MOLECULAR AND METABOLIC EFFECTS OF LOCAL IMMUNE ACTIVATION IN THE RUMINAL EPITHELIUM

A Thesis Submitted to the
College of Graduate and Postdoctoral Studies
In Partial Fulfillment of the Requirements
For the Degree of Doctor of Philosophy
In the Department of Animal and Poultry Science
University of Saskatchewan
Saskatoon

By
Coral Kent-Dennis

PERMISSION TO USE

In presenting this thesis/dissertation in partial fulfillment of the requirements for a Postgraduate degree from the University of Saskatchewan, I agree that the Libraries of this University may make it freely available for inspection. I further agree that permission for copying of this thesis/dissertation in any manner, in whole or in part, for scholarly purposes may be granted by the professor or professors who supervised my thesis/dissertation work or, in their absence, by the Head of the Department or the Dean of the College in which my thesis work was done. It is understood that any copying or publication or use of this thesis/dissertation or parts thereof for financial gain shall not be allowed without my written permission. It is also understood that due recognition shall be given to me and to the University of Saskatchewan in any scholarly use which may be made of any material in my thesis/dissertation.

Requests for permission to copy or to make other uses of materials in this thesis/dissertation in whole or part should be addressed to:

Head of the Department of Animal and Poultry Science
University of Saskatchewan
Saskatoon, Saskatchewan S7N 5A8 Canada

OR

Dean of College of Graduate and Postdoctoral Studies
University of Saskatchewan
116 Thorvaldson Building, 110 Science Place
Saskatoon, Saskatchewan S7N 5C9 Canada

ABSTRACT

Modern dairy and beef cattle efficiently produce large quantities of high value products, milk and meat respectively, for human consumption. In order to meet the energy demands of production, cattle are fed diets consisting of rapidly fermentable carbohydrates. As a result, ruminal acidosis may occur. The acidotic conditions in the ruminal fluid can result in compromised barrier function and, potentially, translocation of microbes and microbe-associated molecular patterns, (**MAMP**) from the lumen across the ruminal epithelium. Translocation of microbes or MAMP may lead to an interaction with the ruminal epithelial cells (**REC**), thus inducing a local, pro-inflammatory response. However, little is known about the capability of REC to initiate such a response as well as the effects of inflammation on the physiological functions of the ruminal epithelium. The objective of this research was to assess the inflammatory response of the ruminal epithelium and to investigate the potential effects of inflammation on nutrient uptake and metabolism using in vivo, ex vivo and primary cell culture models.

In Chapter 3, ruminal papillae biopsies were collected from beef heifers following induction of subacute ruminal acidosis (**SARA**). The papillae were used to evaluate differential gene expression and toll-like receptor (**TLR**) 4 quantification. Despite an increase in ruminal fluid concentration of LPS, gene expression of inflammatory molecules and immunohistofluorescent analysis of TLR4 protein expression indicated an anti-inflammatory response 2 d following the SARA challenge.

The Ussing chamber model was used in Chapter 4 to explore the effects of LPS exposure on the inflammatory response and the potential effects on butyrate flux and metabolism. Analysis of gene expression suggested that the pro-inflammatory response to LPS may have been suppressed or prevented by the epithelial barrier. In tissue exposed to LPS, butyrate flux tended to increase linearly ($P = 0.063$); however, production of β-hydroxybutyrate (**BHB**) was not affected ($P = 0.21$), suggesting that the impact of LPS exposure on metabolism of the ruminal epithelium was minimal.

To further evaluate REC responses to LPS exposure, a cell culture model was established (Chapter 5). Using that model in Chapter 6, I evaluated the effects of dose, duration, and timing of LPS exposure on viability and gene expression of pattern recognition receptors (**PRR**), pro-

inflammatory cytokines, chemokines, and other immunomodulatory molecules in cultured primary REC. There was no indication that LPS negatively impacted cell viability, but exposure to LPS increased *TLR2* and *TLR4* expression and induced a pro-inflammatory response. Results suggested that the REC response was influenced by LPS dose and duration of exposure, and that gene expression may have been regulated to prevent an excessive pro-inflammatory response and potential damage to the cells.

In Chapter 7, cultured REC were exposed to LPS when grown with or without the addition of short-chain fatty acids (**SCFA**) to the cell culture media in order to evaluate the effects of the inflammatory response on metabolic function. Results showed that LPS exposure tended to increase glucose utilization compared to control REC (31.8 versus 28.7 ± 2.7%; P = 0.072). Analysis of gene and protein expression further indicated that nutrient transport and metabolism in the cells may have been moderately altered by the inflammatory response.

Overall, the results of this research indicate that exposure of the REC to LPS activates an inflammatory response, the nature of which is dependent on the dose, duration and timing of exposure. However, the response may differ between whole tissue and cultured REC. The data suggested that although metabolism of the REC may have been altered, the changes observed were moderate, indicating that key functions of the ruminal epithelium are resilient to local inflammatory responses.

ACKNOWLEDGEMENTS

It has been quite a journey getting to this place in my life, and I certainly wouldn't be here if it weren't for all of the people who have helped, encouraged and supported me along the way.

First, I would like to thank my supervisor, Dr. Greg Penner. Thank you for encouraging me to continue my pursuit of a PhD, and providing me with a challenging yet rewarding project. I would also like to acknowledge my committee members, Dr. Tim Mutsvangwa, Dr. Andrew Van Kessel and Dr. Philip Griebel, as well as my graduate chair Dr. Fiona Buchanan, for their guidance and support throughout my program. I'd also like to thank Dr. Jorg Aschenbach and Susanne Trappe for welcoming me into their lab in Berlin and sharing their expertise on the rumen cell culture technique. I am very grateful for that opportunity.

I would also like to acknowledge all of the members of Team Rumen for all of their help and friendship throughout my time at the U of S. I would like to extend a special thanks to Gillian Gratton. Gill, thank you for your patience with all of my ordering requests, and for your willingness to help with any task. Also, thanks to both Gill and Kasia for the much needed coffee breaks.

I would like to thank my friends and family, all around the world, for their love and support, especially my parents, Dan and Sophie, and my siblings, Marie, Eric and Sierra. I am deeply grateful for your unwavering support, and being forever understanding when I couldn't make it to family events. You've always been my bedrock, encouraging my love of science and instilling the importance of critical thinking. I am inspired by all of you.

Finally, I would like to thank my partner, Alex Pasternak, who has stood by my side every step of the way. Alex, thank you for all of the science discussions, even after going on for way too long. Thank you for never telling me something just because it's what I wanted to hear. Thank you for believing in me, even when I didn't believe in myself. Thank you for putting up with my crazy and making sure that neither of us ever completely grow up.

DEDICATION

To Grumpy

Many years ago, when my interest in dairy and agriculture was just beginning to flourish, my grandfather, Eric Lampard, gave me a copy of his PhD dissertation, *The Rise of the Dairy Industry in Wisconsin*. In many ways, my work (57 years later) is a continuation of what he wrote about in his thesis: the use of science and technology to improve agriculture. Inspiration for my pursuit of knowledge and my love of cows can be attributed to him.

TABLE OF CONTENTS

LIST OF TABLES

LIST OF FIGURES

LIST OF ABBREVIATIONS

APC	Antigen-presenting cell
BHB	β-hydroxybutyrate
CTCF	Corrected total cellular fluorescence
DAMP	Damage-associated molecular patterns
DAPI	4',6-diamidino-2-phenylindole
DMI	Dry matter intake
DPBS	Dulbecco's phosphate buffered saline
EU	Endotoxin units
FBS	Fetal bovine serum
GALT	Gut-associated lymphoid tissue
GIT	Gastrointestinal tract
IEC	Intestinal epithelial cells
LBP	LPS-binding protein
LC	Langerhans cells
LCM	Laser capture microdissection
LPS	Lipopolysaccharide
MAMP	Microbe-associated molecular pattern
MEM	Minimum essentials media
PRR	Pattern recognition receptors
REC	Ruminal epithelial cells
ROI	Region of interest

SARA	Subacute ruminal acidosis
SCFA	Short-chain fatty acids
TLR	Toll-like receptor
TMR	Total mixed ration

CHAPTER 1: GENERAL INTRODUCTION

Levels of productivity in both dairy and beef cattle have increased dramatically over the past 75 years (VandeHaar and St-Pierre, 2006; Drouillard, 2018). Milk production by dairy cows has increased from around 2000 kg/cow/year in the 1940s to over 10,000 kg/cow/year in the 2010's and it is not uncommon for high producing cows to exceed 40 kg per day at peak (Baumgard et al., 2017). For beef cattle, current growth standards reflect a high level of efficiency with feedlot steers capable of achieving rates of gain of over 2 kg/d during the finishing period (Zinn et al., 2008; Wierenga et al., 2010). Improvements in productivity can be attributed to selection of superior genetics, advances in nutrition and management techniques such as increased milking frequency and increased emphasis on cow comfort for dairy cows (Connor et al., 2012; Miglior et al., 2017), and the use of growth promotants in beef cattle (Drouillard, 2018).

Provision of highly fermentable carbohydrates in the diet increases the concentrations of short-chain fatty acids (**SCFA**), which are readily absorbed by the ruminal epithelium and constitute a large proportion of the animal's metabolizable energy supply (Plaizier et al., 2008). The increased supply of energy is necessary to support the modern levels of production, whether it is milk yield or muscle growth. However, the increases in the levels of production are not without consequences. Metabolic and nutritional diseases of ruminants are often a result, either directly or indirectly, of inadequately meeting or balancing diets for nutritional requirements (Mulligan and Doherty, 2008). Cattle exposed to rapid dietary changes, such as high yielding transition dairy cows or finishing cattle, are especially at risk.

Highly fermentable diets, especially without adequate levels of physically effective fiber, or without appropriate adaptation to such diets, can lead to ruminal acidosis, a digestive disorder that alters the ruminal environment (Kleen et al., 2003; Penner et al., 2011). Acidosis occurs when ruminal microbial production of organic acids exceeds absorptive capacity and the ability to neutralize those acids. Subsequently, there is a decrease in ruminal pH and an increase in osmolality of the ruminal fluid (Owens et al., 1998). The changes in the ruminal environment lead to a shift in the microbial population and, ultimately, an accumulation of microbe-associated molecular patterns (**MAMP**), particularly free lipopolysaccharide (**LPS**), as a result of increased

bacterial turnover and death (Plaizier et al., 2012). Acidotic conditions in the rumen can lead to a compromised epithelial barrier and increased permeability (Schurmann et al., 2014), and are associated with translocation of microbes or luminal compounds, such as free LPS (Aschenbach et al., 2003; Emmanuel et al., 2007).

A number of consequences are associated with ruminal acidosis. There are marked decreases in dry matter intake (**DMI**) and fiber digestion. Ruminal acidosis is also linked to a number of other metabolic diseases. Poor ruminal health in the transition dairy cow may pre-dispose her to ketosis, fatty liver syndrome and displaced abomasum during early lactation (Nocek, 1997). Translocation of ruminal microbes is thought to lead to colonization of viscera and cause abscesses in the liver (Kleen et al., 2003). Moreover, translocation of MAMPs, such as LPS, and histamine is closely linked to laminitis, which is a leading cause of lameness in both dairy and feedlot cattle. Lameness is the primary welfare issue that ruminant production faces (Nocek et al., 1997).

Systemic inflammation has been well-documented as a consequence of acidotic conditions in the rumen and compromised epithelial barrier function (Gozho et al., 2005; Khafipour et al., 2009). Activation of the immune system is associated with substantial increases in nutrient and energetic demands (McNeil et al., 2016; Kvidera et al., 2017), presumably to meet requirements for proliferation and increased metabolism of immune cells and synthesis of acute phase proteins and immune-modulatory molecules (Calder et al., 2007). In addition to the immediate effects on production, there may also be increased susceptibility to infection, therefore negatively impacting overall health of the animal.

Previous work has shown that the ruminal epithelium is equipped with pattern recognition receptors (Malmuthuge et al., 2012). Although epithelial cells have not traditionally been considered as a part of the active immune system, it is now understood that cells such as intestinal enterocytes and keratinocytes play key roles in microbe-mucosa crosstalk, activation and regulation of epithelial surface inflammation, and immune-modulation (Peterson and Artis, 2014; Bukhari et al., 2019). Translocation of compounds across the ruminal epithelium, in addition to its association with systemic inflammation, may facilitate an interaction with MAMPs, and the initiation of a local inflammatory response by the ruminal epithelial cells (**REC**). However, there is a lack of direct evidence for this response.

The cells that make up the ruminal epithelium, particularly those closest to the basolateral membrane, are specialized epithelial cells that are responsible for transportation of ruminal ions and nutrients, ruminal buffering, regulation of ruminal intracellular pH through uptake and flux of SCFA and extensive cellular metabolism (Graham and Simmons, 2005; Aschenbach et al., 2011). The functions of REC are critical for providing the ruminant with adequate metabolizable energy and ensuring maintenance and productivity. Pro-inflammatory responses at epithelial surfaces have been shown to alter cell metabolism, increase nutrient and energy demands and negatively impact nutrient transport by intestinal epithelial cells (Peuhkuri et al., 2010; Glover and Colgan, 2011). These effects have been demonstrated in intestinal epithelial cells (Thibault et al., 2007) as well as in keratinocytes (Zhang et al., 2018). As they bear many similarities to REC, it is likely that an inflammatory response may also affect metabolic function in REC, however this had not been fully elucidated.

The effects on feed intake and metabolism, as well as inflammation and health, negatively impact milk and milk component yield, and will likely be detrimental to milk production over the entire lactation (Plaizier et al., 2008). For feedlot calves, digestive upset during transition or inadequate adaptation to finishing diets, will also lead to acidosis, which not only can affect growth and overall health, but can also lead to conditions that affect carcass quality (Nagaraja and Chengappa, 1998). Although animal agriculture is highly productive, science and industry must continuously strive to improve efficiency of our modern food systems. Focusing on the physiological mechanisms involved in maintaining or promoting gastrointestinal health will allow for a greater understanding of how to minimize the negative consequences associated with production and to optimize the potential of our animals.

Therefore, the overall aim of my Ph.D. thesis research was to evaluate the potential pro-inflammatory response in the ruminal epithelium and to understand the implications of inflammation on REC metabolic function.

CHAPTER 2: LITERATURE REVIEW

2.1 STRUCTURE AND FUNCTIONS OF THE RUMINAL EPITHELIUM

2.1.1 Organization of the ruminal epithelium

The ruminal epithelium plays several critical roles, including nutrient absorption and metabolism, ion transport and physical protection (Galfi et al., 1991; Baldwin and Connor, 2017). The ruminal epithelium, comprised of specialized cells and structures, has evolved to make efficient use of the end products of microbial fermentation, to provide a robust barrier to the harsh luminal conditions, and to maintain homeostasis within the epithelial tissue (Graham and Simmons, 2005; Aschenbach et al., 2011).

The ruminal epithelium is a mucosal surface of the gastrointestinal tract, although it lacks a mucus layer, consisting of non-glandular, stratified squamous epithelial cells (Connor and Baldwin, 2017). Projections of epithelium, called papillae, increase the absorptive surface area. Ruminal papillae can be found in varying densities ranging from 30 per cm^2 (Kern et al., 2016) to several hundred papillae per cm^2 (Ward, 2008), depending on species, age/stage of development, diet, and region within the rumen (Hofmann, 1989; Josefsen et al., 1996; Lima et al., 2015; Steele et al., 2016). The size and shape can also vary considerably; papillae can be short stubs, long and conical, rounded, tongue-shaped or leaf-shaped (Scott and Gardner, 1973). Increases in epithelial surface area due to an increase in the size and density of ruminal papillae have been associated with an increase in concentrate in the diet and the subsequent increase in short chain fatty acids (**SCFA**) concentrations (Gabel et al., 1987; Bannink et al., 2008).

The epithelium is comprised of four strata including the stratum corneum, stratum granulosum, stratum spinosum and stratum basale (Graham and Simmons, 2005; Figure 1). The epithelial layers surround a central core of lamina propria, which is highly vascularized (Dobson et al., 1956). Small projections of the lamina propria into the epithelium, called papillary bodies, form structures that are akin to epithelial pegs in the skin (Dobson et al., 1956; Ragionieri et al., 2016).

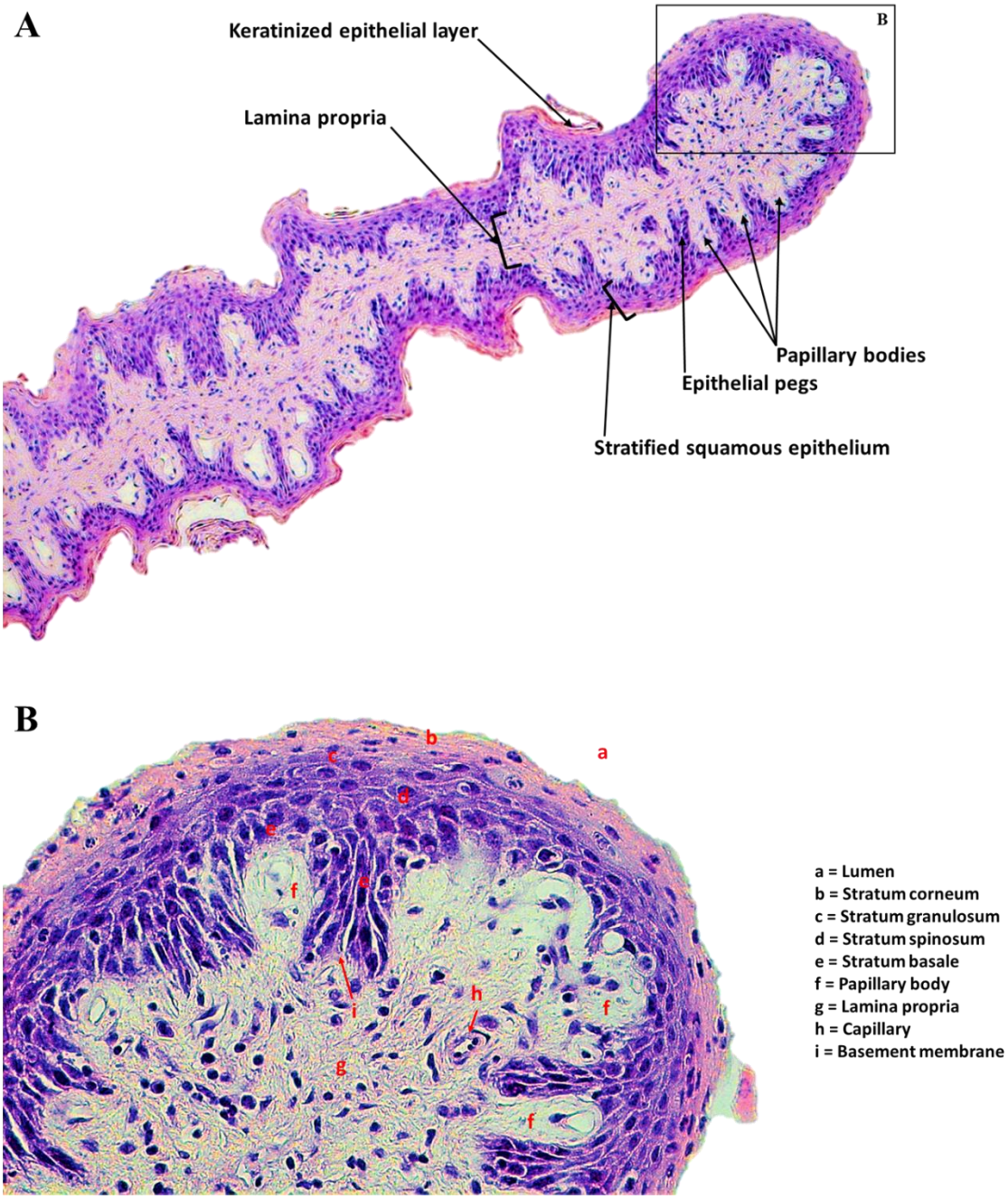

Figure 2.1 H&E staining of ruminal papillae depicting the major morphological features. Images by C. Kent-Dennis.

The stratum basale is a distinct layer of columnar epithelial cells adjacent to the basement membrane (Dobson et al., 1956) and these cells migrate towards the apical surface. The mechanism by which the ruminal epithelial cells (**REC**) migrate from the stratum basale to the stratum corneum is not fully understood (Steele et al., 2016). However, it is proposed to be similar to the processes that occur in the epidermis of the skin (Yohe et al., 2016). The cells of the stratum basale proliferate and differentiate from epithelial stem cells or from progenitor cells (Eckhart et al., 2013). Once these cells detach from the basement membrane, they begin a process of terminal differentiation whereby cells migrate towards the lumen, transforming into keratinocytes (Zouboulis et al., 2008). As these cells become completely cornified, they undergo sloughing into the lumen.

The cells of the stratum basale are considered the most important in terms of the contribution to the metabolic function of the rumen epithelium. Graham and Simmons (2005) used a mitochondrial marker and reported that the density of mitochondria was greatest in the stratum basale. In addition, the same study demonstrated intense immuno-histofluorescent staining of Na^+-K^+-ATPase in the stratum basale cells, indicating that these cells are equipped for secondary active solute transport. Stratum basale cells lack gap junctions (Graham and Simmons, 2005) and most tight junction proteins (Stumpff et al., 2011). Native rumen epithelium in sheep had only diffuse staining for claudin-1 and claudin-3 (Graham and Simmons, 2005; Stumpff et al., 2011).

The stratum spinosum and stratum granulosum are comprised of multiple layers of intermediary cells that are only subtly distinguished from each other in terms of morphology (Tamate et al., 1974). Parabasal spinosum cells are cuboidal or spherical and become flatter with increasing filamentous material as they migrate towards the lumen (Dobson et al 1956). Cells in this stratum are characterized by having numerous mitochondria and other organelles, some granulation, and the presence of desmosomes (Henrikson, 1970). As cells move into the stratum granulosum layer, they become squamous, with increasing amounts of filamentous materials and keratohyalin granules (Lavker and Matoltsy, 1970; Henrikson, 1970). The number of mitochondria decrease and the number of desmosomes as well as gap junctions increase (Graham and Simmons, 2005). Cells of the stratum granulosum, and to some degree the stratum spinosum, have clearly defined intercellular localization of tight junction proteins including claudin-1, -2 and -4 (Stumpff et al., 2011; Liu et al., 2013).

Whereas the underlying strata have no direct contact with ruminal contents, under normal physiological conditions, the stratum corneum provides an important physical barrier between the lumen and the metabolically functional epithelial cells (Steele et al 2016). The cells of this stratum have almost entirely lost their organelles to degradation and may contain up to 85% keratin (Eckhart et al., 2013). The most luminal layer of keratinized cells is made up of horn cells, or corneocytes, which form cytoplasmic protrusions and are subject to sloughing (Scott and Gardner, 1973). In addition to complete degradation of cytoplasmic organelles and nuclei, horn cells are characterized by a proteinaceous cytoskeleton and protein-lipid cross-linking that forms the cornified cell envelope (Lavker and Matoltsy, 1970; Eckhart et al., 2013). These characteristics provide protection against mechanical abrasion, and sloughing of the horn cells occurs as the underlying cells are replenished (Eckhart et al., 2013). The surface of the ruminal papillae is characterized by valleys and grooves (Tamate et al., 1971; Scott and Gardner, 1973; Steele at al., 2011), which are made up of keratinized squamous epithelial cells. Microbial populations reside within the valleys and are loosely associated with the keratinized epithelial cells (Graham and Simmons, 2005).

2.1.2 Mechanisms of absorption across the ruminal epithelium

The ruminal epithelium is highly evolved to facilitate absorption of fermentation products, such as SCFA and ammonia (Bergman, 1990). Short chain fatty acids are absorbed by the REC and transported into the portal drained viscera where they can be utilized for gluconeogenesis, fatty acid synthesis, and ketogenesis in the liver or peripheral tissues. In addition, a substantial proportion of SCFA, especially butyrate, are metabolized by REC (Sehested et al., 1999a). In fact, butyrate is the preferred energy substrate for REC, and the majority that is taken up by the ruminal epithelium is either oxidized to CO_2 or metabolites such as BHB (Sehested et al., 1999a; Kristensen et al., 2005).

In addition, the absorptive mechanisms for SCFA play a critical role in maintenance of ruminal and intracellular pH (Aschenbach et al., 2011). As ruminal pH decreases, there is an increase in undissociated SCFA and the rate of SCFA absorption across the ruminal epithelium increases (Aschencbach et al., 2009). This mechanism is efficient for most lipophilic fatty acids (buytrate > propionate > acetate) at a low pH due to the pKa of 4.8 for SCFA (Aschenbach et al., 2011). Once in the cytosol, rapid dissociation occurs due to the low pKa of SCFA

(approximately 4.8) and this aids in the regulation of intracellular pH (7.4). Even in the lumen, the majority of SCFA are present in their dissociated form and are transported into the epithelial cells through HCO_3^- anion exchange. This exchange is driven by transport of HCO_3^- across the basolateral membrane by Na+/HCO_3^- cotransport (Huhn et al., 2003; Aschenbach et al., 2011) and potentially endogenous production of HCO_3^- through the carbonic anhydrase reaction. However, the importance of intracellular carbonic anhydrase has been questioned (Sehested et al., 1996). The resulting export of HCO_3^- into the lumen contributes to ruminal pH homeostasis by combining with a proton to form H_2CO_3 which is then converted to CO_2 and H_2O (Aschenbach., 2009). To stabilize ruminal pH, the pCO_2 must not increase and CO_2 is removed via eructation. In addition to passive diffusion and HCO_3^- anion exchange, SCFA may also be absorbed by the cells via a protein-mediated transporter (Penner et al., 2009) of which maxi-anion channels are the key contributor (Stumpff, 2019).

In order to protect against intracellular acidification, REC deploy a number of mechanisms in response to incoming protons and outgoing HCO_3^- (Aschenbach 2011). Protons can be exported back into the lumen (Sehested et al., 1996; Muller et al., 2000) or across the basolateral membrane (Muller et al., 2000) via Na^+/H^+ exchangers (NHE). Graham et al. (2007) demonstrated protein expression of NHE1 and NHE2 in the basale, spinosum and granulosum strata of the epithelial cells. Incoming HCO_3^- via the basolateral Na^+/HCO_3^- cotransporter will also neutralize an intracellular proton (Aschenbach et al., 2011).

The mechanisms for export of SCFA across the basolateral membrane are thought to be similar to the apical surface and may also contribute to removal of intracellular protons. However, expression of specific transporters are isolated to basolateral and apical poles (Graham et al., 2007). Despite similar mechanisms, it has been postulated that transport capacity across the basaolateral membrane is greater than the apical membrane to help avoid intracellular loading of SCFA and SCFA metabolites, and in the regulation of intracellular pH (Penner et al., 2009; Stumpff, 2019). Basolateral transport of SCFA occurs via MCT1, a solute transporter with a broad substrate specificity (Halestrap and Wilson, 2012) which appears to be localized to the basolateral membrane of the rumen epithelium (Muller et al., 2002; Kirat et al., 2006; Graham et al., 2007). The broad specificity is important considering the extensive metabolism of butyrate and propionate by the ruminal epithelium and that the transport of end-products of cellular SCFA

metabolism, such as lactic acid (primarily from propionate) and ketone bodies (primarily from butyrate), can also occur via MCT1 (Halestrap and Wilson, 2012).

Extensive metabolism of SCFA occurs by the REC, especially within those of the basale and spinosum strata (Bergman, 1990; Graham and Simmons, 2005). The extent of SCFA metabolism by the ruminal epithelium increases with chain length (Bergman, 1990) and intracellular metabolism of SCFA has been shown to be a driving factor of uptake from the rumen due to gradient between the lumen and cytosol or by promoting $SCFA^-$/ HCO_3^- exchange via CO_2 production (Gäbel et al., 2001). The majority of acetate and approximately 50% of propionate is transported into the portal vein and utilized for fat synthesis and gluconeogenesis, respectively (Britton and Krehbiel, 1993); however, ruminal epithelial cells have been estimated to metabolize up to 50% of propionate to lactate and CO_2 (Pennington and Sutherland, 1956; Gabel and Sehested, 1997). More than 85% of the absorbed butyrate is metabolized by the ruminal epithelium to CO_2, or to ketone bodies by the process of alimentary ketogenesis (Bergman, 1971; Bush and Milligan, 1971). The ketones (BHB and acetoacetate) which can be exported basolaterally to be used as an energy source by other tissues of the portal drained viscera (Kristensen and Harmon, 2004). Although butyrate is the preferred energy substrate for REC, a degree of metabolic flexibility has been demonstrated (El-Kadi et al., 2009); the epithelium may be able to selectively oxidize butyrate or arterial glucose depending on availability to the cells (Baldwin and Jesse, 1992; Wiese et al., 2013).

Ruminal epithelial cells play critical roles in physical protection, absorption of ruminal nutrients and regulation of ruminal and intracellular pH. As such, integrity of the epithelial barrier and function of the REC are critical factors in the development and consequences of metabolic and digestive disorders, such as ruminal acidosis.

2.2 RUMINAL ACIDOSIS

2.2.1 Overview

Diets containing highly fermentable carbohydrates are fed to dairy and finishing feedlot cattle, increasing the production of organic acids in the rumen, in order to meet the demands for metabolizable energy and metabolizable protein that support milk production and rates of gain. However, accumulation of these organic acids can lead to digestive disorders such as ruminal

acidosis, which can be detrimental to the rumen microbial population, health of the animal, and can negatively impact production and growth (Kleen et al., 2003; Penner et al., 2011; Castillo-Lopez et al., 2013).

Ruminal acidosis is generally defined as a digestive disorder characterized by a depression in ruminal pH (Owens et al., 1998). Ruminal pH is regulated by buffering and absorption of organic acids such as SCFA and lactic acid. These mechanisms function by neutralizing and removing H^+ protons in the lumen (Aschenbach et al., 2011). Specific definitions have been developed to characterize the levels of severity of ruminal acidosis, as described below, and depend on the nature of the changes within the rumen. Typically, the definitions have been based on the pH of the ruminal fluid, however it has been suggested that a decrease in pH below a certain threshold is the most useful for diagnosing acidosis, although there is disagreement as to which threshold (Plaizier et al., 2009). Ruminal pH can vary depending on time of day, time of sampling relative to a meal and on the sampling technique, therefore determining the duration that pH is below a given threshold may be more accurate (Gohzo et al., 2005).

Acute acidosis is characterized by a severe drop in ruminal pH, usually below pH 5.2, and has been postulated to primarily occur following excess grain consumption in a single meal (Owens et al., 1998; Nagaraja and Titgemeyer, 2007). That said, acute acidosis may occur following an abrupt change in diet from one of high forage, fed to pre-partum dairy cows or beef steers during the receiving period, to one containing a high proportion of concentrate (Owens et al., 1998). An overload of highly fermentable carbohydrates may also occur due to feeding errors, over-processing of grains, and limiting access to feed followed by provision of feed (Snyder and Credille, 2017). Rapid change to highly fermentable diets without a period of adequate adaptation can result in reduced performance, short and long-term health consequences, involuntary culling and, in some instances, may result in death (Nocek, 1997; Brown et al., 2006; Steele et al., 2009).

With acute acidosis, fermentation of excess starch due to engorgement of grain results in its cleavage to free glucose, which results in increased production of organic acids and decreased ruminal pH, subsequently promoting the growth of lactic acid-producing bacteria (Owens et al., 1998). This leads to an accumulation of lactic acid, especially D-lactic acid as it has a slower rate of absorption and metabolism compared to L-lactic acid, further reducing the pH and impeding

the growth of other microbial species (Nocek, 1997). Acute ruminal acidosis can eventually result in metabolic acidosis as lactate enters circulation and lowers blood pH below physiological levels (Owens et al., 1998).

Subacute ruminal acidosis (**SARA**) is generally defined as a reduction in ruminal pH below a threshold, ranging from 5.2 to 5.9 (Plaizier et al., 2009), for a duration of at least 3 h/d (Gohzo et al., 2005). Decreases in pH occur following a meal, or they can be associated with high risk periods such as during the periparturient transition (Kleen et al., 2003). Besides ruminal pH, SARA is characterized by a number of other factors including changes in blood, urine and fecal pH, milk fat depression, a decrease in body condition, increase disease susceptibility and higher rates of lameness (Oetzel, 2017; Plaizier et al., 2018). Subacute acidosis can be caused by consumption of a diet high in energy, with ruminal pH returning to physiological pH between meals (Kleen et al., 2003), and without sufficient physically effective fiber. It has also been induced through feed restriction followed by re-feeding (Zhang et al., 2013; Pederzolli et al., 2018). As with acute acidosis, adequate adaptation to highly fermentable diets can minimize or prevent negative effects of SARA (Steele et al., 2009; Penner et al., 2011).

2.2.2 Changes in the ruminal environment during acidosis

Ruminal acidosis is characterized by dramatic changes in the ruminal environment including: altered microbial populations; an increase in organic acids especially SCFA and lactic acid; and a subsequent decrease in ruminal pH. High levels of concentrates in the diet favor amylolytic and lactic acid fermenting bacterial species (Goad et al., 1998; Nagajara and Titgemeyer, 2007). In response to highly fermentable diets, microbes in the rumen of cattle have been shown to produce well over 120 mol/day total SCFA (Goad et al., 1998; Bevans et al., 2005; Penner et al., 2007). D/L-lactate can accumulate in the rumen to levels above 40 m*M* during severe acidosis, compared to physiological levels of 5 m*M* (Owens et al., 1998; Nagaraja and Titgemeyer, 2007).

Concurrent with the drop in pH, increased concentration of ruminal solutes, such as free glucose, minerals, and organic acids increase the ruminal osmolality during ruminal acidosis (Owens et al., 1998). Osmolality of ruminal fluid has been shown to be around 265 mOsm/kg with consumption of a forage-based diet and 296 mOsm/kg with a high concentrate diet (Garza et al. 1989). During acidosis, that value may rise to well over 400 mOsm/kg in sheep (Phillip et

al., 1981; Owens et al., 1998) and over 300 mOsm/kg in cattle (Paton et al., 2006; Khafipour et al., 2009). Higher ruminal osmolality can result in an influx of water into the rumen from bloodstream, which may cause damage to the epithelium (Owens et al., 1998).

Another well-documented change in the ruminal environment during ruminal acidosis is increased concentrations of microbial-derived toxins, produced by microbial fermentation and turnover. Bacterial endotoxins (lipopolysaccharide; **LPS**), histamine, tyramine, tryptamine, putrescine, and methylamine have been found at elevated concentrations in ruminal fluid during acidosis (Garner et al., 2002; Khafipour et al., 2009; Wang et al., 2013). Many other molecules, such as fimbrial adhesins, are also suspected to increase as ruminal pH decreases (Gyles, 2007; Plaizier et al., 2009).

The most widely studied of all of the acidosis-related toxins is bacterial LPS, a component of the outer cell wall of gram-negative bacteria (Plaizier et al., 2012). It is produced and shed during growth, as well as following lysis of the bacterial cell (Hurley, 1995). The bioactivity of LPS is typically potent, although its activity depends on the species of bacteria from which it is derived (Aschenbach et al., 2019). The interaction between LPS and host cells can induce robust inflammatory reactions (Cavaillon, 2018). The concentration of free LPS in ruminal fluid is highly variable. Under normal physiological conditions in cows fed high forage diets, ruminal LPS concentrations were found to be as low as 118 EU/mL (Andersen et al., 1994a) and as high as 42,122 EU/mL (Khafipour et al., 2009b). In studies where ruminal acidosis challenges or high grain diets were implemented, the general trend has been an increase in LPS concentration compared to control animals fed a high forage diet (Plaizier et al., 2012). Concentrations under acidotic conditions are also highly variable ranging from 1,487 EU/mL, following a grain over-load (Andersen et al., 1994b) to 145,593 EU/mL, in an alfalfa pellet-based highly-fermentable diet (Khafipour et al., 2009b).

Toxic molecules may be released due to the low ruminal pH creating an environment that is inhospitable to some microbial species, or due to increased bacterial proliferation and turnover. For example, due to the changes in ruminal pH, certain bacteria, especially celluloytic species, cannot survive and will shed free LPS as they die (Plaizier et al., 2012). In addition, there will be an overall increase in microbial growth in response to increased substrate availability, leading to increased rate of microbial turnover, which also increases the level of free LPS in ruminal fluid (Plaizier et al., 2009). At low ruminal pH, the environment is ideal for

species that release potentially toxic molecules as a result of their fermentation. For example, as a result of grain in the diet, histamines from the bacterial species *A. histaminiformans* or leukotoxins from *F. necrophorum* can be produced (Garner et al., 2002; Tadepalli et al., 2009).

2.2.3 Consequences of ruminal acidosis

Acidotic conditions in the rumen are favorable for the development of what has been previously termed the parakeratosis-rumenitis-liver abscess complex (Kleen et al., 2003). Several interrelated factors are proposed to be causative, although the exact interactions that lead to this syndrome are not entirely understood. Development of parakeratosis of the ruminal epithelium, in which REC prematurely undergo keratinization, has been documented in cattle following experimentally-induced acidosis (Steele et al., 2009). Rapid influx of water into the rumen, a result of the increased osmolality, causes swelling and rupture of the ruminal papillae, eventually leading to sloughing of epithelium (Eadie and Mann, 1970; Steele et al., 2009). Subsequently, rumenitis can occur, characterized by micro-abscess formation (Steele et al., 2011), a deterioration of desmosomes and tight cell junctions (Steel et al., 2011; Liu et al., 2013) and, consequently compromised epithelial barrier function. When the mucosal barrier is impaired, potential translocation of microbes and microbe-associated molecular patterns (**MAMPs**) may occur. Abscesses in the liver have long been associated with ruminal acidosis and are purportedly a result of translocation of ruminal bacteria into the portal blood (Kleen et al., 2003). Indeed, cultured microflora, especially *Trueperella pyogenes* and *Fusobacterium necrophorum*, from liver abscesses of feedlot cattle were shown to be strongly correlated with those of ruminal micro-abscesses (Nagaraja and Chengappa, 1998).

Translocation of ruminal-derived microbes and MAMPs can lead to a number of other negative consequences. Besides the liver, bacteria may also colonize the kidneys, lungs, and other parts of the body (Nocek, 1997). Translocation of LPS and histamine are thought to be factors involved in the development of laminitis and lameness in cattle. When released into the bloodstream, these substances are thought to damage the capillaries in the lamellae via arterial dilation and vasoconstriction, causing an increase in blood pressure, hemorrhage and edema within the foot. Subsequent inflammation and mechanical damage to the tissues in the hoof can eventually lead to separation of the lamina and rotation of the pedal bone in the hoof (Nocek, 1997).

Systemic inflammation associated with ruminal acidosis has also been reported. In grain-induced SARA, serum concentration of acute phase proteins, particularly serum amyloid A and haptoglobin, have been found to be elevated compared to the control group (Gozho et al., 2005; Khafipour et al., 2009). This systemic inflammation may be initially triggered by translocation of LPS into the portal blood and subsequent processing by the liver (Dong et al., 2011). It should be noted that other sections of the gastrointestinal tract may also experience acidosis and its consequences as a result of highly fermentable diets, therefore there may be translocation of LPS and other MAMPs across those parts that also contribute to inflammation (Dong et al., 2011).

In addition, translocation of rumen-derived MAMPs may lead to their interaction with rumen epithelium and a potential, local inflammatory response (Plaizier et al., 2018). Dionissopoulos et al. (2012) suggested that SARA may alter the function of the ruminal epithelium. However, there is a paucity of data to support a direct, pro-inflammatory response by the REC.

The implications of ruminal acidosis on production parameters of cattle have been extensively studied and reviewed (Nocek, 1997; Kleen et al., 2003; Stone, 2004; Plaizier et al., 2009). Acidotic animals experience decreased dry matter intake, reduced fiber digestion, increased hindgut fermentation and diarrhea, loss of body condition, increased risk for lameness, decreased milk yield, and milk fat depression. In addition, livers or carcasses may be condemned due to the presence and severity of abscesses and adhesions. Together these amount to significant economic losses associated with acidosis (Nagaraja and Chengappa, 1998; Stone, 2004; Plaizier et al., 2009). An emphasis has been placed on prevention of ruminal acidosis in both the dairy and beef sectors. For example, a balance between dietary fiber and rapidly fermentable carbohydrates can reduce the incidence of SARA, while still maintaining high milk and component yields in dairy cows (Stone, 2004). Moreover, in finishing steers, adequate adaptation to high grain diets is imperative to minimize acidotic insults and ensure a healthy and thriving rumen environment (Brown et al., 2006).

Although the consequences of ruminal acidosis have been a focus of ruminant nutritional physiology for many decades, gaps in the knowledge still exist. More research can further our understanding of the mechanisms that control the response to ruminal acidosis and can provide new insights into prevention and treatment.

2.3 THE MUCOSAL IMMUNE SYSTEM

2.3.1 Overview

Epithelial surfaces provide the first line of defense against invading pathogens. These surfaces are, in general, characterized by secretion of mucus or other anti-microbial substances and the presence of a cellular barrier, comprised of epithelial cells linked by cell to cell junctions. A population of commensal microbes resides at the epithelial surfaces and contributes significantly to the protective function of the mucosa (Cebra, 1999; Sekirov et al., 2008). A highly developed mucosal/epithelial immune system exists in the nasal and oral cavities, gastrointestinal tract, respiratory tract, urogenital tract, the mammary gland, and the skin (McGhee and Fujihashi, 2012). There are many structures and components that interact and contribute to the function of mucosal immunity. It is the collective responsibility of these components to maintain a homeostatic balance in order to respond appropriately and adequately to potential threats (Peterson and Artis, 2014; Kayama and Takeda, 2016). Each mucosal system has unique features and immunological challenges. This review will focus on the immunity at surfaces that most resemble that of the rumen, especially the intestinal and integumentary epithelia.

2.3.2 Protective functions of mucosal epithelial sites

The microflora that resides at mucosal surfaces lives in a symbiotic relationship with the host animal, which benefits from fiber digestion, microbial production of SCFA and vitamins, degradation of toxins, and the ability to out-compete potentially pathogenic microbes (Garland et al., 1982). In order to maintain a healthy relationship between the microflora and host, there must be a compartmentalization between the mucosal surface and the internal tissue. Two major mechanisms, segregation and mediation, facilitate this separation (Peterson and Artis, 2014; Okumura and Takeda, 2017), and help to prevent infection as well as a constant inflammatory response caused by continuous exposure to luminal antigens.

Segregation involves a combination of physical and chemical barriers. Most mucosal surfaces, including the glandular stomach, small and large intestines, the airway, the mammary gland and the urogenital tract, maintain a covering of mucus. Mucus is a viscous material comprised of glycoproteins produced by goblet cells. Due to its high viscosity, mucus physically

obstructs luminal microbes from invading too close to the epithelium (Bakshani et al., 2018). Specific properties of mucus may differ depending on the microbial load and profile of a particular surface (Johansson et al., 2008; Li et al., 2015). In addition, mucus contains a number of bioactive substances with anti-microbial properties. The type and level of antimicrobials also differ depending on the site, but can include defensins, immunoglobulins, especially IgA, cathelicidin, lysozyme, angiogenin, ubiquicidin, phospholipase A_2 and histones (Antoni et al., 2013; Dupont et al., 2014). These substances are produced by specialized Paneth cells, in the small intestine, by lymphocytes or by epithelial cells, and the mucus then acts as a reservoir (Antoni et al., 2013). Along with mucus, a filamentous, mesh-like material called the glycocalyx provides an additional barrier to invading microbes (Kesimer et al., 2013).

The integrity of the epithelial cell layer is maintained by junction complexes. These complexes play direct and supportive roles in upholding barrier function and include tight junctions, adherens junctions, desmosomes and gap junctions (Farquhar and Palade, 1963; Ivanov et al., 2010). These complexes maintain cellular polarity and proximity, while forming a mostly sealed barrier that minimizes paracellular permeability. The degree of permeability of a mucosal epithelial layer is determined by the resistance of the junction complexes, especially tight junctions (Marchiando et al., 2010).

Tight junctions include claudins, occludins, and junctional adhesion molecules, all of which are transmembrane proteins that are localized between adjacent epithelial cells in the most apical region of the lateral surface and form the separation between the apical and basolateral surfaces of the cell (Farquhar and Palade, 1963; Tsukita et al., 2001). Tight junction proteins bind to f-actin of the cytoskeleton through cytosolic connector proteins, ZO1/PDZ (Itoh and Bissell, 2003; Ivanov et al., 2010). Adherens junctions, particularly ecadherin, display many similarities to tight junctions but differ in their structure and molecular composition (Giepmans and van IJzendoorn, 2009). Functions of adherens junctions include maintenance of cell to cell adhesion and regulation of the actin cytoskeleton (Kobielak et al., 2004; Hartsock and Nelson, 2008). Ecadherin, which is more basolaterally located on the lateral surface, interacts with the circumferential F-actin belt, an important cytoskeletal component that regulates mechanical tension and proliferation of epithelial cells (Madara, 1987; Furukawa et al., 2017).

Other important cell to cell molecules include gap junctions and desmosomes. Gap junctions are integral membrane proteins comprised of connexins. They are pore-like and

facilitate cell to cell interactions via diffusion of metabolites and ions. Desmosomes are adherent proteins that help provide structure and resistance to shear force (Giepmans and van IJzendoorn, 2009).

The second major component of mucosal surfaces that contributes to the compartmentalization is mediation of signals between microbes and host cells (Okumura and Takeda, 2017). Homeostasis of the mucosa depends upon a balance between appropriate reactivity to perceived microbial threats and a degree of tolerance to commensal microbes and MAMPs in order to prevent exaggerated inflammatory reactions and potential tissue damage (Karin et al., 2006; Artis, 2008). The degree of reactivity or tolerance varies depending on the mucosal site, and may differ even within regions of the same site. For example, the upper airways maintain a moderate commensal microflora and therefore a greater degree of immune tolerance is ensured. Host cells of the lower respiratory passages, however, are highly reactive to the microbial infiltration (Man et al., 2017). The mechanisms that facilitate tolerance are not completely understood, especially with regards to the "decision-making" abilities of the mucosal immune system (Russell and Ogra, 2010). Undoubtedly, a coordinated and highly developed effort between mechanisms of recognition and intercellular communication maintains the balance between reactivity and tolerance (Artis, 2008; Man et al., 2017).

Recognition of microbes or MAMPs can be accomplished by both the innate and adaptive immune systems. Innate recognition is facilitated by pattern recognition receptors (**PRR**), of which several distinct classes exist, including toll-like receptors (TLR), nod-like receptors (NLR), C-type lectin receptors, and retinoic acid-inducible gene (RIG)-I-like receptors (Takeuchi and Akira, 2010). Within the classes, there are receptors with specific affinities for a wide range of ligands including, LPS, lipoprotein, flagellin, muramyl dipeptide, bacterial and viral nucleic acids, and B-glucan (Takeuchi and Akira, 2010; Hooper, 2015). As is the case with many aspects of the immune system (Nish and Medzhitov, 2011), a degree of redundancy exists within and between receptor families. For example, TLR5 and NLRC4 are both PRR for flagellin, and each can elicit a pro-inflammatory response independently (Vijay-Kumar et al., 2011). Moreover, PRR can have multiple functions. Although often associated with recognition of bacterial lipoproteins, TLR2 has a binding affinity for many molecules of microbial origin including peptidoglycans, lipoteichoic acid, and LPS (Dziarski et al., 2001; Takeuchi and Akira, 2010). Redundancy and pleiotropy are well-described characteristics of the immune system (Paul, 1989;

Ozaki and Leonard, 2002; Kastrukoff et al., 2010) and function to ensure the widest possible coverage of protection in the face of microbial diversity and resistance to host defense mechanisms (Nish and Medzhitov, 2011).

Of the PRR, the most widely studied are the TLRs and perhaps one of the most important for many mucosal surfaces, especially the GIT, is TLR4. The ligand for TLR4 is LPS, which is capable of eliciting a strong, pro-inflammatory response. In immune cells, such as macrophages and polynuclear neutrophils, LPS activation of TLR4 signaling involves several accessory molecules that mediate binding of TLR4 to the ligand (Park and Lee, 2013). These include LPS-binding protein (LBP), CD14 (either as a soluble form or bound to the cell surface) and MD-2. The process is initiated when LPS is transferred to CD14. Although not essential, serum-derived LBP typically mediates this transfer, increasing the efficiency of LPS binding (Song et al., 2001). CD14 is produced by a number of cell types, including immune and epithelial cells (Fichorova et al., 2002; Park and Lee, 2013). MD-2 is a cell surface protein that forms a complex with TLR4 and is necessary for LPS binding (Tsukamoto et al., 2010).

As with the other TLR, TLR4 is a transmembrane glycoprotein that contains three domains, including the N-terminal, central and C-terminal regions (Kim et al., 2007). The N-terminal domain, containing the MD-2 protein, is extracellular, while the C-terminal domain is intracellular (Kim et al., 2007). Upon binding to TLR4, LPS activates a series of transcriptional changes within the cell that leads to the production of pro-inflammatory molecules, in particular cytokines and chemokines. These molecules are crucial mediators of cell to cell communication during the initiation of inflammation (Takeuchi and Akira, 2010). Cytokines are generally categorized as pro-inflammatory, anti-inflammatory, or growth factors; however, many cytokines are pleiotropic (Dinarello, 2000). Cytokines produced by a cell act to signal a threat to other cells locally. As well as their local effects, some cytokines will travel in the circulation and act on various tissues around the body. For example, IL1B is known for its febrile effect (Zaslona et al., 2017) and IL6 acts upon the liver to produce C-reactive protein, a potent acute phase protein (Gani et al., 2009). In addition to cytokines, chemokines are important for recruitment of immune cells, such as neutrophils or lymphocytes, to the aflicted site (Chavakis et al., 2010).

In addition to MAMPs, innate recognition also includes initiating a response to damage-associated molecular patterns (DAMPs), as part of the “danger” sensing mechanism. There are many molecules that act as DAMPs, including ATP, nucleic acids, fibrinogen, uric acid, heat

shock proteins, F-actin and defensins (Roh and Sohn, 2018). In a homeostatic state, within cells, these molecules have important physiological roles. Upon tissue or cell injury, they are released extracellularly and function as DAMPs, capable of inducing potent, pro-inflammatory responses (Venereau et al., 2015). In addition, DAMPs are important for promoting tissue repair. For example, purinergic signalling, involving the release of extracellular ATP, is key in initiating a pro-inflammatory response during cellular stress. However, down-stream purinergic reactions promote an anti-inflammatory response and enhance healing (Di Virgilio et al., 2020).

Many of the DAMPs utilize many of the same PRRs as MAMPs, including TLRs and NLRs, and a large proportion of DAMPs are ligands for TLR4 (Roh and Sohn, 2018). This suggests that in disease states where there is microbial invasion accompanied by tissue damage, such as in inflammatory bowel disease or in acidosis-induced ruminitis, TLR4 activation may occur through binding of either MAMPs or DAMPs.

Many cell types, depending on the mucosal surfaces, play important roles in protection against invading pathogens and mediating the immune response. Certain cells are considered antigen-presenting cells (APC) and include dendritic cells, resident macrophages, and intraepithelial lymphocytes. Collectively, these cell types act as guards or sentinels, sampling luminal antigens at inductor sites (McGhee and Fujihashi, 2012) and provide interactions between the innate and adaptive immune systems. Antigens are internalized and processed by the cell and then presented, via MHCI and MHCII, to $CD8^+$ and $CD4^+$ T lymphocytes, respectively (Clark and Coopersmith, 2007). Resident B lymphocytes are also key APC and produce IgA, which is secreted into the lumen (McGhee and Fujihashi, 2012).

In addition to classical immune cells, epithelial cells also play an important role in mucosal immune responses. Epithelial cells are critical for the recognition of MAMPs via PRR and have been found to initiate pro-inflammatory responses in IEC (Allaire et al., 2018). Moreover, epithelial cells are important sources for the production of many immunomodulatory molecules, which mediate reactiveness and tolerance, and help to promote repair following an inflammatory response (Hooper, 2015). Epithelial cells have even been found to process antigens and subsequently express MHCII on their cell surface, therefore acting as APC (Hershberg et al., 1997). These various mechanisms not only suggest an important role in the mucosal immune system, but also that epithelial cells directly modulate both the innate and adaptive immune responses (Artis, 2008; Hooper, 2015).

2.3.3 Stages of inflammation at mucosal sites

Although largely commensal, there are dense concentrations of microbes at mucosal surfaces, especially the gut. The epithelium must prevent the microbes, commensal or pathogenic, from gaining access to the underlying tissue. In the event of microbial breach of the epithelial barrier, prompt detection by PRRs and activation of pro-inflammatory signaling pathways are critical first steps in eliminating potential threats. In addition, an equally important process, resolution of inflammation, must also occur in order to protect from tissue damage. Many pathologies are associated with autoimmune diseases or chronic inflammation, such as Crohn's disease or atopic dermatitis, both of which are related to the inability to resolve inflammation (Ovsiy et al., 2017; Schett and Neurath, 2018). Resolution is not a passive process, as once thought, but an active one that begins with the initiation of the acute, pro-inflammatory response (Sugimoto et al., 2016). The mechanisms involve both pro-resolution and anti-inflammatory mediators, with the purpose of returning the tissue to a homeostatic state.

During the first stage of inflammation, pro-inflammatory cytokines and chemokines are synthesized. In addition to these molecules, synthesis of lipid mediators of inflammation also occurs and are products of the cyclooxygenase or lipoxygenase (COX and LOX, respectively) pathways that are activated by the metabolism of arachidonic acid (Gilroy et al., 1999; Haeggstrom and Funk, 2011). The COX pathway involves the conversion of arachidonic acid to prostaglandins, such as PGD2 and PGE2, via the enzymatic activity of PTGS1 and PTGS2 (Gilroy et al., 1999). Arachidonic acid can also be converted to leukotrienes in the LOX pathway during acute inflammation, and can elicit potent pro-inflammatory effects (Haeggstrom and Funk, 2011).

These mediators lead to recruitment of immune cells such as neutrophils and macrophages. The cells actively combat foreign material and microbes and further recruit and activate cells of the adaptive immune system (Serhan and Savill, 2005). The onset of acute inflammation; however, is followed closely by the onset of the resolution stage. This stage is characterized by chemokine depletion and negative feedback of pro-inflammatory cytokines (Sugimoto et al., 2016). Both mechanisms will suppress the recruitment of immune cells and the production of pro-inflammatory molecules. In addition, the function of some pro-inflammatory molecules will become anti-inflammatory (Serhan and Savill, 2005; Sugimoto et al., 2016).

Class-switching of the lipid mediators also occurs. Intermediates and enzymes of both prostaglandin and leukotriene synthesis are important regulators of resolution (Serhan et al., 2008). Upregulation of PTGS2 and LTB4 have pro-inflammatory effects in the initial stage of acute inflammation, but they also have anti-inflammatory properties and induce the synthesis of pro-resolution molecules such as resolvins (Gilroy et al., 1999; Campbell et al., 2011). Neutrophils have been shown to release pro-resolution microparticles (Sugimoto et al., 2016), and are important sources of adenosine precursors (Colgan, 2015). Adenosine molecules, and related metabolites, interact with cell surface Ado receptors, activation of which inhibits pro-inflammatory signalling cascades (Khoury et al., 2007; Colgan, 2015). Pro-resolution molecules include lipoxins, AnxA1, maresins, and resolvins (Serhan et al., 2008). Epithelial cells also play a role in promoting resolution and repair following acute inflammation. Along with alternatively-activated macrophages, epithelial cells are a source of IL10 and TGFB, anti-inflammatory cytokines that promote Treg differentiation and suppress pro-inflammatory molecules (Gagliani et al., 2015; Schett and Neurath, 2018). Both pro-resolution and anti-inflammatory molecules function in combination to perpetuate resolution and return the tissue to homeostasis.

2.3.4 Metabolic consequences of inflammation at mucosal sites

Upon initiation of an acute immune response, the energetic and nutrient requirements increase dramatically (Richardson and Davidson, 2003; Wolowczuk et al., 2008). The systemic costs of an immune response have been documented in many species. Mounting an adaptive immune response in birds has been shown to have energetic costs such that reproductive capabilities are compromised (Hanssen et al., 2004). In a study with wild mice, there was a significant allocation of energy away from the respiratory, reproductive, and gastrointestinal systems during an immune response (Derting and Compton, 2003). In an experiment with lactating dairy cows, an acute, systemic immune response resulted in a substantial increase in glucose utilization, estimated at over 1 kg of glucose utilized within a 12-hour period (Kvidera et al., 2017).

Alterations in immune cell metabolism, proliferation of immune cells and the production of immune-modulatory molecules, such as cytokines or immunoglobulins, all contribute to this cost. Induction of inflammation results in metabolic changes in immune cells that enable proper functions, such as rapid response to invading pathogens (Kelly and O'Neill, 2015). Metabolic

changes and requirements differ depending on whether the cells belong to the innate or adaptive immune system. Innate cells, such as dendritic cells, macrophages, and neutrophils are largely recruited to mucosal surfaces during inflammation and the migration of cells requires large amounts of energy (Kominsky et al., 2010). Activation of these innate cells triggers a switch from oxidative phosphorylation to aerobic glycolysis and the production of lactate in the presence of oxygen, a mechanism termed the Warburg effect (Rodriguez-Prados et al., 2010; Kelly and O'Neill, 2015). The shift to glycolytic metabolism is thought to allow for high rates of glucose utilization in low oxygen environments (Van Raam et al., 2008; Kominsky et al., 2010). Resident T and B lymphocytes are highly proliferative, relying on large amounts of glucose (Greiner et al., 1994). These cells favor oxidative phosphorylation of glucose but will also utilize aerobic glycolysis, as well as alternative energy substrates, in order to meet their demands for proliferation (Kominsky et al., 2010). For both innate and adaptive immune cells, as well as non-hematopoietic cells, upregulation of glucose consumption during inflammation is regulated by hypoxia-inducing factor 1-alpha (HIF1A) under hypoxic conditions (Corcoran and O'Neill, 2016).

Inflammatory responses at mucosal surfaces can impact normal barrier functions of epithelial cells, as well as regulate proliferation or apoptosis (Peuhkuri et al., 2010). In addition, the absorptive and metabolic functions of epithelial cells are altered during inflammation. Inflammation of the intestinal mucosa has been shown to impair brush border and intracellular enzyme synthesis, monosaccharide transport, and absorption of some amino acids across the epithelium (Peuhkuri et al., 2010). Oxidative molecules produced by infiltrating neutrophils have been shown not only to be cytotoxic, but will also affect epithelial ion transport (Grisham et al., 1990). Metabolism of butyrate by colonocytes was impaired in mice with experimental colitis (Ahmad et al., 2000). Moreover, Thibault et al. (2007) demonstrated that inflammation of the intestinal mucosa resulted in a down-regulation of MCT1 expression on colonocytes which was correlated with a reduction in butyrate oxidation.

These consequences may have important short- and long-term implications for the health and productivity of an animal. The high energy costs of mounting an immune response may lead to immune suppression and susceptibility to secondary infections (Hanssen et al., 2004). Loss of productivity, in the form of reduced feed intake, milk yield, impaired reproduction or reduced

growth, may occur if animals are immune-challenged and energy is allocated away from those physiological systems (Bradford et al., 2015; Cooke, 2016; Kvidera et al., 2017).

2.3.5 Unique features and functions of the gastrointestinal mucosal immune system

The epithelial barrier of the GIT faces some unique challenges compared to other mucosal surfaces. The most important of these challenges is the immense load of foreign material, including both the microflora and food-derived molecules. The intestinal mucosal immune system must monitor luminal antigens and "decide" whether to respond and how to do so appropriately. As such, there are several distinct structures and mechanisms that help to facilitate these functions.

The intestinal epithelium is comprised of a single layer of columnar epithelial cells, the majority of which are enterocytes, responsible for absorption and transport of food molecules and ions. In addition, goblet cells, enteroendocrine cells and Paneth cells make up the intestinal epithelium. Paneth cells, which are located in the Crypts of Lieberkuhn, are unique to the small intestine and are an important component of the mucosal barrier as they produce many antimicrobial molecules such as host defense peptides and granules containing IgA (Wittkopf et al., 2014).

The intestinal mucosa contains an extensive network of lymphoid tissue, aptly termed gut-associated lymphoid tissue (GALT), which includes Peyer's patches, isolated lymphoid follicles, cecal patches and mesenteric lymph nodes (Hill and Artis, 2010). Specialized intestinal epithelial-like cells, M (microfold) cells, cover GALT and sample the luminal antigens, which are transported to dendritic cells (McGhee and Fujihashi, 2012). Lymphoid tissue contains T cell and B cell domains, which provide a source of memory lymphocytes that can be activated by signals from epithelial cells or APC and subsequently migrate to effector sites (McGhee and FujiHashi, 2012). Compared to other lymphoid tissue, GALT contains the highest density of lymphocytes (Hill and Artis, 2010).

Tight regulation of immune responses at mucosal surfaces is crucial for maintaining homeostasis and depends on highly sophisticated and sensitive cross-talk between the commensal microbiota and the host immune system (Kayama and Takeda, 2012; Wittkopf et al., 2014), the mechanisms of which have not been entirely elucidated. Cross-talk is mediated in part by the epithelial cells through their recognition capabilities and regulation of cell to cell

communication (Wittkopf et al., 2014). During a steady-state, epithelial cells promote tolerance through the production of anti-inflammatory cytokines, such as IL10 and TGFB, promoting the activation of Tregs (Campbell et al., 1999; Wittkopf et al., 2014). Previous work has shown that anti-inflammatory actions by intestinal epithelial cells alters the population of immune cells. For example, dendritic cells were shown to become tolerogenic to luminal antigens (Rimoldi et al., 2005). In contrast, detection of a pathogen or microbial breach via PRR activation promotes a signaling cascade that results in an acute inflammatory response. This response involves up-regulation of pro-inflammatory cytokines and chemokines and down-regulation of anti-inflammatory molecules (Wittkopf et al., 2014).

Another unique aspect of the intestinal mucosal immune system is an interaction between host tissue and microbial-derived immune-modulatory products, specifically SCFA. In monogastrics, and in the hindgut of ruminants, production of significant amounts of SCFA occurs in the cecum or colon, as a result of microbial fermentation of dietary fiber (Roediger, 1980; Allaire et al., 2018). As is the case in the rumen, acetate, propionate and butyrate make up the major proportions of SCFA production. Intestinal epithelial cells utilize SCFA as energy substrates or they are transported into portal circulation (Bloemaen et al., 2009). The relationship between SCFA, especially butyrate, and intestinal immunity has been the subject of a large body of work, of which there are several reviews (Wong et al., 2006; McNabney and Henagan, 2017; Allaire et al., 2018). Butyrate is thought to elicit anti-inflammatory effects on the intestinal epithelium. Previous work has demonstrated beneficial effects of butyrate in alleviating symptoms of Crohn's Disease and colitis through the inhibition of NFkB transcription and subsequent reduction in pro-inflammatory cytokine activity (Segain et al., 2000; Hamer et al., 2008).

2.3.6 Unique features and functions of the cutaneous immune system

The skin surface is normally discussed separately from classic mucosal surfaces; there is no mucus secreted and the epithelial structure differs substantially. However, there are many commonalities between the mucosal and cutaneous immune systems. Although the evolutionary development of epithelial surfaces is largely unknown, the skin of many lower vertebrates, such as fish, closely resembles that of the GIT with goblet cells, antibody secretion and a protective mucus layer, as well a lack of keratinocytes (Hawkes, 1974; Schroder and Bosch, 2016). Many

of the characteristics of mucosal immune system, especially with the GIT, can be applied to the skin as well. A population of commensal microflora resides on the skin surface and interacts with the cells of epidermis (Eyerich et al., 2018). Although mucus is absent, the skin does produce and secrete protective substances such as mild acids, as well as anti-microbial peptides, which provide a chemical barrier to pathogenic or opportunistic microbes (Eyerich et al., 2018). In addition, many innate and adaptive immune cells reside in the epidermis and dermis and the keratinocytes facilitate cross-talk between the microbes and host cells in order to regulate immune reactivity and tolerance (Eyerich et al., 2018).

Aside from the many similarities, there are some unique features and functions of the cutaneous immune system. Unlike many other epithelial surfaces, the epidermis is comprised of several layers of squamous epithelial cells, classified into four strata, starting with a single layer of stratum basale cells that differentiate into stratum spinosum, stratum granulosum and finally stratum corneum (Junqueira, 2009). The stratum corneum is made of keratinized cells that migrate towards the surface, eventually becoming completely cornified, horn cells (Junqueira, 2009), establishing a physical and semi-water-resistant barrier. The structure of the skin epidermis bears substantial similarities to that of the ruminal epithelium (see section 2.1.1 for more details).

The skin also contains some unique subsets of resident immune cells, including Langerhans cells (LC) in the epidermis, dermal dendritic cells, and resident skin macrophages (Nestle et al., 2009; Eyerich et al., 2018). Langerhans cells are often considered the first line of defense, as they detect microbial antigens and present them to effector T lymphocytes (Hunger et al., 2004). However, LC are, in part, responsible for maintaining tolerance in the epidermis through suppression of T cell responses to antigens (Shklovskaya et al., 2011). Resident T cell subsets also contribute to maintaining homeostasis in the skin (Matejuk, 2018). In contrast, antigen detection by dermal dendritic cells and resident macrophages induces a strong, pro-inflammatory response and participate in antigen presentation (Nestle et al., 2009).

Keratinocytes play a key role in skin immunity. As with other epithelial surfaces, a diverse array of PRR have been identified in skin, including TLRs and NLRs and, upon activation, keratinocytes have been shown to initiate pro-inflammatory response to MAMPs (Bukhari et al., 2019). Moreover, keratinocytes mediate the actions of immune cells in skin. For example, a skin-specific chemokine, CCL20, recruits precursors of LC (Dieu-Nosjean et al.,

2000; Matejuk, 2018). Keratinocytes produce a unique profile of other chemoattractant molecules that recruit neutrophils and T cells into the epidermis (Miller and Modlin, 2007; Matejuk, 2018). A study by Yamanaka et al. (2006) also found that keratinocytes produce a growth factor-like cytokine, IL7, which promotes maturation and proliferation of T cells in the skin.

Collectively, these characteristics contribute to a robust cutaneous immune system, capable of sensitive immune-surveillance and rapid responses to potential threats. In addition, the skin is exemplary in its ability to repair and regenerate, allowing for prompt resolution following injury and acute inflammation (Harrison et al., 2019).

2.3.7 Immunity of the ruminal epithelium

There is little, specific information about the mucosal immune system of the rumen. The majority of the inferences made have been a result of extrapolation from the intestinal mucosa. To a lesser extent, the immune system of the rumen epithelium has also been compared to the skin, as there are many similarities between the two. Along with a stratified epithelium, the rumen epithelium contains no goblet cells, and therefore lacks a mucus layer. Like the skin, the REC differentiate into keratinocytes, providing a physical barrier to the luminal environment. In addition to the physical structure, RECs also express PRRs, although information is limited mostly to TLRs. Transcripts for TLR2 and TLR4 have been observed in ruminal tissue in several studies involving dairy cattle (Chen et al., 2012; Dionissopoulos et al., 2013; Minuti et al., 2015; Arroyo et al., 2017). Malmuthuge et al. (2012) showed that most of the known mammalian TLRs are expressed in ruminal tissue in Holstein calves. Besides the TLRs, there is no direct data showing expression of other PRR in REC.

The immune cells that reside in the ruminal mucosa bear remarkable similarities to those of the skin. Although there has been little work done to fully characterize the immune cells and any potential associated lymph tissue, Steven and Marshall (1972) provided evidence of mononuclear leukocytes in ruminal tissue. It was suggested that these cells were a normal component of the ruminal tissue, however it is unknown whether these cells were resident immune cells. Gemmell (1973) identified Langerhans cells engaged in phagocytosis in ruminal epithelial tissue. In addition to Langerhans cells, T cell profiles similar to those of the skin were also identified by Josefsen and Landsverk (1996). Leukocytes have also been found in ruminal

fluid (Trevisi et al., 2014). However, the origin of these cells is unknown; they may have migrated through the ruminal epithelium or been secreted by oral lymphoid tissue. Furthermore, since the concentration of leukocytes in this study was very low (< 5% of total events using flow cytometry analysis), their exact purpose in the lumen of the rumen remains unknown.

Despite the lack of direct evidence, it can be inferred that the immune cells of the ruminal epithelium engage in immune-surveillance and maintenance of tolerance in a manner similar to their counterparts in the cutaneous and gastrointestinal immune systems. However, due to the many unique structures and functions of the ruminal epithelium, extrapolation may not be completely appropriate. Although the epithelial cells of the gastrointestinal tract are similar in many aspects (e.g. absorption of nutrients, expression of tight junctions) the ruminal epithelium is comprised of many layers of cells, some with very different functions. The cells of the stratum basale and spinosum are the most metabolically active of REC, whereas the cells of the stratum granulosum and corneum are tasked with providing a physical barrier (Graham and Simmons, 2005). The degree to which each of these strata contribute to facilitating immune cross talk and mediating tolerance is largely unknown. Moreover, the expression profile of many molecules such as TLRs is known to differ substantially between tissue types, as well as between regions of the same system (McClure and Massari, 2014; Vaure and Liu, 2014). For example, TLR4 signaling is often associated with induction of proliferation in various cell types (Li et al., 2011). In contrast, a study by Iotzova-Weiss et al. (2017) suggested that TLR4 suppressed keratinocyte proliferation. These examples suggest that understanding the specific mechanisms involved in immunity in the rumen epithelium could elucidate the potential effects of inflammatory responses on REC function such as the metabolic consequences of inflammation, a subject that has received little attention. These insights may eventually reveal means of mitigating negative consequences of digestive disorders such as acidosis.

2.4 MODELS FOR STUDYING THE LOCAL INFLAMMATORY RESPONSE IN THE RUMINAL EPITHELIUM

2.4.1 Overview

Common scientific models utilized for studying physiology include *in vivo*, *ex vivo* and *in vitro* systems, each with advantages and disadvantages. While *in vivo* models ultimately

demonstrate the overall outcomes, such as the effects of drugs, disease or nutrition, on the animal, it can be difficult to elucidate the specific physiological functions of a tissue or type of cell. In an *ex vivo* model, whole, native tissue can be studied under more controlled experimental conditions. *In vitro* models, particularly cell culture, can provide invaluable information on the specific functions of a single type of cell. Investigations at the tissue and cell levels both allow for enhanced understanding of the contributions of specific functions to the whole-body physiology, and may indicate opportunities for further study in animal models. In this project, all three models were used to investigate the potential local inflammatory response in ruminal epithelium. This review will briefly describe the Ussing chamber and cell culture models, including their unique advantages and disadvantages.

2.4.2 The Ussing chamber model

For the study of epithelial barriers, *ex vivo* models offer a unique ability to measure the functions of multicellular tissue while maintaining a high level of control over experimental parameters. Tissue morphology and complexity is more representative of *in vivo* physiology, without the "noise" caused by systemic variables (Westerhout et al., 2015). In the 1950s, Hans Ussing developed an *ex vivo* model, aptly named the Ussing chamber model, for studying ion transport across frog skin (Clarke, 2009). Ussing chamber studies have since greatly improved the understanding of epithelial transport mechanisms (Ussing et al., 1951; Skou, 1998).

Since the original design, a number of modified systems have been developed, including inserts that support cultured cells, self-contained systems where all the components are housed within an acrylic block and a multichannel system that supports multiple chambers together (Clark, 2009; Thomson et al., 2019). All of these are based on the principles of the classic system and share several common features including: an ability to hold epithelial tissue while separating the mucosal and serosal sides, means for holding, mixing and exchanging solutions, an ability to maintain a constant temperature and oxygenate the tissue, and the means to measure the electrophysiologic properties of the tissue (Clark, 2009).

For the classical Ussing chamber system, the epithelial tissue, with the serosal layers stripped away, is mounted between two halves of a solid acrylic, cylindrical chamber, the aperture of which varies depending on the tissue type. The two sides are bathed in representative, physiological buffer, creating distinct serosal and mucosal environments. The buffer is contained

within water-jacketed, glass reservoirs. Water is circulated through the jackets in order to maintain the buffers at 37°C. Gas, usually oxygen or carbogen (5% CO_2 and 95% O_2), is bubbled at a constant, low pressure into the buffer. This oxygenates the tissue and helps to maintain a stable pH. In addition, it creates a gas lift, which mixes the buffer within the chamber.

The chambers contain two Ag/AgCl electrodes that pass a current and two calomel electrodes for voltage on each side of the chamber. The electrodes are connected by agar salt bridges. The voltage electrodes are used to measure potential difference of transepithelial resistance across the epithelium. The voltage potential is measured with a voltmeter, connected to the voltage electrodes. The current electrodes can be used to clamp the voltage potential to zero using a voltage clamp device (Clark, 2009). The total ionic current across the tissue, known as short-circuit current (Isc), is the current required to clamp the voltage potential to zero (Li et al., 2004). A brief current across the epithelium can also be applied in order to clamp to a specific, constant voltage, and this can be used to calculate the transepithelial conductance (G_t), or the transepithelial resistance (R_t), using Ohm's law. The pulse current applied causes a corresponding change in the potential difference. The Gt is calculated as Isc/voltage, and the Rt is its reciprocal (Li et al., 2004; Clark, 2009). Measuring Gt or Rt provides an indicator of the integrity of the epithelial barrier. As tissue integrity declines, tissue conductance increases. In this way viability of the tissue can be monitored during the course of an experiment (Clark, 2009). In addition, inflammation of the tissue often results in a compromised barrier, as a result of a breakdown of the tight cell junctional proteins, therefore the G_t is useful for measuring the response to pro-inflammatory stimuli (Thomson et al., 2019).

In addition to the basic electrophysiologic properties, ion or nutrient flux can also be measured using radioisotope tracers or fluorescently-labelled molecules (Etschmann et al., 2009; Clark, 2009). Radioisotopes are highly specific and sensitive, while fluorescent molecules have the advantage of increased safety when handling them (Clark, 2009). Both of these types of markers facilitate precise analysis of bidirectional flux in the absence of a concentration gradient and can allow for the evaluation of specific transport mechanisms and quantification of tissue uptake and oxidation of nutrients (Sehested et al., 1996; Sehested et al., 1999; Etschmann et al., 2009).

The Ussing chamber model has been integral in advancing the understanding of mucosal functions. It is well suited for the study of mechanisms involved in ion and nutrient absorption

and transport across epithelia. Early studies led to discoveries such as the Na^+/K^+ ATPase pump (Ussing et al., 1951; Skou, 1998) and sodium-dependent glucose transport (Clark, 2009). With respect to the rumen, several experiments with Ussing chambers have helped to elucidate flux of molecules such as ions (Gabel et al., 1991), urea (Muschler et al., 2010) and SCFA (Aschenbach et al., 2009; Penner et al., 2009). In addition to transport, Ussing chambers provide an opportunity for measuring subsequent metabolic function and have been important in improving the understanding of the extent of metabolism of nutrients, in gastrointestinal mucosal tissues. A study by Sehested et al. (1999) investigated uptake and metabolism of radio-labelled acetate, propionate and butyrate by the ruminal epithelium. The results demonstrated that SCFA are transported mainly by transepithelial mechanisms, and that a significant proportion of SCFA, especially butyrate, are metabolized to metabolites, such as ketones, or CO_2.

Through the ability to carefully control the environment within the Ussing chambers, the model allows for evaluation of the effects of different conditions on barrier function, absorption and metabolism of the epithelium (Clark, 2009; Westerhout et al., 2015). One question that has been investigated in the rumen is the effect of acidotic conditions, such as changes in pH and osmolality. Sehested et al. (1999) suggested that absorption of SCFA by the ruminal epithelium was influenced by a lower pH in the chamber buffer. A study by Emmanuel et al. (2007) attempted to simulate acidotic conditions in Ussing chambers and observed that there was an increase in epithelial paracellular permeability when ruminal mucosa was exposed to LPS at lower pH. Several additional studies have reported altered permeability of the ruminal epithelium as a result of acidification of Ussing chamber buffer (Penner et al., 2010; Wilson et al., 2012). Recent evidence has indicated that the increases in ruminal epithelial permeability are exacerbated by the combination of low pH and increased SCFA concentration (Meissner et al., 2017). The mechanism for altering the integrity of the epithelium involves a decrease in abundance or re-organization of tight junction complex proteins (Greco et al., 2018).

In addition to the effects of pH, increases in osmolality, a common characteristic of ruminal acidosis (Owens et al., 1998), have been shown to influence epithelial barrier function (Aschenbach et al., 2019). Increased osmolality in the ruminal fluid can cause cellular swelling and rupture of cells of the epithelium (Owens et al., 1998). Widening of the intercellular spaces may occur (Lodemann and Martens, 2006). Schweigel et al. (2005) and Penner et al. (2010)

demonstrated that hyperosmolality impaired barrier function in ruminal epithelium in Ussing chambers.

The effects of pH and osmolality have been implicated in facilitating translocation of ruminal microbes and microbe-associated molecular patterns (**MAMP**) across the epithelium (Kleen et al., 2003). A study by Aschenbach et al. (2000) observed permeability of the ruminal epithelium in Ussing Chambers to histamine. Moreover, LPS was found to translocate across ruminal epithelium (Emmanuel et al., 2007), although it did not appear to be pH-dependent. Translocation of microbes or MAMP is associated with a number of negative consequences, including laminitis, liver abscesses and systemic inflammation (Nocek, 1997; Khafipour et al., 2009). In addition, it has been theorized that local inflammation of the ruminal epithelium may occur (Zebeli and Metzler-Zebeli, 2012). Indeed, a recent study by Pederzolli et al. (2018) demonstrated an increase in expression of genes coding for toll-like receptor-4 in ruminal tissue collected from acidosis-challenged steers. The characterization of inflammation in the ruminal epithelium is limited, however, Ussing chambers have been useful in demonstrating impaired epithelial function in intestinal tissue in an inflammatory state (Thomson et al., 2019). Hardin et al. (2000) also suggested that the metabolism of nutrients was altered when inflammation was induced in jejunal epithelium mounted in Ussing chambers. The model may likewise be useful for evaluating an inflammatory response in ruminal epithelial tissue.

The Ussing chamber model continues to be a valuable tool for measuring uptake and transport mechanisms, flux and metabolism of nutrients and for understanding epithelial barrier functions. However, there are a few key disadvantages. The method is low throughput and labor intensive. In addition, tissue viability is limited to only a short amount of time (~a few hours). Moreover, without many of the whole body physiological functions, such as blood flow or the presence of hormones and growth factors, the tissue responses may differ significantly from *in vivo* responses (Clark, 2009; Westerhout et al., 2015). Overall, despite these limitations, the Ussing chamber method allows for careful control of experimental conditions while maintaining morphological and physiological characteristics of the epithelium.

2.4.3 The Ruminal Epithelial Cell Culture Model

The cultivation of eukaryotic cells has been deployed as a laboratory technique starting in the early 20th century and has since been an invaluable model for the study of cellular physiology

and biochemical processes, testing efficacy and toxicity of compounds and drugs, growing viruses and synthesizing biological substances (Freshney, 2010a). The conditions in which cells are grown can be carefully controlled, allowing for highly consistent data. Results are reproducible and provide information about the function of specific cells types (Freshney, 2010a). The cell culture technique suffers from several key disadvantages. Mainly, monoculture cell culture may not be representative of *in vivo* functions without the complex interactions with diverse cell types and physiological processes such as blood pressure and biochemical modulation, therefore results should be interpreted with caution. In addition, cell culture, especially with primary cells, requires time consuming validation (Freshney, 2010b). Nonetheless, cell culture is a valuable starting point and can lead to discoveries that can be explored further by deploying either *ex vivo or in vivo* methods.

The rumen as an organ of microbial fermentation was described in the 19th century by Hermann von Tappeiner (Bergman, 1990). Early studies confirmed theories that volatile fatty acids (VFA) were absorbed by the rumen into circulation (Barcroft et al., 1944). Studies by Elsden et al. (1946) and Gray et al. (1951) described the rates of production of microbial VFA. Since this early, fundamental work, the functions of the ruminal epithelium, especially with regards to absorption and metabolism of VFA, has been a central focus of study in the field of ruminant physiology. In the mid-20th-century, hundreds of scientific papers on ruminal fermentation and digestion were published. During that time, the understanding of the ruminal mucosa's function in VFA absorption and metabolism increased dramatically, but it wasn't until the 1980s that the specific role of the ruminal epithelial cell (REC) was directly studied.

The method of isolating and culturing REC was first described by Galfi et al. (1981). In this inaugural experiment, epithelial cells were isolated from bovine ruminal mucosa using a serial trypsinization method. The cells obtained were cultured for 10-12 days and the cells were confirmed to be derived from the stratum basale, spinosum and granulosum by detection of carbonic anhydrous isoenzyme. A series of experiments followed characterizing the ruminal epithelial cells under different growing conditions (Innoka et al., 1984; Galfi and Neogrady, 1989; Galfi et al., 1993). Neogrady et al. (1989a,b) discovered that when low levels of sodium butyrate were added to the cell culture media, thymidine incorporation was significantly reduced, indicating a decrease in cell proliferation. Although this is contradictory to effects of butyrate on cell proliferation *in vivo*, similar responses have been noted in other types of cells in culture

(Ginsburg et al., 1973; Sakata, 2019) and may be due to a lack of mediation by hormones or growth factors, such as insulin and insulin-like growth factors (Baldwin et al., 1999). The effect demonstrates a potential pitfall in the cell culture model of mucosal epithelial cells.

Work by Baldwin and Jesse (1991) demonstrated that isolated cells, in a single cell suspension, also known as a suspension culture, were metabolically active and capable of producing BHBA when incubated with sodium butyrate and sodium propionate. Furthermore, a study by Baldwin and Jesse (1992) described the metabolism of butyrate and glucose to BHBA of the developing rumen, showing that ruminal epithelial cells could adapt to utilizing either butyrate or glucose as energy substrates. Subsequent studies suggested that isolated REC were capable of producing not only BHBA but also acetoacetate, lactate and pyruvate following incubations with SCFA (Klotz et al., 2001; Waldron et al., 2002). These studies, however, used REC in a single cell suspension, immediately following trypsinization and therefore do not accurately represent cell metabolism in a culture system.

However, other early studies have provided validation for the use of ruminal epithelial cells through characterizing their functions. Such experiments have shown that primary REC in culture were capable of Na^+/H^+ exchange by studying the rate of amiloride-sensitive Na^+ uptake (Gabel et al., 1996), which was found to be dependent on the amount of non-keratinized cells (Galfi et al., 2002). A study by Muller et al., 2002 not only identified monocarboxylate transporter 1 (MCT1) both in whole ruminal epithelium and isolated, cultured REC, but also demonstrated, through the use of monocarboxylate inhibitors, that REC retained the ability to transport ketone bodies and thus regulate intracellular pH.

The use of isolated REC in culture has had a significant impact on the understanding of the local, cellular mechanisms of the ruminal mucosa. In cells grown in culture, propionate and butyrate decreased DNA synthesis, while insulin and glucagon promoted an increase in DNA synthesis, suggesting a role of hormones in the regulation of cell proliferation (Neogrady et al., 1989; Baldwin et al., 1999). These studies have improved the understanding of the mechanisms involved in ruminal mucosal adaptation (Galfi et al., 1991, Penner et al., 2011). Additionally, intensive patch-clamp experiments have also helped to elucidate the mechanisms involved in transcellular absorption in isolated REC (Stumpff et al., 2009). Stumpff et al. (2011) characterized the localization of the tight junction proteins in both native tissue and polarized

ruminal epithelial cells grown in culture on transwells. The results strongly indicated the ability of cultured ruminal epithelial cells to form a mucosal barrier.

The foundational work has provided a functional model for studying the mechanisms involved in the local, cellular physiology in the rumen mucosa. However, there are many areas and questions yet to be explored using this model. For example, the ruminal epithelial model may be useful in elucidating the effects of compounds, such as non-steroidal anti-inflammatories or other medications, or feed additives on cell metabolism. Some aspects of cellular transport have yet to be fully described (Aschenbach et al., 2011); further development and refinement of the transwell system may allow for a more complete picture and a better understanding of the complex mucosal barrier function.

Another area for further study is with the interactions between the lumen-derived molecules and the ruminal epithelium. Due to diets containing highly fermentable carbohydrates that are fed to high producing dairy cows and finishing feedlot cattle (Penner et al., 2009), acidotic conditions in the rumen can occur, characterized by a decrease in ruminal fluid pH, an increase in osmolality and an increase in free lipopolysaccharide (LPS) (Plaizier et al., 2018). As a consequence of these conditions, loss of barrier function of the ruminal epithelium can occur leading to an increase in permeability and translocation of MAMPs. A plethora of work has suggested that translocation of rumen-derived MAMPs may lead to liver abscesses and a systemic inflammatory response, characterized by increased circulating acute phase proteins (APP) and cytokines (Nagaraja and Chengappa, 1998; Khafipour et al., 2009). These MAMPs may also interact with ruminal epithelial cells and promote a local inflammatory response. Little evidence, however, shows a direct ability of ruminal epithelial cells to initiate this response. Therefore, a focus of the current study was to use the cell culture model to investigate the potential, pro-inflammatory response to MAMPs in the REC, and to elucidate the consequences of inflammation on cellular function and metabolism.

2.5 OVERALL HYPOTHESIS

The overall hypothesis is that ruminal epithelial cells will initiate a pro-inflammatory response to MAMPs, and this response will alter cell metabolism by increasing nutrient uptake and energy substrate utilization.

2.6 OVERALL OBJECTIVE

The objective of this thesis research was to investigate the potential, local pro-inflammatory response in the ruminal epithelium using *in vivo*, *ex vivo* and cell culture models and to determine whether ruminal epithelial cell function and metabolism are influenced by a pro-inflammatory response.

CHAPTER 3: POTENTIAL FOR A LOCALIZED IMMUNE RESPONSE IN THE RUMINAL EPITHELIUM IN BEEF HEIFERS FOLLOWING A SHORT-TERM SUBACUTE RUMINAL ACIDOSIS CHALLENGE

The manuscript "Potential for a localized immune response in the ruminal epithelium in beef heifers following a short-term subacute ruminal acidosis challenge" (Chapter 3) was an in vivo experiment designed to investigate whole tissue responses to a ruminal acidosis challenge. The results revealed novel insight into the expression of molecules relating to local inflammation in the ruminal epithelium, contributing a broader perspective to my thesis.

Original contribution: The in vivo experiment was design by me and my supervisor together. I was responsible for the majority of animal care and sample collection. With the exception of the LPS quantification assay, all sample analysis was conduction by me. Co-authors assisted with imaging techniques and advised me on RNA extraction and real time qPCR analysis. Data analysis was conducted by me. Interpretation of the results was also performed by me, with help from my co-authors and my supervisor. I was responsible for the majority of the writing of the manuscript.

Abstract: The aim of this study was to investigate whether the ruminal epithelium activates a local inflammatory response following a short-term subacute ruminal acidosis challenge. Seven ruminally-cannulated, non-pregnant, non-lactating beef heifers, fed a baseline total mixed ration (**TMR**) with 50:50 forage:concentrate ratio, were used in a crossover design with two periods and two treatments: subacute ruminal acidosis (**SARA**) and control (**CON**). SARA induction was comprised of feed restriction (animals received 25% of DMI for 24 h) followed by a grain overload (30% of baseline DMI), and provision of the full TMR; whereas, the CON received the TMR ad libitum. Ruminal pH was recorded using indwelling probes and ruminal LPS concentration was measured daily for 6 d following the challenge. Ruminal papillae biopsies from the ventral sac were collected on d 2 and 6 following the grain overload and were used for RNA extraction and immunohistofluorescence. Transcript abundance of genes associated with acute inflammation was measured by quantitative real-time PCR, normalized to the geometric mean of three stable

A version of this chapter has been previously published. Kent-Dennis, C., Pasternak, A., Plaizier, J.C., and Penner, G.B. 2019. Potential for a localized immune response by the ruminal epithelium in nonpregnant heifers following a short-term subactute ruminal acidosis challenge. Journal of Dairy Science. 102:7556-7569. doi.org/10.3168/jds.2019-16294.

housekeeping genes. Target genes included toll-like receptor-2 (*TLR2*), *TLR4, TLR9*, tumor necrosis factor-alpha (*TNF*), prostaglandin endoperoxide synthase-1 (*PTGS1*), *PTGS2* transforming growth factor beta-1 *(TGFB1),* and four intermediate enzymes of leukotriene synthesis (*ALOX5, ALOX5AP, LTA4H* and *LTC4S*). Protein localization and expression of TLR4 was quantified by image analysis of fluorescence intensity. Statistical analysis was performed using MIXED PROC of SAS 9.4 as a crossover design with treatment, day, and period as fixed effects. Ruminal pH was below 5.6 for 4.5 h/d and below 5.8 for 6.9 h/d in the SARA group compared to 22 and 72 min, respectively, in CON. Ruminal LPS concentration peaked on d 2 in SARA heifers at 51,481 EU/mL compared to 13,331 EU/mL in CON. Following grain overload, small but statistically significant decreases in the transcriptional abundance of *TLR2, TLR4, TNF, PTGS2, ALOX5* and *ALOX5AP* were observed in SARA versus CON heifers. A functionally relevant decrease in *TLR4* expression was confirmed by a decrease in fluorescence intensity of the corresponding protein following immunohistofluorescent staining of papillae collected from SARA heifers compared to CON. Results from this study indicate a suppression of the inflammatory response in the ruminal epithelium and suggest that it is tightly regulated, allowing for tissue recovery and maintenance of homeostasis following subacute ruminal acidosis.

3.1 INTRODUCTION

Diets for dairy and feedlot cattle often consist of a large proportion of highly fermentable carbohydrates to meet the animal's energy requirements for supporting high milk yields (Penner et al., 2009) and rates of gain (Loerch, 1990). Rapid transition to these diets can cause decreased ruminal pH, increased osmolality of rumen fluid, alters the microbial population in the rumen (Owens et al., 1998), and can lead to digestive disorders such as subacute ruminal acidosis (**SARA**) (Bevans et al., 2005; Plaizier et al., 2008). Exposure to SARA may also reduce DMI, milk yield and milk fat content, and has been implicated as a causative factor in the onset of laminitis and liver abscesses (Plaizier et al., 2008; Wiese et al., 2017). Thus, SARA in cattle has important economic implications (Stone, 2004). Studies examining the effects of SARA on the host have demonstrated increased permeability of the ruminal epithelium when exposed to low pH (Aschenbach and Gabel, 2000; Penner et al., 2010) that could increase the risk for translocation of microbe-associated molecular patterns (**MAMP**), or the microbes themselves, across the epithelium, inducing a systemic acute phase protein response (Gozho et al., 2005; Khafipour et al., 2009; Humer et al., 2017).

Moreover, a local inflammatory response by ruminal epithelium has been hypothesized (Humer et al., 2017) to occur as a consequence of exposure to MAMPs such as lipopolysaccharide (**LPS**). The limited support for this hypothesis comes primarily in the form of studies reporting the expression of genes associated with antigen recognition (Malmuthuge et al., 2012) and inflammation (Zhang et al., 2016). These studies demonstrated an upregulation of immune-associated genes in whole ruminal papillae from cows fed a high-concentrate diet, thereby suggesting a local inflammatory response. However, due to the use of whole ruminal tissue, it is likely that other cell types, such as tissue resident leukocytes could be confounding the results. As such, there is a lack of evidence supporting a direct role of the ruminal epithelium in initiating a local inflammatory response. The objective of the current study was to investigate gene expression and protein localization associated with an inflammatory response in the ruminal epithelium following a moderate, one-day subacute ruminal acidosis challenge.

3.2 MATERIALS AND METHODS

All experimental procedures involving the use of heifers were approved by the University of Saskatchewan Animal Research Ethics Board (protocol no. 20100021), and were conducted in accordance with guidelines set forth by the Canadian Council of Animal Care (Ottawa, ON, Canada).

3.2.1 Experimental Design

Seven crossbred, non-pregnant beef heifers, selected based on availability, previously fitted with ruminal cannulas were used in a crossover design study. The heifers had an average body weight of 720 kg ± 67 SD. The study design included 2 treatments and 2 periods lasting 8 d each with a 28-d recovery phase between the 2 periods. The heifers were housed in individual tie-stalls with rubber mats on the floor and chopped straw was used for bedding. Feed mangers were completely separated by concrete dividers to facilitate measurement of individual intakes, and water was offered free-choice. For 14 d prior to the experiment, at 0900 h, heifers were fed a total mixed ration (31.7% barley silage, 17.6% alfalfa hay, and 23.4% barley grain, 1.8 % canola meal, 24.2% U of S pellet (45.2% ground barley grain, 17.3% ground corn grain, 7.5% pea grain, 7.5% canola meal, 8.3% soybean meal, 2% corn gluten meal, 3.3% corn distillers medium spirits, 2.7% premix, 1.5% EB100, 1.2% molasses, 0.08% biotin, 0.5% R-choline, 0.04% niacin, 0.2% PotMagSulfate, 1.1% sodium bicarbonate, 1.2% limestone, 0.02% Santoquin, 0.5% salt), 0.8% Jeffo RP10, 0.2% limestone, 0.2% Sodium bicarbonate and 0.2% Metasmart, on a DM basis), ad libitum, to allow for environmental and dietary adaptation. Subsequently, heifers were randomly assigned to 1 of 2 treatment sequences. The treatments consisted of either a control (CON) or a subacute ruminal acidosis induction treatment (SARA). Subacute ruminal acidosis was induced for the SARA group by restricting feed to 25% of DMI for 24 h followed by a grain overload (30% of DMI with pelleted barley; adapted from Dohme et al., 2008 and Schwaiger et al., 2013a). The full allocation of each heifer's TMR was provided 2 h after the grain overload. The CON heifers received the TMR ad libitum.

3.2.2 Data and Sample Collection

3.2.2.1 Dry matter intake and ruminal pH. The amount of feed offered and feed refused were recorded throughout the study. Dry matter intake was estimated based on the DM of the

TMR offered and refused. While DMI was determined daily, DMI data from d 0 to d 6, relative to the grain overload, were used for data analysis.

Ruminal pH was measured for 6 consecutive days starting on the day of the grain challenge using an indwelling pH measurement system (Dascor, Escondido, CA, USA; Penner et al., 2006). Before and after placement, the pH systems were standardized in pH buffers 7.0 and 4.0 at 39°C. Placement of the pH systems in the ventral sac of the rumen was maintained using two, 900-g weights attached to a shroud around the electrode to ensure the electrode remained in the ventral sac of the rumen (Penner et al., 2006). The systems were removed and data were downloaded on d 6 after the grain overload. The data were converted from mV to pH using the linear relationship established with the pre- and post-standardization readings and a linear drift over time was assumed. Maximum, mean, and minimum pH, as well as the duration (min) and area (min × pH) that pH was < 5.8 and < 5.6, were calculated for each 24-h interval for d 0 to d 5 relative to the grain overload. As ruminal digesta were removed to facilitate collection of ruminal biopsies, ruminal pH data from the start of the digesta evacuation procedure and that occurring until 1 h following reintroduction of the digesta were removed from the data set.

3.2.2.2 Ruminal Fluid Collection and Preparation. Ruminal fluid samples were collected at 1300 h on the day of the ruminal acidosis induction (day 0 of each sampling period) and on d 1 to 6. Equal volumes of mixed digesta (250 mL) were collected from 3 locations in the rumen (cranial, central-ventral and caudal sacs). Digesta was pooled and then strained through 2 layers of cheesecloth. The resulting ruminal fluid was mixed well, collected in conical centrifuge tubes (Corning Inc, Corning, NY, USA). Ruminal fluid was immediately placed on ice and used for free LPS analysis as described by Khafipour et al. (2009). Briefly, the ruminal fluid samples were centrifuged at 10,000 × *g* for 45 min at 4°C and subsequently filtered through a 0.2 µm sterile syringe filters (Thermo Fisher Scientific, Waltham, MA, USA) into sterile pyrogen-free glass vials with screw caps (Thermo Fisher Scientific). Filtered samples were heated to 100°C for 30 min. After cooling for 10 min, samples were transferred into pyrogen-free 2-mL microcentrifuge tubes (Thermo Fisher Scientific) and stored at -20°C until analyzed for LPS concentration.

3.2.2.3 Rumen Papillae Biopsies. Timing of the first papillae biopsy (d 2 following the ruminal acidosis induction) was based on previous work (Gozho et al., 2005) that showed elevated ruminal LPS, corresponding to ruminal pH below 5.6 on d 2 following the addition of

barley pellets to induce SARA and that SCFA absorption was reduced on d 2 following a similar acidosis induction model (Schwaiger et al., 2013a,b). A second biopsy was collected on d 6 following the SARA induction to investigate whether an effect on gene expression would be detectable in the longer term.

On d 2 and 6 of each sample collection period, ruminal contents from each heifer were partially evacuated through the ruminal cannula and the contents were placed in a clean insulated plastic container in order to access ruminal papillae from the ventral sac. The ventral sac (ventral to the left longitudinal pillar) was partially externalized and approximately 30 papillae were excised using sterile surgical scissors and forceps. Ruminal papillae were immediately rinsed in ice-cold PBS and snap-frozen in liquid nitrogen. Frozen samples were stored at -80°C until analysis. In addition, approximately 5 papillae were placed in embedding cassettes and were fixed in 10% formalin (10% formaldehyde, v/v, in neutral phosphate buffer; Thermo Fisher Scientific).

3.2.3 Sample Analyses

3.2.3.1 Free Ruminal LPS. Ruminal fluid samples were analyzed for ruminal LPS concentration (EU/mL) using a *Limulus* amebocyte lysate assay, relative to a known reference endotoxin (Gozho et al., 2005).

3.2.3.2 RNA Isolation, Primer design and qRT-PCR. Frozen ruminal papillae were ground under liquid nitrogen using a mortar and pestle and total RNA was isolated from approximately 100 mg of ground tissue using a phenol-chloroform extraction and double precipitation to remove contaminants (modified TRIzol protocol, Thermo Fisher Scientific). The RNA was treated with DNase (TURBO DNA-free Kit; Thermo Fisher Scientific) and the quantity of RNA determined using a NanoDrop spectrophotometer ND-1000 (Thermo Fisher Scientific). The RNA integrity was subsequently assessed on a 1.2% (w/v) denaturing agarose gel, where all samples were confirmed to have clear 28S and 18S ribosomal RNA banding patterns. Reverse transcription was carried out with the High Capacity cDNA Reverse Transcription Kit (Thermo Fisher Scientific) following manufacturer's instructions. The resulting cDNA was diluted with nuclease-free water to a final concentration of 10 ng/µl.

Target, immune-related genes were selected based on the hypothesized effects of high LPS concentrations in the rumen. Primers for prostaglandin-endoperoxidase synthase 1 and 2 (*PTGS1*

& PTGS2, arachidonate 5-lipoxygenase (*ALOX5*), arachidonate 5-lipoxygenase-activating protein (*ALOX5AP*), leukotriene A4 hydrolase (*LTA4H*), leukotriene C4 synthase (*LTC4S*), tumor necrosis factor-alpha (*TNF*), Toll-like receptor-2 (*TLR2*), *TLR4*, *TLR9*, transforming growth factor beta-1 (*TGFB1*) and three housekeeping genes (*ACTB*, *GAPDH*, and *HPRT*) were designed using Primer3 software (Untergasser et al., 2007) based on refseq sequence data from National Center for Biotechnology Information (**NCBI**; Bethesda, MD, USA). When possible, primers were designed to span exon-exon junctions as identified by BLAT search against UMD 3.1 and BLAST used to verify target specificity. Primer efficiencies were verified for each primer set using a serial dilution of pooled samples (primer information is presented in Table 3.1). Quantitative real-time polymerase chain reaction (qRT-PCR) was performed using 20 ng of cDNA and was run in duplicate using SsoFast EvaGreen Supermix (Bio-Rad, Hercules, CA, USA) as per manufacturer's instructions in the CFX96 Touch Real-Time PCR Detection System (Bio-Rad). The stability of housekeeping gene expression over treatment and day was verified, and the geometric mean of all three was subsequently used to normalize expression of all genes of interest. Expression data is presented as $2^{-\Delta\Delta Ct}$ form, with treatment held relative to the lowest average biopsy day group.

3.2.3.3 Immunohistofluorescence. In order to analyze slides simultaneously, a subset of samples from the d 2 biopsy were randomly selected for quantification of TLR4 expression in SARA (n=3) and CON (n=4) heifers. This approach, while reducing the number of experimental units, allowed for the control of technical variation in the staining procedure while still enabling the detection of large differences. All slides were processed and imaged concurrently to ensure the same conditions (e.g. incubation times, light exposure).

Tissue processing was performed at Prairie Diagnostic Services (Saskatoon, SK). In brief, tissue was dehydrated in increasing concentrations of ethanol and finally washed in xylene. Subsequently, tissue was embedded in paraffin and 4-µm sections were cut onto glass slides. Four-micron tissue sections were baked at 60°C for 20 min, deparaffinised in xylene (Sigma-Aldrich, St. Louis, Mo, USA), and rehydrated with distilled water using decreasing concentrations of ethanol. Samples were subjected to heat-induced antigen retrieval for 30 min at 90°C in Tris-EDTA buffer (10 m*M* Tris, 1 m*M* EDTA, 0.05% Tween 20, pH 9.0; Sigma-Aldrich).

Table 3.1 Primer used for quantitative real-time PCR

Gene name (official gene symbol)	Source[1]	Sequence (5'-3')	Amplicon size (bp)	Efficiency (%)[2]
Arachidonate 5-lipoxygenase (ALOX5)	NM_001192792.1	F: ACCTGTTCATCAACCGCTTC	108	95
		R: TGACCCGCTCAGAAATAGTGT		
Arachidonate 5-lipoxygenase activating protein (ALOX5AP)	NM_001076293.2	F: GTCCAGAATGGGTTCTTTGC	134	114
		R: GGGTAGGCATCCACACAGTT		
Beta actin (ACTB)	NM_173979.3	F: GAGCTACGAGCTTCCTGACGGGC	109	95
		R: AATGCCGCAGGATTCCATGCCCAG		
Glyceraldehyde-3-phosphate dehydrogenase (GAPDH)	NM_001034034.2	F: GGGTCATCATCTCTGCACCT	101	91
		R: GGAGGCATTGCTGACAATCT		
Hypoxanthine phosphoribosyltransferase 1 (HPRT1)	NM_001034035.2	F: AGGTTGCGAGCTTGCTGAT	103	99
		R: AGGGCATATCCCACAACAAA		
Leukotriene A4 hydrolase (LTA4H)	NM_001034280.1	F: GTCAGTGCCAGGCTATCCAC	97	92
		R: TCTTTGGGGACAGACACCTC		
Leukotriene C4 synthase (LTC4S)	NM_001046098.2	F: TCTACCGAGCCCAAGTGAA	148	93
		R: GCGTAGCCCTGGAAGTAGC		
Prostaglandin-endoperoxidase synthase-1 (PTGS1)	NM_001105323.1	F: CCAAAGGGAAGAAGCAGTTG	114	91
		R: GGGCAAAGAAGGCAAACAT		
Prostaglandin-endoperoxidase synthase-2 (PTGS2)	NM_174445.2	F: GGTGTGAAAGGGAGGAAAGA	117	93
		R: GGCAAAGAATGCAAACATCA		
Transforming growth factor beta-1 (TGFB1)	NM_001166068.1	F: ACTGCTTCAGCTCCACAGAA	148	93
		R: TCCAGGCTCCAGATGTAAGG		
Toll-like receptor-2 (TLR2)	XM_015475330.1	F: TGATGCTGCCATTCTGATTC	107	95
		R: GCCACTCCAGGTAGGTCTTG		
Toll-like receptor-4 (TLR4)	NM_174198.6	F: CCTTGCGTACAGGTTGTTCC	104	90
		R: CTCAGGTCCAGCATCTTGGT		
Toll-like receptor-9 (TLR9)	NM_183081.1	F: CACCAAGACCACCATCTTCA	132	108
		R: TTCTCCAGGGACACCAGACT		
Tumor necrosis factor alpha (TNF)	NM_173966.3	F: CAAGTAACAAGCCGGTAGCC	153	98
		R: AGATGAGGTAAAGCCCGTCA		

[1]National Center for Biotechnology Information (NCBI)

[2]Efficiency= $-1 + 10^{(-1/\text{slope})}$X100

Slides were blocked with fetal bovine serum (Thermo Fisher Scientific) for 2 h at room temperature, followed by incubation with the primary antibody (rabbit anti-TLR4, 1 mg/mL; Thermo Fisher Scientific) in a 1:250 dilution in incubation buffer (1% BSA, 1% horse serum, 0.3% Triton X-100, 0.01% sodium azide in PBS; Sigma-Aldrich) overnight at 4°C. Isotype control slides were previously used to verify absence of non-specific binding. The isotype control antibody matched the primary antibody in species and concentration. Slides were washed 3 times in tris-buffered saline (20 m*M* Tris, 150 m*M* NaCl, 0.1% Tween 20; Sigma-Aldrich), incubated with the secondary antibody at a 1:500 dilution (anti-rabbit Al555, 2 mg/mL; Abcam, Cambridge, UK) for 2 h at room temperature, washed again, and counterstained with 4',6-diamidino-2-phenylindole (**DAPI**) in methanol (Thermo Fisher Scientific). Slides were washed

again and then cover slipped with mowiol mounting medium (Sigma-Aldrich). Slides were imaged at 63x magnification using an Axiovert 200M fluorescent microscope (Zeiss, Oberkochen, Germany).

To quantify TLR4, images were analyzed using ImageJ (1.49v, NIH). Images were captured from the base, middle and tip of each papillae from two to three papillae per heifer for use in measuring tissue fluorescence associated with TLR4 and DAPI. Separate measurements were acquired for the stratum basale (**SB**), stratum spinosum and stratum granulosum combined (**SS/SG**), and the stratum corneum (**SC**) based on the morphology described by (Graham and Simmons, 2005). The procedure for measuring fluorescence intensity was adapted from McCloy et al. (2014). Mean fluorescence intensity was measured within pre-drawn regions of interest (**ROI**; selections in which the measurements are recorded) for TLR4 and DAPI as separate images (i.e. split channels). For every image, two ROI without fluorescence, adjacent to the tissue, were measured as background readings. The corrected total cellular fluorescence (**CTCF**) = integrated density – (area of ROI × mean fluorescence of the background readings) was calculated. In addition to quantifying total fluorescence of TLR4 and DAPI, the number of nuclei within each ROI was recorded manually (in DAPI images only). Data are presented as number of nuclei per mm^2.

3.2.4 Statistical Analysis

Statistical analysis was performed using the MIXED procedure of SAS 9.4 (SAS Inst., Inc). Treatment, day of biopsy, and the treatment × day of biopsy interaction were considered fixed effects, and day of biopsy within period was considered a repeated measure. No effects of period were observed and the variable and associated interactions were subsequently removed from the model. For DMI and pH, day was considered a repeated measure. Fluorescence intensity of TLR4 was analyzed with treatment and cell layer as fixed effects. Ruminal LPS concentrations were not normally distributed and were therefore log transformed. Statistical analysis was performed on the transformed data; however, the means and SEM are presented as EU/mL. Effects were considered significant when $P < 0.05$ and were considered trends when $P < 0.10$.

3.3 RESULTS

Dry matter intake (Table 3.2) did not differ between treatments and there were no treatment × day interactions on DMI. However, there was a tendency for DMI to be less for SARA versus CON (13.1 vs. 14.2 ± 0.36 kg/d; $P = 0.06$). Mean and minimum ruminal pH were 0.3 pH units less for SARA than CON. The SARA heifers had an average duration of 414 minutes below pH 5.8 and 273 minutes below pH 5.6 throughout the 6 d of measurement, whereas, the duration for CON was below 5.8 and 5.6 for an average of 72 and 22 min/d, respectively.

There was a treatment × day interaction ($P < 0.01$) for ruminal LPS concentration (Figure 3.1). The concentration (EU/mL) was greater in the SARA group compared to CON on d 1, 2, and d 3 following the induction of subacute ruminal acidosis. No treatment effects were detected on day 0, 4, 5, or 6.

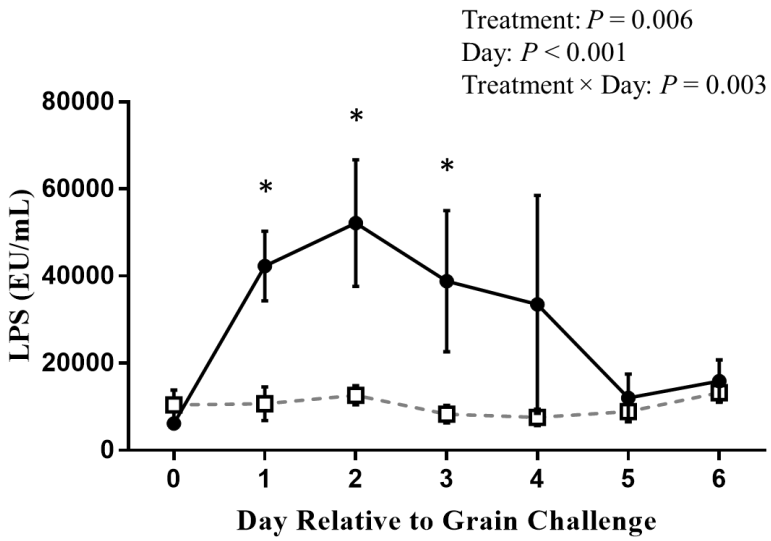

Figure 3.1 Daily mean concentration (EU/mL) of ruminal LPS in subacute ruminal acidosis-induced heifers (SARA, circles) or Control heifers (CON, squares) relative to the day of a grain overload. Statistical analysis was performed on log-transformed data. The asterisk indicates means that differ within a day, $P < 0.05$.

Table 3.2 Dry matter intake and ruminal pH characteristics in subacute acidosis-induced heifers (SARA) or Control (CON).

	Treatment			Day relative to grain over-load							*P* value		
Item	CON	SARA	SEM	0	1	2	3	4	5	SEM	T	D	T × D
DMI (kg/d)	14.2	13.1	0.36	13.3	12.6	13.9	13.7	14.2	14.2	0.63	0.056	0.45	0.27
Minimum pH	6.2[a]	5.9[b]	0.08	5.8	6.0	6.1	6.1	6.0	6.0	0.14	0.021	0.54	0.17
Mean pH	6.6[a]	6.3[b]	0.07	6.3	6.5	6.6	6.6	6.4	6.4	0.13	0.006	0.66	0.61
Maximum pH	7.1[a]	6.7[b]	0.09	7.1	6.9	6.9	6.9	6.8	6.8	0.15	0.013	0.87	0.65
Ruminal pH < 5.8													
Duraton min/d	72[b]	414[a]	69	273	238	208	209	253	275	119	0.005	0.99	0.95
Area, (min × pH)/d	10[b]	143[a]	29	123	64	77	73	66	57	50	0.008	0.95	0.91
Ruminal pH < 5.6													
Duration, min/d	22[b]	273[a]	54	175	137	159	139	139	135	93	0.007	0.99	0.99
Area, (min × pH)/d	1.6[b]	72[a]	20	77	21	40	37	27	18	34	0.028	0.84	0.84

LSmeans for treatments with different letter superscripts within a row were different ($P < 0.05$).
LSmeans for days with different letter superscripts within a row were different ($P < 0.05$).
T = treatment, D = day relative to grain over-load.

A treatment × time interaction affected the expression of *TLR2* (Figure 3.2A) as that abundance was less for SARA on d 2 and d 6 compared to CON with a greater difference on d 2. Transcript abundance of *TLR4* and *TNF* (Figures 3.2B and 3.2D) was less in SARA than CON heifers. We observed no difference in the expression of *TLR9* (Figure 3.2C) and no differences in expression if *TGFB1* (Figure 3.2E).

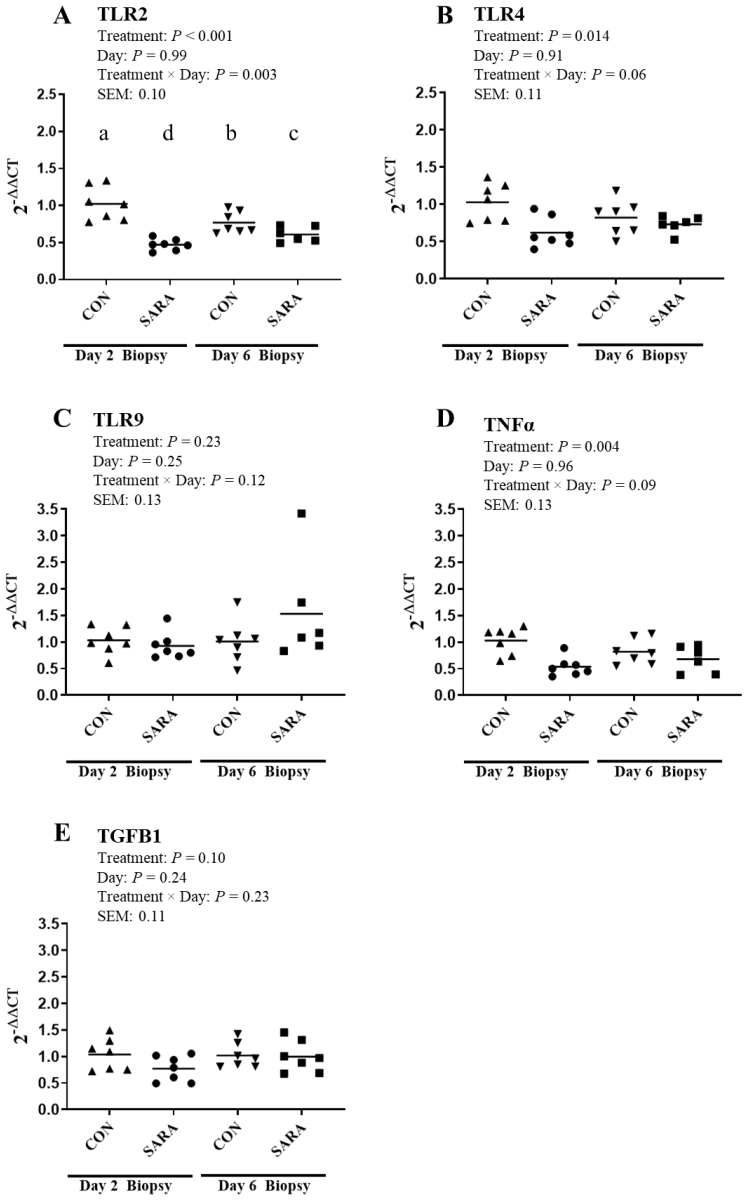

Figure 3.2 Expression of toll-like receptor-2 (TLR2; A), toll-like receptor-4 (TLR4; B), toll-like receptor-9 (TLR9; C), tumor necrosis factor (TNFα; D) and transforming growth factor beta-1 (TGFB1; E) in RNA extracted from ruminal papillae. Means are compared to the treatment group within biopsy day, analyzed using qRT-PCR. Values are expressed as means of fold-change held relative to the baseline measurement, which was the lowest average expression. Means with uncommon letters differ ($P < 0.05$).

Although we observed no difference in expression of *PTGS1* (Figure 3.3A), for *PTGS2* (Figure 3.3B), the expression was less for SARA than CON on d 2 but gene expression was similar at the day 6 biopsy. Transcriptional abundance of *ALOX5*, and *ALOX5AP* (Figures 3.4A and 3.4B) was less in SARA than CON heifers, however no effects were observed for *LTA4H* or *LTC4S* (Figures 3.4C and 3.4D).

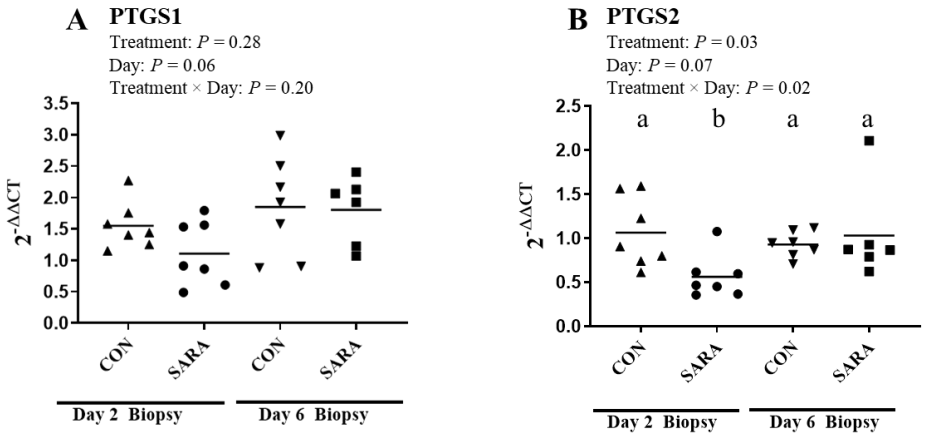

Figure 3.3 Expression of prostaglandin-endoperoxidase synthase-1 and -2 (PTGS1 and PTGS2; A and B, respectively) in RNA extracted from rumen papillae comparing treatment group within biopsy day and analyzed using qRT-PCR. Values are expressed as means of fold-change held relative to the baseline measurement, which was the lowest average expression. Means with different letters differ ($P < 0.05$).

Ruminal epithelial staining for TLR4 was observed in the cytosol and the fluorescence intensity appeared, visually, to be greatest in the cell layers closest to the basal membrane, visibly decreasing in the SC (Figures 3.5A and 3.5B). The CTCF of TLR4 was less in SARA heifers compared with the CON group (Figure 3.6A). In addition, the CTCF of DAPI was also less in SARA versus CON heifers (Figure 3.6B) within the SB. The CTCF of DAPI was affected by a treatment × cell layer interaction ($P = 0.036$). There were fewer nuclei (Figure 3.6C) in SARA vs. CON (94 versus 103 nuclei/mm^2; $P = 0.021$). No treatment differences were observed in the SS/SG or SC. As cells moved from the SB layers towards the lumen, the average number of nuclei decreased from the SB to SS/SG (183 to 84 nuclei/mm^2; $P < 0.001$) and from SS/SG to SC (84 to 28 nuclei/mm^2; $P < 0.001$).

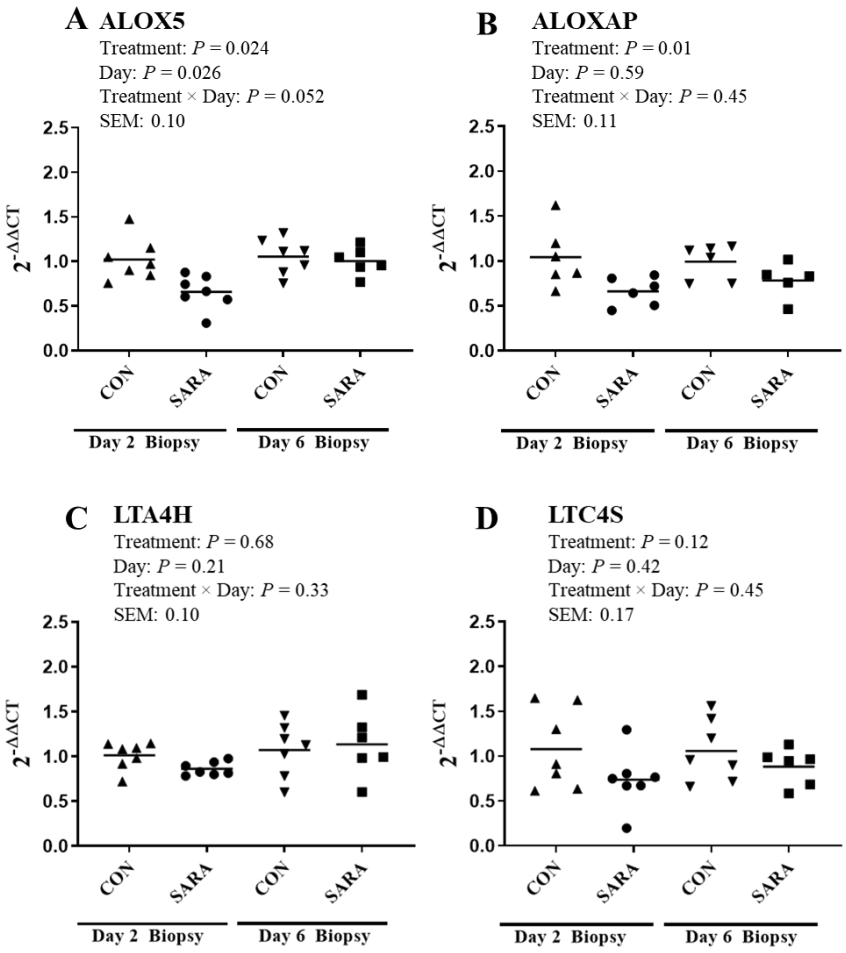

Figure 3.4 Expression of four target genes, arachidonate 5-lipoxygenase (ALOX5; A), arachidonate 5-lipoxygenase-activating protein (ALOX5AP; B), leukotriene A4 hydrolase (LTA4H; C), leukotriene C4 synthase (LTC4S; D), critical genes in the synthesis of leukotrienes from arachidonic acid, in RNA extracted from ruminal papillae comparing treatment group within biopsy day, analyzed using qRT-PCR. Values are expressed as means of fold-change held relative to the baseline measurement, which was the lowest average expression.

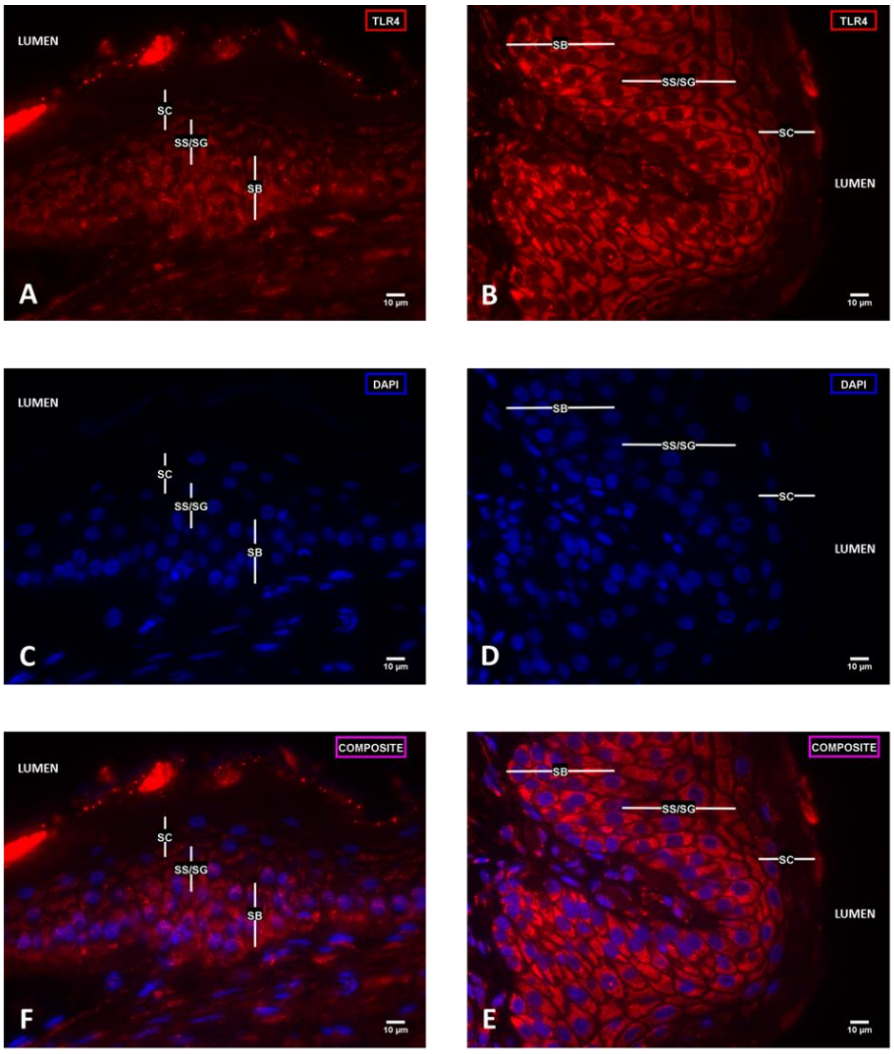

Figure 3.5 Staining for ruminal TLR4 (red) and DAPI (blue) in subacute ruminal acidosis-induced heifers (SARA; A C, and F) or Controls (CON; B,D, and E) from the d-2 biopsy. A composite of both stainings is shown in E and F. White lines indicate the stratified epithelial cell layers: stratum basale (SB), combined stratum spinosum and granulosum (SS/SG) and stratum corneum (SC). Images are representative.

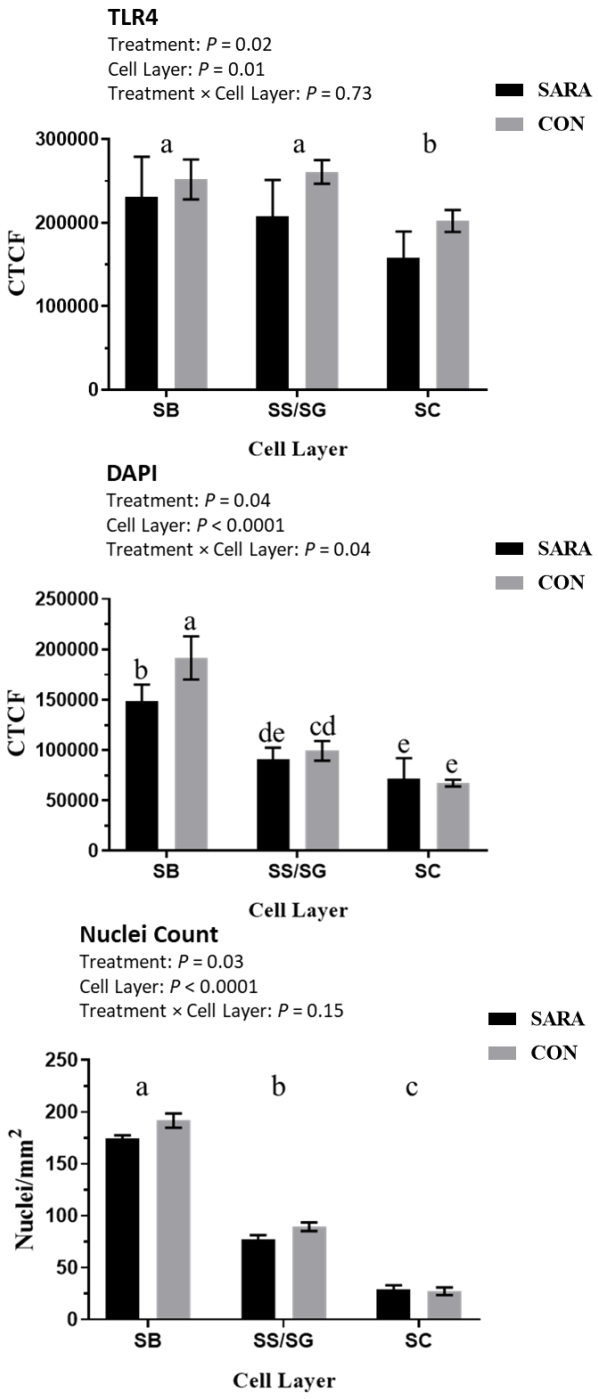

Figure 3.6 Corrected total cellular fluorescence (CTCF) of TLR4 (A) and DAPI (B) in subacute ruminal acidosis-induced (SARA) heifers or controls (CON) within cell layers: stratum basale (SB), combined stratum spinosum and granulosum (SS/SG) and stratum corneum (SC). Mean nuclei count (nuclei/mm2) is shown in C. Means with uncommon letters differ for layer, treatment effect is denoted with P-value only ($P < 0.05$).

3.4 DISCUSSION

The aim of this experiment was to examine the local inflammatory response in the ruminal epithelium following a short-term SARA challenge. Subacute ruminal acidosis has previously been defined as pH falling below a threshold ranging from 5.2 to 5.8 for an extended period of time (Cooper et al., 1999; Kleen et al., 2003; AlZahal et al., 2007; Penner et al., 2007). Deleterious effects of SARA, such as the induction of a systemic immune response (Humer et al., 2017), are often observed with a ruminal pH < 5.6 for at least 3 h/d (Plaizier et al., 2008; Khafipour et al., 2009). In the current study, ruminal pH was below 5.8 and 5.6 for a mean duration of nearly 7 and 5 h/d, respectively, following induction of acidosis. However, only a small decline in mean ruminal pH was observed, therefore induction of moderate SARA was considered successful.

In addition to low ruminal pH, elevated ruminal LPS is thought to play an important role in pro-inflammatory effects in the ruminal epithelium as a consequence of increased permeability and translocation of ruminal antigens (Khafipour et al., 2009; Dong et al., 2011). Following induction of SARA, the increase in LPS concentration is highly variable. In lactating dairy cows, peak levels of LPS were reported at 151,985 EU/mL compared to 29,492 EU/mL in controls (Khafipour et al., 2009). In jersey steers, ruminal LPS concentration increased from 3,715 EU/mL to a peak of 12,589 EU/mL following induction for SARA (Gozho et al., 2005). In addition, caution must be observed when comparing absolute LPS concentrations in different studies, as the LAL assay used to measure LPS is highly sensitive to sampling and assay conditions (Chen and Mozier, 2013). Despite the variability, an increase from baseline in LPS concentrations in ruminal fluid indicates a disruption of the ruminal environment. Consistent with the previous reports, the present study observed that ruminal LPS concentrations increased following SARA induction and peaked at 51,481 EU/mL, compared to average baseline concentrations of 13,331 EU/mL.

Humer et al. (2017) and Plaizier et al. (2018) proposed a model wherein LPS or other MAMPs may interact with specific pattern recognition receptors (PRR), such as TLR4, on the epithelium of the gastrointestinal tract to induce local inflammation. Moreover, there is evidence that following TLR-activation, the ruminal epithelium is capable of inducing an inflammatory response to rumen-derived MAMPs via the production of pro-inflammatory cytokines (Zhang et al., 2016). However, direct evidence for this model is limited. Several studies have shown that

not only are TLR4 (and other TLRs) expressed in ruminal epithelial tissue, but also that the expression may be altered by feeding a high forage diet (Chen et al., 2012; Minuti et al., 2015; Arroyo et al., 2017; Pan et al., 2017). However, results across the literature have been inconsistent. Pan et al. (2017) reported that dairy cows fed a high grain diet had greater transcript and protein expression of *TLR4* compared to those fed a high forage diet. In contrast, Arroyo et al. (2017) reported that of the genes tested, those that were associated with immune function and inflammation, including *TLR4*, were mostly unchanged in the ruminal epithelium of cows with grain-induced acidosis. In the present study, expressions of *TLR4* and *TLR2* were down-regulated in the SARA group. The apparent variability in observations of *TLR* expression in different models of acidosis may suggest that post-exposure expression follows a complex temporal pattern that would only become apparent with more frequent tissue sampling.

In one recent study, Zhang et al. (2016) reported an increase in ruminal LPS concentration from 14,741 to 26,266 EU/mL in dairy cows following prolonged feeding of a high grain diet, and demonstrated significant correlations between ruminal LPS concentration and relative mRNA expression of pro-inflammatory cytokines in the ruminal epithelium. Dionissopoulos et al. (2012) did not detect any differences in transcript abundance of genes associated with pro-inflammatory cytokines, including *TNF*, following grain-induced SARA. In contrast to previous work, the present study demonstrated a down-regulation of *TNF* in the SARA group following a short-term grain overload. Counter regulation of pro-inflammatory cytokines is a key step in the initiation of the resolution phase of acute inflammation (Sugimoto et al., 2016) and the down-regulation of TNF in the present study may be a result of negative feedback in an effort to return to a homeostatic state.

A key step in an acute inflammatory response is the release of arachidonic acid following activation of phospholipase. Free arachidonic acid has two canonical fates: the cyclooxygenase (COX) pathway, responsible for the synthesis of prostaglandins; and the lipoxygenase (LOX) pathway, that culminates in the production of leukotrienes (Medzhitov, 2008). Downstream expression of mediators of each of the distinct pathways can indicate physiological responses to stimuli such as LPS (Medzhitov, 2008). To further investigate the apparent anti-inflammatory effect, or the suppression of a pro-inflammatory response, in the present study, expression of key genes associated with each of these pathways was evaluated, as well as the expression of *TGFB1*.

The enzymatic activity of both prostaglandin-endoperoxide synthase 1 (*PTGS1*) and *PTGS2*, also known as COX1 and COX2, respectively, contributes to the production of prostanoids, such as prostaglandins, from arachidonic acid (Medzhitov, 2008; Ricciotti and FitzGerald, 2011). Under normal conditions, *PTGS1* is constitutively expressed, while *PTGS2* is responsive to stimuli and mediates a pro-inflammatory response (Gilroy et al., 1999; Ricciotti and FitzGerald, 2011). Previous work using knock-out mouse models has shown that expression of *PTGS2* is regulated by *TLR4* signaling (Pasare and Medzhitov, 2005; Fukata et al., 2006). In the present study, there was no change in expression of *PTGS1* as expected, whereas *PTGS2* was down-regulated in the SARA group compared to controls. *TLR4* expression was also reduced in the SARA group and *TLR2* expression on day 2 and day 6 was less in the SARA group, which may partially explain the down-regulation of *PTGS2* in the SARA treatment.

Expression of four genes that regulate production of leukotrienes, arachidonate 5-lipoxygenase (*ALOX5*), arachidonate 5-lipoxygenase-activating protein (*ALOX5AP*), leukotriene A4 Hydrolase (*LTA4H*), and leukotriene C4 synthase (*LTC4S*) were also analyzed. These genes are responsible for the production of molecules that have strong pro-inflammatory effects in response to stimuli (Rinaldo-Matthis and Haeggstrom, 2010). Expression of *ALOX5* and *ALOX5AP* in SARA heifers was down-regulated compared to the CON group. Expression of *TGFB1* did not differ. These results, together with *PTGS2*, *TNF*, *TLR2*, and *TLR4* provide further evidence of an initiation of the resolution phase of acute inflammation (Sugimoto et al., 2016). Expression of *LTA4H* and *LTC4S* did not change. The reduced expression of *ALOX5* and *ALOXAP* may have led to a lack of *LTA4*, upon which these enzymes act.

The inconsistencies across the literature, mentioned above, may be attributed to the common use of whole papillae or pieces of ruminal epithelium. Because ruminal papillae are comprised of a heterogeneous mixture of cell types, including endothelial cells and fibroblasts that are capable of responding to MAMPs, the use of this method in many studies, including the present one, results in an inability to confirm whether the ruminal epithelial cells are directly involved in the induction of a pro-inflammatory response. In addition, the fold changes for many genes in the present study, although statistically significant, are very small, which may be indicative of a local-tissue level effect. It is worth noting that it is possible that the targets in the present study may be altered post-transcriptionally. In order to confirm that the observed decreased *TLR4* transcriptional abundance was in fact occurring in the ruminal epithelium, the

present study quantified protein localization and abundance of the TLR4 receptor using analysis of fluorescence intensity of slides stained with a TLR4 antibody.

Consistent with transcript abundance, analysis of fluorescence intensity indicated that TLR4 expression was less in SARA heifers compared to the CON. In addition, there was clear evidence supporting the intracellular localization of TLR4 within the ruminal epithelium. This finding differs from studies of monogastric small and large intestinal epithelial cells during inflammation of the epithelium, which show localization of TLR4 at the apical and basolateral surfaces (Hamonic et al., 2018). The intracellular localization found in the ruminal epithelium may suggest a reduced sensitivity due to limited interactions with the MAMP ligands, such as LPS.

Fluorescence intensity of the nuclear counterstain DAPI was also analyzed and was also found to be less in the SARA group compared to CON in the SB cells, suggesting a potential difference in the number of cells in that strata. When investigated further, it was found that there were, in fact fewer SB cells in the SARA group. Previous work has demonstrated a non-immune effect of TLR signalling on cell cycle (Hasan et al., 2005). Rakoff-Nahoum et al. (2004) demonstrated a role of TLR signalling in promoting proliferation, tissue repair, and maintaining homeostasis of intestinal epithelial cells. Neal et al. (2012) showed that TLR4 was expressed in progenitor intestinal epithelial cells and that proliferation and apoptosis could be regulated through activation of TLR4. The down-regulation of TLR4 for RA heifers in the present study may be associated with a suppression of proliferation in the SB. Leukotrienes have been previously been shown to promote intestinal epithelial cell proliferation (Paruchuri and Sjölander, 2003), and thus the decreased expression of *ALOX5* and *ALOX5AP* may provide an alternate explanation for changes in cellular density. These findings are also consistent with the decrease in SCFA absorption rates for cattle exposed to SARA (Schwaiger et al., 2013a,b).

In addition to the effect of SARA on TLR expression, the present study also investigated the localization of the receptor in the different strata of the ruminal epithelium. The average fluorescence intensity was greater in the cells closest to the basement membrane and decreased in the cells closest to the lumen. Ruminal epithelial cells lose their nuclei and differentiate into the protective keratinized SC that are in direct contact with the ruminal digesta (Graham and Simmons, 2005). Previous, albeit limited, evidence suggests a degree of tolerance in the rumen epithelium in order to suppress immunogenic reactions towards commensal microbes (Shen et

al., 2016; Shen et al., 2017). Results of the current study indicate a possible tolerogenic effect in the SC that becomes an immuno-reactive effect in the more basal strata, in which TLR4 is highly expressed. This model also supports the concept that reduced barrier function may increase exposure of LPS to cell strata that express TLR4. Endotoxin tolerance has been previously described in ruminants (Gott, 2011; Zebeli et al., 2013) and a down-regulation of TLR4 and pro-inflammatory cytokine expression is associated with LPS tolerance in other species and models (Nomura et al., 2000; Jiang et al., 2018). Gott et al. (2015) observed suppression of a systemic pro-inflammatory response following repeated exposures to LPS. The heifers used in the present study had been previously used in experiments during which they were fed high grain diets. Despite a long adaptation period, it is possible that the heifers may have developed a degree of endotoxin tolerance, however this is purely speculative and cannot be confirmed.

Another possible explanation for the pro-homeostatic response in the present study may be time of sampling. Dionissopoulos et al. (2012) suggested that inconsistencies in the expression of immune-related genes and the observed inflammatory response to a high grain diet may be influenced by time of sampling. We speculate that the anti-inflammatory response is associated with initiation of the resolution phase of the acute inflammatory response. A probable explanation for this effect is that in order to prevent longer-term damage to the tissue, the acute immune response, especially the release of pro-inflammatory cytokines, must be tightly regulated (Buckley et al., 2001; Jura et al., 2008). This regulatory effect may be an important function of ruminal epithelial cells in maintaining tissue homeostasis (Sugimoto et al., 2016). As such, we speculate that ruminal biopsies collected closer in time to the grain overload may have revealed a pro-inflammatory response associated with the initial stages of inflammation and this speculation is supported by the model in Aschenbach et al. (2019). Indeed, recent work from our lab (Pederzolli et al., 2018) reported an upregulation in *TLR4* and *TLR2* in rumen papillae of steers and lambs 24 h following an acidosis challenge, indicating a pro-inflammatory response. Future work, incorporating earlier time points, is needed to further investigate the effects observed in the present study.

3.5 CONCLUSION

In this experiment, it was hypothesized that induction of ruminal acidosis would result in a pro-inflammatory response. However, analysis of gene expression and fluorescence intensity, on d 2, of *TLR4* indicated that inducing ruminal acidosis resulted in a down-regulation of genes associated with inflammation when ruminal papillae biopsies were collected following a grain overload. These data indicate a pro-homeostatic response following acidosis, an effect that may be the result of a tightly-regulated system required to promote resolution and tissue repair following an inflammatory reaction. Differences in the expression level ofeTLR4 protein within the different strata suggest an important role of the ruminal epithelium in regulating local inflammation. Future work is necessary to confirm this hypothesis.

CHAPTER 4: EFFECTS OF LIPOPOLYSACCHARIDE EXPOSURE ON THE INFLAMMATORY RESPONSE, BUTYRATE FLUX, AND METABOLIC FUNCTION OF THE RUMINAL EPITHELIUM USING AN *EX VIVO* MODEL

In Chapter 3, an in vivo experiment was conducted to investigate whole-tissue responses to a ruminal acidosis challenge. This study provided novel data on the expression of molecules relating to local inflammation in the ruminal epithelium. To further understand the results, an *ex vivo* model with Ussing chambers was employed to investigate effects of LPS exposure on inflammation and metabolism of the ruminal epithelium. This technique allowed for the use of native tissue, while providing more control over the experimental conditions.

Abstract: Acidotic conditions in the rumen have been associated with compromised barrier function of the ruminal epithelium and translocation of microbe-associated molecular patterns (**MAMP**) such as lipopolysaccharide (**LPS**). A local, pro-inflammatory response may result from an interaction between MAMPs and the ruminal epithelium. The aim of this study was to evaluate the potential pro-inflammatory response of the ruminal epithelium following LPS exposure in Ussing chambers to investigate whether LPS exposure affects the flux and metabolism of butyrate. Ruminal epithelial tissue from nine Holstein bull calves were mounted into Ussing chambers with a short-chain fatty acid-free buffer and exposed to 0, 10,000, 50,000, or 200,000 EU/mL LPS for a duration of 5 h. Radiolabelled ^{14}C-butyrate (15 m*M*) was added to the mucosal buffer to assess the mucosal-to-serosal flux of ^{14}C-butyrate. Additional Ussing chambers, without radioisotope, were exposed to either 0 or 200,000 EU/mL LPS and were used to measure the release of β-hydroxybutyrate (BHB) and IL1B into the buffer, and to collect epithelial tissue for analysis of gene expression. Genes associated with inflammation (*TNF*, *IL1B*, *CXCL8*, *PTGS2*, *TGFB1*, *TLR2*, *TLR4*), nutrient transport (*MCT1*, *MCT4*, *SLC5A8*, *GLUT1*), and metabolic function (*ACAT1*, *BDH1*, *MCU*, *IGFBP3*, *IGFBP5*) were selected and

A version of this chapter has been accepted by the Journal of Dairy Science. Kent-Dennis, C. and Penner, G.B. 2020. Effects of lipopolysaccharide exposure on the inflammatory response, butyrate flux and metabolic function of the ruminal epithelium using an Ex vivo model.

analyzed using real time qPCR. Butyrate flux was not significantly altered by LPS exposure, however there was a tendency for the mucosal to serosal butyrate flux to increase linearly with LPS dose ($P = 0.063$). Bidirectional release of BHB and IL1B were not affected by LPS exposure. Expression of *PTGS2*, *TGFB1*, *TLR4*, and *MCU* was down regulated following exposure to LPS *ex vivo*. There were no detected effects on the expression of genes associated with nutrient transport. The results of the present study are interpreted to indicate that while the inflammatory response of the ruminal epithelium was suppressed, exposure to LPS may have moderately altered metabolic function.

4.1 INTRODUCTION

During ruminal acidosis, there is an increase in the concentration of short-chain fatty acids (**SCFA**) and subsequently osmolality increases while ruminal pH decreases (Nocek, 1997). Extended exposure to low ruminal pH negatively impacts the activity and abundance of cellulolytic bacteria (Russell and Wilson, 1996; Owens et al., 1998). In combination with increased lysis of gram-negative bacteria, there is increased total bacterial turnover leading to the release of a component of their cell wall, liposaccharide (**LPS**), which may translocate across the ruminal epithelium (Plaizier et al., 2012) as a result of the acidotic (Penner et al., 2010; Wilson et al., 2012) and hyperosmotic conditions (Lodemann and Martens, 2006). Translocation of MAMPs has been associated with a systemic inflammatory response (Khafipour et al., 2009). Additionally, interaction between LPS and pattern recognition receptors (**PRR**) expressed by the ruminal epithelial cells (**REC**) has been shown to induce a pro-inflammatory response (Zhang et al., 2016; Kent-Dennis et al., 2019; Kent-Dennis et al., 2020.

Systemic inflammation is associated with a number of interconnected metabolic perturbations. During an activated state, the immune system increases its nutrient demands thereby consuming greater quantities of amino acids, energy substrates, and micronutrients (Wolowczuk et al., 2008; Kominsky et al., 2010). Although often difficult to accurately quantify, energy expenditure increases substantially (Straub, 2017). The changes in nutrient utilization and metabolism are attributed to several physiological mechanisms including increased proliferation and activity of immune cells (Lanis et al., 2017), increased synthesis of immune-modulatory molecules (Wang and Ye, 2015), a febrile response (Peters, 2006), tissue remodelling (Scoville et al., 2018), and local depletion of nutrients (Kominsky et al., 2010; Lanis et al., 2017).

In particular, an inflammatory response increases glucose demand, especially by immune-related tissues, and many immune cells become obligate glucose users (Kominsky et al., 2010). A study by Kvidera et al. (2017) demonstrated that a systemic LPS challenge in dairy cows resulted in the additional utilization of at least 1 kg of glucose. Previous work has reported that increased glucose utilization by the immune system coincides with a sparing effect that shifts peripheral tissue metabolism away from glucose utilization (Peters, 2006). Local metabolic shifts have also been observed whereby inflammation can alter nutrient availability in the tissue. For example, Glover and Colgan (2011) suggested that inflammation in intestinal epithelial tissue may increase its demand for energy substrates. While not investigated, it could be

speculated that for the ruminal epithelium, a pro-inflammatory response may increase demand for energy substrates such as butyrate. This is particularly relevant given the importance of butyrate as an energy source for the ruminal epithelium (Britton and Krehbiel, 1993) and that the ruminal epithelium modulates metabolism of butyrate and glucose depending on supply (Wiese et al., 2013). These local changes in substrate utilization may in turn play a role in mediating shifts in whole body nutrient utilization.

Inflammation at mucosal surfaces may affect normal functions of epithelial cells. Previous work has demonstrated altered nutrient uptake through impairment of solute transporter function in colonic tissue (Thibault et al., 2007) as well as negative effects on metabolism of energy substrates in colonocytes (Ahmad et al., 2000). It has been suggested, but not proven, based on changes in gene expression that initiation of a pro-inflammatory response may alter the metabolic function of the ruminal epithelium and utilization of energy substrates (Steele et al., 2011). However, while some evidence suggests that absorption of nutrients by the ruminal epithelium can be affected by acidotic conditions (Wilson et al., 2012) and the arising rumintitis (Owens et al., 1998), little if any work has investigated the potential effects of local inflammation on ruminal epithelial metabolism. In the present study, it was hypothesized that exposure of ruminal epithelial tissue to LPS would result in a pro-inflammatory response and a subsequent increase in the utilization of butyrate. In addition, inflammation may impair transport of nutrients across the epithelium. Therefore, the aim of this study was to examine the effects of the dose of LPS on the inflammatory response and butyrate utilization in the ruminal epithelium using an *ex vivo* model.

4.2 MATERIALS AND METHODS

All work involving cattle was pre-approved by the University of Saskatchewan's Animal Research Ethics Board (Protocols 20110127 and 20160076) and was performed following the Canadian Council on Animal Care guidelines (Ottawa, ON, Canada).

4.2.1 Tissue collection and preparation for use in Ussing chambers

Nine Holstein bull calves, approximately 4 mo of age, were housed in an outdoor group pen at the Vaccine and Infectious Disease Organization (VIDO; Saskatoon, SK, Canada) and fed

a common diet comprised of mixed brome-alfalfa hay and 1.7 kg/100 kg BW of a pelleted ration (16 % crude protein; Co-op® Elite Breeder Power Creep Beef Ration DEC Pellet, Saskatoon, SK Canada). Water was provided ad libitum. Calves were euthanized by intravenous administration of Euthanyl (20 mL/45 kg BW; Bimeda-MTC, Cambridge, ON, Canada) and epithelial tissue from the caudal blind sac of the rumen was collected immediately following death. The tissue was washed thoroughly using a physiological transport buffer (Table 4.1) that was oxygenated and pre-heated to 39ºC with pH adjusted to 7.4. The epithelium was then gently separated from the muscular layer by hand, placed in fresh transport buffer, and transported to the lab within 30 min of harvesting the tissue. Buffers used for washing, transportation, and in the Ussing chambers during the experiment are described in Table 4.1.

4.2.2 Ussing chamber Experiment

4.2.2.1 Tissue preparation and electrophysiology. Once in the lab, tissue was cut into 4 cm squares and mounted between two halves of an Ussing chamber with an exposed surface area of 3.14 cm^2. Tissue was incubated with separate mucosal and serosal buffer solutions that were free of SCFA (Table 4.1). Eight chambers were used to evaluate 1-^{14}C-butyrate flux. An additional 4 chambers were used to determine the release of BHB and IL1B and used to measure gene expression. In all cases, buffer pH was adjusted to 7.4 and 5.8 for the serosal and mucosal sides, respectively, in order to simulate physiological conditions. During incubation in Ussing chambers, all buffers were maintained at 39°C with the use of a heated water jacket and were mixed via gas lift with carbogen (5% CO_2, 95% O_2).

The tissues were incubated under short-circuit (**Isc**) conditions as previously described (Aschenbach and Gabel, 2000; Pederzolli et al., 2018) with a computer controlled voltage-clamp device (Dipl.-Ing, K.Mussler, Scientific Instruments, Aachen, Germany). Calomel electrodes (Mettler Toledo, Urdorf, Switzerland), connected to the Ussing chambers by 3*M* KCL-agar salt bridges, were used to measure the inherent potential difference. The ends of the salt bridges were located near the tissue within each side of the chamber. Another pair of Ag-AgCl electrodes, connected to the Ussing chambers with 3*M* NaCl-agar salt bridges, were used to apply a current, which was sufficient to clamp the potential difference to 0 mV. The I_{SC} is the inverse value of the clamp current when applied in the opposite direction. Short, bipolar current impulses were

Table 4.1 Composition of Ussing chamber buffers

BUFFERS			
Substance	Transport and Wash	SCFA-free	
		Serosal	Mucosal
Chemical (mmol/L)			
$CaCl_2$	1	0	0
$MgCl_2$	1.25	0	0
NaCl	15.6	0	0
KCl	5.5	0	0
Ca-gluconate	0	1	1
Mg-gluconate	0	1.25	1.25
Na-gluconate	0	50.6	50.6
K-gluconate	0	5.5	5.5
Na-phosphate	0.6	0.6	0.6
Disodium hydrogen phosphate	2.4	2.4	2.4
Acetic acid	10	0	0
L-glutamine	1	1	1
HEPES-free acid	10	10	10
Na-propionate	10	0	0
Na-butyrate	10	0	0
Na-hydroxide	10	0	0
Na-bicarbonate	25	24	24
Glucose	0	10	10
Gluconic acid	0	0	20
Mannitol	130	112	92
Antibiotics (mg/L)			
Penicillin G Na salt	0	60	60
Kanamycin sulphate	0	100	100
Flurocytosine	0	50	50
Buffer Characteristics			
pH	7.4	7.4	5.8
Osmolality (mOsmol/L)	294 ± 3.3[1]	292 ± 1.7	284 ± 7.4

[1]Mean osmolality ± standard deviation

applied every 6 s and the changes in the potential difference were used to measure the transepithelial conductance (**G_t**) according to Ohm's law. The G_t and Isc were allowed to stabilize for 20 min and the instantaneous G_t was recorded for all tissues. Tissues were then ranked by G_t and assigned to treatment to ensure the treatments were balanced for G_t. Subsequently, G_t and Isc were measured every 6 sec throughout the experiment and averaged for each hour of LPS exposure. All buffer chemicals were purchased from Sigma-Aldrich (St. Louis, MO, USA).

4.2.2.2 Measurement of 14C-butyrate flux. Tissues (8 Ussing chambers) incubated in SCFA-free buffer solutions were used to evaluate the effect of LPS dose on the mucosal-to-serosal butyrate flux (**$J_{ms\text{-}butyrate}$**). In duplicate chambers, LPS (E.coli B055; Sigma) was added to both the mucosal and serosal sides to achieve a final concentration of 0, 10,000, 50,000, or 200,000 EU/mL (Figure 4.1). These doses were selected to represent a physiological range, previously reported in ruminal fluid (Plaizier et al., 2012) and shown to induce a pro-inflammatory response in cell culture experiments (Kent-Dennis et al., 2020). Exposure on both the mucosal and serosal sides was used to ensure cells within the tissue were exposed to LPS. Tissue was incubated with the LPS for one hour (Figure 4.1) before applying butyrate to the mucosal side at a final concentration of 15 m*M*. The butyrate added was spiked with 100 kBq of 1-^{14}C-butyrate (Moravek Biochemicals, Brea, CA, USA) and allowed to equilibrate for 45 min to achieve steady-state flux rates (Sehested et al., 1996). After 45 min, 'hot' (100 µL) and 'cold' samples (500 µL) were collected from the mucosal and serosal sides, respectively. Given the larger volume of the cold samples, an equal volume of fresh buffer was replaced to maintain a constant volume in the chambers to avoid changes in hydrostatic pressure. Hot and cold samples were collected after 3 h and 15 min of incubation. Hot samples were diluted with 400 µL of buffer, and then 4 mL of scintillation cocktail was added to each hot and cold sample (Ultima Gold; PerkinElmer). The specific activity was determined using decays/minute in the cold and hot samples with a liquid scintillation analyzer (Tri-Carb 2910 TR; PerkinElmer). Flux rates were calculated according to Clark (2009) using the specific activity of butyrate on the hot side and the change in activity on the cold side. Values from the duplicate chambers were averaged to yield a single value for each LPS dose from each calf.

4.2.3 Analyses

4.2.3.1 Measurement of BHB and IL1B release. A total of 4 Ussing chambers were used according to Figure 4.1, except that no radioactivity was added. Samples of the buffer in the Ussing chambers were collected at the end of the experiment to evaluate BHB and

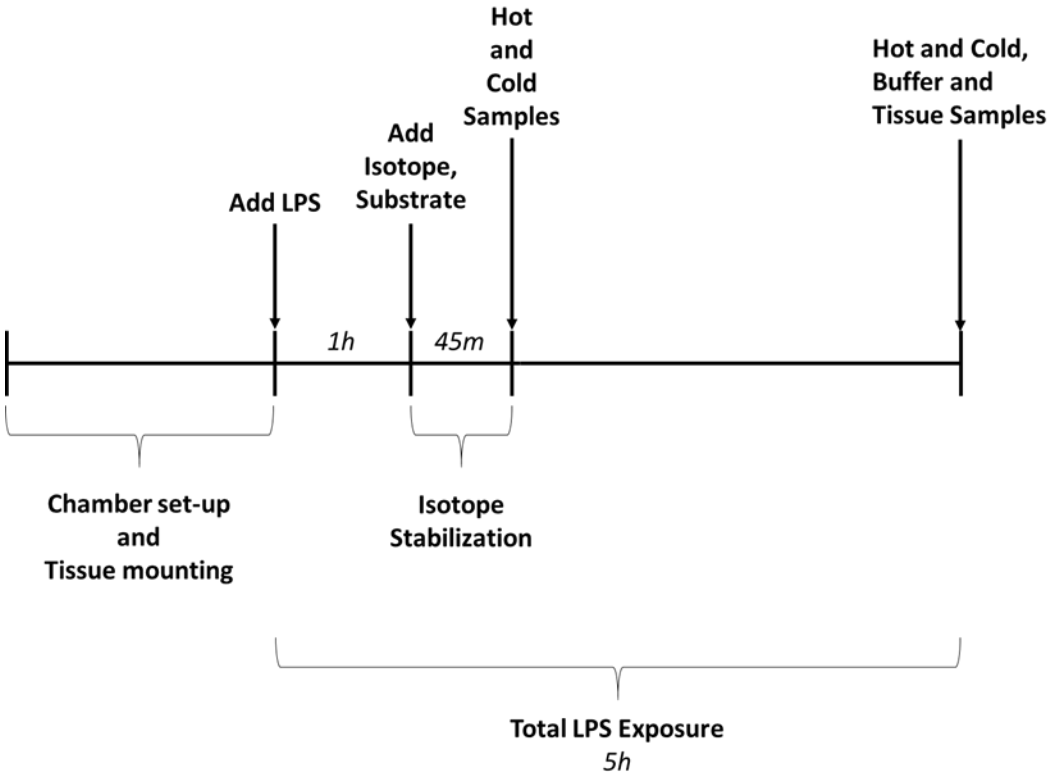

Figure 4.1 Timeline of daily procedures for LPS and substrate administration and subsequent sample collection.

IL1B release following exposure to 0 or 200,000 EU/mL LPS (E. coli B055; Sigma). The buffer samples collected were stored at -20°C until use at which point they were thawed at room temperature.

Production of BHB by the ruminal tissue in Ussing chambers was analyzed based on the method described by Williamson et al. (1962). Briefly, BHB in the samples and standards was oxidized to acetoacetate and NADH by β-hydroxybutyrate dehydrogenase (Roche Holding AG, Basel, Switzerland). Absorbance was determined at 340 nm with a microplate reader (BioTek). The concentrations were then corrected for buffer volume to determine the quantity.

Quantification of IL1B was determined using a commercial bovine IL1B ELISA kit (ESS0027, Thermo Fisher Scientific, Waltham, MA, USA), according to manufacturer's

instructions. Briefly, 96-well microplates (Thermo) were coated overnight at room temperature with anti-bovine IL1B coating antibody at a 1:100 dilution. Plates were blocked for 30 min with 4% bovine serum albumin (Sigma) and 5% sucrose (Sigma) in Dulbecco's PBS (**DPBS**). Samples (neat) and standards were added to the plate in duplicate and incubated for 1 h at room temperature. Plates were then washed six times with wash buffer (DPBS with 0.05% Tween-20 detergent (Sigma). The anti-bovine detection antibody was added to each well at a 1:100 dilution and incubated for 1 h at room temperature, followed by another six washes. Streptavidin-horseradish peroxidase was added to each well at a 1:400 dilution and incubated for 30 min at room temperature. Again, the plates were washed six times. The substrate (3,3′,5,5′-tetramethylbenzidine) was added to each well and incubated in the dark for 20 min followed by the addition of the stop solution (0.16 *M* sulfuric acid). The plates were read immediately on a microplate reader (Biotek) at 450 nm and 550 nm. The 550 nm values were subtracted from the 450 nm values in order to correct for background caused by the microplate. Concentrations were corrected for buffer volume to enable calculations of production rate.

4.2.3.2 RNA extraction and real time qPCR analysis. At the end of the incubation, ruminal papillae from chambers that did not contain radioactivity were clipped off at the base of the tissue. Approximately 10 to 15 papillae from the duplicate chambers were pooled, snap frozen, and stored at -80°C for RNA extraction. Frozen ruminal papillae were ground to a fine powder under liquid nitrogen using a mortar and pestle. Approximately 100 mg of ground tissue was used for extraction of total RNA using a phenol-chloroform extraction (Thermo) for phase separation, followed by double precipitations with ice-cold isopropanol (Kent-Dennis et al., 2019). The concentration of RNA was measured using a Nanodrop 2000 (Thermo). A 1.2% agarose gel was used to analyze RNA integrity and the presence of two distinct 18S and 28S bands was verified in all samples before further use. Upon confirmation of integrity, 1 µg of RNA was used for the synthesis of cDNA using the High Capacity Reverse Transcription Kit (Thermo). The resulting cDNA was diluted to a final concentration of 10 ng/µL. Quantitative real-time polymerase chain reaction (**qPCR**) was performed in duplicate using SsoFast EvaGreen Supermix (Bio-Rad, Hercules, CA, USA) with a CFX96 Touch Real-Time PCR Detection System (Bio-Rad). Primers (Table 4.2) were designed to span exon-exon junctions, where possible, and were obtained from IDT (Coralville, IA, USA). All primers were validated based on achieving efficiency between 90 and 110% and absence of dimer formation evaluated

Table 4.2 Primer used for quantitative real-time PCR

Gene Name (official gene symbol)	Source[1]	Sequence (5'-3')	Amplicon Size	Efficiency %[2]
Housekeeping				
Beta actin (ACTB)	NM_173979.3	F: GAGCTACGAGCTTCCTGACGGGC R: AATGCCGCAGGATTCCATGCCCAG	109	96
Glyceraldehyde-3-phosphate dehydrogenase (GAPDH)	NM_001034034.2	F: GGGTCATCATCTCTGCACCT R: GGAGGCATTGCTGACAATCT	101	91
Hypoxanthine phosphoribosyltransferase 1 (HPRT)	NM_001034035.2	F: AGGTTGCGAGCTTGCTGAT R: AGGGCATATCCCACAACAAA	103	99
Immune-related				
C-X-C motif chemokine ligand 2 (CXCL2)	NM_174299.3	F: CCGAAGTCATAGCCACTCTCA R: CTTCTGTTTTCCACCTGGTCA	128	99
C-X-C motif chemokine ligand 8 (CXCL8)	NM_173925.2	F: AGAGCTGAGAAGCAAGATCCA R: ACCCTACACCAGACCCACAC	150	104
Interleukin 1 beta (IL1B)	NM_174093.1	F: CTGAGGAGCATCCTTTCATTC R: GTCCTGGAGTTTGCACTTTAT	114	97
Prostaglandin-endoperoxidase synthase-2 (PTGS2)	NM_174445.2	F: GGTGTGAAAGGGAGGAAAGA R: GGCAAAGAATGCAAACATCA	117	93
Transforming growth factor 1 beta (TGFB1)	NM_001166068.1	F: ACTGCTTCAGCTCCACAGAA R: TCCAGGCTCCAGATGTAAGG	148	105
Toll-like receptor 2 (TLR2)	XM_015475330.1	F: TGATGCTGCCATTCTGATTC R: GCCACTCCAGGTAGGTCTTG	107	96
Toll-like receptor 4 (TLR4)	NM_174198.6	F: CCTTGCGTACAGGTTGTTCC R: CTCAGGTCCAGCATCTTGGT	104	90
Tumor necrosis factor alpha (TNF)	NM_173966.3	F: CAAGTAACAAGCCGGTAGCC R: AGATGAGGTAAAGCCCGTCA	153	99
Metabolism-related				
Acetyl-CoA acetyltransferase 1 (ACAT1)	NM_001046075.1	F: CGGGTGCAGGAAATAAGGTA R: TAGTGGCTGGCAGAGAGGA	133	103
3-hydroxybutyrate dehydrogenase 1 (BDH1)	NM_001034600.2	F: GACCCTGAGAAAGGCTTGTG R: TCCTTGTAGGTCTCCATGCTG	92	96
Solute carrier family 2 member 1 aka GLUT1 (SLC2A1)	NM_174602.2	F: GGCATCAACGCTGTTTTCTA R: ACACGACAGTGAAGGCTGTG	115	105
Insulin-like growth factor binding protein 3 (IGFBP3)	NM_174556.1	F: GCTGAACCACCTCAAGTTCC R: CGGCACTGCTTTTTCTTGTA	96	99
Insulin-like growth factor binding protein 5 (IGFBP5)	NM_001105327.2	F: CAAGAGAAAGCAGTGCAAACC R: AGTCCCCGTCCACGTACTC	107	98
Mitochondrial calcium uniporter (MCU)	NM_001206102.1	F: CACACAGTTTGGCATTTTGG R: AACATATTCCTGGCGTGTCA	139	97
Solute carrier family 16 member 1 aka MCT1 (SLC16A1)	NM_001037319.1	F: TCCATCGGCTTCTCTTATGC R: GCTGATAGGACCTCCACCAT	144	95
Solute carrier family 16 member 3 aka MCT4 (SLC16A3)	NM_001109980.3	F: TGTGGTGAGCTATGCCAAGG R: TCAGCGAAGCCGTTGAAGAA	183	98
Solute carrier family 5 member 8 (SLC5A8)	NM_001164861.1	F: TGCCTTAGCAGCAGTAACCA R: CAGCACACTCATTCCTTGTGA	100	98

[1]National Center for Biotechnology Information (NCBI)
[2]Efficiency= $-1 + 10^{(-1/\text{slope})}$X100

through the generation of melt curves following amplification. Housekeeping genes (*ACTB*, *GAPDH* and *HPRT*) were determined to be stable as there were no significant effects of treatment detected ($P \geq 0.16$; data not shown). The Ct values of the genes of interest were normalized to the geometric mean of the three housekeeping genes and data are presented as fold change calculated using the $2^{-\Delta\Delta CT}$ method, with treatment means held relative to the mean of the control within each animal.

4.2.4 Statistical analysis

Statistical analysis was performed using the MIXED procedure of SAS 9.4 (SAS Institute Inc, Cary, NC, USA). Treatment (LPS concentration) was considered a fixed effect and chamber within animal was considered random. The BHB and IL1B data were analyzed by mean separation. For isotope flux and electrophysiology data, polynomial contrasts were used to analyze the linear and quadratic effects of LPS concentration. For Gt and Isc, the data were analyzed using repeated measures. Several covariance error structures were tested and compound symmetry was selected as it resulted in the lowest Akaike information criterion and Bayesian information criterion values. Statistical analysis of gene expression data was performed on the ΔCt and results are present as fold change.

4.3 RESULTS

Dose of LPS and hour of incubation did not affect the G_t or Isc (Table 4.3) for ruminal epithelial tissue. The $J_{ms\text{-}butyrate}$ flux rate tended to increase linearly (SEM = 0.32; $P = 0.063$) with exposure to increasing concentrations of LPS.

The production of BHB secreted on the serosal side was 83.6 and 68.6 ± 17.7 μmole/(h × cm^2) and on the mucosal side was 65.5 and 66.2 ± 13.4 μmole/(h × cm^2) for 0 and 200,000 EU/mL LPS, respectively with no difference between treatments ($P \geq 0.21$; Table 4.4). Production of IL1β for the serosal side was 4.3 and 3.7 ± 0.97 pg/(h × cm^2) and on the mucosal side was 0.25 and 0.24 ± 0.06 pg/(h × cm^2) for 0 and 200,000 EU/mL LPS, respectively ($P \geq 0.43$).

Table 4.3 Tissue conductance (Gt), short circuit current (Isc) and Jmucosal-serosal flux of 14C-butyrate in ruminal epithelial tissue exposed to 0, 10,000, 50,000 and 200,000 EU/mL LPS.

	LPS Dose × 1000[1]					*P*-value	
	0	10	50	200	SEM	Linear	Quadratic
Gt, mS/cm^2	5.1	6.9	6.1	5.2	1.5	0.74	0.61
Isc	4.5	4.7	4.4	4.2	1.1	0.78	0.97
Butyrate flux, μmole/h/cm^2	2.0	2.2	2.6	2.4	0.32	0.063	0.61

[1]Endotoxin units/mL

Table 4.4 Rates of BHB and IL1β secretion by ruminal epithelial tissue exposed to 0 or 200,000 EU/mL LPS.

	LPS Dose × 1000[1]			
Measurement	0	200	SEM	P-value
BHBA, μmole/(cm^2 × h)				
Serosal	83.6	68.6	17.7	0.21
Mucosal	65.5	66.2	13.4	0.94
IL1-β, pg/h/cm^2				
Serosal	4.3	3.7	0.97	0.43
Mucosal	0.24	0.25	0.06	0.87

[1]Endotoxin units/mL

Gene expression for *TNF*, *IL1B,* and *CXCL8* (Figure 4.2) was not affected by LPS exposure ($P > 0.18$). However, exposure to LPS, down-regulated *PTGS2* (1.6-fold; $P = 0.025$; Figure 4.3A). Expression of *TGFB1* (1.2-fold; Figure 4.3B) was also downregulated with LPS exposure ($P = 0.016$). Although there was no effect of LPS on expression of *TLR2* (Figure 4.4A), there was a slight downregulation of *TLR4* following exposure to LPS (1.3-fold; $P = 0.024$).

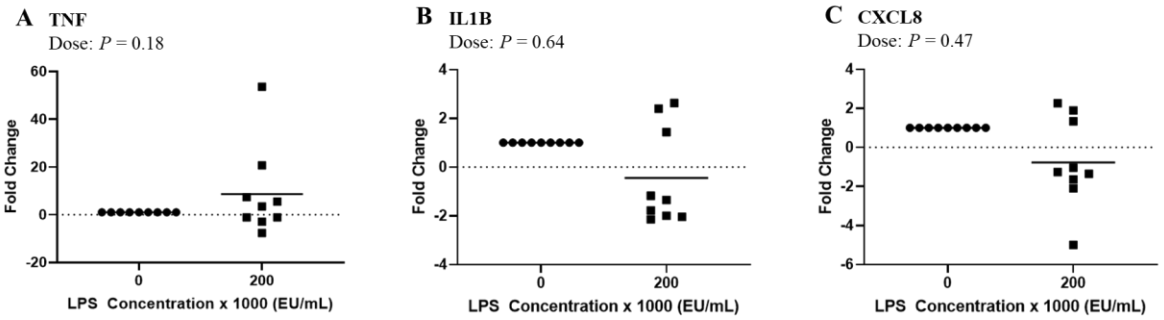

Figure 4.2 Gene expression of pro-inflammatory cytokines, TNF (A) and IL1B (B), and chemokine CXCL8 (C), in ruminal epithelial tissue exposed to 0 or 200,000 EU/mL LPS for 5 h in Ussing chambers. The ΔCt was used for statistical analysis of LPS dose ($P < 0.05$). Results are presented as fold change.

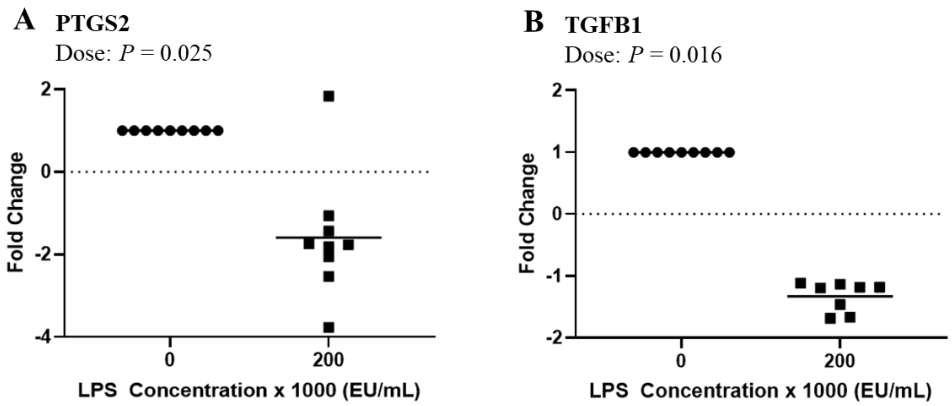

Figure 4.3 Gene expression of a lipid mediator of inflammation, PTGS2 (A) and a growth factor-like cytokine TGFB1 (B), in ruminal epithelial tissue exposed to 0 or 200,000 EU/mL LPS for 5 h in Ussing chambers. The ΔCt was used for statistical analysis of LPS dose ($P < 0.05$). Results are presented as fold change.

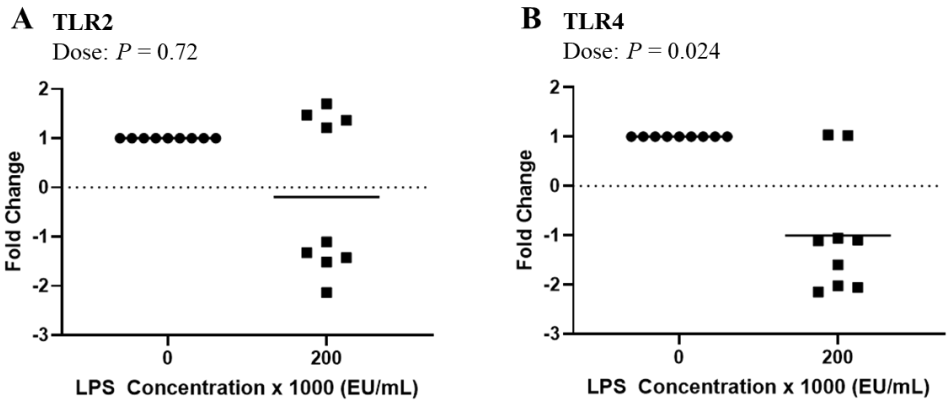

Figure 4.4 Gene expression of toll-like receptors, TLR2 (A) and TLR4 (B), in ruminal epithelial tissue exposed to 0 or 200,000 EU/mL LPS for 5 h in Ussing chambers. The ΔCt was used for statistical analysis of LPS dose ($P < 0.05$). Results are presented as fold change.

There was no effect of LPS exposure on expression of *MCT1*, *MCT4*, *SLC5A8*, or *GLUT1* ($P > 0.21$; Figure 4.5). Expression of *ACAT1* and BDH1 was also not affected by LPS ($P > 0.35$; Figure 6A and B). Expression of *MCU* (Figure 4.6C) was less following LPS exposure (1.3-fold; $P = 0.043$). Expression of *IGFBP3* and *IGFBP5* was not affected ($P > 0.10$; Figure 4.7).

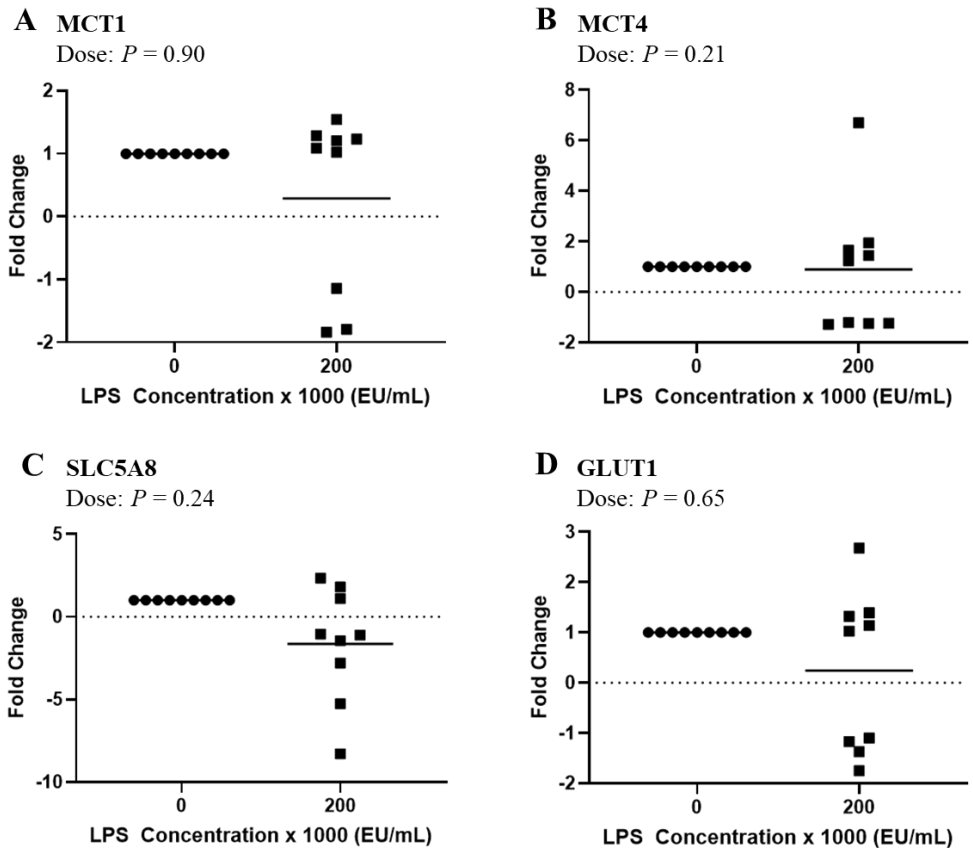

Figure 4.5 Gene expression of solute transporters, MCT1 (A), MCT4 (B), SLC5A8 (C) and GLUT1 (D), in ruminal epithelial tissue exposed to 0 or 200,000 EU/mL LPS for 5 h in Ussing chambers. The ΔCt was used for statistical analysis of LPS dose ($P < 0.05$). Results are presented as fold change.

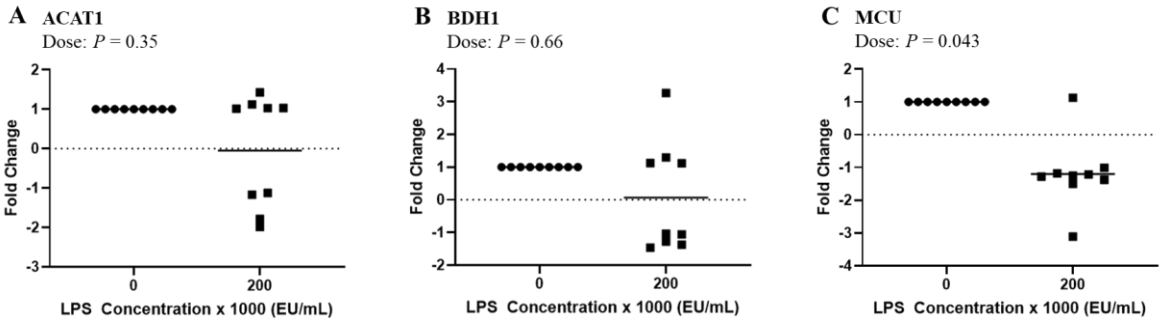

Figure 4.6 Gene expression associated with cell metabolism, ACAT1 (A) BDH1 (B) and MCU (C), in ruminal epithelial tissue exposed to 0 or 200,000 EU/mL LPS for 5 h in Ussing chambers. The ΔCt was used for statistical analysis of LPS dose ($P < 0.05$). Results are presented as fold change.

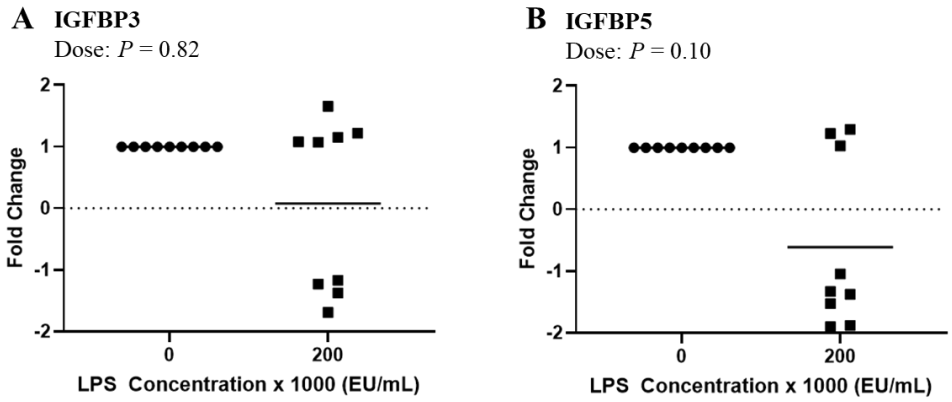

Figure 4.7 Gene expression associated with cell metabolism, IGFBP3 (A) and IGFBP5 (B), in ruminal epithelial tissue exposed to 0 or 200,000 EU/mL LPS for 5 h in Ussing chambers. The ΔCt was used for statistical analysis of LPS dose ($P < 0.05$). Results are presented as fold change.

4.4 DISCUSSION

Nutrient and energy utilization associated with activation of the immune system is difficult to quantify; however, energy expenditure is thought to be substantial. Increased energy expenditures in human pathologies have been reported to account for between 2 and 15% of total energy expenditure (Straub, 2017). Kvidera et al. (2017) administered an intravenous LPS challenge to dairy cows and, through the use of a euglycemic clamp, reported that at least 1 kg of glucose utilization was associated with the inflammatory response. The gastrointestinal tract is not only a crucial source of nutrients for internal tissues, but also is itself a major consumer of nutrients and energy. The splanchnic tissues, which includes the rumen, account for at least 50% of total oxygen utilization of the body (Reynolds, 2005) and Sehested et al. (1999a) suggested that the majority of butyrate, produced in the rumen, is metabolized, to either CO_2 or metabolites, in the ruminal tissue. Ahmad et al. (2000) suggested that local inflammation may alter energy substrate metabolism in intestinal epithelial tissue. As the ruminal epithelium is potentially a major site for MAMP exposure (Malmuthuge et al., 2012), the effects may be similar. In addition, systemic LPS has been shown to inhibit absorption of nutrients such as fatty acids (Liu et al., 2019). Moreover, immune activation at mucosal surfaces may affect the absorptive and metabolic functions of the epithelial cells (Ahmad et al., 2000; Lanis et al., 2017). For example,

transepithelial transport in the intestinal epithelium can be altered by inflammatory conditions such as colitis (Kiela and Ghishan, 2009). The impact on metabolism is thought to be due to diminished barrier function or damage or apoptosis of the epithelial cells, impairing the cell mechanics (Liu et al., 2019). In addition, the microvasculature at the site of inflammation is thought to be a mechanism by which local oxygen levels are reduced, potentially affecting epithelial cell function (Lanis et al., 2017). Inflammation may therefore influence nutrient utilization while also affecting nutrient uptake, which may contribute to energy expenditure, both at a tissue level and systemically.

Previous work has provided evidence for an inflammatory response of the ruminal epithelium as a result of acidotic conditions or elevated LPS in the ruminal fluid (Liu et al., 2013; Zhang et al., 2016). However, the response across studies has not been consistent. Arroyo et al., (2017) found little change in expression of immune-related genes in the ruminal epithelium, and there was no clear systemic response in cows fed a high energy diet. In a recent study (Kent-Dennis et al., 2019), gene expression of pro-inflammatory mediators was down-regulated in the ruminal epithelium, despite increased ruminal fluid LPS and decreased ruminal pH. In the present study, there was no effect of LPS exposure on gene expression of *TNF*, *IL1B,* or *CXCL8*, all three of which are used as indicators of a pro-inflammatory response (Zhang and An, 2007). In addition, expression of *TLR4* and *PTGS2*, also indicators of an inflammatory response, were down-regulated and IL1B protein secretions by the tissue, measured with an ELISA, was not different between treatments. These data suggest that there was a suppression of the pro-inflammatory immune response following 5 h of exposure to LPS. However, it should be noted that the fold changes were small, and therefore the results should be interpreted with caution.

The ruminal environment prior to tissue collection and the conditions during harvest may have affected the response to the treatments in the Ussing chambers. Previous work has suggested that repeated exposure to LPS results in a tolerogenic response (Kent-Dennis et al. 2020), which may have resulted in a suppressed inflammatory response, if the REC were exposed to free LPS, or other MAMPs, in the ruminal fluid. While ruminal fluid normally contains low concentrations of LPS, it was not expected that the calves used in this study would experience ruminal acidosis, therefore it was unlikely that the basal layers of REC would have been exposed to LPS. In addition, during tissue harvest the epithelium was washed thoroughly to

remove ruminal digesta and transported to the lab in approximately 10 L of transport buffer. Therefore the majority of the free LPS would have been washed away, and any remaining free LPS would have been greatly diluted.

Another potential explanation for the response may be that the duration of LPS exposure in the current experiment was not long enough for the transcription of the pro-inflammatory cytokines. Although variable and highly dependent on tissue type, previous work has suggested that peak expression of some pro-inflammatory cytokines such as *TNF* and *CXCL8* may be after 6 hours relative to LPS exposure (Fang et al., 2003; Li et al., 2014). However, expression of TNF and IL1B have been found to be increased even after only one or two hours (Lotter et al., 2006; Godornes et al., 2007). In Kent-Dennis et al. (2020; in review), primary REC exposed to LPS initiated a pro-inflammatory response within 6 h following LPS exposure, with no further increase in expression of pro-inflammatory cytokines at 24 h. In the *ex vivo* model, as the ruminal tissue used was native epithelium, it is possible that exposure to LPS for a longer duration would be necessary to elicit a significant pro-inflammatory response.

In addition to duration of exposure, previous work looking at the inflammatory responses in the epidermis of skin has suggested that keratinocytes are predisposed for immune-tolerance and that a pro-inflammatory response occurs when immune cells of the dermal layer are activated (Shklovskaya et al., 2011). In the current study, it is possible that the LPS interacted with the most luminal REC, which may have been tolerogenic, but that the duration of exposure was not sufficient to activate a pro-inflammatory response in the more basal layers. In support of this theory, Kent-Dennis et al. (2019) demonstrated, using immunohistofluorescence analysis, that TLR4 was highly expressed in the most basal cells of the ruminal epithelium, suggesting that the most luminal cells are less sensitive to LPS. It is possible that the cells of the stratum corneum maintain a degree of tolerance to protect the ruminal epithelium from excessive inflammatory reactions to MAMPs. However, these immune-modulatory mechanisms have not been elucidated in the ruminal epithelium.

To increase probability of LPS exposure to the ruminal epithelial cells within the tissue, we applied LPS on both the mucosal and serosal sides and manually removed the submucosal tissues at the time of tissue preparation. Despite experimental approaches, we cannot confirm exposure of all cells within the ruminal epithelium to LPS due to inherent barrier function properties of the tissue which is further supported by the lack of LPS dose on tissue Gt. It is

possible that other conditions, such as pH, in the chambers could have been altered to increase the chances of increasing permeability. Although the *ex vivo* model allows for greater control over experimental conditions when compared to in vivo settings, the apparent lack of response to LPS may have also been a consequence of quantifying gene expression in whole ruminal papillae, which may have diluted transcript expressed specifically by the epithelial cells. In support of this argument, a study by Zhang et al. (2016) and Kent-Dennis et al. (2020; in review) suggested that isolated REC are capable of initiating a pro-inflammatory response to LPS in culture, while Dionissopoulos et al. (2012) measured expression of pro-inflammatory genes and proteins in whole ruminal papillae obtained from cows following an acidosis challenge and found no effects. The potential inflammatory response of REC should be further explored using in vitro techniques and in vivo techniques but may need to integrate challenge models known to alter epithelial barrier function such as acidic conditions (Meissner et al., 2017, Greco et al., 2018).

Short-chain fatty acids cross the ruminal epithelia via transcellular transport mechanisms including passive diffusion, anion-exchange proteins (Aschenbach et al., 2011), and through maxi-anion channels (Stumpff, 2018). Inflammation of mucosal surfaces is associated with impaired barrier function (Thomson et al 2019) due to the breakdown or altered structure of tight junction complexes leading to increased paracellular transport (Schmitz et al., 1999; Laukoetter et al., 2007). In goats fed a high grain diet, Liu et al. (2013) demonstrated down-regulation (both mRNA and protein) of tight junction complexes, suggesting that there was an impairment of the ruminal epithelial barrier. Emmanuel et al. (2007) suggested that there was an increase in permeability when the tissue was exposed to LPS in Ussing chambers under simulated acidotic conditions, as increased permeability was only detected when the pH on the mucosal side was 4.5. In the current study, the buffer conditions were designed to limit exposure to pH and hyperosmotic challenges to evaluate a direct effect of LPS. With a serosal pH of 7.4 and mucosal pH of 5.8, we did not observe any effect of LPS on G_t and Isc, suggesting resilience of the tissue. Overall the results suggest that integrity of the tissue was maintained regardless of the dose of LPS exposure.

Although the present study was not able to detect a pro-inflammatory response, the results suggest that there was an increase in demand for energy to support the response to LPS by the ruminal epithelium. In the current experiment, to evaluate transport across the epithelium, the

$J_{MS\text{-}butyrate}$ of radiolabelled butyrate was measured. Results indicate that there was a linear tendency for the isotope flux to increase with LPS dose. As there was no effect on G_t, the change in flux should not be attributed to an increase in paracellular permeation. As such, the increased $J_{MS\text{-}butyrate}$ indicated increased movement of butyrate or its metabolites (assuming isotope incorporation) across the epithelium. As butyrate is a preferred energy substrate for the ruminal epithelium, it is possible that the butyrate was metabolized to metabolites such as BHB or to CO_2 (Sehested et al., 1999a; Sehested et al., 1999b). In this experiment we were unable to measure CO_2. The production of BHB was not affected by exposure to LPS and there was a lack of an LPS effect on genes associated with ketogenesis, including *ACAT1* and *BDH1*. On the other hand, while we initially incubated tissues in SCFA-free buffer, we did not measure the initial BHB concentration and thus it is possible that residual butyrate or BHB in the tissue at the start of the incubations may have contributed to the BHB levels detected and therefore led to the large amount of variation. An increase in butyrate flux may also indicate that there is a shift towards utilization of other energy substrates, such as glucose. Previous work has suggested that local inflammation can influence the demand for nutrients and energy substrates to in order to meet requirements for synthesis of immunomodulatory molecules (Wolowczuk et al., 2008; Kominsky et al., 2010). Future research is needed with stable isotopes to evaluate whether LPS affects the metabolism of primary energy substrates (glucose and SCFA) by the ruminal epithelium.

Exposure to LPS reduced the expression of *TGFB1* in the current experiment. Although classically considered an anti-inflammatory mediator, *TGFB1* is a cytokine with multiple functions including regulation of inflammation, cell proliferation, promoting chemotaxis, and cell differentiation (Veldhoen and Stockinger, 2006; Han et al., 2012). *TGFB1* is also involved in formation of both the extracellular matrix and the actin filaments (Boland et al., 1996; Yan et al., 2018). Furthermore, *TGFB1* has been shown to suppress expression of a keratin subtype in keratinocytes (Werner et al., 2000). In support, mitochondrial calcium uniporter (*MCU*), a calcium transporter localized to the inner membrane of the mitochondria, has also been implicated in changes in cytoskeletal organization (Paupe and Prudent, 2018). Expression of *MCU* was also down-regulated following exposure to LPS. Although further study is required to confirm, a decrease in *TGFB1* and *MCU* expression in the current experiment may be indicative of increased keratin expression in response to LPS, therefore altering cell morphology and function. Keratinization has been described as an “active metabolic process”, requiring energy

and nutrients such as lipids (Lorincz and Stoughton, 1958). It may be that this process increased in the energy demand in the ruminal epithelium, in the present study, in response to LPS exposure.

Overall, the metabolic response to LPS was minimal as there were no effects on solute transporters, including *MCT1*, *MCT4*, *SLC5A8*, and *GLUT1*. In addition to the genes associated with ketogenesis, *ACAT1* and *BDH1*, there was also no effect of LPS exposure on expression of *IGFBP3* or *IGFBP5*. These results suggest that LPS exposure may have increased tissue utilization of butyrate as an energy substrate or substrate precursor, but that there were no major perturbations that affected absorption or metabolic function of the ruminal epithelium.

4.5 CONCLUSION

The inflammatory response in the current study was minimal and possibly even suppressed when ruminal epithelium was exposed to LPS in Ussing chambers. The limited response may have resulted in only minor alterations in metabolism, and may have been enhanced by altering conditions such as pH in the chambers. Although a pro-inflammatory response was not evident, LPS may still have had an effect on metabolic function. Butyrate isotope flux tended to increase when exposed to LPS and the results suggested that the energy substrate utilization was altered. Overall, exposing ruminal epithelial tissue to LPS in an *ex vivo* model did not result in a pro-inflammatory response or result in any major perturbations in metabolism. Sampling whole tissue may have obscured the epithelial cell response, especially the expression of mRNA. It may have also provided a degree of protection or tolerance to LPS exposure, leading to resilience of the epithelial barrier. Future work under different experiment conditions in Ussing chambers or the use of *in vitro* techniques may be useful to further elucidate these effects.

CHAPTER 5: DEVELOPMENT OF A PRIMARY RUMINAL EPITHELIAL CELL CULTURE MODEL

In Chapter 3 and 4, whole-tissue responses to ruminal acidosis or LPS exposure *ex vivo*, respectively were investigated to determine whether the ruminal epithelium mounts a pro-inflammatory response. While these chapters provided novel information, the use of whole-tissue cannot confirm whether the response can be attributed to the ruminal epithelia or whether other cell types may have influenced the response. As such, a primary culture model using isolated ruminal epithelial cells was developed to enable more detailed and controlled investigation *in vitro*.

Abstract: The aim of this study was to establish a standardized model for the isolation and culture of primary ruminal epithelial cells (REC), and to characterize the morphological and functional changes that occur during culture. Bovine ruminal epithelial tissue was obtained post-mortem and the ruminal papillae were used for serial trypsinzation to dissociate the REC. Isolated cells were seeded into culture dishes and grown for up to 4 wk. The cells were visually assessed throughout the time in culture for growth characteristics and morphological changes. Fibroblast contamination was evaluated using a CD90 antibody and flow cytometry analysis. Flow cytometry was also used to evaluate the protein expression of epithelial cell markers, including claudin-4 (CLDN4), zonula occludens-1 (ZO1), E-cadherin (ECAD) and a pan-cytokeratin antibodies. Expression of hydroxymethylglutaryl-CoA synthase (HMGCS1) and 3-hydroxybutyrate dehydrogenase-1 (BDH1), ketogenic enzymes, were also evaluated. Quantitative real-time PCR was used to evaluate the expression of genes associated with cytoskeletal organization (*CDH1*, *TGFB1* and *SNAI1*), cell cycle (*CDK1* and *MYC*), and metabolic function (*MCT1*, *MCT4*, *G6PD*, *BDH1*, *ACAT1*, *IGFBP3* and *IGFBP5*). Expression of genes at 2 wk of culture was analyzed relative to expression in the first week of culture. In the first 2 to 4 d following isolation, cells formed small, cobblestone-like clusters, which progressively expanded across the culture plates within the first 2 wk. After 4 wk in culture, cells became large and flat. Fibroblast contamination (>10% of cells) occurred approximately 16% of the time and these cells were discarded. The percent of positive cells for CLDN4 and ZO1 were approximately 50 and 30%, respectively, on d 8, and for ECAD and cytokeratin were 80 and 40% respectively, on d 15. Percent cells positive for BDH1 and HMGCS1 were 84 and 30%,

respectively on d 8. Except for BDH1, the percent of positive cells for all markers decreased after 2 wk. At 2 wk, gene expression of *CDH1* and *MYC* were less, and *TGFB1* and *SNAI1* were greater, compared to wk 1, suggesting that cytoskeletal organization and cell cycle may be altered with time in culture. There was a decrease in expression of *MCT1*, *G6PD,* and *BDH1,* and an increase in expression of *MCT4* and *IGFBP5*. The results of this study indicate that while time in culture may affect cell morphology and indicators of nutrient metabolism, the cultured REC retain characteristics similar to the cells of the spinosum and basale strata for 2 to 3 wk. Isolated and culture REC can therefore be used reliably for experimentation; however, the cells should be carefully monitored for epithelial characteristics.

5.1 INTRODUCTION

Ruminal epithelial cells (**REC**) in the stratum corneum, granuolum, spinosum, and basale form the stratified squamous epithelium of the rumen. This organizational structure enables the most luminal layers to provide physical protection with absorptive and metabolic functions occurring in the most basal layers (Graham and Simmons, 2005; Baldwin and Connor, 2017). Morphologically, the cells of the stratum basale are columnar in shape and gradually become flatter and less uniform as they differentiate towards the lumen (Steele et al., 2016). These stratum basale and stratum spinosum cells are metabolically active, containing many mitochondria and are highly ketogenic. In fact, BHB production, via β-hydroxybutyrate dehydrogenase activity, is a preferred metabolic pathway in REC (Baldwin, 1998). The metabolic functions of REC are progressively lost during differentiation, whereby the cells become increasingly keratinized (Steele et al., 2011). The importance of the stratum basale and spinosum within the REC cannot be understated. These cells are responsible for metabolism and transport of ions and nutrients, especially short-chain fatty acids (**SCFA)**, thus ensuring delivery of metabolites to peripheral tissues (Baldwin and Connor, 2017). In addition, SCFA are a preferred energy substrate for REC and therefore substantial metabolism occurs in the ruminal epithelium (Baldwin, 1998). For these reasons, there has been significant interest in evaluating the specific functions of the REC.

For the study of primary REC in culture, a number of models have been developed, including cell suspension cultures (Baldwin and Jesse, 1991), culture of a non-polarized monolayer of adherent cells (Galfi et al., 1981), and culture of cells in transwells (Stumpff et al., 2011). Each model has its own set of advantages and limitations. Suspension cultures, also called single-cell suspensions, use non-adherent cells that move freely in culture medium. This model allows for the use of cells immediately after the dissociation procedure and eliminates the need to grow cells for any period of time. A number of experiments (Baldwin and Jesse, 1991; Klotz et al., 2001; Waldron et al., 2002) were able to demonstrate the ketogenic activity of isolated REC in single cell suspensions (i.e. non-adherent cells in media). However, these cells had limited application as they were used in short term experiments immediately after the isolation procedure. Normal epithelial function is promoted by adherence to a surface and physical contact with neighboring cells (Jin et al., 2018); therefore, cell suspensions may not be representative of

the normal functions. Additionally, since these cells have been exposed to trypsin digestion immediately prior to use, their function may be altered (Huang et al., 2010).

Culturing adherent cells in a monoculture is the most common model for studying primary REC and allows for the growth of cells under more representative conditions, compared to the cell suspension cultures. Monocultures are limited in that the cells are not polarized and lack adequate cell to cell adhesion molecules, such as tight junctions. Therefore, this model cannot be used to make conclusions about barrier function or transport mechanisms. However, previous work has suggested that REC grown in a monolayer retain some of their characteristics associated with nutrient transport and metabolism. For example, cultured REC express functional monocarboxylate transporters (Muller et al., 2002) and transepithelial transport mechanisms, such as Na^+/H^+ exchange, have been reported (Gabel et al., 1996; Stumpff et al., 2009). Some work has demonstrated that butyrate has a suppressive effect on REC proliferation *in vitro* (Neogrady et al., 1989), which is contradictory to results observed *in vivo* (Penner et al., 2011). The differential responses between *in vitro* and *in vivo* research are common and provide an indication that extrapolation from one experimental method to the other requires a degree of caution (Sakata, 2019).

Culturing REC using transwells has only been reported in one published study (Stumpff et al., 2011). This method allows for the polarization of the cells and the formation of tight junctions, resulting in a functional epithelial barrier. While transwells can be beneficial, namely providing more accurate information about transport functions, there are some significant pitfalls. Mainly, successfully establishing a viable barrier is difficult and the culturing of an adequate numbers of cells is time-consuming (Stumpff et al., 2011).

Primary REC isolation and cultivation was first published in a series of papers in the 1980s (Galfi et al., 1981; Innoka et al., 1984; Galfi and Neogrady, 1989). The initial experiments attempted to optimize the growing conditions and aimed to confirm that the cells obtained from serial trypsin digestion, used to isolate the cells, were characteristic of the metabolically active ruminal epithelial cells (REC). The first published method for isolating REC (Galfi et al., 1981) demonstrated that REC cultured for 10 to 12 d retained expression of carbonic anhydrous isoenzyme, which was used as a marker of cells obtained from the stratum basale, spinosum, and granulosum. Many hours (8 h) were required to obtain the desired cells through the trypsin digestions. However, this study contained little characterization of the different cell fractions

during isolation or description of the cells as they grew in culture. In a subsequent study (Inooka et al., 1984), the isolation time was reduced through the use of 10-min trypsin incubations. In this study, several populations of cells were described immediately following isolation. These included large dead cornified cells, elongated cells, and round cells. The latter two cell types were found to be over 90% viable when analyzed with a trypan blue exclusion test. Culturing the REC, in this same study, resulted in two distinct populations; epithelial cells and fibroblast-like cells. Heterogeneous populations of cells, following isolation of primary REC, were also reported in other previous work (Galfi and Neogrady, 1989; Galfi et al., 1993; Stumpff et al., 2011). Together, results from these studies suggest that markers may be necessary to distinguish the cells types to confirm isolation and culture of the targeted stratum basale.

Previous work (Galfi and Neogrady, 1989; Stumpff et al., 2011) has suggested that morphological changes in the REC may occur over time in culture; however, the details of these changes and how they might impact cell function are limited. In the study by Inooka et al. (1984), REC had to be cultured for > 30 days to reach confluence. This may have been due to the short trypsin incubations, leading to an inadequate number of recovered cells. However, there was no description of the changes in cell characteristics that may have occurred over the 30 days, and there were no indicators of cell function reported.

Primary, cultured REC have proven useful in enhancing the understanding of the physiological functions of the ruminal epithelium (Baldwin, 1998), and more answers can be gleaned from this technique. And although the methodology has been developed over the past several decades, many of the previously discussed studies ultimately indicated that the method may benefit from some additional refinement (Stumpff et al., 2011). In particular, reducing the time of the isolation procedure, increasing the number of useable cells while decreasing time to confluence and confirming epithelial characteristics would be beneficial.

The objective of this study was to establish and describe a standardized primary cell culture model to be subsequently implemented for *in vitro* experiments in order to elucidate the inflammatory response and impacts of inflammation on nutrient utilization in ruminal epithelial cells. In addition, this study aimed to characterize changes in REC morphology and functions during culture.

5.2 MATERIALS AND METHODS

5.2.1 Preparation of reagents and culture plates

All reagent and plates were prepared one day prior to cell isolation and preparation was conducted using aseptic techniques in a biosafety cabinet. Reagents were purchased from Sigma-Aldrich (St. Louis, MO, USA), unless otherwise specified, and were sterile and suitable for cell culture. A single lot of fetal bovine serum (**FBS**) was used within a given experiment. The Dulbecco's phosphate buffered saline (**DPBS**) solutions were purchased as sterile, stock solutions (10-fold concentrated). Deionized water was autoclaved (120°C for 45 min) in 900-mL aliquots for the purpose of diluting the buffer stocks to 1X working concentrations (see below for more detail). All final reagents were maintained at a physiological pH of 7.4. Buffers and media were stored at 4°C until use.

5.2.1.1 Transport and wash buffers. Two buffers were prepared using DPBS without calcium and magnesium (Cat. D1408) to contain 4% (**DPBS-4**) or 1% (**DPBS-1**) of Antibiotic-Antimytotic (**Anti-anti**; Thermo Fisher Scientific, Waltham, MA, USA) solution. An additional buffer was prepared using DPBS containing calcium and magnesium (Cat. D1283) with 1% Anti-anti (**DPBS-CM**). The DPBS-4 buffer contained 40 mL/L of Anti-anti (Final concentrations: 400 U/mL penicillin, 400 µg/mL streptomycin, 1 µg/mL amphoteracin B; Thermo) plus Nystatin (Final concentration: 240 U/mL). Both DPBS-1 and DPBS-CM contained 10 mL/L of Anti-anti (Final concentrations: 100 U/mL penicillin, 100 µg/mL streptomycin, 0.25 µg/mL amphoteracin B; Thermo).

5.2.1.2 Culture media. Two complete media solutions were prepared, one with M199 medium (**M199C**; Cat. M2154) and one with minimum essentials medium (**MEMC**; Cat. M4655). The M199C contained final concentrations of: 0.1 g/L L-glutamine; 15% FBS (Thermo); 20 m*M* HEPES; 1% Anti-anti (Thermo); 240 U/mL Nystatin, 50 mg/mL gentamicin and 100 mg/L kanamycin (Thermo). The composition of MEMC was: 10% FBS (Thermo), 20 m*M* HEPES and 1% Anti-anti (Thermo).

5.2.1.3 Trypsin solution. Sterile trypsin-EDTA solution (0.25% trypsin, 0.02% EDTA; Cat. T4049) was purchased frozen at -20°C. Prior to use, the solution was thawed slowly overnight at 4°C and then 1% Anti-anti was added. During the cell isolation procedure, the

trypsin solution was kept warm to prevent cold shock. A new bottle of trypsin was used for each isolation. Trypsin solution that was remaining after the isolation was aliquoted into 15-mL conical tubes (Thermo) and frozen at -20°C to be used later for passaging.

5.2.1.4 Collagen coating of culture plates. Culture dishes, 60-mm in diameter (Thermo), were coated with bovine collagen I (Thermo). The thin coating procedure, provided by the manufacturer, was followed in order to provide growth substrate recommended for primary cells (Galfi and Neogrady et al., 1989). The collagen stock was diluted with sterile filtered 20 m*M* acetic acid to achieve a final concentration of 5 µg/cm^2. Two millilitres of the diluted collagen were added to each culture plate, which were then incubated at room temperature for 1 h. Subsequently, the collagen solution was aspirated gently and each dish was rinsed three times with 2 mL of DPBS-CM. The plates were stored overnight in the incubator (see below for conditions) with 2 mL of M199C added to each.

5.2.2 Isolation procedure

5.2.2.1 Tissue collection. Bovine tissue was sourced from a local slaughterhouse. Post-mortem collection of tissues was pre-approved by the University of Saskatchewan Research Ethics Board (protocol 20110127; Saskatoon, SK, Canada). Within 30 min of death, epithelial tissue was excised from the central ventral sac of the rumen. Two to three pieces, approximately 10 cm^2 each were collected, depending on the density of papillae. Fat and connective tissue were removed; however, the mucosa was not stripped from the serosal tissue. At the slaughterhouse, the tissue was washed thoroughly with ice-cold DPBS-4 until the majority of digesta was removed and the buffer ran clear (note: DPBS-4 is normally slightly cloudy due to the Nystatin). Once clean, the tissue was submerged in DPBS-4 within a 500-mL plastic screw-cap Erlenmeyer flask (Thermo), which had been previously disinfected with 70% ethanol, and transported on an ice pack back to the lab. Once sealed, the flask was not opened again until inside the biosafety cabinet. All materials in contact with the tissue at this point forward were considered sterile and strict aseptic handling techniques were observed.

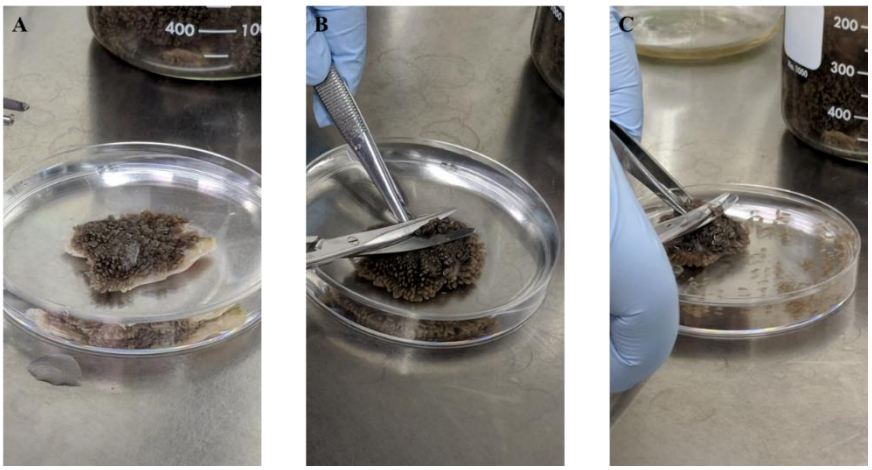

Figure 5.1 Papillae clipped off at their base from pieces of ruminal epithelium submerged in DPBS-1.

Once in the lab, the tissue was kept submerged in the DPBS-4. To collect ruminal papillae, a small piece (4 cm^2) of the epithelium was trimmed off and transferred to a disposable petri dish (Thermo) containing DPBS-1 (Figure 5.1A). Papillae were clipped off at their base with stainless steel scissors (Figure 5.1B and C) being careful to avoid any underlying tissue. The buffer was gently decanted and fresh DPBS-1 was added to the petri dish. The papillae and the buffer were transferred to a beaker. Subsequently, another small piece of epithelium was trimmed off and the process started again. Papillae collected within the same beaker were washed with DPBS-1 three times by adding fresh buffer, vigorously swishing the beaker, followed by decanting. Clean papillae were then transferred to a 250-mL Erlenmeyer flask (Thermo), sealed with a foam plug (Thermo), and aluminum foil over the top. Approximately 30 g, wet weight, of papillae was added to each flask. To determine the weight of the tissue, the sealed flask (including the plug and the foil) was weighed before and after the addition of the tissue. A stirring magnet approximately 3.5 cm in length, which had been soaked in 70% ethanol, was transferred into the flask with the tissue.

5.2.2.2 Trypsin incubations. A 1-L beaker with a vinyl-coated lead flask weight (Thermo) in the bottom and approximately 200 mL of water was placed on a stirring hotplate (Isotemp, Thermo), creating a double water bath that prevented direct contact between the tissue and the hot surface (Figure 5.2A and B). The water temperature was carefully monitored and maintained at 37°C. Trypsin solution (50 mL/30 g tissue) was added to the Erlenmeyer flask,

which was sealed and then placed in the water bath, with the stirring function set to ~100 rpm, for a duration of 30 min. Following the incubation, the supernatant was decanted and fresh trypsin solution was immediately added to the flask. The sealed flask was then returned to the water bath for another 30-min incubation. Supernatants from fractions 1 and 2, containing mostly keratinized cells (Stumpff et al., 2011), were discarded. Supernatants from fractions 3 to 7 were strained, through sterile 4-ply gauze (Medicom, Inc, Pointe-Claire, QC, Canada) set in a glass filling funnel (Thermo), into a 50-mL conical tube (Figure 5.2C). Each of the supernatants from fractions 3 to 7 were centrifuged at 200 × *g* for 5 min at room temperature with the break applied at a moderate setting. The supernatants were discarded and the remaining cell pellets were washed with 10 mL of DPBS-CM. The cells were centrifuged again, under the same settings, and then washed twice more with 10 mL of DPBS-CM.

Figure 5.2 Ruminal epithelial cell isolations utilized a hot stir plate set to 37°C. Flasks containing papillae and trypsin solution were placed in beakers with water (A). In later isolations, a flask ring was used to prevent direct contact between tissue and the hot surface (B). Following each digestion, supernatants were strained through sterile gauze into 50-mL tubes (C)

5.2.2.3 Seeding of cells following isolation. After the final wash, the supernatant was discarded and the pellets were re-suspended and pooled in a minimum of 25 mL of M199C. The final volume was increased by 5 to 10 mL if the cell pellets were larger or contained a lot of cellular detritus, which was identified as larger, flat cells or clumps of irregular cellular material, often brown or gray (Figure 5.3). The volume adjustment was determined subjectively by visually assessing the cell suspension using an inverted microscope set to 10× magnification. A high density of small, round cells that were easily visible amongst the cellular detritus was considered ideal (Stumpff et al., 2011). The M199C in the stored, pre-coated culture dishes was aspirated and discarded. The pooled cell suspension was mixed within the 50-mL tube by

aspirating and dispensing with a 25-mL serological pipet three times. The cell suspension was then added to the plates at 5 mL/plate. Following the seeding procedure, plates were placed in a humidified incubator set to 37°C and gassed with 5% CO_2.

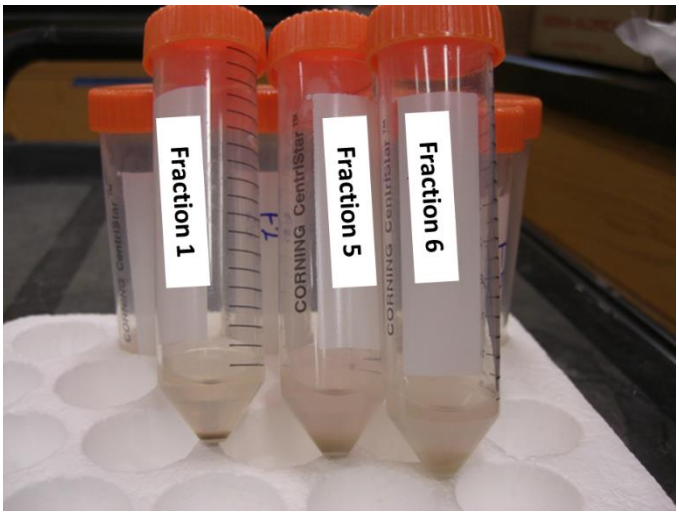

Figure 5.3 Comparison of cell pellets from early and late fractions. Fractions 1 and 2 contained brown/gray cellular detritus. Fractions 3 to 6 were characterized by cream-colored pellets with little or no visible detritus.

5.2.3 Culturing of isolated cells

5.2.3.1 Day 1 and 2 following isolation. The first day after the isolation, media was aspirated and discarded. The plates were then washed three times with DPBS-CM. This was accomplished using a serological pipet to vigorously dispense 5 mL of the buffer/plate over the surface and followed by aspirating and discarding the used buffer. A new pipet was used for each wash for each plate. After the third wash, 5 mL of fresh M199C was added to each plate and the plates were returned to the incubator. On the second day, the plates were again washed with same procedure as described for the first day. After the last wash, the media was replaced with MEMC. Fresh media was replaced every 2 to 3 days thereafter.

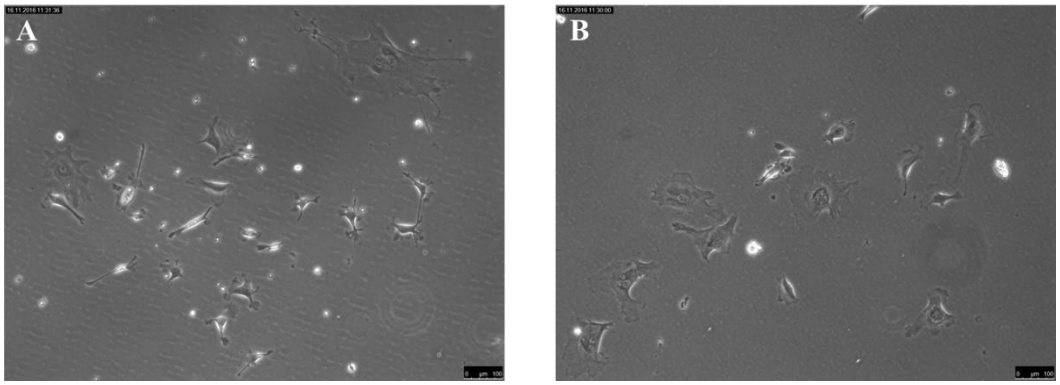

Figure 5.4 Fibroblast-like cells with membrane projections (A) and solitary cells (B) following isolation of REC.

5.2.3.2 Establishment and growth. Each day of the first week, the cells were monitored for growth through visual assessment using an inverted microscope set to 10× magnification. For the first three days, the cells were monitored for adherence, initially characterized as round, "balled up" cells that began to flatten out as their membrane proteins adhered to the surface. Plates were discarded if there was few or no adherent cells. After sufficient adherence, cells were considered to be established when the formation of colonies was observed and, subsequently, progressive proliferation, which normally occurred within the first week. Plates were monitored during this time for abnormally-shaped cells, such as fibroblast-like cells (Figure 5.4A) or for cells growing in solitary (not in contact with neighboring cells; Figure 5.4B). Plates with abnormal growth or cell types were discarded within the first week. In addition to assessing the characteristics of the cells, plates were carefully monitored for bacterial or fungal contamination and any suspects were immediately disposed. After the first week, cells continued to be monitored by visual assessment each time the media was refreshed. When the entire surface of the culture plate was occupied by cells, 100% confluence was achieved (Figure 5.5). Plates that were at least 90% confluent were passaged and reseeded in new culture vessels, which normally occurred 10 to 12 days following initial isolation.

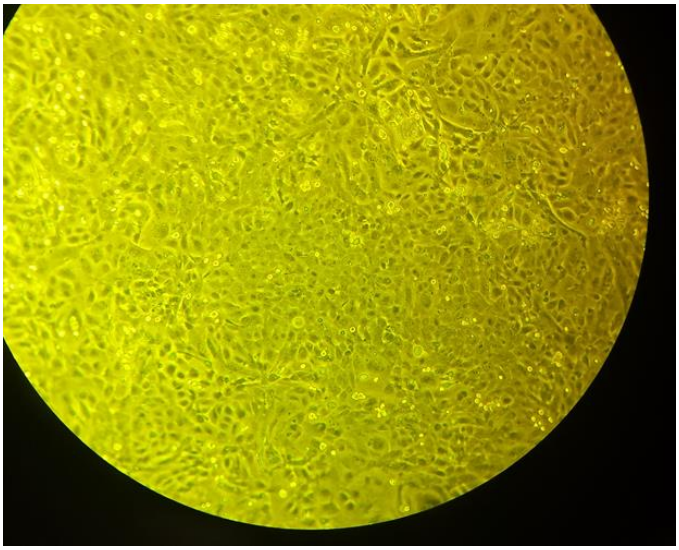

Figure 5.5 Ruminal epithelial cells at 100% confluence. Cells were visualized at 10x magnification using an inverted microscope.

5.2.3.3 Procedure for passaging cells. To passage, the media was aspirated and discarded from the plates, which were then washed two more times, as described for d 1 and 2 old cells. To each plate, 2 mL of warmed trypsin-EDTA (same as for the isolation) was added and the plates were placed in the incubator for 12 min. Immediately following, 4 mL of MEMC was added to each plate and the detached cells were transferred to a 50-mL tube (Thermo). The tubes were centrifuged at 200 × *g* for 5 min at room temperature, the supernatant was decanted, and 10 mL of fresh MEMC was used to re-suspend the cells by aspirating and dispensing three times with a serological pipet. The suspended cells in the 10 mL of MEMC were pipetted into a T75 culture flask (75 cm^2 surface area with filter caps; Thermo). The flasks were not coated with collagen. Reseeded cells were returned to the incubator and the media was again refreshed every 2 to 3 d. Flasks were passaged every 5 to 7 days, or when cells were confluent, splitting (diluting) them 1:3 each time.

5.2.3.4 Detection of fibroblast contamination. When approximately 75% confluence was reached, a single plate was trypsinized (as described above) and the cells used to determine the level of contamination with fibroblasts. An antibody against CD90 (Table 5.1), a fibroblast marker, was used to stain the cells which were then analyzed by flow cytometry (see below for details on the staining procedure and flow cytometry analysis). All isolated cells, destined for an

experiment, were tested for fibroblast contamination. Cells with greater than 10% fibroblasts were discarded (Kisselbach et al., 2009).

5.2.4 Assessment of the characteristics of cultured primary REC

5.2.4.1 Cell characteristics in weeks 1 to 4. Using antibody staining and flow cytometry, the expression of epithelial cell markers, claudin-4 (CLDN4), zonula occludens-1 (ZO1), E-cadherin (ECAD) and a pan-cytokeratin were evaluated. In addition, expression of hydoxymethylglutaryl-CoA synthase (HMGCS1), a ketogenic enzyme, was also analyzed. Antibody sources and working concentrations are summarized in Table 5.1. Cells isolated from six cattle over a 4-month period were collected by trypsinization on d 8, 15, 22, and 30 following isolation. Cytokeratin was only evaluated at d 15. Prior to the staining procedure, the concentration of viable cells was determined. Some flasks of cells were maintained (by

Table 5.1 Description, sources and working concentrations of antibodies used for flow cytometry analysis.

Antibody	Species	Clone ID	Source	Function	Final Concentration
Primary					
CD90	Mouse IgG1 kappa	AF-9	Novus[1]	Fibroblast marker	0.02 mg/mL
CLDN4	Rabbit	Polyclonal	Abcam[2]	Tight junction marker	5 µg/mL
Cytokeratin	Mouse IgG1 kappa	AE-1/AE-3	Novus	Epithelial marker	1 µg/mL
ECAD	Rabbit	Polyclonal	Abcam	Epithelial marker	1 µg/mL
HMGCS1	Rabbit	Polyclonal	Thermo[3]	Ketogenic enzyme	0.04 mg/mL
ZO1	Rat IgG_{2a}	R40.76	SCBT[4]	Tight junction marker	2 µg/mL
Secondary					
Alexa Fluor 488	Goat anti-mouse IgG preadsorbed		Abcam	Detection	4 µg/mL
Alexa Fluor 488	Goat anti-rabbit IgG H&L		Abcam	Detection	4 µg/mL
Alexa Fluor 488	Donkey anti-rat IgG H&L preadsorbed		Abcam	Detection	1 µg/mL

[1]Novus Biologicals, Centennial, CO, USA
[2]Abcam, Cambridge, UK
[3]Thermo Fisher Scientific, Waltham, MA, USA
[4]Santa Cruz Biotechnology Inc, Dallas, TX, USA

passaging and splitting as described above) beyond 4 wk of age to assess morphology changes, but were not collected for qualitative measurements.

In a separate experiment, cells were used to evaluate the effects of time in culture on indicators for physiological and metabolic changes. Genes associated with cytoskeletal organization (*CDH1*, *TGFB1* and *SNAI1*) and cell cycle (*CDK1* and *MYC*) were selected as indicators for structural and morphological changes. To evaluate changes in metabolic function, expression of *MCT1*, *MCT4*, *G6PD*, *BDH1*, *ACAT1*, *IGFBP3*, and *IGFBP5* were evaluated. Cells from nine yearling beef heifers were collected by lysis in 1 mL of Trizol (Thermo) during week 1 (d 4 or 5) or at 2 wk (d 13 to 15) following isolation. Samples were frozen at -80°C for RNA extraction and analysis by real time qPCR. Prior to collection, all cells were also analyzed for fibroblast contamination, as described above. Cells collected in wk 1 were < 50% confluent and were collected directly from the 60-mm dishes. Cells collected at 2 wk were passaged on d 10 to 12 and re-seeded into 24-well culture plates at a rate of 10×10^4 cells/mL. Cell samples were collected when 100% confluence was achieved.

5.2.4.2 Cell counting and viability. To count the number of live and dead cells, a subsample of 50 µL of the cell suspension was used. The cell suspension was diluted with a 1:2 ratio of cell suspension:Trypan Blue (Sigma) mixed together in a 0.6-mL microcentrifuge tube by briefly (< 1 s) vortexing. Ten microliters were then pipetted into the chamber of a hemocytometer (Thermo) and cell viability was determined with a Trypan Blue exclusion test (the number of uncolored cells versus those that take up the blue dye). Cells were counted in all four, 4 × 4 corner squares. The concentration of cells reseeded was dependent on the vessel.

5.2.4.3 Cell staining and flow cytometry. Between 2 and 4×10^6 cells/mL were incubated in a 96-well round bottom plate (Thermo) for 1 h at 4°C in 200 µL of fixation/permeabilization reagent solution using the FoxP3/Transcription Factor staining buffer kit (eBioscience, San Diego, CA, USA). The solution was prepared as a 3:1 ratio of fixation/permeabilization diluent:concentrate (provided with the kit). The plate was then centrifuged at 500 × *g* for 3 min at room temperature and the supernatant was removed by inverting the plate with a single but rapid snapping motion. The cells were blocked with 200 µL FBS (neat) for 15 min at room temperature. The plate was centrifuged, under the same conditions, and the supernatant removed again. Cells were then incubated with 10 µL of primary antibody for 10 min at room temperature. The plates were washed twice by adding 200 µL of

permeabilization buffer (provided with the kit; diluted 1:10), centrifuged under the same conditions, and again the supernatant was removed. The cells were incubated with 10 µL of secondary antibody for 10 min at room temperature in the dark and the plate was subsequently washed twice, using the same method described above. After the last wash 200 µL of permeabilization buffer was used to resuspend the cells in 1.5-mL microcentrifuge tubes (Thermo). Cells were analyzed using an Accuri C6 flow cytometer (BD Biosciences, Franklin Lakes, NJ, USA). Data analysis was performed with FlowJo version 10.0.7 (BD). This experiment was designed as a pilot study and not all proteins were measured at each time point. Therefore, the data did not allow for statistical analysis.

5.2.4.4 RNA extraction and real time qPCR. RNA was isolated using a phenol-chloroform extraction procedure modified from the protocol provided with the Trizol reagent (Thermo). The cell samples in Trizol were thawed at room temperature and 200 µL of chloroform was added to each sample. The tubes were mixed vigorously and centrifuged at 10,000 × *g* for 10 min at 4°C. Subsequently, 500 to 600 µL of the aqueous phase was transferred to a new tube and an equal volume of isopropanol was added to each tube. Linear acrylamide (Thermo) was added as a co-precipitant at a final concentration of 15 µg/mL, in order to visualize the RNA pellet. Samples were incubated on ice for 1 h. The samples were then centrifuged at 14,000 × *g* for 15 min at 4°C. The supernatant was carefully aspirated and the pellet was washed by adding 1 mL of 100% ethanol, centrifuged at 14,000 × *g* for 15 min at 4°C, and the supernatant was aspirated. The pellet was re-suspended in 200 µL of nuclease-free water and a second precipitation was performed by adding 200 µL isopropanol and 10 µL of 3 *M* sodium acetate to each tube and incubating the samples overnight at -20°C. The following day, the ethanol wash, described above, was repeated and the pellet was resuspended in 13 µL of nuclease-free water.

Samples were analyzed using a Nanodrop (ND2000c; Thermo) for purity and to quantify the RNA concentration. A 1.2% agarose gel was used to analyze the samples for RNA integrity. SYBR Safe (Final concentration: 0.007%; Thermo) was used to visualize the RNA with a gel imager (UVP, Upland, CA, USA). Distinct 28S and 18S bands were confirmed in all samples before they were used in subsequent steps.

The High Capacity Reverse Transcription kit (Thermo) was used to synthesize cDNA from 2 µg of RNA. Reverse transcription was performed with a thermocycler (Eppendorf, Hamburg, Germany) under the following conditions: 25°C for 10 min, 37°C for 120 min, 85°C for 5 min and then cooled to 4°C. The resulting cDNA was diluted with nuclease-free water to a final concentration of 10 ng/µL and stored at -20°C.

Quantitative real-time PCR was performed using 20 ng of cDNA with 7.5 µL of SsoFast EvaGreen Supermix (Bio-Rad, Hercules, CA, USA) on a CFX96 Real-Time PCR Detection system (Bio-Rad). Samples were run in duplicate under the following conditions: 1 cycle at 95°C, 30 sec, for enzyme activation and 40 cycles at 95°C followed by 60°C, 10 sec, for denaturing and annealing. Primer pairs, listed in Table 5.2, were designed using the National Center for Biotechnology Information database and were obtained from IDT (Coralville, IA, USA). Primers were designed to span exon-exon junctions, where possible, and were validated by assessing efficiency (-1+10 (-1/slope) × 100) of a serial dilution of pooled cDNA. Primers with efficiencies between 90 and 110% were considered acceptable. Melt curves were performed following the last annealing cycle and assessed for dimer formation and to verify the presence of a single product.

The Ct values for the target genes were normalized to the geometric mean of three housekeeping genes (*ACTB*, *GAPDH* and *STX5*). Statistical analysis was performed on the ΔCt using the MIXED procedure of SAS 9.4 (SAS Institute, Cary NC, USA) with time as a fixed effect and animal within plate as random. Data are presented as fold change with the mean expression of week 2 held relative to the mean expression of week 1 within each heifer.

Table 5.2 Primer used for quantitative real-time PCR

Gene Name (official gene symbol)	Source[1]	Sequence (5'-3')	Efficiency[2]
Housekeeping			
Beta actin (ACTB)	NM_173979.3	F: GAGCTACGAGCTTCCTGACGGGC R: AATGCCGCAGGATTCCATGCCCAG	96
Glyceraldehyde-3-phosphate dehydrogenase (GAPDH)	NM_001034034.2	F: GGGTCATCATCTCTGCACCT R: GGAGGCATTGCTGACAATCT	91
Syntaxin 5 (STX5)	NM_001075444.1	F: CCATTCAGAGGATCGACGAG R: GGATGTGACCGACTGGAAGT	103
Cytoskeletal organization and cell cycle			
Cyclin dependent kinase 1 (CDK1)	NM_174016.2	F: GGGCACTCCCAATAATGAAG R: ACATTTTCGAGAGCAGATCCA	95
E cadherin (CDH1)	NM_001002763.1	F: GCTGGACCGTGAGAGTTTTC R: TGGGAGCATTATCATTGGTG	95
MYC proto-oncogene, bHLH transcription factor (MYC)	NM_001046074.2	F: GACCAGTAGCGACTCTGAGGA R: GACTAACGGGCTGTGAGGAG	106
Snail family transcription repressor 1 (SNAI1)	NM_001112708.1	F: GCACGACTCTTCTCCAGAGC R: CAGATGAGTGTCGGCAAGG	98
Transforming growth factor beta 1 (TGFB1)	NM_001166068.1	F: ACTGCTTCAGCTCCACAGAA R: TCCAGGCTCCAGATGTAAGG	105
Metabolism			
Acetyl-CoA acetyltransferase 1 (ACAT)	NM_001046075.1	F: CGGGTGCAGGAAATAAGGTA R: TAGTGGCTGGCAGAGAGGA	103
3-hydroxybutyrate dehydrogenase 1 (BDH1)	NM_001034600.2	F: GACCCTGAGAAAGGCTTGTG R: TCCTTGTAGGTCTCCATGCTG	96
Glucose-6-phosphate dehydrogenase (G6PD)	NM_001244135.2	F: TGGGGGCTACTTTGATGAAT R: GCACCTTGACCTTCTCATCG	95
Insulin-like growth factor binding protein 3 (IGFBP3)	NM_174556.1	F: GCTGAACCACCTCAAGTTCC R: CGGCACTGCTTTTTCTTGTA	99
Insulin-like growth factor binding protein 5 (IGFBP5)	NM_001105327.2	F: CAAGAGAAAGCAGTGCAAACC R: AGTCCCCGTCCACGTACTC	98
Solute carrier family 16 member 1 aka MCT1 (SLC16A1)	NM_001037319.1	F: TCCATCGGCTTCTCTTATGC R: GCTGATAGGACCTCCACCAT	95
Solute carrier family 16 member 3 aka MCT4 (SLC16A3)	NM_001109980.3	F: TGTGGTGAGCTATGCCAAGG R: TCAGCGAAGCCGTTGAAGAA	98

[1]National Center for Biotechnology Information (NCBI)
[2]Efficiency= $-1 + 10^{(-1/\text{slope})}X100$

5.3 RESULTS

5.3.1 Visual observations

5.3.1.1 Isolation. Cell pellets from fractions 1 and 2 during isolation contained mostly cellular detritus, which could be grossly observed and was characterized as brown or gray material that clumped together and could not easily be dispersed. This material was still present in the subsequent fractions but was substantially less (Figure 5.3). Fractions 3 to 7 were characterized by a cream-colored cell pellet that could be easily re-suspended.

When assessed microscopically, three distinct cell types were typically observed: large flat cells, small round cells, and small elongated cells (Figure 5.6). More large flat cells were observed in the earlier fractions, whereas the small round cells were predominant in later fractions (data not presented). An increasing number of small, elongated cells were visible if the papillae were incubated for more than 7 fractions. In addition to cells, indistinct cellular material was often observed immediately following the isolation (data not presented).

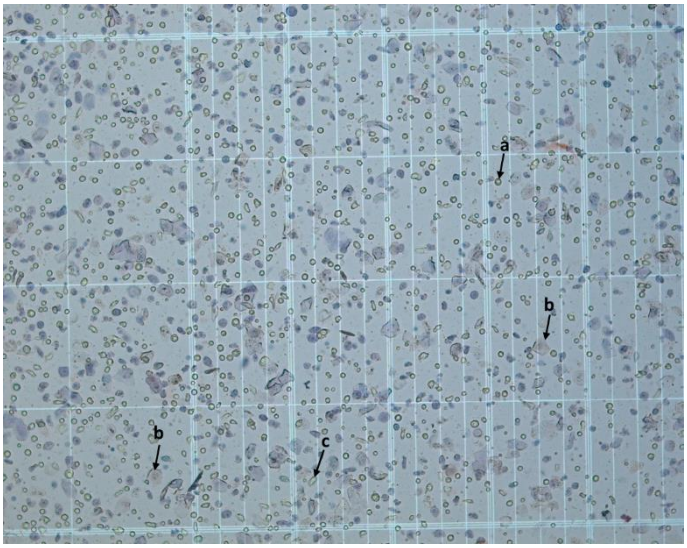

Figure 5.6 Abundant small, round cells (a), large, flat cells (b) and elongated cells (c) following isolation of ruminal epithelial cells. Image captured at 10x magnification.

5.3.1.2 Establishment and growth. On the first day following isolation, after removal of all loose materials via the washing steps, cells that survived the isolation procedure were observed adhered to the plate surface. Small, elongated cells did not readily adhere. Large flat cells were occasionally observed adhered to the surface. Most of the adhered cells remained round and "balled up" for the first 2 to 3 d, but would gradually flatten. Large nuclei became easily visible at 10x magnification. Between d 2 and 4, cells began to form small colonies, which were initially observed as cobblestone-like clusters of 5 to 20 cells (Figure 5.7A). Subsequently, colonies progressively grew in size (Fraction 5.7B) with the rate of growth appearing to increase (by visual assessment) each day. Cell colonies continued to proliferate and expand across the plates until confluence had occurred usually between d 10 and 12 relative to cell isolation. After passaging, cells proliferated and morphology remained similar for another 7 to 10 d, at which point cells gradually became larger and less uniform. After 4 to 6 wk in culture, cells became very large with striations in their cytoplasm (data not shown).

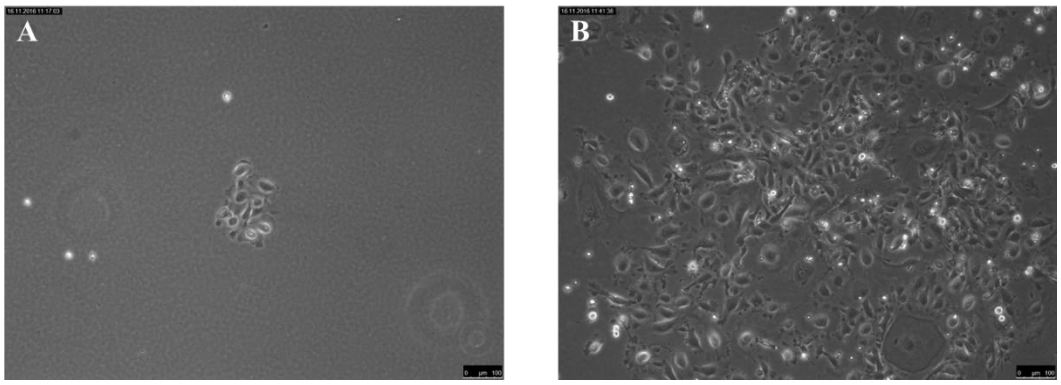

Figure 5.7 Ruminal epithelial cells in culture. A: small colonies began to form 2 to 4 days in culture. B: Cells progressively proliferated and expanded across the culture plate within the first 2 weeks.

5.3.2 Flow cytometry

5.3.2.1 Fibroblast contamination. Out of 19 isolation events, 3 were found to contain more than 10% fibroblasts (Figure 5.8). Within the isolations where cells contained less than 10% fibroblasts, the majority contained less than 5%.

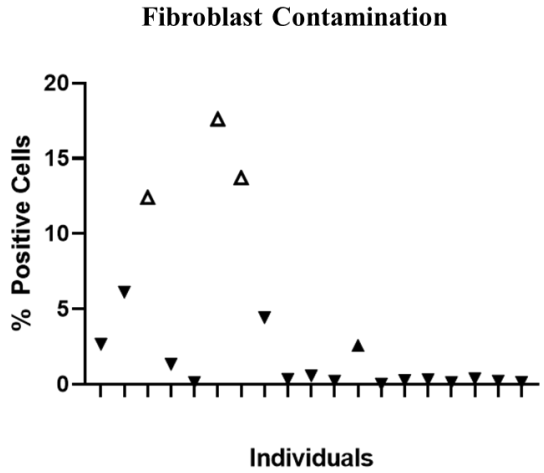

Figure 5.8 Fibroblast contamination determined in cultured primary ruminal epithelial cells using a CD90 antibody and flow cytometry analysis. Cells with greater than 10% fibroblasts (open triangles) were discarded. Cells with less than 10% fibroblasts (filled triangles) were used for experiments.

5.3.2.2 Expression of epithelial cell markers. The percent of cells positive for CLDN4 (Figure 5.9A) was approximately 50% on d 8, decreased to below 10% on d 15, and below 5% on d 22. By d 30, expression of CLDN4 was below detection limits. The percent of cells expressing ZO1 (Figure 5.9B) was > 30% on d 8 and was 13% at d 22. Expression of ECAD (Figure 5.9C) was detected on approximately 80% of the cells on d 15 but decreased to below the detection limit by d 22. While only evaluated at d 15, cytokeratin (Figure 5.9D) was expressed in 38% of the cells at this time point. The percent of cells expressing BDH1 was 83.6, 89, and 81.2 % on d 8, 15, and 22, respectively (Figure 5.10A). HMGCS1 (Figure 5.10B) was > 30% on d 8 but the proportion decreased by 50% by d 22. Expression of HMGCS1 remained constant from d 22 to 30.

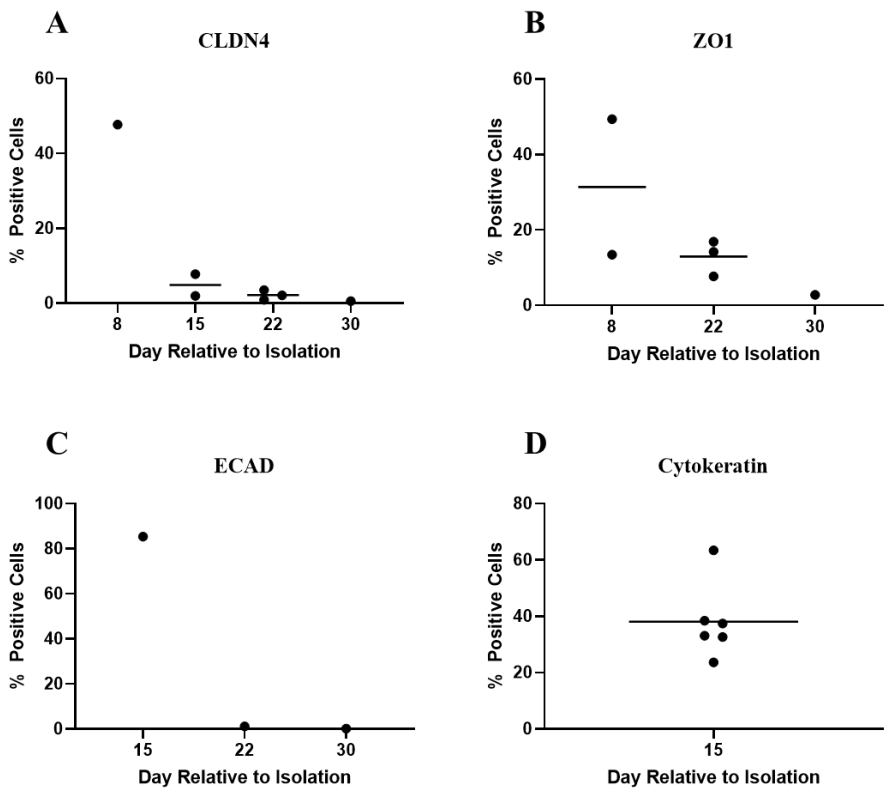

Figure 5.9 Percent of cells positive for epithelial cell markers claudin-4 (CLDN4; A), zonula occludens-1 (ZO1; B), ecadherin (ECAD; C) and cytokeratin (D) analyzed by flow cytometry. Data are presented for individual animals. Not all proteins were measured at each time point. At some time points, only a single measurement could be obtained, therefore statistical analysis was not conducted. Cytokeratin was only evaluated at d 15.

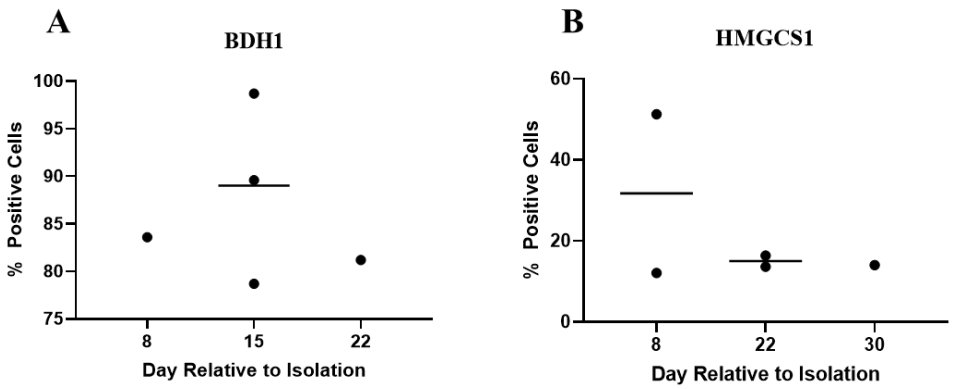

Figure 5.10 Percent of cells positive for epithelial cell markers Beta-hydroxybutryrate dehydrogenase (BDH1; A) and hydroxymethylglutaryl-CoA synthase (B) analyzed by flow cytometry. Data are presented for individual animals. Not all proteins were measured at each time point. At some time points, only a single measurement could be obtained, therefore statistical analysis was not conducted.

5.3.3 Gene expression.

In cells collected at 2 wk of age, expression of *CDH1* (Figure 5.11A) was decreased 17-fold ($P = 0.002$) compared to those collected within the first week; whereas, expression of *TGFB1* (Figure 5.11B) and *SNAI1* (Figure 5.11C) increased at 2 wk (2.8-fold; $P < 0.001$ and 4-fold; $P = 0.050$, respectively) relative to the first wk. While *CDK1* (Figure 5.12A) expression was not influenced ($P = 0.28$), *MYC* (Figure 5.12B) decreased 1.4-fold ($P = 0.001$) at for 2-wk old cells relative to the first wk.

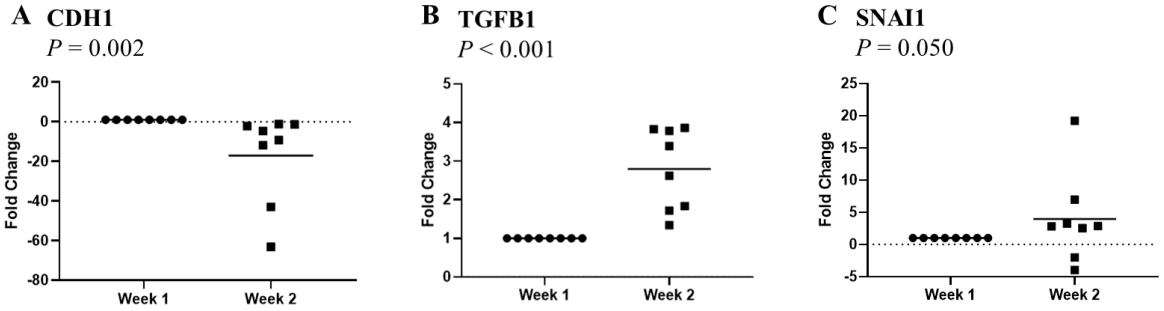

Figure 5.11 Expression of genes associated with cytoskeletal organization in primary ruminal epithelial cells culture in week 1 or at week 2. Data are presented as fold change with expression at week 2 held relative to the mean expression of week 1 within each animal.

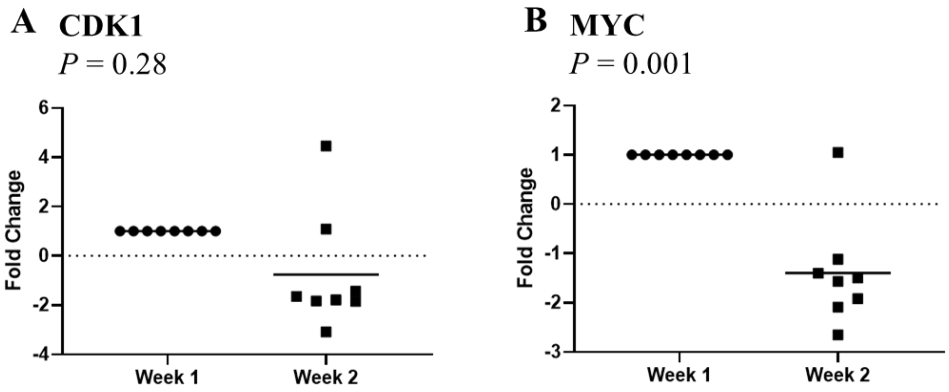

Figure 5.12 Expression of genes associated with cell cycle progression in primary ruminal epithelial cells culture in week 1 or at week 2. Data are presented as fold change with expression at week 2 held relative to the mean expression of week 1 within each animal.

Compared to cells collected in the first week following isolation, expression of *MCT1* (Figure 5.13A) was decreased 1.7-fold ($P = 0.003$) and *MCT4* (Figure 5.13B) was increased 26.6-fold ($P = 0.004$) for 2-wk old cells. Expression of both *G6PD* (Figure 5.14A) and *BDH1* (Figure 5.14B) were decreased for 2 wk (3.1-fold; $P = 0.002$ and 4.4-fold; $P < 0.001$, respectively) compared to cells collected in the first week of culture.

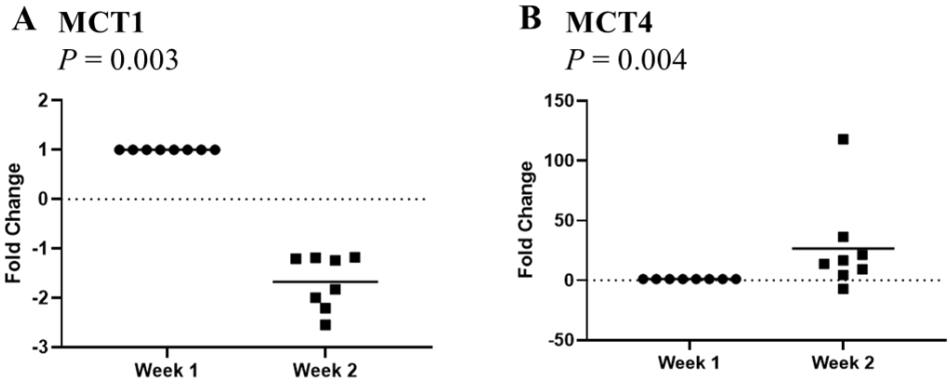

Figure 5.13 Expression of genes associated with nutrient transport in primary ruminal epithelial cells culture in week 1 or at week 2. Data are presented as fold change with expression at week 2 held relative to the mean expression of week 1 within each animal.

Neither the expression of *ACAT1* (Figure 5.14C) or *IGFBP3* (Figure 5.15A) were affected ($P > 0.10$); however, *IGFBP5* (Figure 5.15B) increased by 5.5-fold at 2 wk ($P < 0.001$) relative to cells collected during the first week following isolation.

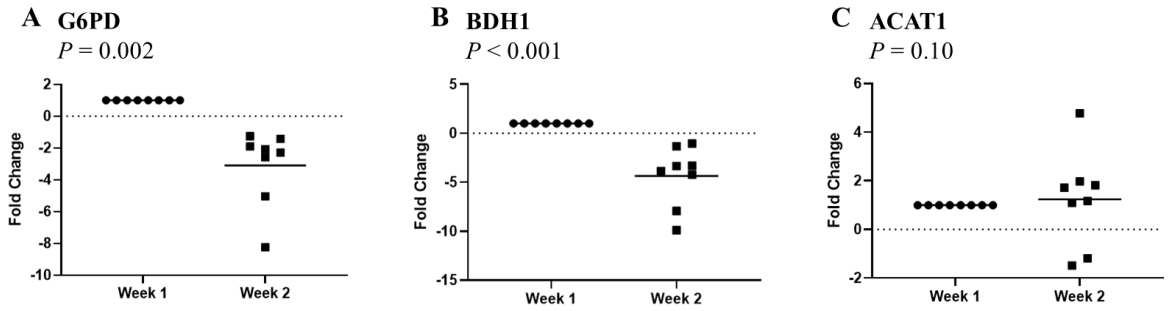

Figure 5.14 Expression of genes associated with cellular metabolism in primary ruminal epithelial cells culture in week 1 or at week 2. Data are presented as fold change with expression at week 2 held relative to the mean expression of week 1 within each animal.

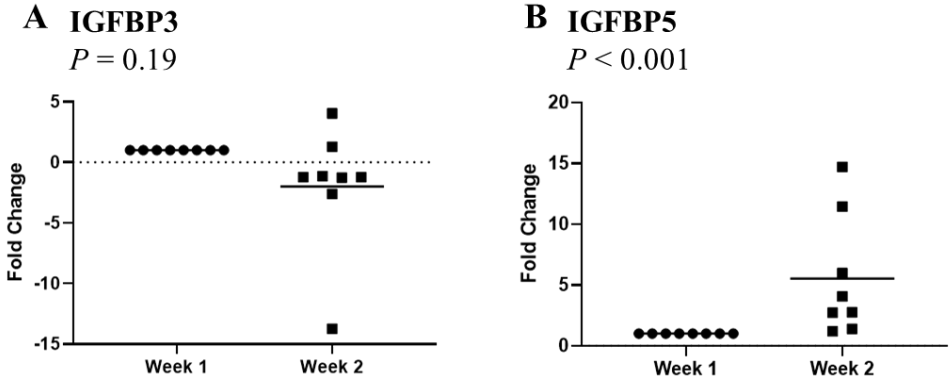

Figure 5.15 Expression of genes associated with cellular metabolism in primary ruminal epithelial cells culture in week 1 or at week 2. Data are presented as fold change with expression at week 2 held relative to the mean expression of week 1 within each animal.

5.4 DISCUSSION

The aim of this study was to establish and document a standardized procedure for isolation and culture of REC, which was based on previously published work (Galfi et al., 1981; Galfi et al., 1993; Muller et al., 2002). To evaluate inflammation and its impact on the metabolism of the REC, it is important that isolated cells were primarily derived from the spinosum and basale strata, which are the metabolically functional units of the epithelium. Stratum basale cells are not only the most metabolically active (Graham and Simmons, 2005) but are also undifferentiated cells making them an obvious target for use in cell culture. However, stratum basale cells are protected by keratinized cells in the stratum corneum and extensive cell to cell junctional proteins within the stratum granulosum and spinosum. Galfi et al. (1981) reported that the number of cornified cells substantially decreased by the third fraction during isolation of bovine REC, and that after the third fraction, the majority of cells obtained were from the stratum spinosum and the stratum basale, particularly those from fractions 6 and 7. Baldwin and Jesse (1991) described isolated REC from fractions 3 to 5 as relatively homogeneous with cells having metabolic activity when evaluated as a single cell suspension. In our study, an adherent, monoculture was used because this model allows for more representative, epithelial characteristics to be observed and measured.

In the present study, only fractions 3 to 7 were collected for subsequent culture. These fractions were characterized by large numbers of small round cells, which has previously been reported as an indicator of cells within the spinosum and basale strata (Baldwin and Jesse, 1991) and have shown to be a determining factor in the success rate of establishing the cells in culture (Stumpff et al., 2011). Beyond the 7^{th} fraction, in the present experiment, an increasing number of small elongated cells were visually observed. Although this cell type could be observed to some extent in all of the fractions, when these were the majority, the success of establishing cells in culture was nearly zero. Therefore, the trypsin incubations were terminated following the 7^{th} fraction. Although the elongated cells were not identified, a study by Inooka et al. (1984) also observed them following isolation of REC and suggested that they may have been fibroblast-like cells. These cells were initially found to be viable; however, the study by Inooka et al. (1984) demonstrated that fibroblastic cells could only be established in culture 10% of the time. In the present study, fibroblast contamination was detected at a rate of 16%. Fibroblast contamination is a commonly reported problem when isolating primary epithelial cells and may cause spurious

results since fibroblasts can contain some of the same markers as epithelial cells (Kisselbach et al., 2009). Fibroblasts can also have similar functions as epithelial cells, such as initiating a pro-inflammatory response if stimulated with MAMPs. Moreover, fibroblasts are more rigorous in culture and can easily out-grow epithelial cells (Kisselbach et al., 2009). Results from previous work with isolated REC (Inooka et al., 1984), and from the present study, suggest that fibroblast contamination from ruminal papillae may not have as much of an impact compared to other epithelial tissues. The reason for this is unknown, but it may be that due to the multiple layers of epithelial cells of ruminal papillae, the exposure of trypsin and dissociation of the fibroblastic cells is limited, therefore limiting their ability to out-grow REC. However, cells should still be monitored to prevent any confounding effects of cultured fibroblasts.

Following the isolation procedure in the present study, adherent cells initially began to form small cobblestone-like colonies, consisting of a few cells which grew progressively over the first two weeks in culture. The cell morphology closely resembled previous reports (Galfi et al., 1981; Galfi et al., 1993). These two studies, used immunohistofluorescent markers, carbonic anhydrase isozyme and cytokeratin, respectively, to verify that the cells in culture were of epithelial origin. Innoka et al. (1984) showed that cell isolation from ruminal epithelium resulted in epithelial-like cells that grew in clusters, as well as fibroblastic cells that appeared to grow apart from one another. In agreement, primary epithelial cells grown in a monolayer are typically described as growing in colonies with a cobblestone appearance (Halldorsson et al., 2007; Jin et al., 2018).

In the current study, cells that were grown in culture exhibited some morphological changes over time that became visibly noticeable after 3 to 4 wk of culture. Cells became larger and flatter, with cytoplasmic striations. These changes were also observed by Stumpff et al. (2011) who suggested that maturation or differentiation of the REC occurred in culture. In support of this theory, cells in the current study were nearly 40% positive for cytokeratin. Cytokeratins are molecules that are unique to the cytoskeleton of epithelial cells and are used as markers of epithelial differentiation (Heyden, et al., 1992; Pastuszak et al., 2015). Although cytokeratin was only evaluated at a single time point in the present experiment (d 15), its expression indicates that the cells are of epithelial origin (Galfi et al., 1993; Muller et al., 2000).

In addition to the visual observations, expression of epithelial markers was evaluated in the REC at 8, 15, 22, and 30 d in culture. Less than 50% of the cells were positive for CLDN4 and

ZO1, proteins of the tight junction complex, at d 8 and expression decreased over time, particularly at around 2 weeks. Tight junctions promote epithelial barrier function and help to maintain polarization of epithelial cells (Ivanov et al., 2010). In addition, multiple studies have shown that there is little expression of tight junction proteins in the stratum basale but they are highly expressed in the granuolum and spinuosum strata (Graham and Simmons, 2005; Stumpff et al., 2011; Liu et al., 2013). The expression is then almost completely lost as the cells differentiate into keratinocytes (Graham and Simmons, 2005). This suggests that in the present study, at d 8, the majority of the cells were derived from the stratum basale and stratum spinosum. In addition, as the cells were not grown on transwells, it was expected that the expression of tight junction proteins would decrease with time in culture (Kauffman et al., 2013). In support, expression of ECAD, both at the mRNA and protein levels, also decreased; however, protein expression remained at 80% of cells at d 15. E cadherin is a cell adhesion molecule specific to epithelial cells and is used as a marker to distinguish epithelial cells from other cell types (Zeisberg and Neilson, 2009). Although the ECAD protein in the present study decreased substantially by d 22, the high percentage of expression at d 15 suggests that the cells were in fact epithelial in origin and suitable for use in subsequent experiments.

Insulin-like growth factor binding proteins mediate the functions of IGF and mediate nutrient utilization (Clemmons, 2012). Previous work has suggested that IGF-binding proteins may be altered by dietary changes or perturbations of the ruminal environment (Steele et al., 2012). In the present study, expression of *IGFBP3* was not changed, but expression of *IGFBP5* was upregulated in cells at 2 weeks. In addition to the roles in metabolism, IGFBPs are also important molecules that promote cell proliferation (Kiepe et al., 2005). Moreover, expression of *G6PD*, the first enzyme in the pentose phosphate pathway, was significantly down-regulated in cells at 2 weeks. The pentose phosphate pathway is a major source of NADPH and is mediated, in part, by *G6PD* (Kowalik et al., 2017). Its activity is closely associated with cell cycle and proliferation (Du et al., 2013). The results of the present study suggest that specific aspects of cell growth may be affected by time in culture. In support, *MYC*, a central regulator of proliferation and apoptosis (Bettess et al., 2005), was up-regulated in cells at 2 wk of age. However, expression of *CDK1* was not affected, suggesting that not all stages of cell cycle were affected. Further exploration revealed changes in the cytoskeletal organization, as expression of both *TGFB1* and *SNAI1* increased at 2 wk of age. These two genes work in tandem to mediate

cell development and differentiation (Lamouille et al., 2014). Together with the morphological changes, observed visually but not presented in this thesis, these results further suggest that the cells may be undergoing maturation or differentiation, which has been previously observed in cultured REC (Galfi and Neogrady, 1989; Stumpff et al., 2011). The *SNAI1* gene is also readily used as a marker of an epithelial to mesenchymal transition, a commonly occurring process in cultured primary epithelial cells (Lamouille et al., 2014; Canciello et al., 2017). Further work is necessary to fully elucidate the morphological and functional changes observed in this study and previous work.

Nutrient transport was explored by evaluating gene expression of *MCT1* and *MCT4*. These molecules are found at epithelial barriers and transport various solutes including SCFA, lactate, pyruvate, and ketones (Halestrap et al., 2012). In the ruminal epithelium, previous studies have demonstrated that MCT1 protein localizes to the basolateral membrane of cells in the stratum basale (Kirat et al., 2005; Graham et al., 2007). Muller et al. (2002) detected MCT1 protein in cells of the stratum basale in the ruminal epithelium, and found that it was also widely expressed in isolated REC that had been grown in culture for 12 to 14 d. The authors concluded that the cultured cells were similar to those in the stratum basale of the native tissue. Likewise, expression of MCT4 protein was found to be localized primarily in the cells of the spinosum and basale strata (Kirat et al., 2007). In the current study, the cultured REC expressed both genes. Interestingly, there was a decrease (1.7-fold) in *MCT1* expression in cells after 2 wk in culture. This could be an additional indicator that REC may begin to differentiate, as MCT1 protein expression has been shown to gradually decrease as the cells migrate towards the lumen (Graham et al., 2007). Kirat et al. (2007) showed that the MCT1 protein was also almost entirely absent from the cells of the corneum and granulosum strata. In addition, in the present study, there was a 26-fold increase in the expression of *MCT4* at 2 wk relative to wk 1. One explanation for the up-regulation of *MCT4* may be an increase in lactate consumption, a process that is observed in cultured epithelial cells following an increase in production of lactate (Zagari et al., 2013). However, lactate levels were not evaluated in the present study. Expression of *MCT4* may have also increased in order to compensate for the decrease in *MCT1*, as the two transporters can bind similar substrates and a degree of flexibility has been demonstrated for *MCT4* (Park et al., 2018).

Cells within the ruminal epithelium are metabolically active and are responsible for primary ketogenesis (Sehested et al., 1999). In fact, in the fed state, most of the circulating

ketones arise from ruminal ketogenesis (Kristensen et al., 2005). In the present study, more than 80% of the REC were positive for BDH1, an enzyme that catalyzes an energy-dependent reaction (Baldwin, 1998). Approximately 30% of cells also expressed HMGCS1 at d 8. These enzymes are both involved in ketone production in the ruminal epithelium (Steele et al., 2012). The lower percentage of cells positive for HMGCS1 may reflect differences in temporal expression patterns compared to BDH1. It may also indicate that there was a shift towards ketone oxidation (Grabacka et al., 2016) or towards an alternative ketogenic pathway that is independent of HMGCS1 (Kristensen et al., 2005). The cultured REC continued to express the HMGCS1 protein, albeit at lower levels, at d 22 and d 30, but BDH1 was expressed in just over 80% of cells at d 22, suggesting that the cells retained their key metabolic function even at 3 wk in culture. Expression of mRNA encoding for *ACAT1* and *BDH1* were also detected in REC. *ACAT1* catalyzes a rate-limiting reaction in the ketogenic pathway. In the present study, while *ACAT1* was not altered by time in culture, expression of *BDH1* decreased 3-fold by week 2. The addition of butyrate to the culture media may also alter the expression of ketogenic enzymes, however this was not evaluated in the present study.

Although the results of the current study suggest that the morphology and metabolic function of REC may be altered over time in culture, the major changes do not occur until approximately 3 wk. Moreover, expression patterns over time of key molecular markers, especially MCT1, MCT4, and BDH1, are interpreted to indicate that the cultured REC retain characteristics similar to the cells of the spinosum and basale strata in native ruminal epithelium, and are therefore suitable for use in experiments within the first 2 to 3 wk after isolation.

5.5 CONCLUSIONS

This study was successful in establishing a standardized method for isolating and culturing primary REC that could be used for *in vitro* experiments. The cultured cells reached confluence and were ready for use after 10 to 12 d. While detected in some isolations, fibroblast contamination did not pose a significant challenge. Changes in cell morphology, including tight junction proteins and epithelial cell markers, were observed over time and suggested that the cells may gradually undergo differentiation. However, molecules associated with nutrient utilization and metabolism indicated that the cultured REC maintained epithelial characteristics

for up to 3 wk. By careful selection of the fractions used for culture, and monitoring of the cells for epithelial characteristics, this method can be used to reliably isolate and culture REC from ruminal papillae. However, time-dependent morphological and functional alterations suggest that the cells should be used for experimentation within the first 2 to 3 wk following isolation.

CHAPTER 6: EFFECTS OF LIPOPOLYSACCHARIDE EXPOSURE IN PRIMARY BOVINE RUMINAL EPITHELIAL CELLS

Following the establishment of a primary cell culture model, Chapter 5, cultured ruminal epithelial cells were used in two controlled in vitro experiments, in order to determine whether these cells can mount a pro-inflammatory response when exposed to LPS. In addition, these experiments were designed to elucidate the nature of the response with regards to LPS dose, duration and timing of exposure. One of the main objectives of this thesis project was to investigate the potential inflammatory response of the ruminal epithelial cells. The manuscript "Effects of lipopolysaccharide exposure in primary bovine ruminal epithelial cells" (Chapter 6) was therefore conducted using primary cells grown in culture. While Chapter 3 provided insight into a whole tissue response, Chapter 6 allowed for an understanding of the responses of the specific cell type of interest in a highly controlled experimental environment. These data contributed a more reduced perspective to the thesis.

Original contribution: My supervisor assisted with the experimental design. All cell culture work and sample collection were performed by me. Co-authors provided assistance with the cell culture techniques. Sample and data analysis were also performed by me. Co-authors assisted with interpretation of the results. I was responsible for the majority of the writing of the manuscript.

Abstract: The objective of this study was to investigate whether cultured ruminal epithelial cells (**REC**) responded to lipopolysaccharide (**LPS**) stimulation and determine if LPS induced a pro-inflammatory response. Primary bovine REC were isolated and grown in culture for two studies. In Study 1, REC were isolated from Holstein bull calves (n = 8) and grown in culture for 10-12 days. Cells were then exposed to 0, 10,000, 50,000 or 200,000 EU/mL LPS for either 6 or 24 h. Effect of LPS exposure on cell viability was analyzed by flow cytometry using a propidium iodide stain. In Study 2, cells were isolated from Holstein bull calves (n = 5) and yearling beef heifers (n = 4). Cells were exposed to either 1,000 or 50,000 EU/mL of LPS using the following conditions: 1) Medium alone time-matched controls (**CON**); 2) 12 h LPS exposure (**12H**); 3)

A version of this chapter has been previously published. Kent-Dennis, C, Aschenbach, J.R., Griebel, P.J., and Penner, G.B. 2020. Effects of lipopolysaccharide exposure in primary ruminal epithelial cells. Journal of Dairy Science. 103:9587-9603. doi.org/10.3168/jds.2020-18652.

24 h LPS exposure (**24H**); 4) 36 h LPS exposure (**36H**); 5) 12 h LPS exposure followed by LPS removal for 24 h before re-stimulating with LPS for an additional 12 h (**RPT**) and 6) 12 h of LPS exposure followed by LPS removal for 36 (**RVY**). For both experiments, total RNA was extracted from REC and real time qPCR was performed to determine relative expression of genes for toll-like receptors (***TLR2*** and ***TLR4***), pro-inflammatory cytokines (***TNF*** and ***IL1B***), chemokines (***CXCL2*** and ***CXCL8***), a lipid mediator (***PTGS2***), and growth factor-like cytokines (***CSF2*** and ***IL7***). In study 1, LPS exposure did not negatively affect cell viability. Treatment of cells with LPS resulted in increased transcript abundance for all genes analyzed. *TLR2, IL7* and *TLR4* had a greater magnitude of change at 6 h compared to 24 h. Quadratic expression patterns were detected for *TNF, IL1B, CXCL2, CXCL8,* and *CSF2*. These results suggest that REC increase expression of a pro-inflammatory genes following exposure to LPS. In study 2, all genes analyzed were up-regulated in a quadratic manner following exposure to LPS for different time intervals. *TLR4, TNF, CXCL2, CXCL8, CSF2,* and *IL7* gene expression was significantly greater after a single 12 h LPS exposure than RPT exposure, suggesting repeated exposure of REC to LPS may induce a tolerogenic effect. When LPS was removed from the media (RVY), transcript abundance for all genes analyzed decreased and expression of *TLR2, TLR4* and *IL7* returned to baseline levels, suggesting REC recovered following exposure to LPS. Overall, the data suggest cultured REC respond to LPS stimulation by increasing transcription of pro-inflammatory genes and this transcriptional response is influenced by the dose, duration, and frequency of LPS exposure.

6.1 INTRODUCTION

To meet their energy requirements, diets containing highly fermentable carbohydrates are often fed to high producing dairy cows (Penner et al., 2009) and finishing beef cattle (Loerch, 1990; Wierenga et al., 2010). However, diets that result in rapid rates of carbohydrate fermentation also increase the risk for ruminal acidosis. As such, ruminal acidosis occurs with rapid rates of short chain fatty acid (**SCFA**) production leading to decreased ruminal pH and increased ruminal osmolality (Nocek, 1997; Penner et al., 2010). In addition, an increase in the concentration of microbe-associated molecular patterns (**MAMP**) molecules such as LPS in ruminal fluid has been reported in cattle fed highly fermentable diets (Nagaraja et al., 1978; Khafipour et al., 2009), presumably as a result of increased bacterial cell lysis (Plaizier et al., 2008).

Low ruminal pH with increased SCFA concentration of ruminal fluid, as well as increased osmolality, have been reported to disrupt epithelial barrier function, increasing the permeability of the ruminal epithelium (Aschenbach and Gabel, 2000; Penner et al., 2010; Meissner et al., 2017), which may lead to translocation of ruminal LPS, bacteria, or other MAMP molecules into peripheral tissue and the induction of a systemic inflammatory response (Khafipour et al., 2009; Aschenbach et al., 2019). Through binding with pattern recognition receptors (**PRR**), such as toll-like receptors (**TLR**), this translocation of MAMP may result in an interaction between luminal-derived MAMP and ruminal epithelial cells (**REC**), potentially triggering a local innate immune response (Li et al., 2013; Pan et al., 2017).

Bovine ruminal tissue has been reported to express PRR (Malmuthuge et al., 2012), but PRR expression can occur in many different cell types present within a tissue (Schilling et al., 2003; Najar et al., 2017). Previous studies (Dionissopoulos et al., 2012; Liu et al., 2013; Arroyo et al., 2017) used ruminal papillae to investigate local inflammatory responses. Pan et al. (2017) showed that expression of genes encoding for pro-inflammatory cytokines, *TNF*, *IL1B* and *IL6*, was up-regulated in ruminal epithelial tissue in dairy cows fed high grain diets. Other studies, despite detecting increased ruminal fluid LPS following high grain diets, have reported no effect (Dionissopoulos et al., 2012), or even an anti-inflammatory effect (Minuti et al., 2015; Kent-Dennis et al., 2019), suggesting that the inflammatory response in the ruminal epithelium is tightly regulated, as is the case in other tissues (Sugimoto et al., 2016). A direct role of REC in these inflammatory responses, however, could not be ascertained due to the heterogenous nature

of ruminal tissue. Zhang et al. (2016) provided evidence that cultured REC increased expression of pro-inflammatory cytokine genes, including *IL1B, TNF* and *CXCL8*, in response to LPS stimulation, suggesting that REC respond canonically. In addition to the classical, pro-inflammatory cytokines, molecules that regulate the phases of inflammation, such as lipid mediators and growth factor-like cytokines, may also be differentially expressed in the ruminal epithelium (Kent-Dennis et al., 2019). However, expression of such molecules has not been previously evaluated in REC. Further investigation is necessary to elucidate the potential for and regulation of a local inflammatory response initiated by REC. The purpose of the present study was to investigate changes in expression of pro-inflammatory genes when isolated REC were exposed to different concentrations, durations and frequencies of LPS exposure to better elucidate the potential role of REC in the local inflammatory response.

6.2 MATERIALS AND METHODS

This study was preapproved by the University of Saskatchewan Animal Research Ethics Board (protocol 20110127), and was conducted in accordance with guidelines set forth by the Canadian Council of Animal Care (Ottawa, ON, Canada). Tissue for this study was obtained from Holstein bull calves (protocol 20160076) and yearling beef heifers (protocol 20100021) which were euthanized for use in unrelated experiments, the conditions of which were not expected to alter the rumen epithelium. Bull calves were euthanized by intravenous injection of 20 mL Euthanyl (Bimeda-MTC, Cambridge, ON, Canada) /45 kg body weight and beef heifers were euthanized by captive bolt stunning followed by exsanguination.

6.2.1 Experiment 1: Dose-Dependent Cytotoxicity and Inflammatory Response to LPS

6.2.1.1 Animals and Tissue Collection. Tissues for this experiment were obtained from 4-month old Holstein bull calves (n = 8) group housed in an outdoor, dry-lot pen. Calves had ad libitum access to water, mixed brome-alfalfa hay and were fed 1.7 kg pelleted ration (16 % crude protein; Co-op® Elite Breeder Power Creep Beef Ration DEC Pellet, Saskatoon, SK Canada)/100 kg body weight/day. Within 15 minutes after euthanasia, ruminal tissue (~ 20 cm^2) was excised from the ventral sac. The tissue was washed thoroughly with ice-cold Ca^{2+}- and Mg^{2+}-free Dulbecco's phosphate buffered saline (**DPBS**; Sigma-Aldrich, St. Louis, MO, USA)

containing antibiotics (final concentration: 400 U/mL penicillin, 400 µg/mL streptomycin and 1 µg/mL amphotericin B; Thermo Fisher Scientific, Waltham, MA, USA) and an antimycotic agent (Nystatin, 240 U/mL; Sigma), and then transported in the same buffer on ice to the laboratory.

6.2.1.2 Ruminal Epithelial Cell Isolation and Cultivation. The procedure for isolation and cultivation of RECs was adapted from Galfi et al. (1981). All DPBS used with the ruminal tissue, upon arrival in the laboratory, contained an antibiotic-antimycotic at a final concentration of 100 U/mL penicillin, 100 µg/mL streptomycin and 0.25 µg/mL amphotericin B (Thermo Fisher).

Ruminal papillae were cut off at their base and washed thoroughly in Ca^{2+}- and Mg^{2+}-free DPBS solution. Papillae were subjected to serial trypsinization using a trypsin-EDTA solution (0.25% trypsin and 0.02% EDTA; Sigma), with an initial papillae to trypsinization solution ratio of 30 g/50 mL. Papillae were agitated in the trypsin solution at 37°C and the supernatant was collected and replaced with fresh solution every 30 min. The first two fractions of supernatant were discarded. Fractions 3 through 6 were strained through sterile gauze to remove cellular detritus. Each fraction was centrifuged at 200 × *g* at room temperature for 5 min. Cell pellets were re-suspended in with sterile DPBS with Ca^{2+} and Mg^{2+} and washed three times using the same centrifugation conditions as described above. Cell pellets from fractions 3 through 6 were then pooled and re-suspended in 20 to 30 mL M199 cell culture medium (Sigma) containing fetal bovine serum (15% v/v; Thermo Fisher), L-glutamine (1.36 mM; Sigma), HEPES (20 m*M*; Sigma), antibiotic-antimycotic (final concentrations of 100 U/mL penicillin, 100 µg/mL streptomycin, 0.25 µg/mL amphotericin B (Thermo Fisher), plus 240 U/mL nystatin (Sigma), 50 mg/L gentamycin (Sigma), and 100 mg/L kanamycin (Thermo Fisher). Cell suspensions were seeded into 60-mm cell culture plates coated with bovine collagen I (Thermo Fisher). Seeding was conducted to ensure a high density of small round cells (Stumpff et al., 2011). Plates were placed in an incubator at 37°C with 5% CO_2 humidified atmosphere. One day after seeding, plates were washed with DPBS containing Ca^{2+} and Mg^{2+} to remove non-attached cellular detritus and fresh culture media was added. On day 2, cells were washed again with DPBS and the media was replaced with Minimum Essential Media (**MEM**) cell culture medium with stable L-glutamine (Sigma) containing fetal bovine serum (10% v/v; Thermo Fisher), HEPES (20m*M*; Sigma) and antibiotic-antimycotic combination (final concentrations of 100 U/mL penicillin, 100

µg/mL streptomycin, 0.25 µg/mL amphotericin B (Thermo Fisher)). Culture media was then replaced every 2 to 3 days. After 10 to 12 days in culture, a subset of cells were stained with a mouse anti-CD90 antibody (final concentration: 0.02 mg/mL; Novus Biologicals, Centennial, CO, USA) followed by a goat-anti mouse Alexa Fluor 488 secondary (Abcam, Cambridge, UK). Percentage of fibroblast contamination was then determined by flow cytometry using an Accuri C6 (BD Biosciences, Franklin Lakes, NJ, USA) based on a minimum of 5000 events and data analysis was performed with FlowJo version 10.0.7 (BD). Cultures with <10% CD90 positive cells were considered acceptable (Kisselbach et al., 2009) and were re-seeded into 24-well culture plates (Thermo Fisher) at a rate of 8×10^4 cells/mL (1 mL medium per well). Cells were grown for 3 days, until approximately 90% confluent, at which point they were used for the LPS exposure experiment. REC isolated from each animal were cultured as separate cell lines.

6.2.1.3 LPS Dose Response and Stimulation Time. The LPS used in this study was from E. coli O55:B5 (L6529, Lot 126M4087V; Sigma) and was reconstituted in sterile DPBS to a stock concentration of 2.1×10^6 EU/mL. The LPS used for the entire experiment was derived from the same lot to maintain consistent LPS activity levels. The stock was stored in 200 µl aliquots at -20°C, as per manufacturer's instructions. The isolated REC were exposed to 0, 10,000, 50,000, or 200,000 EU/mL of LPS (three replicate wells per treatment), for either 6 or 24 h, with one plate per time point for each biological replicate of isolated REC. Following exposure to LPS, one well for each LPS dose/time point was trypsinized and cells were immediately analyzed viability using propidium iodide (BioVision Inc, Milpitas, CA, USA) staining to quantify the percent dead cells with a flow cytometer (BDC6, BD, Franklin Lakes, NJ, USA). The remaining two wells for each dose/time point were lysed in 1 mL Trizol (Thermo Fisher), pooled, and frozen at -80°C until used for RNA extraction.

6.2.1.4 Extraction of RNA and analysis of gene expression. Total RNA was isolated by phenol-chloroform extraction with two isopropanol precipitations (Kent-Dennis et al., 2019) and the addition of linear acrylamide (Thermo Fisher) as a co-precipitant. RNA integrity was analyzed with a 1.2% (w/v) denaturing agarose gel and distinct 28S and 18S ribosomal RNA bands were confirmed in all samples before use in subsequent steps. The High Capacity cDNA Reverse Transcription Kit (Thermo Fisher) was used to reverse transcribe 1 µg of RNA. The resulting cDNA was diluted to a final concentration of 10 ng/µl with nuclease-free water. Quantitative real-time polymerase chain reaction (qRT-PCR) was performed using 20 ng cDNA,

run in duplicate using SsoFast EvaGreen Supermix (Bio-Rad, Hercules, CA, USA) using a CFX96 Touch Real-Time PCR Detection System (Bio-Rad). Primers (IDT, Coralville, IA, USA) were designed to span exon-exon junctions, where possible, and were assessed for dimer formation by generating melt curves following amplification in order to verify the presence of a single product. Primers designed for housekeeping genes and genes of interest are listed in Table 6.1. Prior to qRT-PCR analysis, primer efficiencies were calculated from a serial dilution of pooled cDNA samples. Housekeeping genes were assessed for effects of treatment and time, and no significant effects were detected ($P \geq 0.22$; data not shown). Therefore, all three genes were determined to be stable. The Ct values of the genes of interest were normalized to the geometric mean of the three housekeeping genes. Changes in gene expression were calculated as fold change using the formula $2^{-\Delta\Delta Ct}$ (Pasternak et al., 2020). Expression of treatments was held relative to the mean of the time-matched medium control (CON), within animal.

6.2.2 Experiment 2: Repeated LPS exposure

6.2.2.1 Animals and Tissue Collection. Ruminal papillae collected from the ventral sac of 4-mo old Holstein bull calves (n = 5) and yearling beef heifers (n = 4) were used for this experiment. The procedures for ruminal tissue collection and for isolation and cultivation of REC were performed as described for Experiment 1.

6.2.2.2 LPS Dose, Stimulation Time and Frequency. Isolated REC were exposed to either **low** or **high** (1000 or 50,000 EU/mL, respectively) concentrations of LPS and subjected to one of the following exposure conditions (Figure 6.1): 1) 0 LPS exposure (**CON**); 2) 36 h of exposure (**36H**); 3) 24 h of exposure (**24H**); 4) 12 h of exposure (**12H**); 5) 12 h of exposure followed by removal of LPS for 24 h and then 12 h of exposure was repeated (**RPT**); and 6) 12 h of exposure followed by removal of LPS and a recovery period of 36 h (**RVY**). The starting point for administration of LPS was staggered such that cell collections from all cultures occurred at the same time. Two wells (for each treatment/time point) were lysed in 1 mL of Trizol (Thermo Fisher), pooled, and frozen at -80°C until used for RNA extraction.

6.2.2.3 Extraction of RNA and analysis of gene expression. Extraction of RNA and real time qPCR analysis procedures were performed as described for Experiment 1. The Ct values of the genes of interest were normalized to the geometric mean of three stable housekeeping genes. Changes in gene expression were calculated as described previously.

Table 6.1 Primer used for quantitative real-time PCR

Gene Name (official gene symbol)	Source[1]	Sequence (5'-3')	Amplicon Size	Efficiency %[2]
Housekeeping				
Beta actin (ACTB)	NM_173979.3	F: GAGCTACGAGCTTCCTGACGGGC R: AATGCCGCAGGATTCCATGCCCAG	109	96
Glyceraldehyde-3-phosphate dehydrogenase (GAPDH)	NM_001034034.2	F: GGGTCATCATCTCTGCACCT R: GGAGGCATTGCTGACAATCT	101	91
Hypoxanthine phosphoribosyltransferase 1 (HPRT)	NM_001034035.2	F: AGGTTGCGAGCTTGCTGAT R: AGGGCATATCCCACAACAAA	103	99
Genes of Interest				
Colony stimulating factor 2 (CSF2)	NM_174027.2	F: CATGTGGATGCCATCAAGG R: TTGGTTCCTGGGAGTCAAAC	112	108
C-X-C motif chemokine ligand 2 (CXCL2)	NM_174299.3	F: CCGAAGTCATAGCCACTCTCA R: CTTCTGTTTTCCACCTGGTCA	128	99
C-X-C motif chemokine ligand 8 (CXCL8)	NM_173925.2	F: AGAGCTGAGAAGCAAGATCCA R: ACCCTACACCAGACCCACAC	150	104
Interleukin 1 beta (IL1B)	NM_174093.1	F: CTGAGGAGCATCCTTTCATTC R: GTCCTGGAGTTTGCACTTTAT	114	97
Interleukin 7 (IL7)	NM_173924.2	F: TTTTTGAATCGTGCTTCTCG R: TCTTCCTTTACCCTTGCTGGT	135	
Prostaglandin-endoperoxidase synthase-2 (PTGS2)	NM_174445.2	F: GGTGTGAAAGGGAGGAAAGA R: GGCAAAGAATGCAAACATCA	117	93
Toll-like receptor 2 (TLR2)	XM_015475330.1	F: TGATGCTGCCATTCTGATTC R: GCCACTCCAGGTAGGTCTTG	107	96
Toll-like receptor 4 (TLR4)	NM_174198.6	F: CCTTGCGTACAGGTTGTTCC R: CTCAGGTCCAGCATCTTGGT	104	90
Tumor necrosis factor alpha (TNF)	NM_173966.3	F: CAAGTAACAAGCCGGTAGCC R: AGATGAGGTAAAGCCCGTCA	153	99

[1]National Center for Biotechnology Information (NCBI)
[2]Efficiency= $-1 + 10^{(-1/\text{slope})}$X100

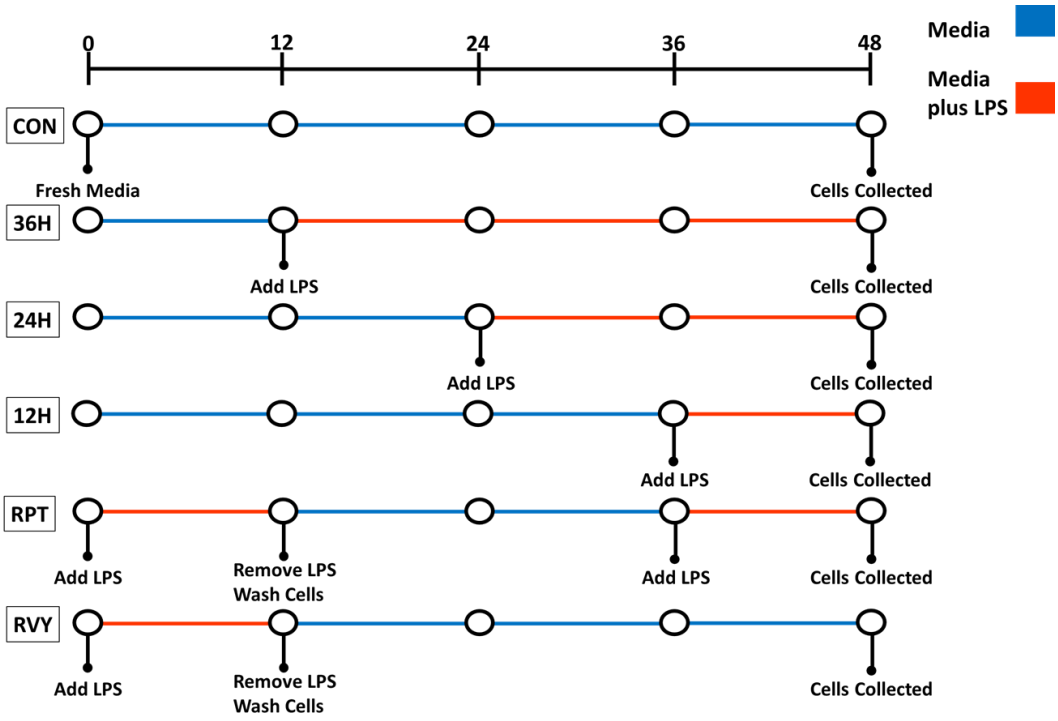

Figure 6.1 Schematic diagram of experimental conditions used in Experiment 2. Treatments included: 0 LPS exposure (CON), 12 h of exposure followed by removal of LPS for 24 h and then 12 h of exposure was repeated (RPT), 12 h of exposure followed by removal of LPS and a recovery period of 36 h (RVY), 36 h of exposure (36H), 24 h of exposure (24H) and 12 h of exposure (12H). Administration of treatments and sample collections for cells from individual animals occurred in a sequence that facilitated collection of cells from all cultures at the same 48 h time point.

6.2.3 Statistical Analysis

All statistical analyses were performed as a mixed model using the MIXED procedure of SAS 9.4 (SAS Institute, Inc, Cary, NC, USA). Analysis of qRT-PCR data were performed on ΔCT and results are presented as fold-change. Significance was declared at $P < 0.05$.

6.2.3.1 Experiment 1. Data were analyzed with polynomial contrasts to evaluate whether viability or gene expression responded to LPS concentration in a linear or quadratic pattern and coefficients were determined to account for unequal spacing. Treatment, duration (h of exposure), and the treatment × duration interaction were considered fixed effects. Triplicate well (of culture plate) within animal was considered as the random effect.

6.2.3.2 Experiment 2. Treatment (exposure to LPS), dose (concentration of LPS), and the treatment × dose were considered fixed effects. The interaction was not significant ($P > 0.078$) and was therefore removed from the model. Well (of culture plate) within animal and animal type (calf or heifer) were considered as random effects. Data were analyzed for the effects of duration and dose by mean separation and using polynomial contrasts to evaluate the linear and quadratic patterns associated with duration of LPS exposure. The effect of repeated exposure to LPS (RPT) was analyzed with mean separation, comparing CON, 12H, RPT and RVY.

6.3 RESULTS

6.3.1 Experiment 1

There was a linear decrease ($P = 0.011$; Figure 6.2) in the percent dead REC as LPS exposure increased from 0 (9.7 ± 0.8) to 200,000 EU/mL LPS (7.5 ± 0.8). No significant time ($P = 0.34$) or LPS dose × time ($P = 0.71$) effects were observed.

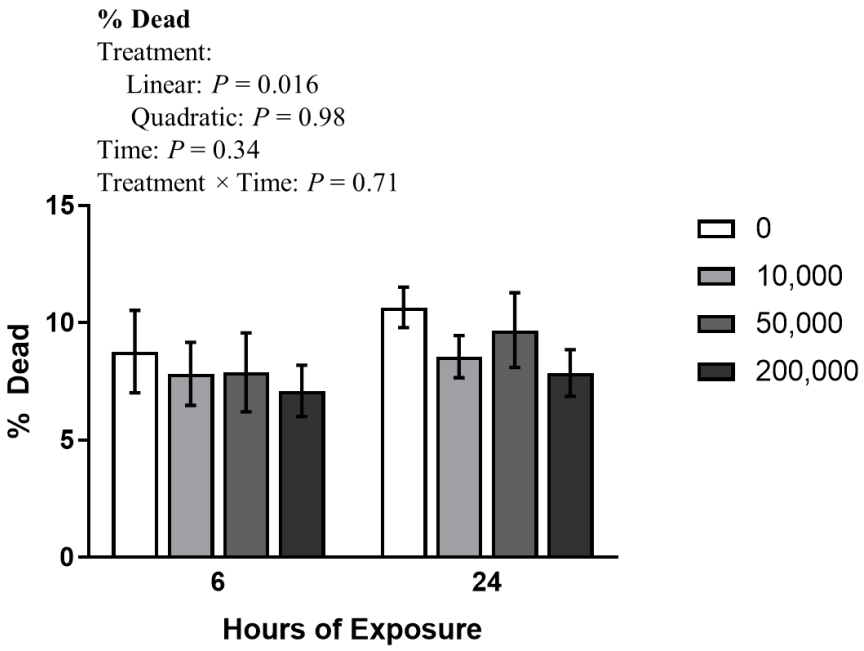

Figure 6.2 Percent dead ruminal epithelial cells, measured with flow cytometry, when exposed to 0, 10,000, 50,000 or 200,000 EU/mL LPS and following either 6 or 24 h of exposure. A significant ($P < 0.05$) linear dose effect was observed.

There were treatment × time interactions for *TLR2* and *TLR4* ($P < 0.001$, Figure 6.3) with all LPS-treated groups showing higher *TLR2* and *TLR4* expression than their time-specific CON. The treatment × time interaction for *TLR2* expression was based on greater values in REC exposed to 10,000 and 50,000 EU/mL with LPS exposure for 6 h (5.4 and 4.7-fold, respectively) compared to 24 h (2.2 and 2.0-fold, respectively). However, there was no significant ($P = 0.14$) time effect following exposure to 200,000 EU LPS/mL (Figure 6.3A). The treatment × time interaction for *TLR4* (Figure 6.3B) did not reveal differences between *TLR4* LPS individual means for each LPS concentration after 6 vs. 24 h of exposure. However, a general trend for a greater expression of *TLR4* after 6 h than 24 h was observed as described for *TLR2*.

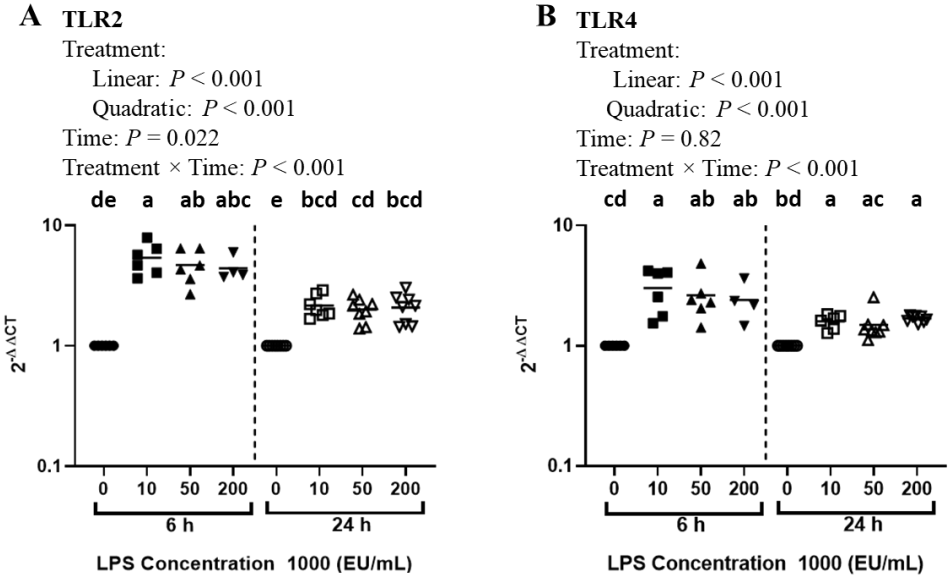

Figure 6.3 Expression of toll-like receptor genes (A: TLR2 and B: TLR4) in cultured ruminal epithelial cells exposed to 0 (control), 10,000, 50,000 or 200,000 EU/mL LPS for 6 or 24 hours. Data are presented as fold change (2-ΔΔCT) relative to the average ΔCq value for each gene in the control group. Unique letters denote statistical significance ($P < 0.05$).

Gene expression increased (quadratic $P < 0.001$) in response to all doses of LPS, regardless of time, for *TNF* (17.5-fold, Figure 6.4A), *IL1B* (276.9-fold, Figure 6.4B), *CXCL2* (13.9-fold Figure 6.4C) and *CXCL8* (46.9-fold, Figure 6.4D), respectively.

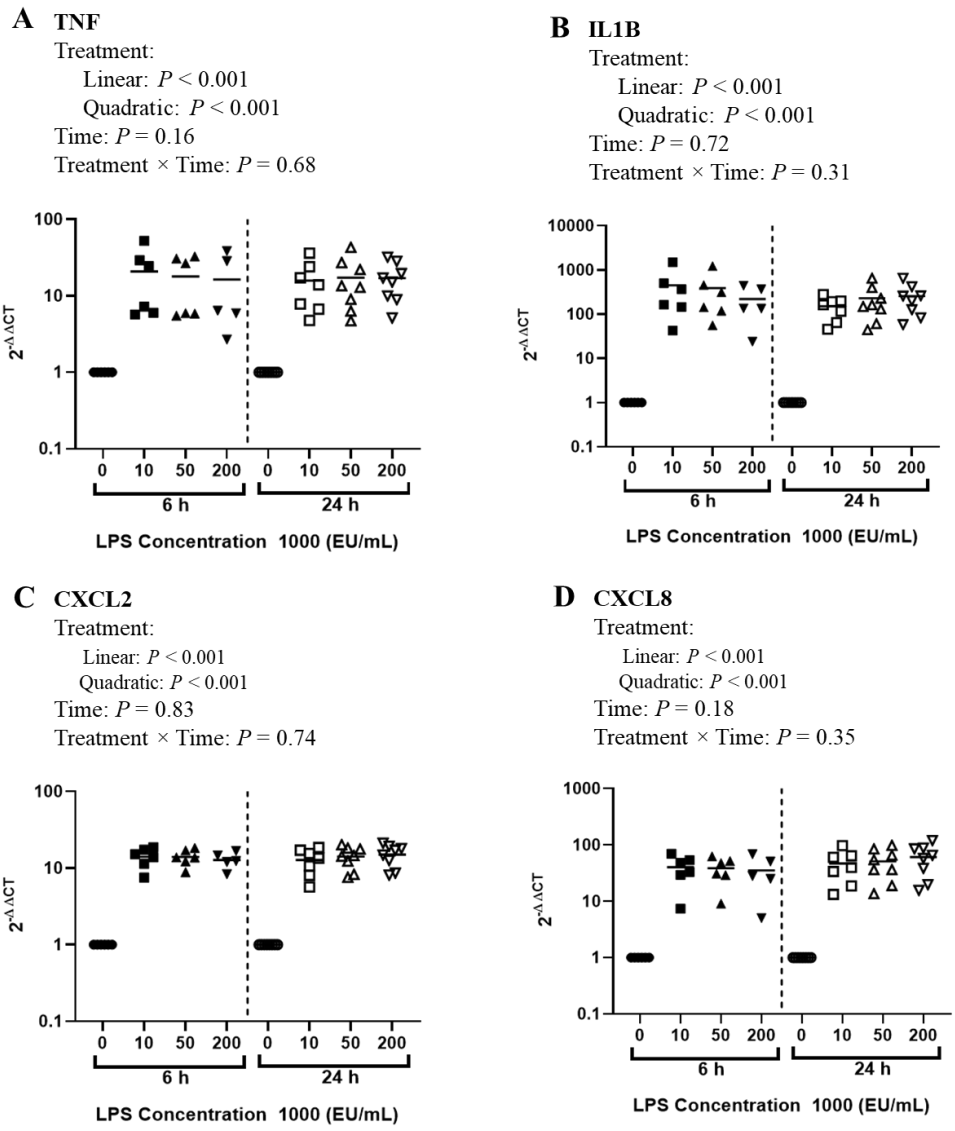

Figure 6.4 Expression of pro-inflammatory cytokine genes (A: TNF and B: IL1B) and chemokine genes (C: CXCL2 and D: CXCL8) in cultured ruminal epithelial cells exposed to 0 (control), 10,000, 50,000 or 200,000 EU/mL LPS for 6 or 24 hours. Data are presented as fold change (2-ΔΔCT) relative to the average ΔCq value for each gene in the control group. Unique letters denote statistical significance (P < 0.05).

There was a treatment × time interaction for *PTGS2* (Figure 6.5A; $P < 0.001$) with all LPS-treated groups showing higher expression than their time-specific CON and the magnitude of the change in expression tending to be greater at 24 h compared to 6 h. Expression of *CSF2* increased (quadratic $P < 0.001$) in response to LPS, regardless of time (12.9 and 15.6-fold,

respectively; Figure 6.5B). There was also a treatment × time interaction for *IL7* (Figure 6.5C). The expression of *IL7* was increased by all LPS doses over their time-specific CON; however, the expression following exposure to 10,000 and 50,000 EU/mL was greater after 6 h (17.1 and 13.1-fold, respectively) compared to 24 h (3.7 and 4.8-fold, respectively; $P = 0.003$).

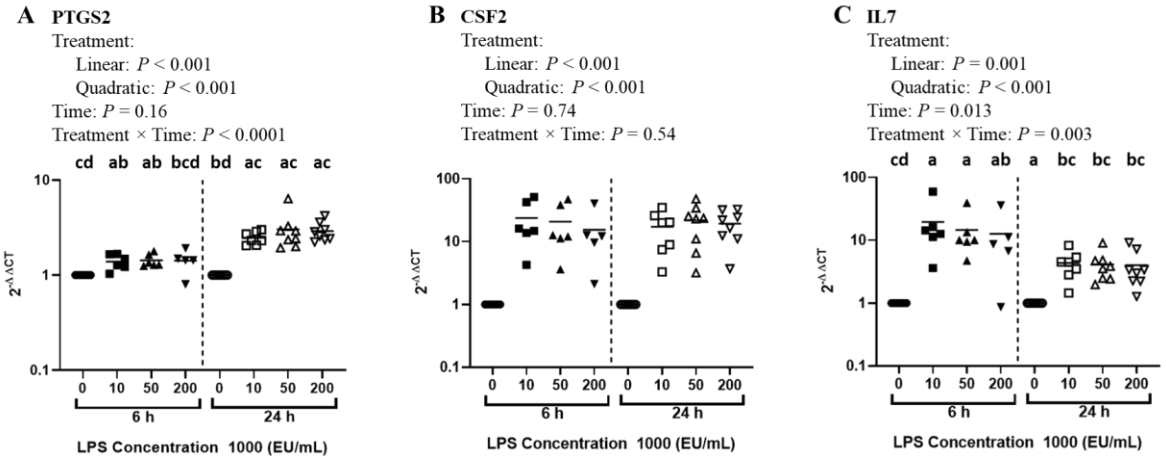

Figure 6.5 Expression of gene involved in generation of a lipid mediator of inflammation (A: PTGS2) and growth factor-like cytokine genes (B: CSF2 and C: IL7) in cultured ruminal epithelial cells exposed to 0 (control), 10,000, 50,000 or 200,000 EU/mL LPS for 6 or 24 hours. Data are presented as fold change (2-ΔΔCT) relative to the average ΔCq value for each gene in the control group. Unique letters denote statistical significance ($P < 0.05$).

6.3.2 Experiment 2

6.3.2.1 Effect of the duration of LPS exposure. Exposure of REC to LPS, regardless of dose, quadratically increased the expression of all genes measured with increasing duration of exposure independent of dose ($P < 0.001$, Figures 6.6 to 6.8). Expression of *TLR4*, *CXCL2* and *CSF2* at 24H was less compared 12H and 36H ($P < 0.001$; Figures 6.6B, 6.7C and 6.8B, respectively).

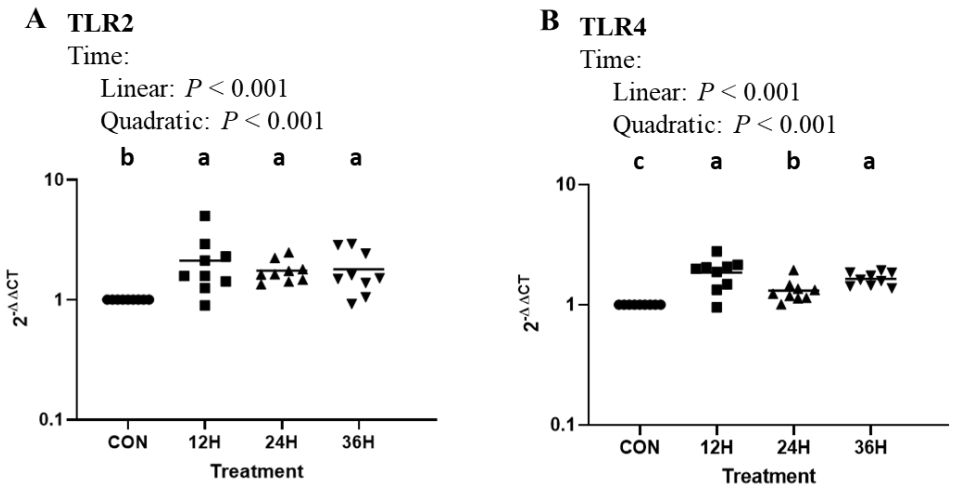

Figure 6.6 Time-dependent changes in gene expression of Toll-like receptors (A: TLR2 and B: TLR4) in cultured ruminal epithelial cells exposed to either a Low (1000 EU/mL) or High (50,000 EU/mL) LPS dose. The dose × treatment interaction was not significant and the dose data was combined. The following treatments were compared: control (no LPS; CON), 12h LPS exposure (12H), 24h of LPS exposure (24H) and 36h of LPS exposure (36H). Data are presented as fold change (2-ΔΔCT) relative to the average ΔCq value for each gene in the control group. The dose × treatment interaction was not significant and was removed from the model. Unique letters denote statistical significance ($P < 0.05$).

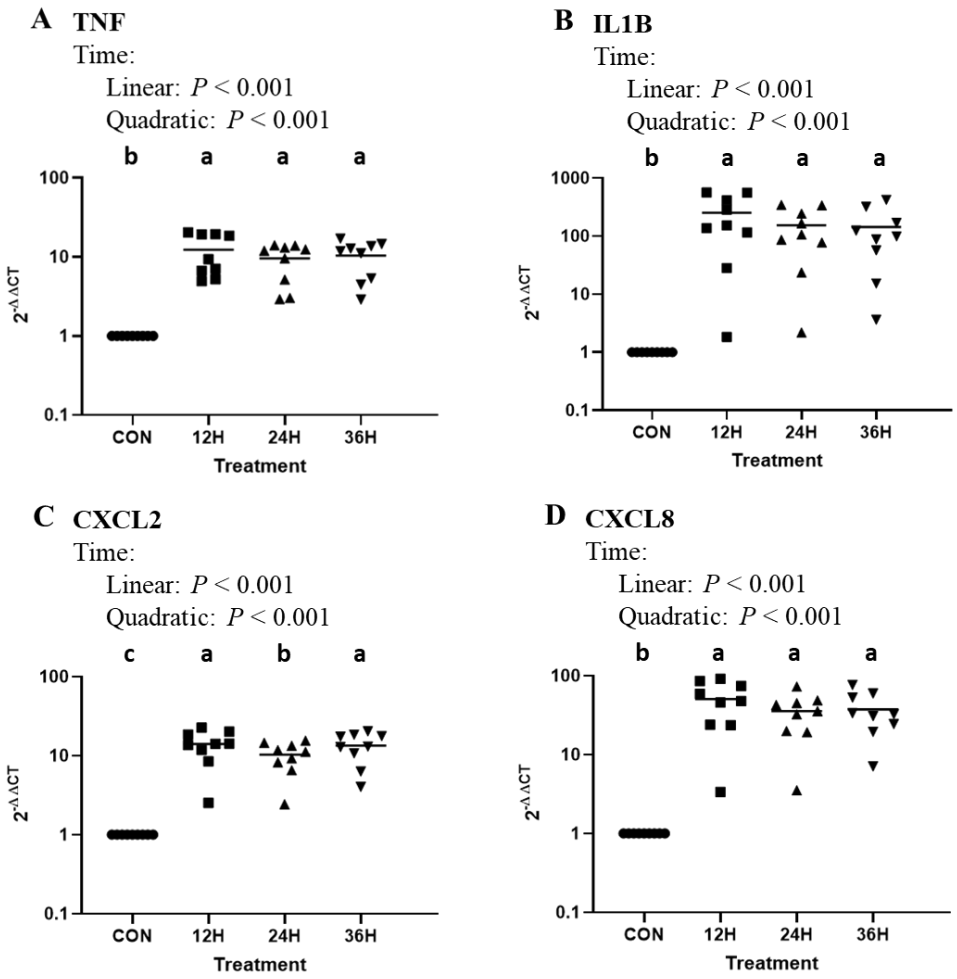

Figure 6.7 Time-dependent changes in gene expression of pro-inflammatory cytokines (A: TNF and B: IL1B) and chemokines (C: CXCL2 and D: CXCL8) in cultured ruminal epithelial cells exposed to either a Low (1000 EU/mL) or High (50,000 EU/mL) LPS dose. The dose × treatment interaction was not significant and the dose data was combined. The following treatments were compared: control (no LPS; CON), 12h LPS exposure (12H), 24h of LPS exposure (24H) and 36h of LPS exposure (36H). Data are presented as fold change (2-ΔΔCT) relative to the average ΔCq value for each gene in the control group. The dose × treatment interaction was not significant and was removed from the model. Unique letters denote statistical significance ($P < 0.05$).

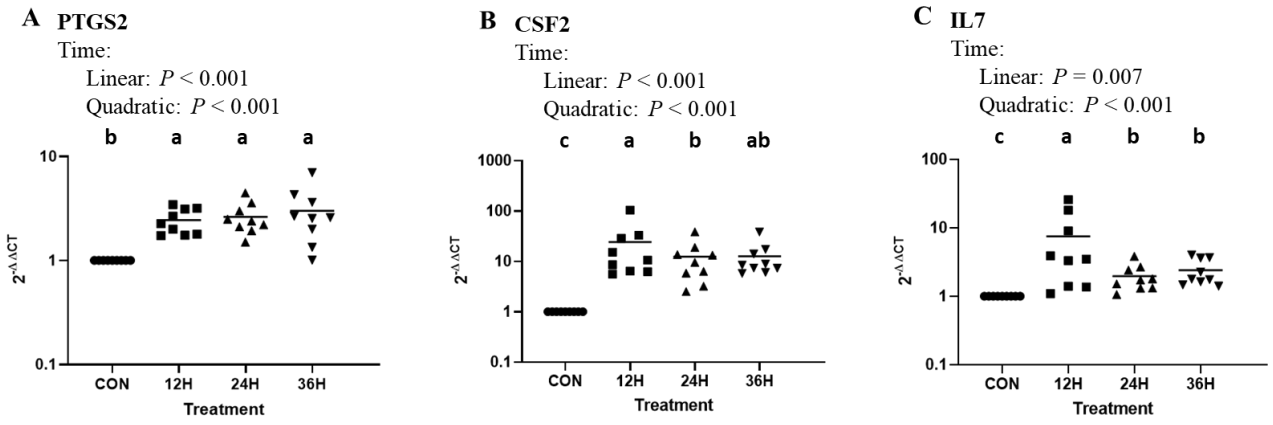

Figure 6.8 Time-dependent changes in gene expression of lipid mediator of inflammation (A: PTGS2) and growth factor-like cytokines (B: CSF2 and C: IL7) in cultured ruminal epithelial cells exposed to either a Low (1000 EU/mL) or High (50,000 EU/mL) LPS dose. The dose × treatment interaction was not significant and the dose data was combined. The following treatments were compared: control (no LPS; CON), 12h LPS exposure (12H), 24h of LPS exposure (24H) and 36h of LPS exposure (36H). Data are presented as fold change (2-ΔΔCT) relative to the average ΔCq value for each gene in the control group. The dose × treatment interaction was not significant and was removed from the model. Unique letters denote statistical significance ($P < 0.05$).

6.3.2.2 Effect of repeated LPS exposure. For all genes, except *TLR4* and *IL7*, expression was greater with re-exposure to LPS when compared to CON ($P < 0.001$; Figures 6.9 to 6.11). The RPT and 12H groups had greater *TLR2* expression compared to RVY ($P = 0.024$) (Figure 6.9A). Expression of *TLR4* (Figure 6.9B) was greatest when exposed to LPS for 12H and least for CON, RVY and RPT ($P < 0.001$).

Expression levels of *TNF*, *CXCL2* and *CXCL8* were greater when exposed to LPS for 12H compared to RVY or RPT, with CON having lowest expression ($P = 0.001$, Figure 6.10A, C and D) There was no difference in expression of *IL1B* for the 12H and RPT groups ($P = 0.14$; Figure 10B). For *TNF*, *IL1B*, *CXCL2* and *CXCL8*, expression of RVY was greater than CON, but less compared to 12H and RPT ($P < 0.001$)

The expression of *PTGS2* did not differ between 12H and RPT ($P = 0.52$) with both being greater than CON ($P < 0.001$; Figure 6.11A). Expression was greater after 12H compared to RPT for *CSF2* ($P = 0.011$, Figure 6.11B). For both *PTGS2* and CSF2, RVY had greater expression than CON, but was less compared to 12H and RPT ($P < 0.001$). The expression level of *IL7* was greatest at 12H compared with CON, RVY and RPT ($P < 0.001$; Figure 6.11C).

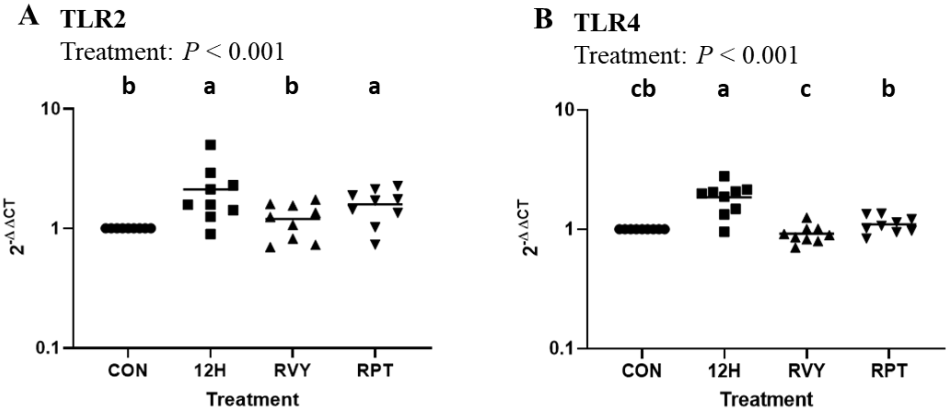

Figure 6.9 Expression of Toll-like receptor genes (A: TLR2 and B: TLR4) in cultured ruminal epithelial cells exposed to either Low (1000 EU/mL) or High (50,000 EU/mL) LPS dose. The dose × treatment interaction was not significant and the dose data was combined. The following treatments were compared: control (no LPS; CON), 12h LPS exposure (12H), 12h of LPS exposure followed by 36h of no exposure (RVY), and 12h of LPS exposure followed by 24h of no exposure followed by another 12h of exposure (RPT). Data are presented as fold change (2-ΔΔCT) relative to the average ΔCq value for each gene in the control group. The dose × treatment interaction was not significant and was removed from the model. Unique letters denote statistical significance ($P < 0.05$).

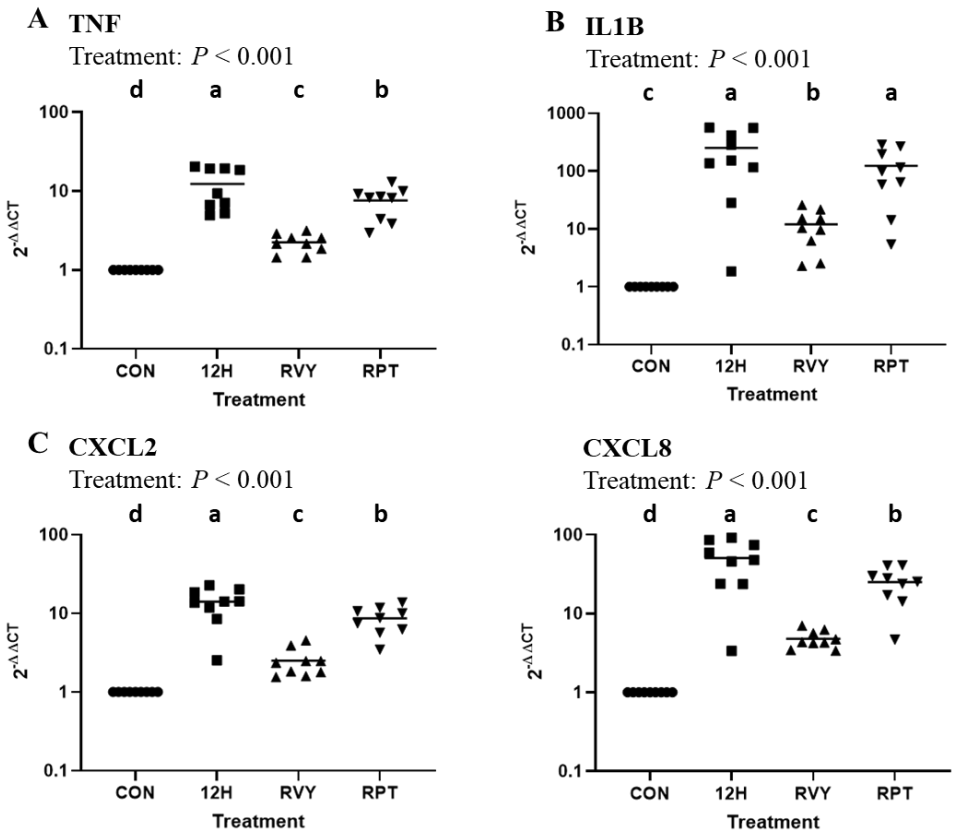

Figure 6.10 Gene expression of pro-inflammatory cytokines (A: TNF and B: IL1B) and chemokines (C: CXCL2 and D: CXCL8) in cultured ruminal epithelial cells exposed to either a Low (1000 EU/mL) or High (50,000 EU/mL) LPS dose. The dose × treatment interaction was not significant and the dose data was combined. The following treatments were compared: control (no LPS; CON), 12h LPS exposure (12H), 12h of LPS exposure followed by 36h of no exposure (RVY), and 12h of LPS exposure followed by 24h of no exposure followed by another 12h of exposure (RPT). Data are presented as fold change (2-ΔΔCT) relative to the average ΔCq value for each gene in the control group. The dose × treatment interaction was not significant and was removed from the model. Unique letters denote statistical significance ($P < 0.05$).

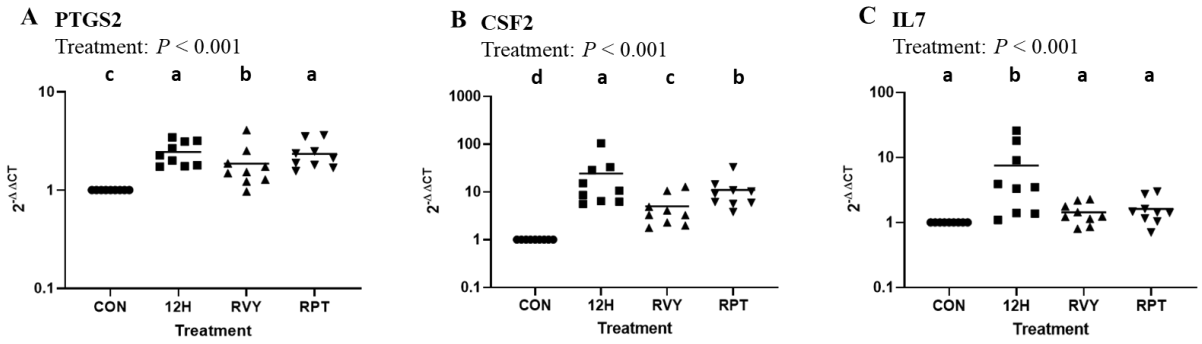

Figure 6.11 Gene expression of lipid mediator of inflammation (A: PTGS2) and growth factor-like cytokines (B: CSF2 and C: IL7) in cultured ruminal epithelial cells exposed to either a Low (1000 EU/mL) or High (50,000 EU/mL) LPS dose. The dose × treatment interaction was not significant and the dose data was combined. The following treatments were compared: control (no LPS; CON), 12h LPS exposure (12H), 12h of LPS exposure followed by 36h of no exposure (RVY), and 12h of LPS exposure followed by 24h of no exposure followed by another 12h of exposure (RPT). Data are presented as fold change (2-ΔΔCT) relative to the average ΔCq value for each gene in the control group. The dose × treatment interaction was not significant and was removed from the model. Unique letters denote statistical significance ($P < 0.05$).

6.4 DISCUSSION

It is widely accepted that intestinal epithelial cells (**IEC**) play a direct role in gastrointestinal mucosal immunity through PRR expression and signaling that activates pro-inflammatory signalling pathways (Jung et al., 1995; Stadnyk, 2002; Chin et al., 2006; Hirotani et al., 2008; Kern et al., 2017). Similarly, the interaction between REC and luminal microbes or MAMPs may initiate a local inflammatory response (Steele et al., 2009; Plaizier et al., 2018), but the potential for REC directly mediating these responses has not previously been well characterized.

6.4.1 Detection of LPS by REC

Translocation of ruminal LPS across the ruminal epithelium is thought to occur when consumption of a highly fermentable diet causes acidosis and hyperosmotic conditions in the rumen which compromise the epithelial barrier (Owens et al., 1998; Kleen et al., 2003; Khafipour et al., 2009). During the process of translocation, LPS may interact directly with REC (Emmanuel et al., 2007; Plaizier et al., 2018), thereby affecting REC function. In fact, a dose-dependent cytotoxic effect of LPS has been reported for cultured IEC, with cell viability decreasing at an LPS concentration of 50 µg/mL (Chin et al., 2006). At LPS concentrations exceeding 800 µg/mL, the viability of Caco-2 cells dropped to 30% of control cells (Hirotani et al., 2008). However, the LPS concentrations reported above are considered very high and may not be representative of physiological concentrations present in the rumen (Yagi et al., 2002; Guo et al., 2013). For the present study, a range of LPS concentrations was selected to reflect ruminal LPS concentrations reported in the literature (Plaizier et al., 2012). We observed a slight reduction in the percentage of dead cells when LPS increased from 0 to 200,000 EU/mL (20 µg/mL). The reason for this increased viability is not known but the relatively small numerical (< 3%) difference was not considered biologically relevant. Thus, our interpretation of the data is that exposing REC to moderate LPS concentrations does not have a cytotoxic effect.

Expression of PRR, such as *TLR2* and *TLR4*, which are receptors for the detection of MAMPs such as LPS (Dziarski et al., 2001), has been demonstrated in ruminal epithelial tissue (Chen et al., 2012; Dionissopoulos et al., 2012; Liu et al., 2013). Indeed, mRNA for nearly all mammalian TLRs 1 through 10) has been detected in the ruminal tissue of Holstein calves (Chen

et al., 2012; Malmuthuge et al., 2012). However, the majority of work on inflammation in the ruminal epithelium has utilized whole ruminal papillae tissue (Malmuthuge et al., 2012; Liu et al., 2013; Arroyo et al., 2017), which is comprised of multiple cell types capable of detecting MAMPs and inducing a pro-inflammatory response. A recent study by Kent-Dennis et al. (2019) confirmed localization of TLR4 protein in REC, suggesting that REC alone may be capable of initiating a pro-inflammatory response. Supporting the previously mentioned findings, we observed that the expression of *TLR4* was up-regulated when cultured REC were exposed to LPS, regardless of the concentration in Experiment 1 or 2. Expression of *TLR2* was also up-regulated when REC were exposed to LPS and the response to LPS was greater when measured after 6H compared to 24H. TLR2 has a wide variety of ligands, including LPS which has been shown to activate TLR2 signalling (Takeuchi et al., 1999; Yang et al., 1999). Dampening of this response with longer duration of LPS exposure may serve to limit the capacity of REC to respond to LPS. This down-regulation of TLR2 gene transcript may protect against potential tissue damage caused by inflammation (Lee et al., 2008). The results may also indicate that some of the doses of LPS selected for this study exceeded the cells capacity to respond (Sugimoto et al., 2016) and future research should evaluate lower exposure doses.

6.4.2 Initiation of a pro-inflammatory response by REC

As a result of LPS-activated TLR signalling, a number of pro-inflammatory molecules including cytokines (Jung et al., 1995; Stadnyk, 2002), chemokines (Vallee et al., 2003; De Plaen et al., 2006), and lipid mediators of inflammation (Grishin et al., 2006; Fukata et al., 2006), are produced by non-hematopoietic cells including IEC during the acute phase of inflammation. A study by Liu et al., (2013) reported increased mRNA expression of pro-inflammatory cytokines *TNF* and interferon gamma (*IFNG*) in ruminal epithelia collected from goats fed a high grain diet compared to those fed hay. Similarly, when dairy cows were fed a high starch diet, both gene and protein expression for TLR4, IL1B, IL7, and TNF were greater compared to a low starch diet (Pan et al., 2017). Little research, however, has demonstrated a direct role for REC in initiating the local inflammatory response. Zhang et al. (2016) has reported a correlation between LPS exposure and production of pro-inflammatory cytokines in isolated REC. In the current study, cultured REC were exposed to LPS in a dose-dependent manner and for increasing time intervals to further characterize the REC pro-inflammatory response. In Experiment 1, expression of *TNF*

and *IL1B* were up-regulated following exposure to LPS confirming REC are capable of expressing pro-inflammatory cytokine genes. Both *CXCL2* and *CXCL8* were also up-regulated following exposure to LPS. These chemokines are important chemo-attractants for the recruitment of leukocytes during inflammatory responses. *CXCL2* is associated with an increased recruitment of neutrophils and mucosal lymphocytes (Ohtsuka et al., 2001) and CXCL8 is known to be a potent neutrophil recruiter and is a critical component of acute inflammation (Harada et al., 1994). The expression of *TNF*, *IL1B*, *CXCL2*, and *CXCL8* were similar when REC were exposed to LPS for 6 or 24 h suggesting transcript abundance was maintained. Data from Experiment 2 confirmed transcript abundance for all genes remained elevated when REC were exposed to LPS for as long as 36 h. These results suggest that RECs may be directly involved in initiating a pro-inflammatory response in the rumen to LPS, and this REC response may be sustained for at least 36 h. However, expression of *TLR4*, *CXCL2* and *CSF2* at 24H was less compared with 12H and 36H, suggesting that there may have been an effect of duration of LPS exposure.

In addition, in Experiment 1, there was a treatment × time interaction, where expression of *PTGS2* following exposure to LPS was up-regulated to a greater extent at 24 h than 6 h. In Experiment 2, there was a quadratic up-regulation of *PTGS2* with longer exposure to LPS, regardless of dose. Prostaglandins are synthesized during inflammation from arachidonic acid via two enzymes, PTGS1 and PTGS2 (formally known as COX1 and COX2). Whereas PTGS1 is constitutively expressed, PTGS2 is considered a pro-inflammatory lipid mediator of prostaglandin synthesis (Ricciotti and FitzGerald, 2011). Increased expression of *PTGS2* further supports the conclusion that REC may play a role in initiating inflammation in the ruminal epithelium.

Intestinal epithelial cells are involved in coordinating crosstalk with immune cells, such as resident dendritic cells (Loss et al. 2018; Loss et al., 2019), intra-epithelial lymphocytes and lamina propria T and B lymphocytes (Clark and Coopersmith, 2007; Hooper, 2015). During acute inflammation, IEC have been shown to produce molecules that promote and regulate immune cell functions (Hooper, 2015). To further explore this role in REC, two "growth factor-like" cytokines, CSF2 and IL7, were selected in this study. Colony-stimulating factor-2 is expressed by many cell types including IEC during inflammation (Egea et al., 2010), and promotes differentiation and survival of myeloid cells, especially tissue-resident mononuclear

phagocytes (Mortha et al., 2014). Production of CSF2 by colonic epithelial cells has been reported to play a role in epithelial cell repair and recovery following induction of colitis (Egea et al., 2013). In the present study, CSF2 was expressed in REC at significantly greater levels when cells were exposed to LPS compared to CON, regardless of LPS concentration and exposure time, suggesting CSF2 function in REC may be similar to that in IEC.

The growth factor-like cytokine IL7 is critical for development and survival of T and B lymphocytes (Mackall et al., 2011). It is mainly produced by non-haematopoietic stromal cells (Mackall et al., 2011), but IEC have also been shown to produce IL7 in response to infection (Zhang et al., 2015). In the intestinal epithelia, elevated levels of IL7 may be important for the regulation of tissue-resident lymphocyte function (Watanabe et al., 1995). In Experiment 1 of the present study, IL7 was up-regulated when REC were exposed to LPS; however, expression was less after 24 h of exposure compared to 6 h with more than a 5-fold difference. Further, results from Experiment 2 showed that expression of *IL7* decreased when duration of exposure was increased to 24 and 36 h. These results suggest that *IL7* may be involved in the acute phase of inflammation but is tightly regulated. Indeed, previous work has shown evidence for stringent regulation of *IL7* production and expression of the *IL7* receptor, which may control proliferation of T cells and epithelial cells (Mackall et al., 2011). Expression of *IL7* by REC may have similar feedback mechanisms. The expression patterns of *IL7* and *CSF2* observed in the present study suggest that the rumen epithelial mucosa may interact with either infiltrating or tissue-resident immune cells (Steele et al., 2009; Trevisi et al., 2014).

6.4.3 Tolerance of REC to LPS

An important regulatory mechanism for epithelial cells in the gastrointestinal tract is the development of dampened responses to luminal MAMPs and other antigens to reduce tissue damage by pro-inflammatory molecules (Christiakov et al., 2015). Endotoxin tolerance has been reported in IEC (Lotz et al., 2007; Lee et al., 2008), and previous studies have suggested that repeated exposure to LPS reduces the magnitude of the pro-inflammatory response (Nomura et al., 2000; Beutler and Rietschel et al., 2003). The concept of endotoxin tolerance has also been explored in mucosal surfaces of ruminants (Bieniek et al., 1998; Petzl et al., 2011; Gott et al., 2015). Despite the fact that the REC may have multiple exposures to ruminal LPS during their progression from stratum basale to the stratum granulosum and finally the stratum corneum,

endotoxin tolerance has not been previously evaluated in the ruminal epithelium. In Experiment 2, when REC were exposed to a single dose of LPS for 12h, regardless of concentration, expression of all genes was increased, suggesting a rapid, pro-inflammatory response to LPS by the REC. Following a period without LPS exposure, REC were exposed to a second, 12 h-dose of LPS. Although there was still an increase in expression of most genes evaluated when compared to CON, the second dose of LPS resulted in lower fold-changes for *TLR4, TNF, CXCL2, CXCL8, CSF2*, and *IL7* as compared to a first 12 h LPS exposure.

These results suggest a dampening of pro-inflammatory gene expression in RECs following repeated or prolonged exposures to LPS. In previous work, pre-treatment with LPS was administered and a decreased response to subsequent LPS exposure was apparent with decreased expression of classical pro-inflammatory cytokines (Harada et al., 1994). In agreement with these results, an *in vivo* study by Petzl et al. (2011) observed decreased mRNA abundance for *TNF* and *CXCL8* when an intra-mammary pre-treatment with LPS was given prior to a bacterial challenge. Additionally, prolonged LPS exposure is associated with endotoxin tolerance in a variety of cells types and tissues (Seeley and Ghosh, 2016). In support, a continuous dose of TNF, infused into adipose tissue of dairy cows, resulted in a suppressed inflammatory response suggesting that pro-inflammatory cytokines may also have a tolerogenic effect (Martel et al., 2014).

In the present experiment, expression of *CSF2* was less when the REC were re-stimulated, compared to 12H. Expression of *CSF2* is closely associated with *TNF* expression and may be important in regulating acute inflammation by modulating pro-inflammatory cytokines and chemokines production (Nierhaus et al., 2017). Moreover, *IL7* did not appear to response at all to the second dose, as its expression in the RPT group was the same as the control. A study by Julian et al. (2015) demonstrated that IL7 is involved in immune tolerance and may be important for reversing tolerance in splenocytes, suggesting that IL7 helps to promote and restore T cell function.

Expression of *IL1B* following the second LPS exposure was similar to that of the initial response. The reason for this effect is unknown, however previous work has shown that circulating *IL1B* has a positive feedback effect on itself (Dinarello et al., 1987) and also that other pro-inflammatory cytokines can sustain *IL1B* expression for more than 24 h (Schindler et al., 1990). Following the second LPS exposure, expression of *TLR2* was also similar to that of

the initial response. Considering the expression of *TLR2* in Experiment 1, results suggest that *TLR2* signalling in REC may be influenced more by LPS dose or duration, rather than repeated LPS exposure.

In Experiment 2, when LPS was removed from the media (RVY), the expression of all genes measured was decreased significantly 36 h after exposure, compared to the single, 12-h of LPS exposure. In addition, *TLR2*, *TLR4* and *IL7* expression levels returned to baseline. These data suggest that although moderate exposure of LPS to ruminal epithelium induces a pro-inflammatory response, the effects are not sustained if the exposure is limited. However, *TNF*, *IL1B*, *CXCL2*, *CXCL8*, *PTGS2* and *CSF2* were all significantly up-regulated compared to the control. These results demonstrate that the REC were able to recover after the LPS exposure, although there was still expression of some of the pro-inflammatory genes even after the LPS had been removed, suggesting that some residual transcription had occurred.

6.5 CONCLUSION

Previous research has provided evidence for a local inflammatory response in ruminal papillae, presumably a consequence of translocation of microbes or MAMPs during ruminal acidosis. Our data provide evidence that REC have the capacity to play a direct role in initiating pro-inflammatory responses when exposed to LPS. Moreover, the results of the present study suggest that when REC are repeatedly exposed to LPS, there is a dampened expression of some pro-inflammatory genes, suggesting a potential tolerogenic response. Finally, following LPS induction of a pro-inflammatory gene response, REC are able to recover but increased expression of some pro-inflammatory genes may remain elevated for at least 36 h after the LPS is removed. Overall, our results suggest that the REC response to LPS is dependent on several exposure conditions, such as LPS dose, duration of LPS exposure, and frequency of LPS stimulation.

CHAPTER 7: EFFECTS OF A PRO-INFLAMMATORY RESPONSE ON METABOLIC FUNCTION OF CULTURED, PRIMARY RUMINAL EPITHELIAL CELLS

Chapter 6 demonstrated that LPS can induce a pro-inflammatory response in REC in vitro. However, it remains unclear whether this response can affect the metabolic function of the cells. Therefore, an experiment was conducted whereby an inflammatory response was induced in cultured REC. Utilization of energy substrates and molecules to indicate shifts in cellular metabolism were evaluated. The potential effects of inflammation on REC metabolism have not been previously evaluated.

Abstract: Inflammation of ruminal epithelium may occur during ruminal acidosis as a result of translocation and interaction of ruminal epithelial cells (**REC**) with molecules such as lipopolysaccharide (**LPS**). Such inflammation has been reported to alter cellular processes such as nutrient absorption, metabolic regulation, and energy substrate utilization in other cell types but has not been investigated for REC. The objectives of this study were to investigate the effects of LPS on metabolism of short chain fatty acids (**SCFA**) by primary REC, as well as to investigate the effects of SCFA on the pro-inflammatory response. Ruminal papillae from nine yearling Speckle Park beef heifers were used to isolate and culture primary REC. Cells were grown in minimum essentials media (**MEM**) for 12 d before use and then reseeded in 24-well culture plates. The study was conducted as a 2 × 2 factorial where cells were grown in normal MEM (**REG**) or media containing 2 m*M* butyrate and 5 m*M* propionate (**SCFA**) with (50,000 EU/mL; **+LPS**) or without LPS **(-LPS**) for 24 h. Supernatant samples were collected for analysis of glucose and SCFA consumption. Cells were collected to determine the expression of mRNA for genes associated with inflammation (*TNF*, *IL1B*, *CXCL2*, *CXCL8*, *PTGS2,* and *TLR4*), purinergic signaling (*P2RX7*, *ADORAB2,* and *CD73*), nutrient transport (*MCT1*, *MCT4*, *SLC5A8,* and *MCU*) and cell metabolism (*ACAT1*, *GLUT1*, *IGFBP3,* and *IGFBP5*). Protein expression of TLR4 and ketogenic enzymes (BDH1 and HMGCS1) were also analyzed using flow cytometry.

A version of this chapter has been accepted by the Journal of Dairy Science. Kent-Dennis, C. and Penner, G.B. 2020. Effects of a pro-inflammatory response on metabolic function of cultured, primary ruminal epithelial cells.

Statistical analysis was conducted with the MIXED model of SAS with media, LPS exposure, and the media × LPS interaction as fixed effects and animal within plate as a random effect. Cells tended to consume more glucose when exposed to LPS compared to without (31.8 vs 28.7 ± 2.7 %; $P = 0.072$), but consumption of propionate and butyrate were not influenced by LPS ($P \geq 0.11$). Expression of *TNF* and *IL1B* were upregulated when exposed to LPS ($P < 0.001$), and expression of *CXCL2* and *CXCL8* were increased following LPS exposure with SCFA (media × LPS; $P < 0.001$). For cells exposed to LPS, there was a downregulation of *ACAT1* and *IGFBP5*, and an upregulation of *GLUT1*, *MCT4*, *MCU*, and *IGFBP3* ($P \leq 0.031$). Media with SCFA led to greater expression of *MCU* ($P = 0.002$). *MCT1* was upregulated in cells incubated with SCFA and without LPS compared to the other groups ($P = 0.001$). Protein expression of ketogenic enzymes was not affected; however, BDH1 mean fluorescence intensity (**MFI**) expression tended to be less in cells exposed to LPS ($P = 0.076$). These data are interpreted to indicate that when REC are exposed to LPS, they may increase glucose metabolism. Moreover, transport of solutes was affected by SCFA in the media and exposure to LPS. Overall, the results suggest metabolic function of REC *in vitro* is altered by a pro-inflammatory response, which may lead to a greater glucose requirement.

7.1 INTRODUCTION

The rumen is uniquely designed for efficient uptake and metabolism of nutrients, especially for short-chain fatty acids (**SCFA**). These functions are facilitated by the ruminal epithelium, which is comprised of stratified squamous epithelial cells, organized into the stratum corneum, granulosum, spinosum, and basale (Graham and Simmons, 2005). The highly specialized cells of the spinosum and basale strata are responsible for the transcellular transport and metabolism of large quantities of SCFA (Stumpff, 2018) and SCFA serve as a primary substrate for whole body energy supply but are also important energy substrates for the cells (Britton and Krehbiel, 1993; Sehested et al., 1999).

Ruminal acidosis, a potential consequence of feeding highly fermentable diets, leads to an increase in the concentration of microbe-associated molecular patterns (**MAMP**) in ruminal fluid, of which lipopolysaccharide (**LPS**) has been the most widely studied (Plaizier et al., 2012). Previous work has provided evidence that acidotic conditions can lead to translocation of bacteria or MAMP across the ruminal epithelium. These conditions play a causative role in the induction of liver abscesses, laminitis, systemic inflammation, and may negatively impact production whether it be milk yield (Khafipour et al., 2009; Plaizier et al., 2012) or growth and feed conversion (Castillo-Lopez et al., 2014). Ruminal MAMP may be capable of interacting with the ruminal epithelial cells (**REC**) and initiate a local inflammatory response (Plaizier et al., 2018; Kent-Dennis et al., 2019).

At a whole-body level, inflammation markedly increases glucose (Kvidera et al. 2017) and amino acid cost (McNeil et al., 2016) in ruminants. While the liver is a central organ that is involved, localized pro-inflammatory responses have been shown to alter nutrient transport and metabolic function in intestinal mucosa (Peuhkuri et al., 2010; Glover and Colgan, 2011). Inflammation in the intestinal epithelium not only results in increased permeability, but also impairs proton-coupled nutrient transport (Thibault et al., 2007). Moreover, in experimental colitis models, butyrate oxidation by colonocytes was decreased and the secretion of ketone bodies reduced (Ahmad et al., 2000). Pathologies, such as inflammatory bowel diseases, of the intestinal mucosa have also been reported to increase the demands for oxygen and energy substrates, especially glucose, in inflamed mucosa (Glover and Colgan, 2011). Metabolic function of keratinocytes, which bare many similarities to REC, may also be altered by

inflammation of the skin (Zhang et al., 2018). The increased energy costs during inflammation have been attributed to an increase in cell proliferation, especially for leukocytes, as well as an increase in production of immune-modulatory molecules such as cytokines which have additional regulatory effects on metabolism (Richardson and Davidson, 2003).

Acidotic conditions in the rumen driving a local inflammatory response in the ruminal epithelium have been speculated to alter metabolic function of the REC (Steele et al., 2011; Zhao et al., 2017). However, there is little direct evidence of the effects of inflammation on REC metabolism. As substantial metabolism of energy substrates occurs in the REC (Britton and Krehbiel, 1993; Penner et al., 2011), it could be speculated that initiation of a pro-inflammatory response to ruminally-derived MAMP may alter nutrient transport and cell metabolic function. In addition, SCFA, especially butyrate, are known to have protective or anti-inflammatory functions in intestinal epithelial cells when exposed to LPS or during active inflammation (Correa-Oliveira et al., 2016; Parada et al., 2019). These functions have not been well characterized in the ruminal epithelium (Zhan et al., 2019). In this experiment, it was hypothesized that primary REC would increase utilization of energy substrates when exposed to LPS. In addition, butyrate and propionate added to the culture media would have a protective effect, resulting in a suppressed pro-inflammatory response. Therefore, the aim of this study was to investigate the effects of LPS on nutrient transport and metabolic function of primary REC in culture, as well as to understand how SCFA affect the pro-inflammatory response, by evaluating energy substrate consumption, and by analyzing the expression of genes and proteins involved in inflammation and metabolism.

7.2 MATERIALS AND METHODS

This study was approved by the University of Saskatchewan Research Ethics Board (protocol no. 20100021) and was conducted in accordance with the Canadian Council of Animal Care guidelines (Ottawa, ON, Canada).

7.2.1 Rumen epithelial cell isolation and cultivation

Yearling beef heifers (n = 9) were housed in individual pens for 28 d and fed a diet of 40.0 % barley silage, 10.0 % grass hay, 33.2 % dry-rolled barley, 16.4 % vitamin and mineral pellet,

and 0.34 % limestone, on a DM basis. Heifers were allowed ad libitum water consumption. On d 28, heifers were euthanized by captive bolt followed by exsanguination and pithing. Heifers were staggered such that only one animal per day was euthanized for sample collection. Ruminal epithelial tissue was excised from the ventral sac and was subsequently washed and transported to the lab in ice-cold Ca^{2+}- and Mg^{2+}-free Dulbecco's phosphate buffered saline (**DPBS**; Sigma-Aldrich, St. Louis, MO, USA) containing Antibiotic-Antimycotic (**Anti-Anti**; final concentration: 400 U/mL Penicillin, 400 µg/mL Streptomycin and 1 µg/mL Amphoteracin B; Thermo Fisher Scientific, Waltham, MA, USA) and Nystatin (240 U/mL; Sigma). Ruminal papillae were cut off at the base, washed in DPBS solution containing Anti-Anti (final concentration: 100 U/mL Penicillin, 100 µg/mL Streptomycin and 0.25 µg/mL Amphoteracin B; Thermo Fisher) and approximately 30 g (initial wet weight) of tissue was subjected to serial trypsinization with 50 mL of a trypsin-EDTA solution (0.25% trypsin and 0.02% EDTA; Sigma) at 37°C. Fresh trypsin-EDTA solution was replaced every 30 min. The first two fractions of supernatant contained highly keratinized cells and were discarded. The subsequent four fractions were each strained through sterile gauze and centrifuged for 5 min at 200 × *g* at room temperature. The resulting cell pellet was washed and centrifuged three times with sterile DPBS containing Ca^{2+} and Mg^{2+}. Pellets from the four fractions were pooled, resuspended, and seeded into 60-mm cell culture plates that were pre-coated with bovine collagen I (Thermo Fisher). Cells were grown in M199 cell culture medium (M2154; Sigma) with the addition of fetal bovine serum (15% v/v; Thermo Fisher), L-glutamine (1.36 m*M*; Sigma), HEPES (20 m*M*; Sigma), Anti-Anti (final concentration: 100 U/mL Penicillin, 100 µg/mL Streptomycin and 0.25 µg/mL Amphoteracin B; Thermo Fisher), Nystatin (240 U/mL; Sigma), Gentamycin (50 mg/L; Sigma), and Kanamycin (100 mg/L; Thermo Fisher) for 2 d and then the media was switched to minimum essentials medium (**MEM**) with stable L-glutamine (M4655; Sigma) and the addition of fetal bovine serum (10% v/v; Thermo Fisher), HEPES (20 m*M*; Sigma) and Anti-Anti (final concentration: 100 U/mL Penicillin, 100 µg/mL Streptomycin and 0.25 µg/mL Amphoteracin B; Thermo Fisher). Fresh media was replaced every 2 to 3 days and cells were cultured for 10 to 12 days until 80 to 90% confluency was attained. An anti-CD90 antibody (final concentration: 0.02 mg/mL; Novus Biologicals, Centennial, CO, USA) was used to determine fibroblast contamination (Kent-Dennis et al., 2020). Cells that were < 10% positive for CD90 were considered acceptable for experimentation (Kisselbach et al., 2009). Cells from each animal were

then re-seeded into two 24-well culture plates (Thermo Fisher) at a rate of 10×10^4 cells/mL and used for the experiment.

7.2.2 Experimental procedure

The day of re-seeding was considered as d 0 of the experiment (Figure 7.1). The total experiment for each batch of REC was conducted over a duration of 5 days. Cells were re-seeded in regular MEM cell culture media (**REG**). On Day 2, fresh media was added to the wells with one plate/animal receiving REG media while the other plate received MEM media with Na-butyrate and Na-propionate (2 m*M* and 5 m*M* final concentrations, respectively; **SCFA**). The concentration of butyrate selected was expected to be sufficient to influence cell functions without causing cytotoxic effects (Galfi et al., 1991) and the propionate concentration was selected to maintain the butyrate to propionate ratio based on Klotz et al. (2001). On d 4, fresh REG and SCFA media were added to the respective wells. Subsamples of each media source, prior to adding it to the cells, were collected and frozen at -20°C. On d 4, cells were exposed to the treatments, which were arranged in a 2 × 2 factorial, with a total of four wells per treatment. Cells were incubated in REG or SCFA media and with or without LPS (50,000 EU/mL; E. coli 055:B5, Sigma) resulting in the following treatment groups: REG without LPS (Control; **REG-LPS**); REG with LPS added (**REG+LPS**); SCFA without LPS (**SCFA-LPS**); and SCFA with LPS added (**SCFA+LPS**). The experiment ended 24 h later on d 5. Supernatant from each well was collected and frozen at -20°C. Cells from two wells/treatment were collected by trypsinization for immediate analysis of TLR4, BDH1 and HMGCS1 staining by flow cytometry. The cell lysate from two wells/treatment was also collected and pooled in 1-mL of Trizol (Thermo). Samples were frozen at -80°C for later RNA extraction.

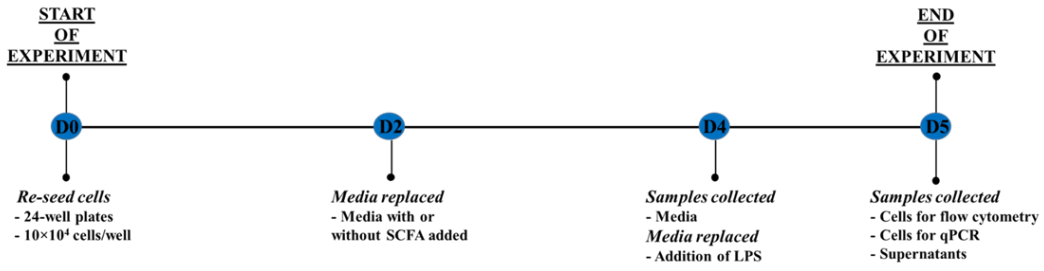

Figure 7.1 Timeline of treatments and sample collections of cultured REC.

7.2.3 Analysis of supernatants

7.2.3.1 Glucose consumption. Glucose concentration in the media and supernatant were quantified using an enzymatic assay modified from that used to assess glucose concentration in plasma. The reaction utilized a peroxidase-glucose oxidase enzyme solution (Sigma) and o-dianisidine (Sigma) as the substrate. Absorbance was determined using a plate reader (Epoch2; BioTek Instruments, Winooski, VT, USA) at a wavelength of 450 nm. Glucose consumption (disappearance) was calculated based on the differences in concentration between the fresh media and supernatants and the volume of the media and supernatant.

7.2.3.2 Butyrate and propionate consumption. Concentrations of butyrate and propionate in the media and supernatants were determined as described by Khorasani et al. (1996) using gas chromatography (Agilent Technologies, Santa Clara, CA, USA) equipped with a Zebron capillary column (ZB-FFAP; 30m × 0.32 mm i.d × 0.25 µm film thickness; Phenomenex, Torrence, CA, USA) with minor modifications. For detection of SCFA in cell culture media, a 1:5 split ratio was used with a 1-µl injection volume. The injector temperature was 225°C. The oven temperature was initially ramped up to 90°C and then increased to 170°C at a rate of 10°C/min, where the temperature was held for 2 min. The detector temperature was held constant at 250°C. Isocaproic acid was used as the internal standard. Consumption (disappearance) of butyrate and propionate by the cells was determined by calculating the difference between concentrations in the media and the supernatants and corrected to account for well volume and time as described for glucose.

7.2.4 Cell staining and flow cytometry

The expression of TLR4, BDH1, and HMGCS1, as well as the percent of dead and apoptotic cells, were analyzed using flow cytometry. The staining and analysis were performed as described by Kaser et al. (2016). Single marker staining was conducted using the antibodies described in Table 1. Following trypsinization, cells were resuspended in 5 mL of media to neutralize the trypsin, centrifuged at 200 × *g* for 5 min at room temperature, and then the supernatant was decanted. Cells were incubated in 96-well round bottom plates (Thermo Fisher) for 1 h at 4°C in fixation/permeabilization reagent (3:1 ratio of diluent to concentrate) from the FoxP3/Transcription Factor staining buffer kit (Ebioscience, San Diego, CA, USA). Plates were then centrifuged at 500 × *g* at room temperature and the supernatant was removed. Cells were

Table 7.1 Description of antibodies used to evaluate inflammatory and metabolic effects of LPS exposure on cultured ruminal epithelial cells.

Antibody	Description	Clone ID	Source	Function	Final Concentration
Primary					
BDH1	Mouse IgG1	1A5	Thermo	Ketogenic enzyme	0.1 mg/mL
CD90	Mouse IgG1 kappa	AF-9	Novus	Fibroblast marker	0.02 mg/mL
HMGCS1	Rabbit	Polyclonal	Thermo	Ketogenic enzyme	0.04 mg/mL
TLR4	Rabbit	Polyclonal	Thermo	Pattern recognition receptor	0.1 mg/mL
Secondary					
Alexa Fluor Ms488	Goat anti-mouse IgG preadsorbed		Abcam		4 µg/mL
Alexa Fluor Rb488	Goat anti-rabbit IgG H&L		Abcam		4 µg/mL

blocked with fetal bovine serum (neat) for 15 min at room temperature. Plates were centrifuged again, the supernatant was removed, and cells were incubated with 10 µL of primary antibody for 10 min at room temperature. Plates were washed twice with 200 µL of permeabilization buffer provided with the kit (diluted 1:10 with water), centrifuged, and the supernatant was removed. Cells were then incubated with 10 µL of secondary antibody for 10 min without light exposure at room temperature. Plates were washed twice, using the same method described above. After the last wash, the cells were re-suspended in 200 µL permeabilization buffer, transferred to a 2-mL microcentrifuge tube (Thermo Fisher), and analyzed using an Accuri C6 flow cytometer (BD Biosciences, Franklin Lakes, NJ, USA) based on a minimum of 5000 events. Data analysis of percent positive and mean fluorescence intensity (**MFI**) were performed using FlowJo Software (BD Biosciences).

A subset of samples (n = 3) were used to monitor the effect of the treatments on apoptosis and cell death by staining cells with annexin and propidium iodide markers, respectively (Annexin V-FITC Apoptosis kit Plus, Biovision Inc, Milpitas, CA, USA). Following trypsinization, cells were resuspended in 100 µL of binding buffer provided with the kit and 1 µL each of Annexin and propidium iodide was added to the cell suspension. Cells were incubated with the markers for 10 min in the dark at room temperature and then analyzed with the flow cytometer. Each marker was incubated and analyzed in separate tubes.

7.2.5 RNA extraction and real time quantitative PCR

Samples of cell lysate, in Trizol, were thawed and a phenol-chloroform RNA extraction (Thermo Fisher) was used with two precipitation steps using isopropanol following phase separation. Linear acrylamide (Thermo Fisher) was used as a co-precipitant (final concentration of 15 µg/mL) in order to visualize the pellet. The concentration of RNA was determined using a Nanodrop (ND2000c; Thermo Fisher). A 1.2% denaturing agarose gel was used to determine RNA integrity. The presence of distinct 18s and 28s bands in all samples was confirmed before RNA was used. Subsequently, 2 µg of RNA was converted to cDNA using the High Capacity Reverse Transcription kit (Thermo Fisher). The cDNA was diluted with nuclease-free water to a final concentration of 10 ng/uL.

Primer pairs for housekeeping and target genes were obtained from IDT (Coralville, IA, USA) and are listed in Table 7.2. Primers were designed to span exon-exon junctions, where possible, and were assessed for efficiency (calculated as: -1+10(-1/slope) × 100) using a serial dilution of pooled cDNA. Melt curves for primers were assessed for dimer formation in order to verify the presence of a single product.

Quantitative real-time PCR (qRT-PCR) was performed using 20 ng cDNA, run in duplicate, using SsoFast EvaGreen Supermix (Bio-Rad, Hercules, CA, USA) on a CFX96 Real-Time PCR Detection System (Bio-Rad). The Ct values for the target genes were normalized to the geometric mean of the three housekeeping genes (*ACTB, GAPDH* and *STX5*), and statistical analysis was performed on ΔCt. Data are presented as fold changes, with treatments held relative to the mean value of REG-LPS.

7.2.6 Statistical Analysis

Data were analyzed using the MIXED procedure of SAS 9.4 (SAS Institute, Cary, NC, USA) with LPS treatment, media, and the treatment × media interaction as fixed effects. Animal within plate was considered random. Data were analyzed using mean separations. For gene expression, statistical analysis was performed on ΔCt and data are presented as fold change.

Table 7.2 Primers used for quantitative real-time PCR

Gene Name (official gene symbol)	Source[1]	Sequence (5'-3')	Amplicon Size	Efficiency %[2]
Housekeeping Genes				
Beta actin (ACTB)	NM_173979.3	F: GAGCTACGAGCTTCCTGACGGGC R: AATGCCGCAGGATTCCATGCCCAG	109	96
Glyceraldehyde-3-phosphate dehydrogenase (GAPDH)	NM_001034034.2	F: GGGTCATCATCTCTGCACCT R: GGAGGCATTGCTGACAATCT	101	91
Syntaxin 5 (STX5)	NM_001075444.1	F: CCATTCAGAGGATCGACGAG R: GGATGTGACCGACTGGAAGT	95	103
Inflammation-Related Genes				
C-X-C motif chemokine ligand 2 (CXCL2)	NM_174299.3	F: CCGAAGTCATAGCCACTCTCA R: CTTCTGTTTTCCACCTGGTCA	128	99
C-X-C motif chemokine ligand 8 (CXCL8)	NM_173925.2	F: AGAGCTGAGAAGCAAGATCCA R: ACCCTACACCAGACCCACAC	150	104
Interleukin 1 beta (IL1B)	NM_174093.1	F: CTGAGGAGCATCCTTTCATTC R: GTCCTGGAGTTTGCACTTTAT	114	97
Transforming growth factor 1 beta (TGFB1)	NM_001166068.1	F: ACTGCTTCAGCTCCACAGAA R: TCCAGGCTCCAGATGTAAGG	148	105
Toll-like receptor 2 (TLR2)	XM_015475330.1	F: TGATGCTGCCATTCTGATTC R: GCCACTCCAGGTAGGTCTTG	107	96
Toll-like receptor 4 (TLR4)	NM_174198.6	F: CCTTGCGTACAGGTTGTTCC R: CTCAGGTCCAGCATCTTGGT	104	90
Tumor necrosis factor alpha (TNF)	NM_173966.3	F: CAAGTAACAAGCCGGTAGCC R: AGATGAGGTAAAGCCCGTCA	153	99
Metabolism-Related Genes				
Acetyl-CoA acetyltransferase 1 (ACAT1)	NM_001046075.1	F: CGGGTGCAGGAAATAAGGTA R: TAGTGGCTGGCAGAGAGGA	133	103
Adenosine A2b receptor (ADORA2B)	NM_001075925.1	F: CGTCCCGCTCAGGTATAAGA R: TGGCAATTTTTCTGTCGTTC	128	103
3-hydroxybutyrate dehydrogenase 1 (BDH1)	NM_001034600.2	F: GACCCTGAGAAAGGCTTGTG R: TCCTTGTAGGTCTCCATGCTG	92	96
Hypoxia inducible factor 1a (HIF1A)	NM_174339.3	F: GCCACTCCCCCATAATGTAA R: ATCCAAATCACCAGCATCCA	106	98
Insulin-like growth factor binding protein 3 (IGFBP3)	NM_174556.1	F: GCTGAACCACCTCAAGTTCC R: CGGCACTGCTTTTTCTTGTA	96	99
Insulin-like growth factor binding protein 5 (IGFBP5)	NM_001105327.2	F: CAAGAGAAAGCAGTGCAAACC R: AGTCCCCGTCCACGTACTC	107	98
Mitochondrial calcium uniporter (MCU)	NM_001206102.1	F: CACACAGTTTGGCATTTTGG R: AACATATTCCTGGCGTGTCA	139	97
MYC proto-oncogene, bHLH transcription factor (MYC)	NM_001046074.2	F: GACCAGTAGCGACTCTGAGGA R: GACTAACGGGCTGTGAGGAG	148	106
5'-nucleotidase ecto aka CD73 (NT5E)	NM_174129.4	F: GGAACAATGGCACGATTACC R: CTTCAGGGTGGAGCCTTTTA	95	98
Purinergic receptor P2X 7 (P2RX7)	NM_001206516.1	F: CTTGCAGGGGAACTCCTTTT R: TCAGAGGAACAGAGCGTCCT	108	108
Solute carrier family 2 member 1 aka GLUT1 (SLC2A1)	NM_174602.2	F: GGCATCAACGCTGTTTTCTA R: ACACGACAGTGAAGGCTGTG	115	105
Solute carrier family 5 member 8 (SLC5A8)	NM_001164861.1	F: TGCCTTAGCAGCAGTAACCA R: CAGCACACTCATTCCTTGTGA	100	98
Solute carrier family 16 member 1 aka MCT1 (SLC16A1)	NM_001037319.1	F: TCCATCGGCTTCTCTTATGC R: GCTGATAGGACCTCCACCAT	144	95
Solute carrier family 16 member 3 aka MCT4 (SLC16A3)	NM_001109980.3	F: TGTGGTGAGCTATGCCAAGG R: TCAGCGAAGCCGTTGAAGAA	183	98

[1]National Center for Biotechnology Information (NCBI)
[2]Efficiency= $-1 + 10^{(-1/\text{slope})}$X100

7.3 RESULTS

7.3.1 Glucose and SCFA concentrations in cell supernatants

The percent of glucose (Table 7.3) that was consumed by REC incubated with SCFA was 13.9% compared to 46.6% when incubated with REG (SEM = 3.7; $P < 0.001$). Cells exposed to LPS tended to consume more glucose compared those in media without LPS (31.8 versus 28.7 ± 2.7 %; $P = 0.072$), but the amount of butyrate and propionate consumed was not affected by LPS exposure. Collectively, cells incubated with SCFA consumed 0.42 m*M* (21.2 %) of the butyrate and 0.38 m*M* (7.6 %) of the propionate (Table 7.3).

Table 7.3 Percent consumption[1] of energy substrates in primary ruminal epithelial cells exposed to 0 (-LPS) or 50,000 EU/mL LPS (+LPS), with or without the addition of SCFA to the culture media.

	Media[2]			Treatment			*P* Values		
	REG	SCFA	SEM[3]	-LPS	+LPS	SEM	Media	Treatment	Media × Treatment
Glucose, %	46.6	13.9	3.7	28.7	31.8	2.7	< 0.001	0.072	0.80
Butyrate, %	nd	21.2	-	23.8	18.5	2.5	-	0.12	-
Propionate, %	nd	7.6	-	4.0	11.1	3.2	-	0.11	-

[1]Calculated by subtracting the amount measured in the supernatants from the amount measured in media subsamples prior to use
[2]REG = regular culture media, SCFA = Media with 2 m*M* butyrate and 5 m*M* propionate added
[3]SEM = Standard error of the mean of each factor

7.3.2 Cell staining

The MFI for TLR4, BDH1, and HMGCS1 (Table 7.4) were not affected by media or LPS treatment, and there were no interactions detected. However, there was a tendency for less BDH1 MFI in cells exposed to LPS ($P = 0.076$). Compared to REG, exposure to SCFA resulted in a reduced number of cells positive for TLR4 (94.8 versus 87.0 ± 2.5 %; $P = 0.046$) and BDH1 (83.4 versus 66.4 ± 4.6 %; $P = 0.020$), but HMGCS1 was not affected. The percent of positive cells was not influenced by exposure to LPS. Cell death (propidium iodide) and apoptosis (Annexin) were not affected by SCFA or LPS exposure (Table 7.4).

Table 7.4 Percent positive and mean fluorescence intensity for markers in primary ruminal epithelial cells.

	Media[1]			Treatment			*P* Values		
	REG	SCFA	SEM[5]	-LPS	+LPS	SEM	Media	Treatment	Media × Treatment
TLR4									
% Positive	94.8	87.0	2.5	90.8	91.0	2.7	0.046	0.82	0.60
MFI[2]	87794	94273	12953	89856	92211	9299.2	0.73	0.47	0.51
BDH1									
% Positive	83.4	66.4	4.6	76.4	73.4	3.6	0.020	0.31	0.60
MFI	49199	46997	5545.5	50109	46086	4061.6	0.78	0.076	0.49
HMGCS1									
% Positive	66.0	47.9	7.4	56.4	57.5	5.5	0.101	0.72	0.88
MFI	33872	34002	5331.6	32744	35129	3961.0	0.99	0.33	0.62
Annexin[3]									
% Positive	9.5	10.8	4.7	10.1	10.2	3.4	0.85	0.93	0.73
Propidium Iodide[4]									
% Positive	8.0	7.3	3.8	7.4	7.9	2.7	0.91	0.38	0.54

[1]REG = regular media, SCFA = media with 2 m*M* butyrate and 5 m*M* propionate added
[2]Mean fluorescence intensity, arbitrary unit
[3]Apoptotic cells
[4]Dead cells
[5]SEM = Standard error of the mean of each factor

7.3.3 Gene expression

Expression of *TNF* (Figure 7.2A) and *IL1B* (Figure 7.2B) was greater ($P < 0.001$) following LPS exposure. The addition of SCFA to the media also resulted in greater expression of *TNF* and *IL1B* compared to REG ($P < 0.001$). When compared to REG-LPS, REG+LPS and SCFA-LPS increased expression of both CXCL2 (Figure 7.2C) and CXCL8 (Figure 7.2D), and there was greatest expression of *CXCL2* and *CXCL8* in cells exposed to LPS with SCFA in the media (LPS × media, $P < 0.001$).

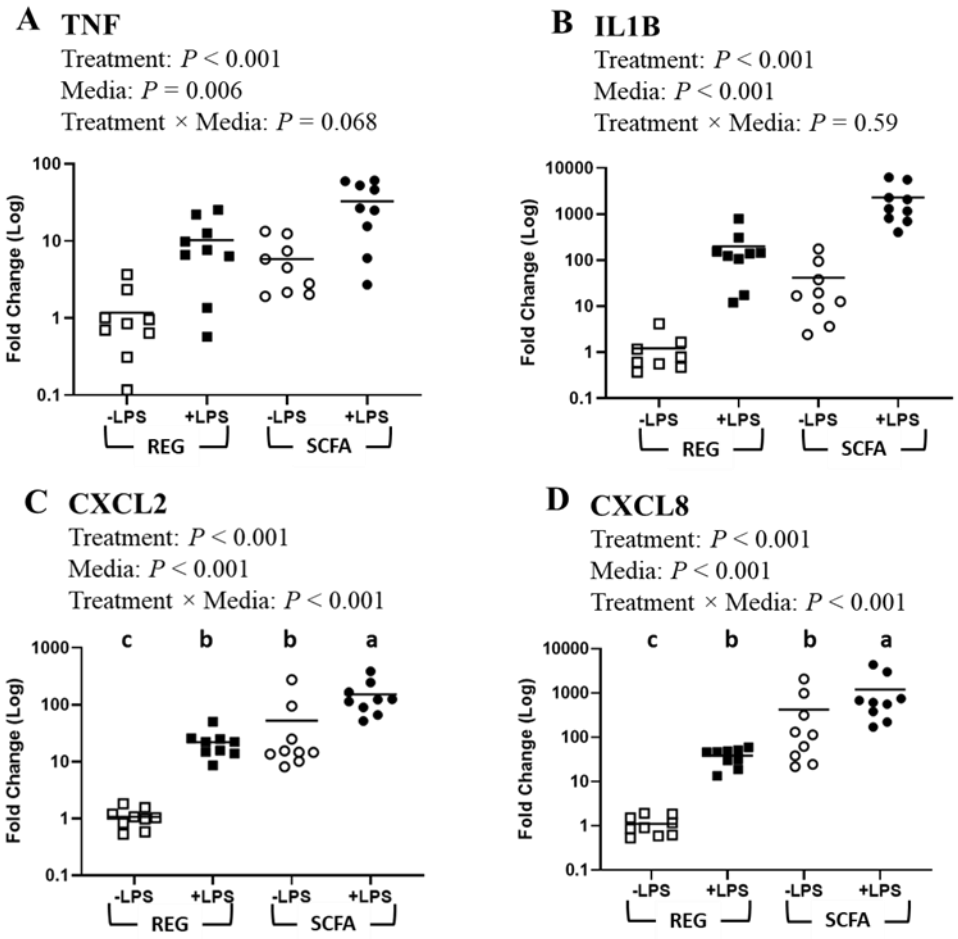

Figure 7.2 Gene expression of pro-inflammatory cytokines, TNF (A) and IL1B (B), and chemokines, CXCL2 (C) and CXCL8 (D), in cultured ruminal epithelial cells exposed to either 0 or 50,000 EU/mL LPS with (SCFA) or without (REG) the addition of SCFA (2 m*M* butyrate and 5 m*M* propionate) in the culture media. The ΔCt was used for statistical analysis ($P < 0.05$) and results are presented as fold change (log), with each individual plotted. The bar represents the mean.

A tendency for the same response was also the case for *TNF* (LPS × media, $P = 0.068$). Exposure to LPS resulted in increased expression of *PTGS2* (Figure 7.3A; $P < 0.001$); however, PTGS2 expression was not influenced by SCFA. Expression of *TLR4* (Figure 7.3B) also increased with LPS exposure ($P < 0.001$); however, SCFA added to the media down-regulated *TLR4* ($P = 0.008$). Neither LPS nor SCFA influenced *TGFB1* (Figure 7.3C).

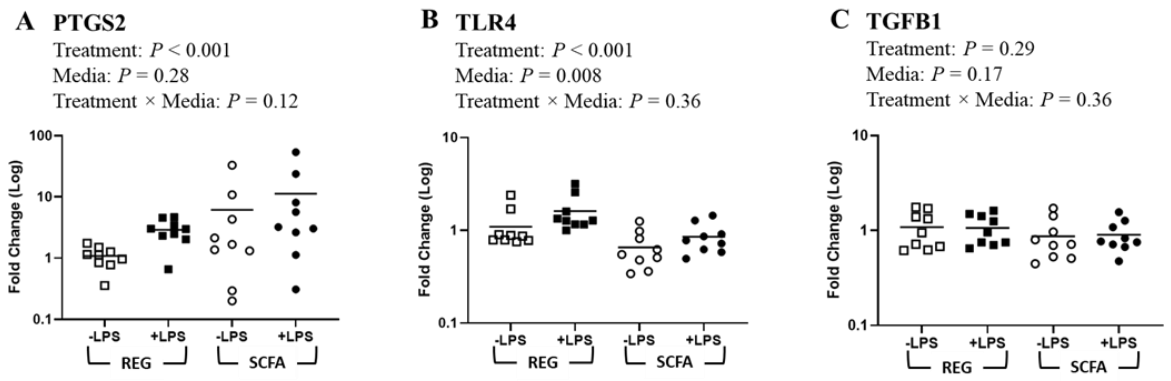

Figure 7.3 Gene expression of a lipid mediator of inflammation, PTGS2 (A), toll-like receptor, TLR4 (B), and growth factor-like cytokine, TGFB1 (C), in cultured ruminal epithelial cells exposed to either 0 or 50,000 EU/mL LPS with (SCFA) or without (REG) the addition of SCFA (2 m*M* butyrate and 5 m*M* propionate) in the culture media. The ΔCt was used for statistical analysis ($P < 0.05$) and results are presented as fold change (log), with each individual plotted. The bar represents the mean.

There was a significant treatment × media interaction such that expression of *P2RX7* (Figure 7.4A) was less for cells exposed to LPS in REG media (1.3-fold; $P = 0.006$) compared to the other treatments. Exposure to LPS increased expression of *ADORA2B* (Figure 7.4B; $P < 0.001$) and decreased expression of *CD73* (Figure 7.4C; $P = 0.002$).

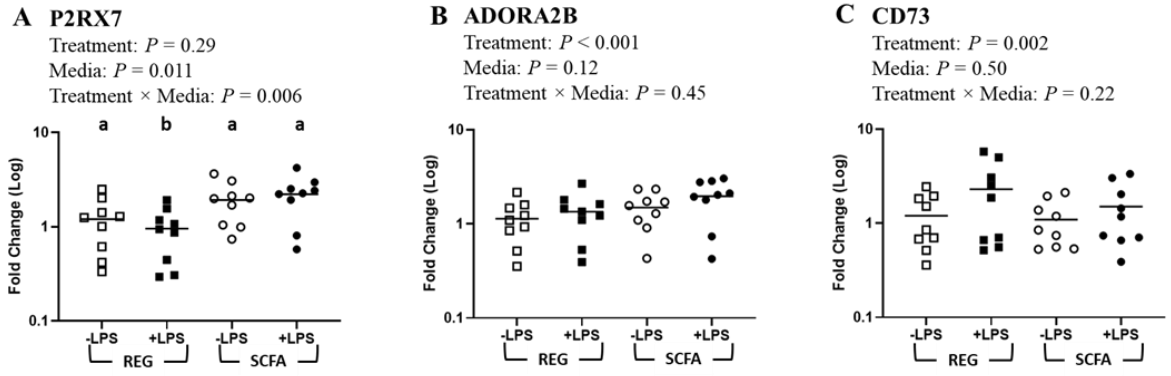

Figure 7.4 Gene expression of purinergic receptors, P2RX7 (A) and ADORA2B (B), and surface enzyme, CD73 (C) in cultured ruminal epithelial cells exposed to either 0 or 50,000 EU/mL LPS with (SCFA) or without (REG) the addition of SCFA (2 m*M* butyrate and 5 m*M* propionate) in the culture media. The ΔCt was used for statistical analysis ($P < 0.05$) and results are presented as fold change (log), with each individual plotted. The bar represents the mean.

Although *HIF1A* (Figure 7.5A) was not affected by LPS or media, SCFA-LPS had decreased expression of *GLUT1*, compared to REG+LPS and SCFA+LPS (Figure 7.5B; treatment × media $P = 0.010$). A treatment × media interaction resulted in an upregulation of *MCT1* (Figure 7.6A; treatment × media $P = 0.001$) when SCFA was added to the media without LPS exposure. Expression of *MCT4* (Figure 7.6B) and *SLC5A8* (Figure 7.6C) were greater ($P = 0.031$ and $P = 0.004$, respectively) following LPS exposure compared to cells incubated without LPS. Exposure to LPS did not affect *MCU* expression (Figure 7.6D); however, the addition of SCFA increased expression (1.6-fold; $P = 0.002$).

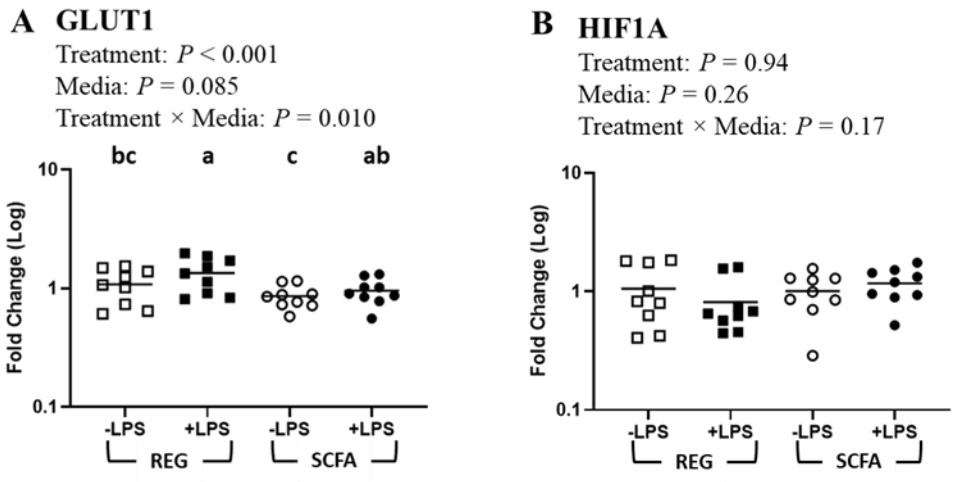

Figure 7.5 Gene expression of hypoxia-inducible factor, HIF1A (A), glucose transporter, GLUT1 (B), in cultured ruminal epithelial cells exposed to either 0 or 50,000 EU/mL LPS with (SCFA) or without (REG) the addition of SCFA (2 m*M* butyrate and 5 m*M* propionate) in the culture media. The ΔCt was used for statistical analysis ($P < 0.05$) and results are presented as fold change (log), with each individual plotted. The bar represents the mean.

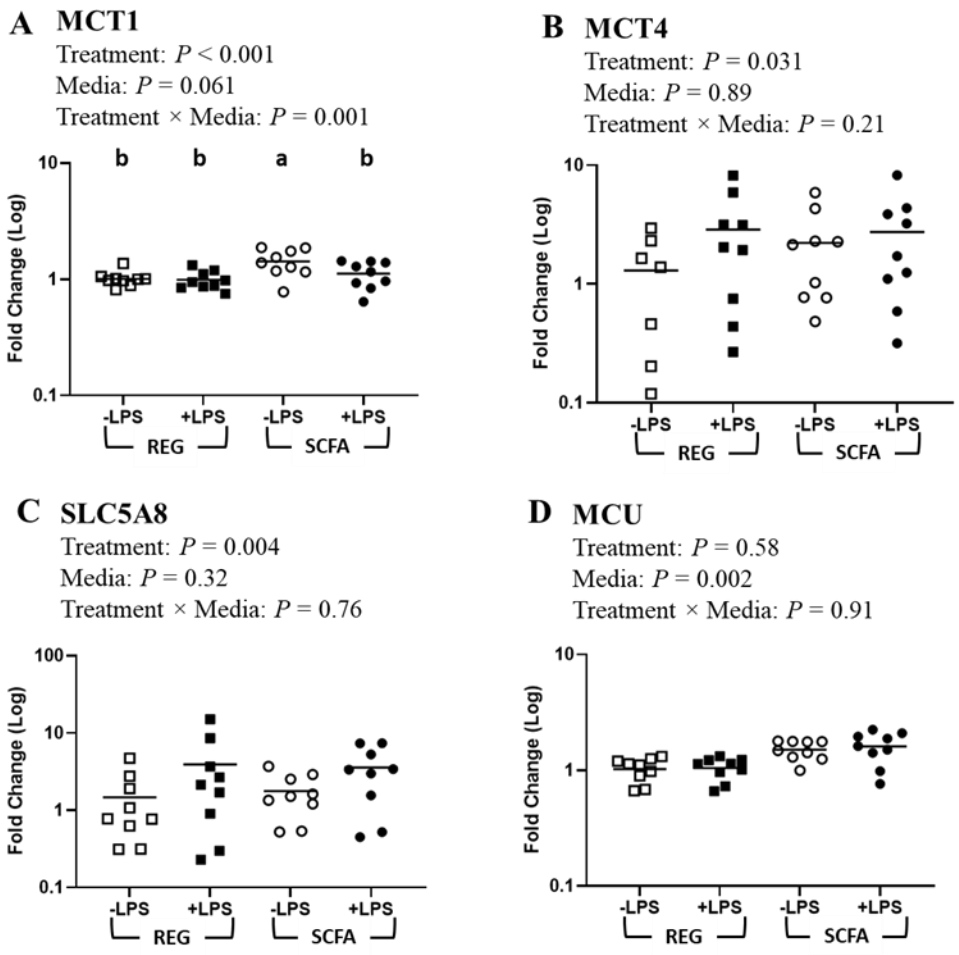

Figure 7.6 Gene expression of ketogenic enzymes, ACAT1 (A) and BDH1 (B), and IGFBP3 (C) and IGFBP5 (D) in cultured ruminal epithelial cells exposed to either 0 or 50,000 EU/mL LPS with (SCFA) or without (REG) the addition of SCFA (2 m*M* butyrate and 5 m*M* propionate) in the culture media. The ΔCt was used for statistical analysis ($P < 0.05$) and results are presented as fold change (log), with each individual plotted. The bar represents the mean.

There was a down-regulation of *ACAT1* (Figure 7.7A; $P < 0.001$) and *BDH1* (Figure 7.7B; $P = 0.001$) following exposure to LPS. However, *BDH1* increased in expression (1.4-fold; $P = 0.046$) when SCFA were added to the media and this also tended to be the case for *ACAT1* ($P = 0.072$). Both LPS and SCFA increased expression of *IGFBP3* (Figure 7.7C; 4.7-fold; $P = 0.001$ and 6.3-fold; $P < 0.001$, respectively), and exposure to LPS resulted in a down-regulation of *IGFBP5* (Figure 7.7D; 1.1-fold; $P < 0.001$). For *IGFBP5* there was tendency for a treatment × media interaction ($P = 0.050$).

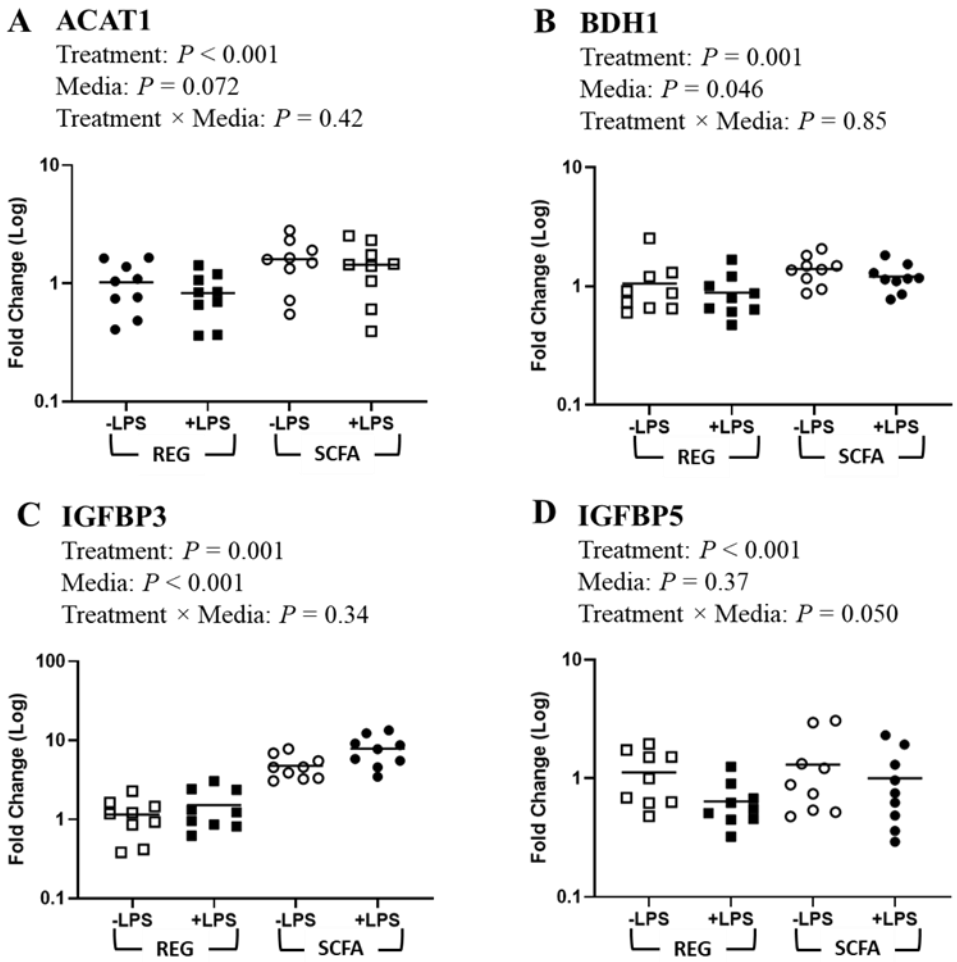

Figure 7.7 Gene expression of ketogenic enzymes, ACAT1 (A) and BDH1 (B), and IGFBP3 (C) and IGFBP5 (D) in cultured ruminal epithelial cells exposed to either 0 or 50,000 EU/mL LPS with (SCFA) or without (REG) the addition of SCFA (2 m*M* butyrate and 5 m*M* propionate) in the culture media. The ΔCt was used for statistical analysis ($P < 0.05$) and results are presented as fold change (log), with each individual plotted. The bar represents the mean.

7.4 DISCUSSION

A pro-inflammatory response at a mucosal surface is initiated, whether by immune cells or non-hemopoietic cell types, by the binding of MAMPs to pattern recognition receptors (**PRR**) activating a signaling cascade that leads to transcription of cytokines, chemokines, and other immune-modulatory molecules (Pott and Hornef, 2012). Recent work has suggested that REC are capable of initiating a pro-inflammatory response (Zhang et al., 2016; Kent-Dennis et al.,

2020). In addition to epithelial cells, large numbers of immune cells, such as neutrophils, macrophages, and lymphocytes are recruited to the site of the insult and further promote inflammation in order to eliminate the threat, repair cellular damage, and return the tissue to a homeostatic state (Peterson and Artis, 2014). As a consequence, metabolic function of the tissue may be altered; however, effects of a local inflammatory response on ruminal epithelial metabolism has not been explored.

Carbohydrate digestion in the gastrointestinal tract results in the production of SCFA by the resident microflora. These end-products of fermentation, especially butyrate, have been extensively studied as they are important energy substrates, and may also help to maintain epithelial barrier function, modify cellular processes such as proliferation, and mediate the inflammatory response in the mucosal tissue (Correa-Oliveira et al., 2016). In particular, the potential anti-inflammatory effects of SCFA on intestinal epithelial cells have been of interest as a possible therapy for pathologies such as ulcerative colitis and Crohn's disease (Parada et al., 2019). However, the effects of SCFA have been inconsistent, with both pro- and anti-inflammatory responses reported (Li et al., 2018). The addition of SCFA to culture media of colon epithelial cells suppressed the production of pro-inflammatory cytokines (Hung and Suzuki, 2018). Conversely, SCFA have been shown to enhance expression of inflammation-induced TLRs (Lin et al., 2015; Xiao et al., 2018), increase levels of pro-inflammatory cytokines (Vancamelbeke et al., 2019), and may stimulate recruitment of first-responder cells, such as neutrophils (Correa-Oliveira et al., 2016). In the present study, exposure to LPS and the addition of SCFA to the media independently resulted in increased expression of *TLR4*, *TNF,* and *IL1B.* Moreover, expression of *CXCL2* and *CXCL8*, chemokines that recruit neutrophils during acute inflammation, were enhanced by the combination of LPS and SCFA. Although the reasons for the apparent paradoxical effects of SCFA have not been elucidated, the effects observed in the present study suggest that SCFA can modulate the inflammatory response to LPS in REC, and may have further effects on cellular processes or metabolism. In agreement, Zhan et al. (2019) demonstrated an enhanced immune response in the presence of SCFA in cultured REC, providing further evidence that SCFA play a regulatory role in the inflammatory response in the ruminal epithelium.

Chemotaxis of neutrophils is intimately linked to purinergic signaling, a process that causes the release of ATP into the extracellular environment as a consequence of cellular stress,

injury, or infection (Ferrari et al., 2016). The free ATP acts as a signaling molecule in order to fine tune immune cell responses and prevent excessive tissue damage caused by inflammation (Ferrari et al., 2016). Two main types of receptors, P2 and P1, mediate the signaling pathway. The P2 receptors, of which there are the P2XR and P2YR groups, bind extracellular ATP, inducing a pro-inflammatory response, leading to secretion of chemokines and recruitment of immune cells (Pastore et al., 2007; Idzko et al., 2014). The ATP is then converted to AMP facilitated by CD39. Adenosine is then produced from the AMP, by the action of CD73, and binds to one of the four subtypes (A_1, A_{2A}, A_{2B} or A_3) of the P1 receptor group (Antonioli et al., 2013). In the current study, gene expression patterns of CD73, and both a P2 receptor (*P2RX7*) and a P1 receptor (*ADORA2B*) were evaluated. Following exposure to LPS, without SCFA added to the media, REC expression of *P2RX7* was down-regulated. Expression of *CD73* and *ADORA2B*, however, were up-regulated in response to LPS exposure. Production of adenosine and binding to P1 receptors is associated with an anti-inflammatory response (Ferrari et al., 2016). The present results are consistent with the literature, whereby activation of P2 and P1 receptors invoke opposing effects (Ferrari et al., 2016) and suggest that the pro-inflammatory response in REC may be regulated to prevent cell damage.

Inflammation can result in increased catabolism and increased energy, nitrogen, and micronutrient demands (Lennie et al., 1995). Inflammation has been associated with altered metabolic activity at systemic and tissue levels (Staal-van den Brekel et al., 1995; Hardin 2000). Production of immune-modulatory molecules and increases in cell turnover, both systemically and locally, are implicated in the changes in metabolic demands. Using an intravenous LPS challenge in dairy cows, Kvidera et al. (2017) demonstrated that a systemic inflammatory response increased whole body glucose requirements. At a tissue level, an ex vivo experiment with rabbit intestinal epithelium showed that pro-inflammatory cytokines were associated with an increase in metabolic demands and increased glucose absorption (Hardin et al., 2000). In the present experiment, exposure to LPS increased expression of *TLR4*, *PTGS2*, and cytokines *TNF* and *IL1B*, suggesting the REC had initiated a pro-inflammatory response. Following LPS exposure, REC tended to consume more glucose indicating that the response may have increased the energetic demand. However, the amount of butyrate and propionate consumed by the cells was not affected by LPS exposure. The increase in glucose utilization may indicate a metabolic shift towards glycolysis or oxidation. However, we did not assess lactate formation arising from

glucose consumption and therefore cannot conclude whether glucose was partially metabolized or completely oxidized. Immune cells (Kominsky et al., 2010), airway epithelial cells (Garnett et al., 2016), and keratinocytes (Wickersham et al., 2017) also favor glycolysis under inflammatory conditions, suggesting that REC may do so as well.

Exposure to LPS increased the expression of *GLUT1* in REC, supporting the increase in glucose consumption observed. Interestingly, the addition of SCFA, without LPS, resulted in a down-regulation of *GLUT1*. Ability to alter the energy substrate use, depending on their availability, has previously been demonstrated in ruminal epithelial tissue (Wiese et al., 2013). These data suggest that in the presence of SCFA, there may be a shift away from glucose utilization. As well as its function in glucose transport, previous work has shown that *GLUT1* may be important for modulating inflammation in the skin (Zhang et al., 2018). *GLUT1* was also found to increase during inflammation-induced hypoxia, a result of depleted oxygen and increased glycolysis at sites of inflammation (Corcoran and O'Neill, 2016; Zhang et al., 2019). The present results show that *GLUT1* expression in the SCFA+LPS cells was greater than without LPS, suggesting that the presence of SCFA may be promoting inflammation. Others have also shown that SCFA have a modulating effect on REC when exposed to a variety of challenges (Meissner et al., 2017). Inflammation-induced hypoxia is mediated by *HIF1A*. In the present study *HIF1A* was not affected by either treatment; however, *HIF1A* is tightly regulated with a half-life of only a few minutes (Masoud and Li, 2015), therefore a change in mRNA expression may not have been detectable.

Expression of *IGFBP3* increased in response to SCFA in the media. Insulin-like growth factor (**IGF**) is an important homeorhetic molecule of metabolism that acts as a signal of adequate nutrient availability (Clemmons, 2012). Although tissue dependent, previous work has shown that IGF1 increases glucose transport into non-hepatic cells (Simpson et al., 2004) and regulates utilization of nutrients such as oxidation of free fatty acids (Clemmons, 2012). In addition, IGF1 is well-known for its effects on cell proliferation (Kiepe et al., 2005; Zheng et al., 2018). At a systemic level, IGFBP3 and IGFBP5 proteins bind to a tertiary molecule, acid-labile subunit (ALS), and together act to increase total serum IGF1 levels by prolonging its half-life (Clemmons, 2018). However, all IGF binding proteins are pleiotropic and have local tissue-specific functions that are sometimes independent of IGF1 (Baxter, 2001; Zheng et al., 2018). Perks et al. (2000) reported that IGFBP3 and IGFBP5 have opposing functions, which was also

observed in ruminal epithelial tissue by Steele et al. (2011), where a high grain diet increased gene expression of *IGFBP3* while *IGFBP5* was down-regulated. In contrast, *IGFBP3* was decreased while *IGFBP5* increased when butyrate was infused into the rumen in neonatal lambs (Liu et al., 2019). In the present study, *IGFBP3* increased with the addition of SCFA; however, *IGFBP5* was not affected by the media. Previous work has suggested that butyrate, through its regulatory action on growth factors such as IGF, influences cellular proliferation and apoptosis of REC (Penner et al., 2011). Neogrady et al. (1989) indicated that butyrate may inhibit REC apoptosis in culture. However, in the present study, rates of apoptosis of the REC were not influenced by SCFA in the culture media. The mechanisms that mediate cell turnover in the ruminal epithelium in response to dietary changes involve many interconnected processes that have not been fully elucidated and warrant further investigation.

The inflammatory response has also been found to regulate the expression of IGFBP (O'Connor et al., 2008). The present results suggested that LPS increased expression of *IGFBP3* but decreased *IGFBP5* supporting the results of Steele et al. (2011) when imposing a rumen acidosis induction model. Previous work has suggested that IGF may increase in response to stimulation by pro-inflammatory cytokines (Clemmons, 2012). However, expression of *IGFBP3* is also associated with protective functions in response to inflammation (O'Connor et al., 2008; Kim and Hwang, 2018). Further research is required to elucidate the potential homeorhetic and immune-modulatory effects in REC.

As further evidence that LPS influenced metabolic activity in the present experiment, expression of *ACAT1*, a key mitochondrial enzyme, was down-regulated in cells that had been exposed to LPS, which may suggest a shift away from ketogenesis. In the first step in the formation of ketone bodies, *ACAT1* catalyzes the reaction that combines two acetyl-CoA molecules to form acetoacetyl-CoA, and, depending on substrate availability, it also catalyzes the reverse reaction. Moreover, *BDH1*, a ketogenic enzyme that facilitates BHBA formation, was also down-regulated in cells exposed to LPS. The MFI of BDH1 protein tended to be less, suggesting that, in addition to mRNA, protein expression was also affected. In agreement with the present results, Memon et al. (1992) demonstrated that LPS-induced inflammation, by way of pro-inflammatory cytokines *IL1B* and *TNF*, resulted in reduced production of ketone bodies in mice *in vivo*. The inflammation-induced inhibition of ketogenesis was also observed in hepatocytes by Pailla et al. (1998) and Pailla et al. (2001).

A state of inflammation not only increases metabolic demands, it may also alter nutrient transport by epithelial cells (Peuhkuri et al., 2010). Previous work has demonstrated detrimental effects of experimental colitis on energy substrate uptake and metabolic function of colonocytes (Ahmad et al., 2000). Thibault et al. (2010) suggested that inflammatory bowel disease was associated with dysregulation of *MCT1* and thus uptake of butyrate. In the gastrointestinal epithelia, *MCT1* is an apically-localized SCFA transporter (Graham et al., 2007), while *MCT4* is thought to be primarily on the basolateral membrane (Kirat et al., 2007), although there is evidence that these expression patterns may be reversed in ruminal epithelium (Stumpff, 2018). In the present study, REC not exposed to LPS had greater expression of *MCT1* but only in the presence of SCFA. This is in agreement with findings by Villodre Tudela et al. (2015), where MCT1 was also found to increase following incubation with butyrate. Additionally, in the present study, expression of *MCT4* and *SLC5A8* were both up-regulated following exposure to LPS. Increased expression of *MCT4* was also observed by He et al. (2018) in intestinal epithelium afflicted with inflammatory bowel disease. The authors suggest that MCT4 may be increased in response to greater levels of lactate. Lactate production is commonly reported in cultured cells and can indicate metabolic shifts (Hu et al., 1987; Zagari et al., 2013). Although lactate was not measured in the current experiment, the up-regulation in MCT4 may have occurred in an effort to mediate lactate accumulation due to increased glycolysis. *SLC5A8*, a sodium-coupled monocarboxylate transporter, is involved in the apical transport of SCFA as well as lactate and ketone bodies (Sivaprakasam et al., 2018). Martin et al. (2006) suggested that, in addition to transport of solutes, *SLC5A8* may also play a regulatory role in maintaining the energy status in some tissues.

In the REC incubated with SCFA, there was a decrease in glucose consumption, compared to those incubated with REG media. Although not affected by LPS treatment, the addition of SCFA to the culture media resulted in increased expression of *MCU*, a transporter localized to the inner mitochondrial membrane that controls the influx of calcium (Paupe and Prudent, 2018). Calcium is a regulator of mitochondrial dehydrogenases and plays a key role in the ATP production (Finkel et al., 2015). The increase in *MCU* expression in the REC further suggests that metabolic function was altered in culture by the presence of SCFA. Together with the expression patterns of BDH1, MCT1 and ACAT1, the results suggest a shift towards butyrate

metabolism in cells incubated with SCFA in culture and indicate the ability of REC to utilize SCFA in the culture model.

7.5 CONCLUSION

The current study demonstrated the complexity of the inflammatory response in REC and explored how the response affected nutrient transport and metabolism. The results suggested that REC consumed more glucose following exposure to LPS, presumably as a result of the pro-inflammatory response. However, the difference was small, and the response did not appear to influence utilization of SCFA added to the culture media. Nonetheless, the results of this study suggest that the inflammatory response to LPS altered the metabolic activity of REC in culture through differential expression of genes associated with nutrient uptake. Although the exact role of SCFA on the inflammatory response was not fully elucidated, the results of this study demonstrate evidence for regulatory roles of SCFA in REC, especially in the recruitment of immune cells, such as neutrophils. Many questions still remain and future research should focus on understanding the mechanisms by which the inflammatory response in REC affects nutrient transport and shifts metabolism including the metabolic fates of glucose. Overall, this study provides evidence that, while the effects on energy substrate consumption may be limited, the pro-inflammatory response, as a result of the interaction between ruminal epithelium and ruminal MAMPs, may alter cellular processes and metabolism.

CHAPTER 8: GENERAL DISCUSSION

Gastrointestinal tract functions impact all physiological processes in the body and are a determining factor for animal performance and overall health (Celi et al., 2017). The steady state of the gastrointestinal tract, and alterations due to disease or dysfunction have long been in the research spotlight for humans and animals alike, and ruminants are no exception. Perturbations in the diet can dramatically impact microbe-mucosal interactions, mucosal barrier function, and transport and absorption of luminal molecules (Peuhkuri et al., 2010). These physiological changes can impact the availability of glucose, amino acids, and micronutrients while also increasing the demand for these nutrients (Celi et al., 2017). Consequently, there can be serious implications on health, welfare, and productivity of agriculture animals (Plaizier et al., 2018). The importance of the gastrointestinal tract is emphasized given that digestive disorders are prevalent in production ruminants and can affect a substantial percentage of a herd (Plaizier et al., 2019). For example, 18 to 40% of dairy cows may be afflicted by subacute ruminal acidosis (**SARA**) during their lactation (Zebeli and Metzler-Zebeli, 2012).

Modern dairy and beef cattle are efficient at converting feed to milk and muscle, respectively. Adequate energy and other nutrients must be provided to support production. To meet the metabolizable energy and metabolizable protein demands, cattle are fed highly fermentable diets. However, diets without sufficient physically effective NDF or those provided without adequate adaptation, can lead to digestive disorders such as ruminal acidosis (Plaizier et al., 2018). Due to an increase in SCFA production, ruminal acidosis can occur, and is characterized by a decrease in ruminal pH and an increase in osmolality (Owens et al., 1998). Subsequently, the ruminal epithelial barrier may be compromised, leading to translocation of microbes or microbe-associated molecular patterns (**MAMP**), such as lipopolysaccharide (**LPS**), across the epithelium (Nocek et al., 1997). Translocation of MAMPs into systemic or lymphatic circulation has been implicated as a key factor in the development of laminitis, liver abscesses, and systemic inflammation (Nocek et al., 1997; Kleen et al., 2003; Khafipour et al., 2009). Inflammation can alter whole body metabolism, such as increasing the demand for glucose (Kvidera et al., 2017) and amino acids (McNeil et al., 2016) and may also affect local metabolic functions of epithelial cells (Peuhkari et al., 2010). Translocation may result in MAMPs

interacting with ruminal epithelial cells (**REC**) by way of pattern recognition receptors (**PRR**), potentially leading to local inflammatory response (Malmuthuge et al., 2012; Zhang et al., 2016). However, the capability of REC to initiate a pro-inflammatory response had not been fully elucidated prior to completion of research within this thesis. Furthermore, it was unknown whether the local inflammatory response in REC influences epithelial metabolism or cellular functions. Therefore the overall hypothesis of this project was that MAMPs, specifically LPS, would stimulate a pro-inflammatory response in REC, and this response would alter cell metabolism by increasing nutrient uptake and energy substrate utilization.

8.1 Confirmation that REC can induce a pro-inflammatory response when exposed to LPS

Chapter 3 explored the effects of a grain challenge on the inflammatory response in ruminal epithelial tissue *in vivo*. Evidence from previous work (Zhang et al., 2016; Pan et al., 2017; Pederzolli et al., 2018) had suggested that a local inflammatory response in the ruminal epithelium may occur as a result of highly fermentable diets and/or ruminal acidosis. As an epithelial surface of the gastrointestinal tract, it is probable that REC are equipped with mechanisms for detection of microbes and MAMPs undergoing translocation. Indeed, a number of studies have demonstrated the expression of genes encoding PRR, such as toll-like receptors (**TLR**; Chen et al., 2012; Pan et al., 2017). Malmuthuge et al. (2012) showed that most of the previously described TLRs were expressed in the ruminal tissue of Holstein calves. In Chapter 3, in addition to mRNA, immuno-histofluorescence analysis demonstrated cytosolic localization of TLR4 in REC, especially cells closer to the basolateral membrane. Taniguchi et al. (2010) reported a number of differentially expressed genes when dairy cows were fed diets with low and high levels of concentrate, including pro-inflammatory cytokines and molecules that regulated the immune response. Chapters 6 and 7 demonstrated increased gene expression of *TLR2* and *TLR4* in primary REC in response to LPS exposure. Moreover, there was differential expression of genes coding for pro-inflammatory cytokines, chemokines and other immune-modulatory molecules. However, we could not confirm the mechanism by which immune activation occurred in REC. While it is probably that when REC are exposed to LPS they initiate TLR4 signalling, it is possible that other PRRs play a role in the mechanism. In Chapter 7, genes involved in purinergic signalling were differentially expressed. This suggests that it is possible that the

response may be, in part, due to cell damage and the subsequent release of DAMPs, which are also capable of inducing a potent, pro-inflammatory response (Venereau et al., 2015). Overall, my results confirm previous suggestions that REC express PRR, and this was investigated at both the mRNA and protein levels with whole tissue and isolated cells indicating that the ruminal epithelium can initiate a local inflammatory response.

8.2 Use of in vitro, ex vivo, and in vivo models to evaluate a tissue-specific inflammatory response.

While it is clear that REC can induce a pro-inflammatory response, evidence for a direct link to ruminal acidosis has not been consistent. For example, expression of *TLR4* was up-regulated in ruminal tissue collected from calves with ruminal acidosis (Pederzolli et al., 2018) and Pan et al. (2017) also reported that mRNA and protein expression of TLR4, as well as the pro-inflammatory cytokines IL1B, IL6 and TNF, were all up-regulated in the ruminal epithelium of dairy cows fed a high grain diet. In contrast, several studies have found that expression of immune-related molecules in the ruminal tissue were not changed following exposure to ruminal acidosis (Dionissopoulos et al., 2012; Arroyo et al., 2017). Moreover, in Chapter 3, mRNA expression of *TLR4*, *IL1B* and *TNF* were down-regulated in the ruminal tissue following induction of transient acidosis *in vivo*. In Chapter 3, ruminal papillae were collected on d 2 in order to evaluate the potential inflammatory response following acidosis. Previous work indicated that there was elevated LPS in ruminal fluid 2 d following a grain overload (Gohzo et al., 2005). Another biopsy, in Chapter 3, was collected at d 6 to detect any persistent effects. These results suggest that there was an anti-inflammatory response in the ruminal epithelium following the acidosis challenge. Expression of *TLR2* and *PTGS2* were down-regulated (and *ALOX5* tended to be) on d 2 following the challenge and were not changed on d 6. Pederzolli et al. (2018) reported that there was in increase in transcript abundance of *TLR2* and *TLR4* 24 h following acidosis in steers, suggesting that the pro-inflammatory response may occur earlier. A transient model for gastrointestinal epithelial responses has also previously been reported (Aschenbach et al., 2018). Indeed, the results in Chapter 6 indicate that a pro-inflammatory response to LPS in an *in vitro* REC culture model could be detected at 6 h after exposure to LPS.

A drawback to *in vivo* experimentation is the reduced control of physiological conditions, particularly when studying functions of specific tissue types. To study effects in specific tissues,

such as absorption or immune responses in regions of the gastrointestinal tract, an *ex vivo* model may be more appropriate (Westerhout et al., 2015). Ussing chambers are a suitable method for studying physiological processes in complex tissues, while also allowing greater control over the tissue milieu, such as pH, temperature, osmolality and availability of nutrients and hormones. Although there are some key disadvantages, namely issues with viability and a large degree of variability, data from the Ussing chamber is more representative of the *in vivo* status when compared to *in vitro* techniques.

In Chapter 4, the Ussing chamber model was used to further explore the potential inflammatory response in ruminal epithelium. With the goal of inducing a pro-inflammatory response, the tissue was exposed to LPS in the chambers for a duration of five hours, after which papillae were clipped off and used for gene expression analysis. Similar to Chapter 3, there was a down-regulation of several pro-inflammatory molecules in tissue exposed to LPS, including *TNF*, *TLR4* and *PTGS2*, and no effect on expression of *IL1B*, *CXCL8* or *TLR2*. These results seemed to indicate that the inflammatory response may have been suppressed. Analysis of the G_t data revealed that LPS did not influence permeability. In agreement, Arroyo et al. (2017) showed that tight junction complexes were not altered by higher energy diets in dairy cows. The results of the immunohistofluorescence analysis in Chapter 3 demonstrated that *TLR4* was highly expressed in the basale, spinosum and granulosum strata of the ruminal epithelium, but decreased significantly in cells of the stratum corneum. This suggests that interactions with the more basal strata within the ruminal epithelium is necessary to induce a pro-inflammatory response. Although contradictory to the results from Chapter 6, five hours in the present study may have been too short a duration to detect a response. In previous work, peak expression of pro-inflammatory molecules has been found to occur only after six hours of direct LPS exposure in some experimental situations (Fang et al., 2003; Li et al., 2014).

Besides the duration of LPS exposure, disruption of the ruminal epithelial barrier function has been shown to occur from a combination of SCFA and low ruminal pH (Aschenbach et al., 2019). In Chapter 4, the buffer on the mucosal side of the Ussing chambers was maintained at 5.8; however, Meissner et al. (2017) found an increase in ruminal epithelial permeability at a pH of 5.1. Moreover, in another study (Emmanuel et al., 2007) also reported that there was an increase in rumimal epithelial permeability but only when the buffer in the

Ussing chambers was at a pH of 4.5, compared to 5.5 and 6.5. In the present study, the pH of the buffer may not have been sufficiently low to alter barrier function.

While the data from Chapter 3 and 4 appear to at least partially agree, with regards to the inflammatory response, the results from the REC culture experiments are not consistent. The discrepancies may reflect differences in the response to LPS in the most luminal layers of cells versus those in the most basal layers. Previous work with skin epidermis has demonstrated that the outer-most keratinocytes promote tolerance, whereas those in the most basal layers and cells of the dermis are highly responsive to MAMPs such as LPS (Nestle et al., 2009; Bukhari et al., 2019). The results from Chapter 3 and 4 may indicate that the REC of the outer strata in the ruminal epithelium respond to LPS through down-regulating an inflammatory response, to protect the tissue from excessive damage from the action of pro-inflammatory molecules; whereas, the more basal cells induce inflammation, as demonstrated in Chapter 6 and 7.

Additional factors may contribute to the differences observed between models using whole, native tissue and those using monocultures of a specific cell type. In previous work studying the effects of diet or acidosis on the ruminal epithelium, nearly all samples are collected as native tissue, either excised post-mortem or papillae collected using a biopsy performed through a ruminal cannula. Biopsies in particular are a valuable method that are minimally invasive and allow for multiple measurements to be taken for a single animal (Kelly et al., 1993). Ruminal papillae are covered with multiple layers of REC and the exposure to MAMPs, especially the cells of the more basal strata, may be limited due to the structural arrangement of the tissue. Papillae are also comprised of connective tissue and supportive cells, such as fibroblasts, endothelial cells (Baldwin, 1998) and potentially professional immune cells (Chihaya et al., 1988; Josefsen and Landsverk, 1996). All of these non-epithelial cell types possess pattern recognition receptors and are capable of readily initiating a pro-inflammatory reaction to microbes or MAMPs. The inconsistent responses reported in the literature (Dionissopoulos et al., 2012; Arroyo et al., 2017; Pan et al., 2017) and that in Chapters 3 and 4, may be partially explained by the use of whole papillae to draw conclusions about epithelial function. The many different cell types contribute to the total RNA extracted and can be a source of significant noise when analyzing gene expression with qPCR, as transcripts in one cell types may be diluted by large changes in gene expression in other cell types (Steele et al., 2013).

Alternative methods to whole tissue sampling include laser capture microdissection (LCM), antibody staining of specific cell components using in situ hybridization, immunohistochemistry or immunohistofluorescence, and cell culture. Highly specific cell populations can be isolated using the LCM technique, increasing the precision of RNA and protein analyses (Hoffmann et al., 2017). The method has been employed with ruminal papillae to isolate individual REC (Steele et al., 2013). However, LCM has several critical challenges, including limited ability to obtain sufficient RNA or protein and high rates of RNA degradation (Hoffmann et al., 2017).

Histological staining techniques are valuable for visualizing the localization of proteins or nucleic acids in cells within a tissue. In Chapter 3, to further explore the anti-inflammatory response indicated by mRNA analysis, IHF was used to stain ruminal epithelial tissue with an antibody against TLR4. The fluorescence intensity analysis indicated that, indeed, expression of TLR4 was less in animals following the acidosis challenge compared to the controls. However, in order to make accurate measurements, all procedures involving antigen-retrieval, antibody staining, and imaging must be carefully controlled to maintain consistency. Moreover, antibodies must undergo rigorous validation and only a small number of proteins can be analyzed at one time. Immunohistofluorescence is therefore limited in its practicality as it is a time-consuming, low through-put technique.

Cell culture is a widely used method for biomedical research, production and testing of compounds and drugs and for studying cellular processes (Freshney, 2010a). Primary cells, which are isolated directly from the tissues of interest, are especially valuable for studying the physiological functions of specific cell types. Compared to immortalized cell lines, primary cells retain more of their functional characteristics, albeit normally only for limited number of passages (Freshney, 2010b). This allows for the direct study of specific cellular functions while producing more relevant results. Isolation and culture of REC was developed in the 1980's to better understand the absorptive and metabolic function of the ruminal epithelium. Interest in this method has increased in recent years to study the specific functions of the REC. In the current project, the method for isolating REC was further developed and the cells were subsequently used to conduct *in vitro* experiments.

Overall, the *in vivo* and *ex vivo* results appear to differ from results obtained with the cell culture model, suggesting that the pro-inflammatory characteristics in native epithelial tissue are

different from the cultured REC, which are generated from the most basal layers. This may indicate that while the most luminal cell layers induce an anti-inflammatory response, or no response, the most basal cells initiate a pro-inflammatory response to MAMPs. In addition, there are some methodological limitations that may contribute to the inconsistencies observed between the different models, including, reduced control over experimental conditions and the use of whole tissue.

8.3 The effects of LPS exposure on the pro-inflammatory response in cultured primary REC

A major goal of this project was to evaluate the response of REC when exposed to a MAMP. Many molecules, including LPS, amines, lactate, fimbrial adhesins, lipoteichoic acid, microbial-derived nucleic acids, and flagellin are present in ruminal fluid and can potentially induce a pro-inflammatory response (Dong et al., 2011). Of these many molecules, only a few have been evaluated for their concentrations in ruminal fluid and their potential effects on the host. Histamine was found to be increased in ruminal fluid of heifers following a grain overload (Ahrens, 1967) and Aschenbach et al. (2000) investigated the effect of histamine on permeability of the ruminal epithelium in Ussing chambers. By far, LPS is the most widely used molecule in the literature for the induction of a predictable, pro-inflammatory response. In ruminal fluid, free LPS is a normal constituent generated by cell lysis during bacterial turnover, occurring at low baseline levels (Plaizier et al., 2012). During instances of increased dietary concentrates and ruminal acidosis, concentrations of LPS in ruminal fluid often increase substantially (Plaizier et al., 2012).

Previous *in vitro* studies have demonstrated that intestinal epithelial cells detect LPS, and via activation of PRRs can initiate a pro-inflammatory response (Campbell et al., 1999; Guo et al., 2015). Cario et al. (2000) demonstrated that LPS induced TLR-activation and signaling pathways in several intestinal epithelial cell lines. A number of studies have shown that, in response to LPS, intestinal epithelial cells can produce immune-modulatory molecules such as pro-inflammatory cytokines and chemokines (Jung et al., 1995; Stadnyk, 2002). Increasingly, intestinal epithelial cells are being recognized for their central role in mediating immune cross-talk across the mucosal barrier (Kagnoff, 2014). However, this characteristic does not appear to be limited to the gastrointestinal tract. Superbasal and basal keratinocytes also express pattern recognition receptors, such as TLR4 (Iotzova-Weiss et al., 2017) and play an important role in

initiating and regulating inflammatory response in the skin (Bukhari et al., 2019). The epidermis shares several structural and functional similarities with the ruminal epithelium. Both surfaces are comprised of stratified squamous epithelial cells that provide physical protection with their outer-most corneocytes and metabolic functions with their most basal cells (Graham and Simmons, 2005; Eyerich et al., 2018). Therefore, extrapolating from the observations in the intestines and skin, it was hypothesized in the current study that the REC would be involved in mediating an inflammatory response when exposed to LPS in culture.

A previous study by Zhang et al. (2016) suggested that there was a correlation between cytokine mRNA and LPS exposure in REC in culture. However, while the LPS dose was correlated with an upregulation of some pro-inflammatory cytokines, others were either the opposite or not affected. In Chapters 6, two experiments were conducted whereby LPS was added to the cell culture media with the goal of inducing a pro-inflammatory response in REC and to evaluate the nature of this response. In the first experiment, REC were exposed to differing concentrations of LPS for a duration of 6 or 24 hours. The concentrations of LPS, 0, 10,000, 50,000 and 200,000 EU/mL, were selected to represent the LPS range that has previously been observed in ruminal fluid following consumption of highly fermentable diets and/or during an acidosis challenge (Plaizier et al., 2012). The LPS selected for this study was purified from E. coli. Viability of REC may be affected by higher doses of LPS. In support of this theory, excessive levels of LPS reduced viability of epithelial cells grown in culture (Chin et al., 2006). In Chapter 6, as well as Chapter 7, the percent dead cells was rarely more than 10% and cell viability was not significantly affected by LPS dose or duration of exposure. In addition, LPS did not increase the percentage of cells undergoing apoptosis (Chapter 7 only). These results suggest that REC are more resilient to higher levels of LPS, at least compared to intestinal epithelial cells.

Results from the first experiment, in Chapter 6, demonstrated that, following exposure to LPS, cultured REC are capable of initiating an inflammatory response. Although increasing levels of LPS did not result in an obvious dose-dependent effect, expression of pro-inflammatory cytokines and chemokines increased substantially following exposure to LPS. Expression of both *TLR2* and *TLR4* increased following exposure; however, *TLR2* transcript was less after 24 hours when compared to 6 hours. The expression patterns of CSF2 and IL7 further suggested that REC

regulated the response to LPS and may have been involved in the resolution phase of inflammation (Mackall et al., 2011; Egea et al., 2013).

A second experiment was designed to further explore the pro-inflammatory response and the potential regulatory effects in REC. In this experiment, a single, 12-hour dose of LPS resulted in an up-regulation of pro-inflammatory molecules. However, after a second LPS exposure, expression of *TLR4*, *TNF*, *CXCL2*, *CXCL8*, *CSF2* and *IL7* had decreased. In addition, compared to 12 hours, 24 hours of exposure resulted in a decrease of *TLR4*, *CXCL2*, *CSF2* and *IL7*. These results indicate a potential tolerogenic response to either multiple or prolonged exposures. Endotoxin tolerance is a well-known response in intestinal epithelial cells (Lotz et al., 2006; Lee et al., 2008). The process has been shown to occur following repeated exposure to LPS (Beutler and Rietschel, 2003). Throughout their life, or even within a single lactation in dairy cows, high producing ruminants are likely to experience multiple episodes of ruminal acidosis which may therefore result in multiple exposures of REC to MAMPs. However, endotoxin tolerance has not been previously evaluated in the ruminal epithelium. The current study provides evidence that REC may also promote a tolerogenic response to repeated LPS exposures.

The data from Chapter 6, together with the *in vivo* results, suggest that inflammation in the ruminal epithelium is tightly regulated, presumably to prevent damage due to excessive inflammation from exposure to LPS (Sugimoto et al., 2016). In the second *in vitro* experiment in Chapter 6, REC were exposed to LPS for 12 h, which stimulated an up-regulation in gene expression of pro-inflammatory molecules. When the LPS was removed and the cells allowed to recover for 36 h, expression of these same genes was significantly less, several of which were not different from baseline levels. These data further suggest that the inflammatory response is tightly regulated. Overall, the results from the current studies demonstrate that cultured REC are capable of initiating a pro-inflammatory response. However, the expression of immune-modulatory molecules and the nature of the response are dependent on dose, duration and pattern of exposure to LPS.

8.4 Effect of Inflammation on nutrient metabolism by REC

Inflammation can negatively impact production, growth, reproduction, and overall health in animals (Lochmiller and Deerenberg, 2003; Plaizier et al., 2018). The effects can be especially

pronounced in dairy cows, as demonstrated with mastitis challenge models where milk production is decreased (Grohn et al., 2004). Kvidera et al. (2017) observed an 80% reduction in milk yield following a systemic LPS challenge. Despite the decrease in demand for milk synthesis, there was an increase in whole body glucose utilization. The authors suggested that the effect on milk synthesis may be a response to spare glucose. In support, previous work has shown that glucose utilization decreases in non-essential, non-immune tissue, while increasing in immune cells and related tissues (Lang et al., 1993). In addition to glucose, sheep subjected to an endotoxemia challenge altered specific tissue use of amino acids (McNeil et al., 2016).

Activation of the immune system is characterized by a rapid increase in immune cell activation, proliferation, and migration (McNeil et al., 2013; Colgan et al., 2016). Biosynthetic processes involved in the production of immune-modulatory molecules, enzymes and mediators of resolution and tissue remodeling (Chen et al., 2018) are also up-regulated. These physiological responses to inflammation have a profound impact on whole body metabolism as the nutrient and energetic demands of the immune system are increased (Wang and Ye, 2015; Kvidera et al., 2017). The abrupt change in energetic demands initially results in a state of hyperglycemia as the body increases availability of glucose for immune cells and tissues (McGuinness, 2005). Subsequently, a shift to hypoglycemia occurs and glucose utilization decreases in non-essential, non-immune tissues (Lanis et al., 2017; Peters, 2006). Increases in lipid and protein catabolism also occur to provide substrates for energy or for immune-related processes. For example, the production of acute phase proteins in response to inflammation is associated with net protein catabolism (Bruins et al., 2000).

Contributing to whole body metabolism are tissue-specific demands for energy and nutrients. At a basal level, the gastrointestinal tract has a large and disproportional requirement for energy and other nutrients (Britton and Krehbiel, 1993). The portal-drained viscera collectively consumes a substantial amount of oxygen due to the high rates of metabolic activity and rapid tissue turnover (Reynolds, 1995). Previous work has shown that there is substantial metabolism of SCFA in the ruminal epithelium (Goosen, 1976; Kristensen et al., 1998) and butyrate is a preferred energy substrate for REC. Serosal uptake and metabolism of arterial glucose has also been demonstrated (Kristensen et al., 2005). Energy substrates are oxidized to CO_2 (Sehested et al., 1999a) or converted to a number of metabolites such as ketone bodies and lactate (Stevens and Stettler, 1966; Bergman, 1990).

Another goal of my PhD program, addressed in Chapters 4 and 7, was to evaluate how the potential inflammatory response would affect nutrient transport and metabolism of the ruminal epithelium. During an inflammatory state, evidence suggests that tissue-specific requirements for glucose and amino acids increase (Yu et al., 2000; McGuinness, 2005). Little work has evaluated the effects of inflammation on ruminal epithelial metabolism; however, energy metabolism in the intestinal mucosa is altered by inflammation (Lanis et al., 2017). During potential translocation of MAMPs, the interaction with REC may have similar results as observed with intestinal epithelial tissue.

Although there did not appear to be an increase in pro-inflammatory molecules in tissue exposed to LPS in the Ussing chambers (in Chapter 4), there was some indication that exposure influenced metabolism. Mucosal-to-serosal flux of ^{14}C-butyrate tended to increase linearly with LPS dose. These results suggest that LPS exposure influenced removal of butyrate from the mucosal side, by either transport across the epithelia or oxidation. Analysis of G_t and Isc data ruled out an increase in paracellular or ion-coupled transport as the explanation for the effects on flux rates. In support of this, there were no differences detected in the expression of solute transporters. An increase in flux may be a response by the tissue to increase energy or nutrient supply (Hardin et al., 2000; McNeil et al., 2016). Altered transport of ions and nutrients at mucosal surfaces has also been observed, as a result of an inflammatory response, both at a systemic level and locally. Liu et al. (2019) demonstrated impaired intestinal absorption of fatty acids when mice were systemically challenged with LPS. In pathologies such as Crohn's disease or ulcerative colitis, nutrient absorption and metabolism of intestinal epithelial cells may be affected, either from increased permeability or from impairments of cell functions (Peuhkuri et al., 2010). When the results of Chapter 4 are considered in the context of previous research, despite no clear pro-inflammatory response to LPS, nutrient utilization and aspects of cell metabolism may have been altered. However, the effects that were observed were subtle and did not appear to be detrimental to epithelial function. Further exploration into the reasons for the responses is required to fully understand whether inflammation has a significant impact on metabolism of the ruminal epithelium.

In Chapter 7, an experiment was designed to evaluate the potential consequences of LPS-induced inflammation in REC on cell function and metabolism. A pro-inflammatory response was induced in REC using 50,000 EU/mL LPS with or without the addition of butyrate and

propionate to the cell culture media. This study provided evidence that a pro-inflammatory response by the REC may influence cellular transport of nutrients. Although previous work has often shown detrimental effects of inflammation on transport functions of epithelial cells (Peuhkuri et al., 2010), in the present study, there was an up-regulation in the expression of both *MCT4* and *SLC5A8*. This is consistent with findings in intestinal epithelium with inflammatory bowel disease (He et al., 2018). Along with SCFA, these transporters may play a role in the transport of other solutes, such as ketones and lactate, in or out of REC (Stumpff et al., 2018). In this experiment, cells were not polarized and as a result the directionality of solute transport is unknown. However, the expression patterns suggests that REC nutrient transport is altered in response to LPS exposure.

REC metabolism may have also been affected by exposure to LPS. Although there was no effect of LPS on consumption of the SCFA, cells exposed to LPS tended to consume more glucose (31.8 compared to 28.7% in the controls). Previous work has shown that an inflammatory state leads to an increase in glucose metabolism (Johnson et al., 2016). Interestingly, expression of *ACAT1* in the REC was down-regulated following exposure to LPS. Moreover, *BDH1* expression was also down-regulated. Together these results indicate a shift away from ketogenesis and are consistent with previous studies that found an inhibitory effect of pro-inflammatory cytokines on ketone body production (Pailla et al., 1998; Pailla et al., 2001). This is in contrast, however, to the observations in Chapter 4 where the mucosal-to-serosal butyrate flux increased with increasing LPS dose. Part of the discrepancy in the response may be due to the duration of exposure. In the cell culture experiment (Chapter 7), REC were exposed to LPS for a duration of 24 hours, compared to the 5 hours that the ruminal epithelium was exposed to LPS in the Ussing chambers. Metabolism via pathways such as the ketogenesis are dynamic and depends on a number of factors such as enzyme and substrate availability and regulation by transcription factors (Puchalska and Crawford, 2017). Timing of the exposure and sample collected may in part explain the observed differences. In addition, the extent of exposure may have also been a factor. Whereas all of the cells in the culture experiment would have been exposed to LPS, the most basal layers of cells in the epithelium in the Ussing chambers may have had limited or no exposure. The cells of the most basal strata are highly metabolically active compared to the more luminal layers. Therefore, the effect of LPS exposure of the basal cells would have the most impact on metabolism. However, caution should be taken when

comparing data from two different methodologies, since results from *in vitro* experiments are known to deviate from those measured in whole tissue or *in vivo*.

Although the results of Chapter 7 indicated that exposure to LPS may have altered metabolic function in REC, the magnitude of the responses was not pronounced. In addition, although there was a slight increase in glucose utilization, LPS exposure did not appear to affect butyrate or propionate use. These data indicate a degree of resilience, such that a pro-inflammatory response may not have led to significant metabolic perturbations.

The moderate metabolic effect in the cultured REC may be a consequence of using isolated epithelial cells, thus eliminating potential communication between other cell types. Inflammation at mucosal surfaces has been associated with metabolic shifts in epithelial cells, involving a local hypoxic response (Colgan et al., 2016). However, during an inflammatory state, epithelial cells interact intimately with resident and recruited immune cells. Studies have suggested that metabolic responses at a tissue level are promoted or significantly enhanced by recruited leukocytes (Lewis et al., 1999; Colgan et al., 2016). In this experiment, due to the use of isolated ruminal epithelial cells, this interaction was not possible. Likewise, further recruitment of immune cells could not occur in the Ussing chambers with isolated tissue segments. The response (in Chapter 7) to LPS, and SCFA in the media, suggested that REC play an important role in the recruitment of leukocytes. Re-evaluation of the effects of inflammation on ruminal epithelial metabolic function *in vivo* may therefore be warranted.

Some of the limitations of Chapter 7 may have been resolved through the use of transwells, in order to establish polarity in the cultured REC. The current, and commonly used, method cultivates isolated REC as a monolayer. Growing cells in this way, on a surface, can be informative and, depending on the question, may even yield similar results as those obtained from polarized cells (Reza et al., 2005). However, aspects of epithelial cell function may be altered by the loss of a proper barrier and a lack of polarity. For example, polarized retinal pigment epithelial cells produced greater amounts of growth factors compared to their non-polar counterparts (Sonoda et al., 2009). Epithelial cells grown on transwells or using 3-D models retain many native, structural components, which likely influences nutrient and ion transport (Sun et al., 2008). In Chapter 7, differential expression of genes relating to nutrient transport appeared to be influenced by LPS exposure. However, the transporters analyzed, *MCT1*, *MCT4* and *SLC5A8*, are localized to either the apical or basolateral membrane. As the REC in the

present experiment were not polarized, the membrane surfaces were indistinguishable. Transport and metabolic functions may have therefore been altered. Establishing cells on transwells is a complex process and success rates can be low (Sun et al., 2008). With isolated REC only one study has been published where the cells were successfully seeded onto transwells (Stumpff et al., 2011). Development of a more robust model would allow future work to elucidate the effects of nutrient transport in REC. However, the results of the present study are not without benefit. The data offer insights into how the metabolic function in the ruminal epithelium may be regulated when exposed to LPS. Moreover, the results suggested that SCFA may impact the pro-inflammatory response initiated by REC.

While the results of Chapter 7 offered some insight into of the effects of protein expression, most of the conclusions of this thesis have been drawn solely from gene expression analysis. Quantification of protein abundance would provide valuable phenotypic information about the REC under inflammatory conditions. As the relationship between transcript and protein abundance is inherently complex, there is not necessarily a direct or simple correlation between the two (Liu et al., 2016). Protein expression, especially that of cytokine production, may enhance the understanding of the exact role REC play in responding to a pro-inflammatory stimulus. For example, gene expression occurs prior to protein translation. Knowing the expression pattern of proteins in addition to mRNA may give a clearer picture of the timing of the inflammatory response. However, gene expression analysis is a robust method that is widely used to draw physiological conclusions about cells and tissues (Liu et al., 2016). In the present study, it was a practical means of indicating the effects of LPS exposure to the ruminal epithelium and cultured REC.

CHAPTER 9: GENERAL CONCLUSIONS

The induction of SARA in vivo resulted in a decrease in ruminal pH and an increase in the concentration of free LPS in the ruminal fluid, which remained elevated for 3 days following the grain overload. Rumen tissue collected on day 2 after the challenge had down-regulated expression of *TLR2* and *PTGS2* for the SARA treatment relative to the control. Heifers exposed to ruminal acidosis also had less expression of *TLR4*, *TNF*, *ALOX5* and *ALOXAP* compared to the controls. Moreover, immunohistofluorescence analysis demonstrated that TLR4 protein expression was also less when SARA was induced. The results from this study suggested that there was an anti-inflammatory response following an acidosis challenge.

In ruminal papillae exposed to LPS in Ussing chambers, gene expression of pro-inflammatory cytokines *TNF*, *IL1B* and *CXCL8*, as well as *TLR2*, did not differ compared to the controls. Expression of *PTGS2* and *TLR4* were down-regulated following exposure to LPS. These data were interpreted to indicate that the inflammatory response to LPS may have been suppressed and appear to be in agreement with in vivo results.

Contradicting the results from Chapters 3 and 4, exposing primary REC to LPS in culture resulted in an increase in gene expression of immune-regulatory molecules including *TLR2*, *TLR4*, *TNF*, *IL1B*, *CXCL2*, *CXCL8*, *PTGS2*, *CSF2* and *IL7*. The pro-inflammatory response was dependent on the dose, duration and timing of the LPS exposure. The expression patterns suggested that the response was regulated and that a degree of tolerance may have occurred in REC when exposed to repeated doses of LPS. These observations indicate a physiological mechanism to prevent damage to the cells, caused by an excessive, pro-inflammatory reaction.

In whole, native tissue, as in the in vivo and ex vivo experiments, the local inflammatory response may have been influenced by the timing of the sample collection, extent of LPS exposure, the heterogeneous nature of the tissue, or the structural organization of the ruminal epithelium. However, the cell culture experiments clearly demonstrated that primary REC exhibit a pro-inflammatory response when exposed to LPS in culture. The results from this research suggests that while a local inflammatory can be induced, the response is tightly regulated. In addition, the overall results indicate that exposure to LPS may lead to different responses depending on the whether the effected cells are more luminal or more basal. The cells

of the stratum corneum and granulosum function primarily to provide protection from the ruminal environment, whereas the cells of the stratum spinosum and basale function as the absorptive and metabolically active units of the ruminal epithelium (Graham and Simmons, 2005). It stands to reason that the more luminal cells would exhibit tolerance towards MAMP, in order to protect the tissue from excessive inflammatory responses. Likewise, penetration of these MAMP into the more basal cells, which may occur under acidotic conditions, would trigger an appropriate pro-inflammatory response. In Chapters 3 and 4, it may have been that only the most luminal cell layers were exposed to LPS, whereas the cultured REC, derived from the most basal cell layers, were directly exposed. Therefore, the inconsistent results between whole, native epithelial tissue and the culture REC may reflect the differences in exposure between luminal and basal cell layers.

Despite the lack of a pro-inflammatory response in ruminal epithelium exposed to LPS in the Ussing chambers, there was a tendency for mucosal to serosal butyrate flux to increase linearly with increasing concentrations of LPS. In cultured, primary REC exposure to LPS tended to increase glucose consumption. Analysis of nutrient transporters *MCT4* and *SLC5A8* showed that expression of these genes was increased following exposure to LPS. Moreover, gene and protein expression of ketogenic enzymes was less when the REC were exposed to LPS. These results suggest that exposure to LPS altered nutrient transport and metabolism of the REC.

The results from this research confirm the ability of REC to induce an inflammatory response and show that the response is influenced by dose, duration and timing of the exposure of LPS. However the response appears to differ in whole, native tissue, which exhibited an anti-inflammatory response, or no response, under acidotic conditions or when exposed to LPS in Ussing chambers. The data also provide evidence that uptake and metabolism of the ruminal epithelium is affected by inflammation; however, the changes appear to be moderate, suggesting a degree of resilience. Therefore, although a local inflammatory response to MAMP by the REC may occur, the metabolic activity, a critical function for the ruminal epithelium, does not appear to be greatly altered. Overall, this research contributes to the understanding of the nature of the local inflammatory response by REC and provides insights into the effects of the local inflammatory response on the metabolic functions of the ruminal epithelium.

LITERATURE CITED

Ahmad, M. S., S. Krishnan, B. S. Ramakrishna, M. Mathan, A. B. Pulimood, and S. N. Murthy. 2000. Butyrate and glucose metabolism by colonocytes in experimental colitis in mice. Gut. 46:493-499. doi: 10.1136/gut.46.4.493.

Ahrens, F. A. 1967. Histamine, lactic acid, and hypertonicity as factors in the development of rumenitis in cattle. Am. J. Vet. Res. 28:1335-1342.

Allaire, J. M., S. M. Crowley, H. T. Law, S. Y. Chang, H. J. Ko, and B. A. Vallance. 2018. The Intestinal Epithelium: Central Coordinator of Mucosal Immunity. Trends Immunol. 39:677-696. doi: 10.1016/j.it.2018.04.002.

AlZahal, O., E. Kebreab, J. France, and B. W. McBride. 2007. A mathematical approach to predicting biological values from ruminal pH measurements. J. Dairy Sci. 90:3777-3785. doi: 10.3168/jds.2006-534.

Andersen, P. H., B. Bergelin, and K. A. Christensen. 1994a. Effect of feeding regimen on concentration of free endotoxin in ruminal fluid of cattle. J. Anim. Sci. 72:487-491. doi: 10.2527/1994.722487x.

Andersen, P. H., M. Hesselholt, and N. Jarlov. 1994b. Endotoxin and arachidonic acid metabolites in portal, hepatic and arterial blood of cattle with acute ruminal acidosis. Acta Vet. Scand. 35:223-234.

Antoni, L., S. Nuding, D. Weller, M. Gersemann, G. Ott, J. Wehkamp, and E. F. Stange. 2013. Human colonic mucus is a reservoir for antimicrobial peptides. J. Crohns Colitis. 7:e652-664. doi: 10.1016/j.crohns.2013.05.006.

Antonioli, L., P. Pacher, E. S. Vizi, and G. Hasko. 2013. CD39 and CD73 in immunity and inflammation. Trends Mol. Med. 19:355-367. doi: 10.1016/j.molmed.2013.03.005.

Arroyo, J. M., A. Hosseini, Z. Zhou, A. Alharthi, E. Trevisi, J. S. Osorio, and J. J. Loor. 2017. Reticulo-rumen mass, epithelium gene expression, and systemic biomarkers of metabolism and inflammation in Holstein dairy cows fed a high-energy diet. J. Dairy Sci. 100:9352-9360. doi: 10.3168/jds.2017-12866.

Artis, D. 2008. Epithelial-cell recognition of commensal bacteria and maintenance of immune homeostasis in the gut. Nat. Rev. Immunol. 8:411-420. doi: 10.1038/nri2316.

Aschenbach, J. R., S. Bilk, G. Tadesse, F. Stumpff, and G. Gabel. 2009. Bicarbonate-dependent and bicarbonate-independent mechanisms contribute to nondiffusive uptake of acetate in the ruminal epithelium of sheep. Am. J. Physiol. Gastrointest. Liver Physiol. 296:G1098-1107. doi: 10.1152/ajpgi.90442.2008.

Aschenbach, J. R., and G. Gabel. 2000. Effect and absorption of histamine in sheep rumen: significance of acidotic epithelial damage. J. Anim. Sci. 78:464-470.

Aschenbach, J. R., R. Oswald, and G. Gabel. 2000. Transport, catabolism and release of histamine in the ruminal epithelium of sheep. Pflugers Arch. 440:171-178.

Aschenbach, J. R., G. B. Penner, F. Stumpff, and G. Gabel. 2011. Ruminant Nutrition Symposium: Role of fermentation acid absorption in the regulation of ruminal pH. J. Anim. Sci. 89:1092-1107. doi: 10.2527/jas.2010-3301.

Aschenbach, J. R., T. Seidler, F. Ahrens, W. Schrodl, I. Buchholz, B. Garz, M. Kruger, and G. Gabel. 2003. Luminal salmonella endotoxin affects epithelial and mast cell function in the proximal colon of pigs. Scand. J. Gastroenterol. 38:719-726. doi: 10.1080/00365520310003129.

Aschenbach, J. R., Q. Zebeli, A. K. Patra, G. Greco, S. Amasheh, and G. B. Penner. 2019. Symposium review: The importance of the ruminal epithelial barrier for a healthy and productive cow. J. Dairy Sci. 102:1866-1882. doi: 10.3168/jds.2018-15243.

Bakshani, C. R., A. L. Morales-Garcia, M. Althaus, M. D. Wilcox, J. P. Pearson, J. C. Bythell, and J. G. Burgess. 2018. Evolutionary conservation of the antimicrobial function of mucus: a first defence against infection. NPJ Biofilms Microbiomes. 4:14. doi: 10.1038/s41522-018-0057-2.

Baldwin, R. L. 1999. The proliferative actions of insulin, insulin-like growth factor-I, epidermal growth factor, butyrate and propionate on ruminal epithelial cells in vitro. Small Rumin. Res. 32:261-268. doi: Doi 10.1016/S0921-4488(98)00188-6.

Baldwin, R. L. t. 1998. Use of isolated ruminal epithelial cells in the study of rumen metabolism. J. Nutr. 128:293S-296S.

Baldwin, R. L. t., and E. E. Connor. 2017. Rumen Function and Development. Vet. Clin. North Am. Food Anim. Pract. 33:427-439. doi: 10.1016/j.cvfa.2017.06.001.

Baldwin, R. L. t., and B. W. Jesse. 1991. Technical note: isolation and characterization of sheep ruminal epithelial cells. J. Anim. Sci. 69:3603-3609.

Baldwin, R. L. t., and B. W. Jesse. 1992. Developmental changes in glucose and butyrate metabolism by isolated sheep ruminal cells. J. Nutr. 122:1149-1153. doi: 10.1093/jn/122.5.1149.

Bannink, A., J. France, S. Lopez, W. J. J. Gerrits, E. Kebreab, S. Tamminga, and J. Dijkstra. 2008. Modelling the implications of feeding strategy on rumen fermentation and functioning of the rumen wall. Anim. Feed Sci. and Technol. 143:3-26. doi: https://doi.org/10.1016/j.anifeedsci.2007.05.002.

Barcroft, J., R. A. McAnally, and A. T. Phillipson. 1944. Absorption of Volatile Acids from the Alimentary Tract of the Sheep and Other Animals. J. Exp. Biol. 20:120.

Baumgard, L. H., R. J. Collier, and D. E. Bauman. 2017. A 100-Year Review: Regulation of nutrient partitioning to support lactation. J. Dairy Sci. 100:10353-10366. doi: 10.3168/jds.2017-13242.

Baxter, R. C. 2001. Signalling pathways involved in antiproliferative effects of IGFBP-3: a review. Mol. Pathol. 54:145-148. doi: 10.1136/mp.54.3.145.

Bergman, E. N. 1971. Hyperketonemia-ketogenesis and ketone body metabolism. J. Dairy Sci. 54:936-948. doi: 10.3168/jds.S0022-0302(71)85950-7.

Bergman, E. N. 1990. Energy contributions of volatile fatty acids from the gastrointestinal tract in various species. Physiol. Rev. 70:567-590.

Bettess, M. D., N. Dubois, M. J. Murphy, C. Dubey, C. Roger, S. Robine, and A. Trumpp. 2005. c-Myc is required for the formation of intestinal crypts but dispensable for homeostasis of the adult intestinal epithelium. Mol. Cell Biol. 25:7868-7878. doi: 10.1128/mcb.25.17.7868-7878.2005.

Beutler, B., and E. T. Rietschel. 2003. Innate immune sensing and its roots: the story of endotoxin. Nat. Rev. Immunol. 3:169-176. doi: 10.1038/nri1004.

Bevans, D. W., K. A. Beauchemin, K. S. Schwartzkopf-Genswein, J. J. McKinnon, and T. A. McAllister. 2005. Effect of rapid or gradual grain adaptation on subacute acidosis and feed intake by feedlot cattle. J. Anim. Sci. 83:1116-1132.

Bieniek, K., A. Szuster-Ciesielska, T. Kaminska, M. Kondracki, M. Witek, and M. Kandefer-Szerszen. 1998. Tumor necrosis factor and interferon activity in the circulation of calves

after repeated injection of low doses of lipopolysaccharide. Vet. Immunol. Immunopathol. 62:297-307. doi: 10.1016/s0165-2427(98)00102-0.
Bloemen, J. G., K. Venema, M. C. van de Poll, S. W. Olde Damink, W. A. Buurman, and C. H. Dejong. 2009. Short chain fatty acids exchange across the gut and liver in humans measured at surgery. Clin. Nutr. 28:657-661. doi: 10.1016/j.clnu.2009.05.011.
Boland, S., E. Boisvieux-Ulrich, O. Houcine, A. Baeza-Squiban, M. Pouchelet, D. Schoevaert, and F. Marano. 1996. TGF beta 1 promotes actin cytoskeleton reorganization and migratory phenotype in epithelial tracheal cells in primary culture. J. Cell Sci. 109 (Pt 9):2207-2219.
Bradford, B. J., K. Yuan, J. K. Farney, L. K. Mamedova, and A. J. Carpenter. 2015. Invited review: Inflammation during the transition to lactation: New adventures with an old flame. J. Dairy Sci. 98:6631-6650. doi: 10.3168/jds.2015-9683.
Britton, R., and C. Krehbiel. 1993. Nutrient metabolism by gut tissues. J. Dairy Sci. 76:2125-2131. doi: 10.3168/jds.S0022-0302(93)77547-5.
Brown, M. S., C. H. Ponce, and R. Pulikanti. 2006. Adaptation of beef cattle to high-concentrate diets: performance and ruminal metabolism. J. Anim. Sci. 84 Suppl:E25-33. doi: 10.2527/2006.8413_supple25x.
Bruins, M. J., P. B. Soeters, and N. E. Deutz. 2000. Endotoxemia affects organ protein metabolism differently during prolonged feeding in pigs. J. Nutr. 130:3003-3013. doi: 10.1093/jn/130.12.3003.
Buckley, C. D., D. Pilling, J. M. Lord, A. N. Akbar, D. Scheel-Toellner, and M. Salmon. 2001. Fibroblasts regulate the switch from acute resolving to chronic persistent inflammation. Trends Immunol. 22:199-204.
Bukhari, S., A. F. Mertz, and S. Naik. 2019. Eavesdropping on the conversation between immune cells and the skin epithelium. Int. Immunol. 31:415-422. doi: 10.1093/intimm/dxy088.
Bush, R. S., and L. P. Milligan. 1971. ENZYMES OF KETOGENESIS IN BOVINE RUMEN EPITHELIUM. Can. J. Anim. Sci. 51:129-133. doi: 10.4141/cjas71-017.
Calder, P. C., G. Dimitriadis, and P. Newsholme. 2007. Glucose metabolism in lymphoid and inflammatory cells and tissues. Curr. Opin. Clin. Nutr. Metab. Care. 10:531-540. doi: 10.1097/MCO.0b013e3281e72ad4.
Campbell, E. L., C. N. Serhan, and S. P. Colgan. 2011. Antimicrobial aspects of inflammatory resolution in the mucosa: a role for proresolving mediators. J. Immunol. 187:3475-3481. doi: 10.4049/jimmunol.1100150.
Campbell, N., X. Y. Yio, L. P. So, Y. Li, and L. Mayer. 1999. The intestinal epithelial cell: processing and presentation of antigen to the mucosal immune system. Immunol. Rev. 172:315-324. doi: 10.1111/j.1600-065x.1999.tb01375.x.
Canciello, A., V. Russo, P. Berardinelli, N. Bernabo, A. Muttini, M. Mattioli, and B. Barboni. 2017. Progesterone prevents epithelial-mesenchymal transition of ovine amniotic epithelial cells and enhances their immunomodulatory properties. Sci. Rep. 7:3761. doi: 10.1038/s41598-017-03908-1.
Cario, E., I. M. Rosenberg, S. L. Brandwein, P. L. Beck, H. C. Reinecker, and D. K. Podolsky. 2000. Lipopolysaccharide activates distinct signaling pathways in intestinal epithelial cell lines expressing Toll-like receptors. J. Immunol. 164:966-972.
Castillo-Lopez, E., T. J. Klopfenstein, S. C. Fernando, and P. J. Kononoff. 2013. In vivo determination of rumen undegradable protein of dried distillers grains with solubles and

evaluation of duodenal microbial crude protein flow. J. Anim. Sci. 91:924-934. doi: 10.2527/jas.2012-5323.
Castillo-Lopez, E., B. I. Wiese, S. Hendrick, J. J. McKinnon, T. A. McAllister, K. A. Beauchemin, and G. B. Penner. 2014. Incidence, prevalence, severity, and risk factors for ruminal acidosis in feedlot steers during backgrounding, diet transition, and finishing. J. Anim. Sci. 92:3053-3063. doi: 10.2527/jas.2014-7599.
Cavaillon, J. M. 2018. Exotoxins and endotoxins: Inducers of inflammatory cytokines. Toxicon. 149:45-53. doi: 10.1016/j.toxicon.2017.10.016.
Cebra, J. J. 1999. Influences of microbiota on intestinal immune system development. Am. J. Clin. Nutr. 69:1046S-1051S. doi: 10.1093/ajcn/69.5.1046s.
Celi, P., A. J. Cowieson, F. Fru-Nji, R. E. Steinert, A. M. Kluenter, and V. Verlhac. 2017. Gastrointestinal functionality in animal nutrition and health: New opportunities for sustainable animal production. Anim. Feed Sci. and Technol. 234:88-100. doi: https://doi.org/10.1016/j.anifeedsci.2017.09.012.
Chavakis, E., E. Y. Choi, and T. Chavakis. 2009. Novel aspects in the regulation of the leukocyte adhesion cascade. Thromb. Haemost. 102:191-197. doi: 10.1160/TH08-12-0844.
Chen, L., H. Deng, H. Cui, J. Fang, Z. Zuo, J. Deng, Y. Li, X. Wang, and L. Zhao. 2018. Inflammatory responses and inflammation-associated diseases in organs. Oncotarget. 9:7204-7218. doi: 10.18632/oncotarget.23208.
Chen, L., and N. Mozier. 2013. Comparison of Limulus amebocyte lysate test methods for endotoxin measurement in protein solutions. J. Pharm. Biomed. Anal. 80:180-185. doi: 10.1016/j.jpba.2013.03.011.
Chen, Y., M. Oba, and L. L. Guan. 2012. Variation of bacterial communities and expression of Toll-like receptor genes in the rumen of steers differing in susceptibility to subacute ruminal acidosis. Vet. Microbiol. 159:451-459. doi: 10.1016/j.vetmic.2012.04.032.
Chihaya, Y., K. Matsukawa, S. Mizushima, and Y. Matsui. 1988. Ruminant forestomach and abomasal mucormycosis under rumen acidosis. Vet. Pathol. 25:119-123. doi: 10.1177/030098588802500203.
Chin, A. C., A. N. Flynn, J. P. Fedwick, and A. G. Buret. 2006. The role of caspase-3 in lipopolysaccharide-mediated disruption of intestinal epithelial tight junctions. Can. J. Physiol. and Pharmacol. 84:1043-1050. doi: 10.1139/Y06-056.
Chistiakov, D. A., Y. V. Bobryshev, E. Kozarov, I. A. Sobenin, and A. N. Orekhov. 2015. Intestinal mucosal tolerance and impact of gut microbiota to mucosal tolerance. Front. Microbiol. 5:781-781. doi: 10.3389/fmicb.2014.00781.
Clark, J. A., and C. M. Coopersmith. 2007. Intestinal crosstalk: a new paradigm for understanding the gut as the "motor" of critical illness. Shock. 28:384-393. doi: 10.1097/shk.0b013e31805569df.
Clarke, L. L. 2009. A guide to Ussing chamber studies of mouse intestine. Am. J. Physiol. Gastrointest. Liver Physiol. 296:G1151-1166. doi: 10.1152/ajpgi.90649.2008.
Clemmons, D. R. 2012. Metabolic actions of insulin-like growth factor-I in normal physiology and diabetes. Endocrinol. Metab. Clin. North Am. 41:425-443, vii-viii. doi: 10.1016/j.ecl.2012.04.017.
Clemmons, D. R. 2018. Role of IGF-binding proteins in regulating IGF responses to changes in metabolism. J. Mol. Endocrinol. 61:T139-T169. doi: 10.1530/JME-18-0016.
Colgan, S. P. 2015. Neutrophils and inflammatory resolution in the mucosa. Semin. Immunol. 27:177-183. doi: 10.1016/j.smim.2015.03.007.

Colgan, S. P., E. L. Campbell, and D. J. Kominsky. 2016. Hypoxia and Mucosal Inflammation. Annu. Rev. Pathol. 11:77-100. doi: 10.1146/annurev-pathol-012615-044231.

Connor, E. E., J. L. Hutchison, K. M. Olson, and H. D. Norman. 2012. Triennial Lactation Symposium: Opportunities for improving milk production efficiency in dairy cattle. J. Anim. Sci. 90:1687-1694. doi: 10.2527/jas.2011-4528.

Cooper, R. J., T. J. Klopfenstein, R. A. Stock, C. T. Milton, D. W. Herold, and J. C. Parrott. 1999. Effects of imposed feed intake variation on acidosis and performance of finishing steers. J. Anim. Sci. 77:1093-1099.

Corcoran, S. E., and L. A. O'Neill. 2016. HIF1alpha and metabolic reprogramming in inflammation. J. Clin. Invest. 126:3699-3707. doi: 10.1172/JCI84431.

Corfe, B. M., D. Majumdar, A. Assadsangabi, A. M. Marsh, S. S. Cross, J. B. Connolly, C. A. Evans, and A. J. Lobo. 2015. Inflammation decreases keratin level in ulcerative colitis; inadequate restoration associates with increased risk of colitis-associated cancer. BMJ Open Gastroenterol. 2:e000024. doi: 10.1136/bmjgast-2014-000024.

Correa-Oliveira, R., J. L. Fachi, A. Vieira, F. T. Sato, and M. A. Vinolo. 2016. Regulation of immune cell function by short-chain fatty acids. Clin. Transl. Immunology. 5:e73. doi: 10.1038/cti.2016.17.

De Plaen, I. G., X. B. Han, X. Liu, W. Hsueh, S. Ghosh, and M. J. May. 2006. Lipopolysaccharide induces CXCL2/macrophage inflammatory protein-2 gene expression in enterocytes via NF-kappaB activation: independence from endogenous TNF-alpha and platelet-activating factor. Immunology. 118:153-163. doi: 10.1111/j.1365-2567.2006.02344.x.

Derting, T. L., and S. Compton. 2003. Immune response, not immune maintenance, is energetically costly in wild white-footed mice (Peromyscus leucopus). Physiol. Biochem. Zool. 76:744-752. doi: 10.1086/375662.

Di Virgilio, F., A. C. Sarti, and R. Coutinho-Silva. 2020. Purinergic signaling, DAMPs, and inflammation. Am. J. Physiol. Cell Physiol. 318:C832-C835. doi:10.1152/ajpcell.00053.2020.

Dieu-Nosjean, M. C., C. Massacrier, B. Homey, B. Vanbervliet, J. J. Pin, A. Vicari, S. Lebecque, C. Dezutter-Dambuyant, D. Schmitt, A. Zlotnik, and C. Caux. 2000. Macrophage inflammatory protein 3alpha is expressed at inflamed epithelial surfaces and is the most potent chemokine known in attracting Langerhans cell precursors. J. Exp. Med. 192:705-718. doi: 10.1084/jem.192.5.705.

Dinarello, C. A. 2000. Proinflammatory cytokines. Chest. 118:503-508.

Dionissopoulos, L., M. A. Steele, O. AlZahal, J. C. Plaizier, and B. W. McBride. 2012. A characterization of inflammatory and structural markers within the rumen epithelium during grain-induced ruminal acidosis in lactating dairy cattle. Am. J. Animal Vet. Sci. (Journal Article (Published)) doi: https://doi.org/10.7939/R30R9MH7D.

Dobson, M. J., W. C. Brown, A. Dobson, and A. T. Phillipson. 1956. A histological study of the organization of the rumen epithelium of sheep. Q. J. Exp. Physiol. Cogn. Med. Sci. 41:247-253. doi: 10.1113/expphysiol.1956.sp001186.

Dong, G., S. Liu, Y. Wu, C. Lei, J. Zhou, and S. Zhang. 2011. Diet-induced bacterial immunogens in the gastrointestinal tract of dairy cows: impacts on immunity and metabolism. Acta Vet. Scand. 53:48. doi: 10.1186/1751-0147-53-48.

Drouillard, J. S. 2018. Current situation and future trends for beef production in the United States of America - A review. Asian-Australas. J. Anim. Sci. 31:1007-1016. doi: 10.5713/ajas.18.0428.

Du, W., P. Jiang, A. Mancuso, A. Stonestrom, M. D. Brewer, A. J. Minn, T. W. Mak, M. Wu, and X. Yang. 2013. TAp73 enhances the pentose phosphate pathway and supports cell proliferation. Nat. Cell Biol. 15:991-1000. doi: 10.1038/ncb2789.

Dupont, A., L. Heinbockel, K. Brandenburg, and M. W. Hornef. 2014. Antimicrobial peptides and the enteric mucus layer act in concert to protect the intestinal mucosa. Gut Microbes. 5:761-765. doi: 10.4161/19490976.2014.972238.

Dziarski, R., Q. Wang, K. Miyake, C. J. Kirschning, and D. Gupta. 2001. MD-2 enables Toll-like receptor 2 (TLR2)-mediated responses to lipopolysaccharide and enhances TLR2-mediated responses to Gram-positive and Gram-negative bacteria and their cell wall components. J. Immunol. 166:1938-1944. doi: 10.4049/jimmunol.166.3.1938.

Eadie, J. M., J. Hyldgaard-Jensen, S. O. Mann, R. S. Reid, and F. G. Whitelaw. 1970. Observations on the microbiology and biochemistry of the rumen in cattle given different quantities of a pelleted barley ration. Br. J. Nutr. 24:157-177. doi: 10.1079/bjn19700018.

Eckhart, L., S. Lippens, E. Tschachler, and W. Declercq. 2013. Cell death by cornification. Biochim. Biophys. Acta. 1833:3471-3480. doi: 10.1016/j.bbamcr.2013.06.010.

Egea, L., C. S. McAllister, O. Lakhdari, I. Minev, S. Shenouda, and M. F. Kagnoff. 2013. GM-CSF produced by nonhematopoietic cells is required for early epithelial cell proliferation and repair of injured colonic mucosa. J. Immunol. 190:1702-1713. doi: 10.4049/jimmunol.1202368.

El-Kadi, S. W., R. L. t. Baldwin, K. R. McLeod, N. E. Sunny, and B. J. Bequette. 2009. Glutamate is the major anaplerotic substrate in the tricarboxylic acid cycle of isolated rumen epithelial and duodenal mucosal cells from beef cattle. J. Nutr. 139:869-875. doi: 10.3945/jn.108.103226.

Elsden, S. R., M. W. Hitchcock, and et al. 1946. Volatile acid in the digesta of ruminants and other animals. J. Exp. Biol. 22:191-202.

Emmanuel, D. G., K. L. Madsen, T. A. Churchill, S. M. Dunn, and B. N. Ametaj. 2007. Acidosis and lipopolysaccharide from Escherichia coli B:055 cause hyperpermeability of rumen and colon tissues. J. Dairy Sci. 90:5552-5557. doi: 10.3168/jds.2007-0257.

Etschmann, B., A. Suplie, and H. Martens. 2009. Change of ruminal sodium transport in sheep during dietary adaptation. Arch. Anim. Nutr. 63:26-38. doi: 10.1080/17450390802506885.

Eyerich, S., K. Eyerich, C. Traidl-Hoffmann, and T. Biedermann. 2018. Cutaneous Barriers and Skin Immunity: Differentiating A Connected Network. Trends Immunol. 39:315-327. doi: 10.1016/j.it.2018.02.004.

Fang, W. H., Y. M. Yao, Z. G. Shi, Y. Yu, Y. Wu, L. R. Lu, and Z. Y. Sheng. 2003. The mRNA expression patterns of tumor necrosis factor-alpha and TNFR-I in some vital organs after thermal injury. World J. Gastroenterol. 9:1038-1044. doi: 10.3748/wjg.v9.i5.1038.

Farquhar, M. G., and G. E. Palade. 1963. Junctional complexes in various epithelia. J. Cell Biol. 17:375-412. doi: 10.1083/jcb.17.2.375.

Ferrari, D., E. N. McNamee, M. Idzko, R. Gambari, and H. K. Eltzschig. 2016. Purinergic Signaling During Immune Cell Trafficking. Trends Immunol. 37:399-411. doi: 10.1016/j.it.2016.04.004.

Fichorova, R. N., A. O. Cronin, E. Lien, D. J. Anderson, and R. R. Ingalls. 2002. Response to Neisseria gonorrhoeae by cervicovaginal epithelial cells occurs in the absence of toll-like receptor 4-mediated signaling. J. Immunol. 168:2424-2432. doi: 10.4049/jimmunol.168.5.2424.

Finkel, T., S. Menazza, K. M. Holmstrom, R. J. Parks, J. Liu, J. Sun, J. Liu, X. Pan, and E. Murphy. 2015. The ins and outs of mitochondrial calcium. Circ. Res. 116:1810-1819. doi: 10.1161/CIRCRESAHA.116.305484.

Freshney, R. I. 2010a. Introduction, Culture of Animal Cells. John Wiley & Sons, Inc. p. 1-10.

Freshney, R. I. 2010b. Primary Culture, Culture of Animal Cells. John Wiley & Sons, Inc. p. 163-186.

Fukata, M., A. Chen, A. Klepper, S. Krishnareddy, A. S. Vamadevan, L. S. Thomas, R. Xu, H. Inoue, M. Arditi, A. J. Dannenberg, and M. T. Abreu. 2006. Cox-2 is regulated by Toll-like receptor-4 (TLR4) signaling: Role in proliferation and apoptosis in the intestine. Gastroenterology. 131:862-877. doi: 10.1053/j.gastro.2006.06.017.

Gabel, G., P. Galfi, S. Neogrady, and H. Martens. 1996. Characterization of Na+/H+ exchange in sheep rumen epithelial cells kept in primary culture. Zentralbl. Veterinarmed. A. 43:365-375. doi: 10.1111/j.1439-0442.1996.tb00464.x.

Gabel, G., F. Muller, H. Pfannkuche, and J. R. Aschenbach. 2001. Influence of isoform and DNP on butyrate transport across the sheep ruminal epithelium. J. Comp. Physiol. B. 171:215-221.

Gabel, G., and J. Sehested. 1997. SCFA transport in the forestomach of ruminants. Comp. Biochem. Physiol. A. Physiol. 118:367-374. doi: 10.1016/s0300-9629(96)00321-0.

Gabel, G., S. Vogler, and H. Martens. 1991. Short-chain fatty acids and CO2 as regulators of Na+ and Cl- absorption in isolated sheep rumen mucosa. J. Comp. Physiol. B. 161:419-426. doi: 10.1007/bf00260803.

Gaebel, G., H. Martens, M. Suendermann, and P. Galfi. 1987. The effect of diet, intraruminal pH and osmolarity on sodium, chloride and magnesium absorption from the temporarily isolated and washed reticulo-rumen of sheep. Q. J. Exp. Physiol. 72:501-511. doi: 10.1113/expphysiol.1987.sp003092.

Gagliani, N., M. C. Amezcua Vesely, A. Iseppon, L. Brockmann, H. Xu, N. W. Palm, M. R. de Zoete, P. Licona-Limon, R. S. Paiva, T. Ching, C. Weaver, X. Zi, X. Pan, R. Fan, L. X. Garmire, M. J. Cotton, Y. Drier, B. Bernstein, J. Geginat, B. Stockinger, E. Esplugues, S. Huber, and R. A. Flavell. 2015. Th17 cells transdifferentiate into regulatory T cells during resolution of inflammation. Nature. 523:221-225. doi: 10.1038/nature14452.

Galfi, P., G. Gabel, and H. Martens. 1993. Influences of extracellular matrix components on the growth and differentiation of ruminal epithelial cells in primary culture. Res. Vet. Sci. 54:102-109. doi: 10.1016/0034-5288(93)90018-b.

Galfi, P., and S. Neogrady. 1989. Epithelial and non-epithelial cell- and tissue culture from the ruminal mucosa. Asian-Australas. J. Anim. Sci. 2:143-144.

Galfi, P., S. Neogrady, and G. Gabel. 2002. Na+/H+ exchange in primary, secondary and n-butyrate-treated cultures of ruminal epithelial cells: short communication. Acta Vet. Hung. 50:211-215. doi: 10.1556/AVet.50.2002.2.10.

Galfi, P., S. Neogrady, and F. Kutas. 1981. Culture of epithelial cells from bovine ruminal mucosa. Vet. Res. Commun. 4:295-300. doi: 10.1007/bf02278507.

Gálfi, P., S. Neogrády, and T. Sakata. 1991. Effects of Volatile Fatty Acids on the Epithelial Cell Proliferation of the Digestive Tract and Its Hormonal Mediation. In: T. Tsuda, Y. Sasaki

and R. Kawashima, editors, Physiological Aspects of Digestion and Metabolism in Ruminants. Academic Press, San Diego. p. 49-59.
Gani, D. K., D. Lakshmi, R. Krishnan, and P. Emmadi. 2009. Evaluation of C-reactive protein and interleukin-6 in the peripheral blood of patients with chronic periodontitis. J. Indian Soc. Periodontol. 13:69-74. doi: 10.4103/0972-124X.55840.
Garland, C. D., A. Lee, and M. R. Dickson. 1982. Segmented filamentous bacteria in the rodent small intestine: Their colonization of growing animals and possible role in host resistance toSalmonella. Microb. Ecol. 8:181-190. doi: 10.1007/BF02010451.
Garner, M. R., J. F. Flint, and J. B. Russell. 2002. Allisonella histaminiformans gen. nov., sp. nov. A novel bacterium that produces histamine, utilizes histidine as its sole energy source, and could play a role in bovine and equine laminitis. Syst. Appl. Microbiol. 25:498-506. doi: 10.1078/07232020260517625.
Garnett, J. P., K. K. Kalsi, M. Sobotta, J. Bearham, G. Carr, J. Powell, M. Brodlie, C. Ward, R. Tarran, and D. L. Baines. 2016. Hyperglycaemia and Pseudomonas aeruginosa acidify cystic fibrosis airway surface liquid by elevating epithelial monocarboxylate transporter 2 dependent lactate-H(+) secretion. Sci. Rep. 6:37955. doi: 10.1038/srep37955.
Garza, J. D., F. N. Owens, and J. E. Breazile. 1989. Effects of diet on ruminal liquid and on blood serum osmolality and hematocrit in feedlot heifers. Animal science research report, Oklahoma agriculture experiment station.
Gemmell, R. T. 1973. Langerhans cells in the ruminal epithelium of the sheep. J. Ultrastruct. Res. 43:256-259. doi: 10.1016/s0022-5320(73)80037-1.
Giepmans, B. N., and S. C. van Ijzendoorn. 2009. Epithelial cell-cell junctions and plasma membrane domains. Biochim. Biophys. Acta. 1788:820-831. doi: 10.1016/j.bbamem.2008.07.015.
Gilroy, D. W., P. R. Colville-Nash, D. Willis, J. Chivers, M. J. Paul-Clark, and D. A. Willoughby. 1999. Inducible cyclooxygenase may have anti-inflammatory properties. Nat. Med. 5:698-701. doi: 10.1038/9550.
Ginsburg, E., D. Salomon, T. Sreevalsan, and E. Freese. 1973. Growth inhibition and morphological changes caused by lipophilic acids in mammalian cells. Proc. Natl. Acad. Sci. U S A. 70:2457-2461. doi: 10.1073/pnas.70.8.2457.
Glover, L. E., and S. P. Colgan. 2011. Hypoxia and metabolic factors that influence inflammatory bowel disease pathogenesis. Gastroenterology. 140:1748-1755. doi: 10.1053/j.gastro.2011.01.056.
Goad, D. W., C. L. Goad, and T. G. Nagaraja. 1998. Ruminal microbial and fermentative changes associated with experimentally induced subacute acidosis in steers. J. Anim. Sci. 76:234-241.
Godornes, C., B. T. Leader, B. J. Molini, A. Centurion-Lara, and S. A. Lukehart. 2007. Quantitation of rabbit cytokine mRNA by real-time RT-PCR. Cytokine. 38:1-7. doi: 10.1016/j.cyto.2007.04.002.
Goosen, P. C. 1976. Metabolism in rumen epithelium oxidation of substrates and formation of ketone bodies by pieces of rumen epithelium. Z. Tierphysiol. Tierernahr. Futtermittelkd. 37:14-25. doi: 10.1111/j.1439-0396.1976.tb00037.x.
Gott, P. N. 2011. Endotoxin Tolerance in Lactating Dairy Cows. Ohio State University.
Gott, P. N., J. S. Hogan, and W. P. Weiss. 2015. Effects of various starch feeding regimens on responses of dairy cows to intramammary lipopolysaccharide infusion. J. Dairy Sci. 98:1786-1796. doi: 10.3168/jds.2014-8638.

Gozho, G. N., J. C. Plaizier, D. O. Krause, A. D. Kennedy, and K. M. Wittenberg. 2005. Subacute ruminal acidosis induces ruminal lipopolysaccharide endotoxin release and triggers an inflammatory response. J. Dairy Sci. 88:1399-1403. doi: 10.3168/jds.S0022-0302(05)72807-1.

Grabacka, M., M. Pierzchalska, M. Dean, and K. Reiss. 2016. Regulation of Ketone Body Metabolism and the Role of PPARalpha. Int. J. Mol. Sci. 17doi: 10.3390/ijms17122093.

Graham, C., I. Gatherar, I. Haslam, M. Glanville, and N. L. Simmons. 2007. Expression and localization of monocarboxylate transporters and sodium/proton exchangers in bovine rumen epithelium. Am. J. Physiol. Gastrointest. Liver Physiol. 292:R997-1007. doi: 10.1152/ajpregu.00343.2006.

Graham, C., and N. L. Simmons. 2005. Functional organization of the bovine rumen epithelium. Am. J. Physiol. Regul. Integr. Comp. Physiol. 288:R173-181. doi: 10.1152/ajpregu.00425.2004.

Gray, F. V., A. F. Pilgrim, and R. A. Weller. 1951. Fermentation in the rumen of the sheep. I. The production of volatile fatty acids and methane during the fermentation of wheaten hay and lucerne hay in vitro by micro-organisms from the rumen. J. Exp. Biol. 28:74-82.

Greco, G., F. Hagen, S. Meissner, Z. Shen, Z. Lu, S. Amasheh, and J. R. Aschenbach. 2018. Effect of individual SCFA on the epithelial barrier of sheep rumen under physiological and acidotic luminal pH conditions. J. Anim. Sci. 96:126-142. doi: 10.1093/jas/skx017.

Greiner, E. F., M. Guppy, and K. Brand. 1994. Glucose is essential for proliferation and the glycolytic enzyme induction that provokes a transition to glycolytic energy production. J. Biol. Chem. 269:31484-31490.

Grisham, M. B., T. S. Gaginella, C. von Ritter, H. Tamai, R. M. Be, and D. N. Granger. 1990. Effects of neutrophil-derived oxidants on intestinal permeability, electrolyte transport, and epithelial cell viability. Inflammation. 14:531-542. doi: 10.1007/bf00914274.

Grishin, A. V., J. Wang, D. A. Potoka, D. J. Hackam, J. S. Upperman, P. Boyle, R. Zamora, and H. R. Ford. 2006. Lipopolysaccharide induces cyclooxygenase-2 in intestinal epithelium via a noncanonical p38 MAPK pathway. J. Immunol. 176:580-588.

Grohn, Y. T., D. J. Wilson, R. N. Gonzalez, J. A. Hertl, H. Schulte, G. Bennett, and Y. H. Schukken. 2004. Effect of pathogen-specific clinical mastitis on milk yield in dairy cows. J. Dairy Sci. 87:3358-3374. doi: 10.3168/jds.S0022-0302(04)73472-4.

Guo, S., R. Al-Sadi, H. M. Said, and T. Y. Ma. 2013. Lipopolysaccharide causes an increase in intestinal tight junction permeability in vitro and in vivo by inducing enterocyte membrane expression and localization of TLR-4 and CD14. Am. J. Pathol. 182:375-387. doi: 10.1016/j.ajpath.2012.10.014.

Guo, S., M. Nighot, R. Al-Sadi, T. Alhmoud, P. Nighot, and T. Y. Ma. 2015. Lipopolysaccharide Regulation of Intestinal Tight Junction Permeability Is Mediated by TLR4 Signal Transduction Pathway Activation of FAK and MyD88. J. Immunol. 195:4999-5010. doi: 10.4049/jimmunol.1402598.

Gyles, C. L. 2007. Shiga toxin-producing Escherichia coli: an overview. J. Anim. Sci. 85:E45-62. doi: 10.2527/jas.2006-508.

Haeggstrom, J. Z., and C. D. Funk. 2011. Lipoxygenase and leukotriene pathways: biochemistry, biology, and roles in disease. Chem. Rev. 111:5866-5898. doi: 10.1021/cr200246d.

Halestrap, A. P., and M. C. Wilson. 2012. The monocarboxylate transporter family--role and regulation. IUBMB Life. 64:109-119. doi: 10.1002/iub.572.

Halldorsson, S., V. Asgrimsson, I. Axelsson, G. H. Gudmundsson, M. Steinarsdottir, O. Baldursson, and T. Gudjonsson. 2007. Differentiation potential of a basal epithelial cell line established from human bronchial explant. In Vitro Cell Dev. Biol. Anim. 43:283-289. doi: 10.1007/s11626-007-9050-4.

Hamer, H. M., D. Jonkers, K. Venema, S. Vanhoutvin, F. J. Troost, and R. J. Brummer. 2008. Review article: the role of butyrate on colonic function. Aliment. Pharmacol. Ther. 27:104-119. doi: 10.1111/j.1365-2036.2007.03562.x.

Hamonic, G., J. A. Pasternak, and H. L. Wilson. 2018. Recognizing conserved non-canonical localization patterns of toll-like receptors in tissues and across species. Cell Tissue Res. 372:1-11. doi: 10.1007/s00441-017-2767-9.

Hanssen, S. A., D. Hasselquist, I. Folstad, and K. E. Erikstad. 2004. Costs of immunity: immune responsiveness reduces survival in a vertebrate. Proc. Biol. Sci. 271:925-930. doi: 10.1098/rspb.2004.2678.

Harada, A., N. Sekido, T. Akahoshi, T. Wada, N. Mukaida, and K. Matsushima. 1994. Essential involvement of interleukin-8 (IL-8) in acute inflammation. J. Leukoc. Biol. 56:559-564.

Hardin, J., K. Kroeker, B. Chung, and D. G. Gall. 2000. Effect of proinflammatory interleukins on jejunal nutrient transport. Gut. 47:184-191. doi: 10.1136/gut.47.2.184.

Harrison, O. J., J. L. Linehan, H. Y. Shih, N. Bouladoux, S. J. Han, M. Smelkinson, S. K. Sen, A. L. Byrd, M. Enamorado, C. Yao, S. Tamoutounour, F. Van Laethem, C. Hurabielle, N. Collins, A. Paun, R. Salcedo, J. J. O'Shea, and Y. Belkaid. 2019. Commensal-specific T cell plasticity promotes rapid tissue adaptation to injury. Science. 363doi: 10.1126/science.aat6280.

Hartsock, A., and W. J. Nelson. 2008. Adherens and tight junctions: structure, function and connections to the actin cytoskeleton. Biochim. Biophys. Acta. 1778:660-669. doi: 10.1016/j.bbamem.2007.07.012.

Hasan, U. A., G. Trinchieri, and J. Vlach. 2005. Toll-like receptor signaling stimulates cell cycle entry and progression in fibroblasts. J. Biol. Chem. 280:20620-20627. doi: 10.1074/jbc.M500877200.

Hawkes, J. W. 1974. The structure of fish skin. I. General organization. Cell Tissue Res. 149:147-158. doi: 10.1007/bf00222270.

He, L., H. Wang, Y. Zhang, L. Geng, M. Yang, Z. Xu, K. Zou, W. Xu, and S. Gong. 2018. Evaluation of Monocarboxylate Transporter 4 in Inflammatory Bowel Disease and Its Potential Use as a Diagnostic Marker. Dis. Markers. 2018:2649491. doi: 10.1155/2018/2649491.

Henrikson, R. C. 1970. Ultrastructure of ovine ruminal epithelium and localization of sodium in the tissue. J. Ultrastruct. Res. 30:385-401. doi: 10.1016/s0022-5320(70)80070-3.

Hershberg, R. M., P. E. Framson, D. H. Cho, L. Y. Lee, S. Kovats, J. Beitz, J. S. Blum, and G. T. Nepom. 1997. Intestinal epithelial cells use two distinct pathways for HLA class II antigen processing. J. Clin. Invest. 100:204-215. doi: 10.1172/JCI119514.

Heyden, A., H. S. Huitfeldt, H. S. Koppang, P. S. Thrane, M. Bryne, and P. Brandtzaeg. 1992. Cytokeratins as epithelial differentiation markers in premalignant and malignant oral lesions. J. Oral Pathol. Med. 21:7-11. doi: 10.1111/j.1600-0714.1992.tb00960.x.

Hill, D. A., and D. Artis. 2010. Intestinal bacteria and the regulation of immune cell homeostasis. Annu. Rev. Immunol. 28:623-667. doi: 10.1146/annurev-immunol-030409-101330.

Hirotani, Y., K. Ikeda, R. Kato, M. Myotoku, T. Umeda, Y. Ijiri, and K. Tanaka. 2008. Protective effects of lactoferrin against intestinal mucosal damage induced by

lipopolysaccharide in human intestinal Caco-2 cells. Yakugaku Zasshi. 128:1363-1368. doi: 10.1248/yakushi.128.1363.
Hoffmann, J., J. Wilhelm, and G. Kwapiszewska. 2017. Laser Capture Microdissection of Tissue Sections for High-Throughput RNA Analysis. Methods Mol. Biol. 1627:325-340. doi: 10.1007/978-1-4939-7113-8_21.
Hofmann, R. R. 1989. Evolutionary steps of ecophysiological adaptation and diversification of ruminants: a comparative view of their digestive system. Oecologia. 78:443-457. doi: 10.1007/BF00378733.
Hooper, L. V. 2015. Epithelial cell contributions to intestinal immunity. Adv. Immunol. 126:129-172. doi: 10.1016/bs.ai.2014.11.003.
Hu, W. S., T. C. Dodge, K. K. Frame, and V. B. Himes. 1987. Effect of glucose on the cultivation of mammalian cells. Dev. Biol. Stand. 66:279-290.
Huang, H. L., H. W. Hsing, T. C. Lai, Y. W. Chen, T. R. Lee, H. T. Chan, P. C. Lyu, C. L. Wu, Y. C. Lu, S. T. Lin, C. W. Lin, C. H. Lai, H. T. Chang, H. C. Chou, and H. L. Chan. 2010. Trypsin-induced proteome alteration during cell subculture in mammalian cells. J. Biomed. Sci. 17:36. doi: 10.1186/1423-0127-17-36.
Huhn, K., F. Muller, K. U. Honscha, H. Pfannkuche, and G. Gabel. 2003. Molecular and functional evidence for a Na(+)-HCO3(-)-cotransporter in sheep ruminal epithelium. J. Comp. Physiol. B. 173:277-284. doi: 10.1007/s00360-003-0333-0.
Humer, E., J. R. Aschenbach, V. Neubauer, I. Kroger, R. Khiaosa-Ard, W. Baumgartner, and Q. Zebeli. 2018. Signals for identifying cows at risk of subacute ruminal acidosis in dairy veterinary practice. J. Anim. Physiol. Anim. Nutr. (Berl). 102:380-392. doi: 10.1111/jpn.12850.
Hung, T. V., and T. Suzuki. 2018. Short-Chain Fatty Acids Suppress Inflammatory Reactions in Caco-2 Cells and Mouse Colons. J. Agric. Food Chem. 66:108-117. doi: 10.1021/acs.jafc.7b04233.
Hunger, R. E., P. A. Sieling, M. T. Ochoa, M. Sugaya, A. E. Burdick, T. H. Rea, P. J. Brennan, J. T. Belisle, A. Blauvelt, S. A. Porcelli, and R. L. Modlin. 2004. Langerhans cells utilize CD1a and langerin to efficiently present nonpeptide antigens to T cells. J. Clin. Invest. 113:701-708. doi: 10.1172/JCI19655.
Hurley, J. C. 1995. Endotoxemia: methods of detection and clinical correlates. Clin. Microbiol. Rev. 8:268-292.
Idzko, M., D. Ferrari, and H. K. Eltzschig. 2014. Nucleotide signalling during inflammation. Nature. 509:310-317. doi: 10.1038/nature13085.
Inooka, S., S. Ohwada, and H. Tamate. 1984. Cell cultivation of bovine rumen mucosa tissues. Can. J. Anim. Sci. 64:110-111. doi: 10.4141/cjas84-180.
Iotzova-Weiss, G., S. N. Freiberger, P. Johansen, J. Kamarachev, E. Guenova, P. J. Dziunycz, G. A. Roux, J. Neu, and G. F. L. Hofbauer. 2017. TLR4 as a negative regulator of keratinocyte proliferation. PLoS One. 12:e0185668. doi: 10.1371/journal.pone.0185668.
Itoh, M., and M. J. Bissell. 2003. The organization of tight junctions in epithelia: implications for mammary gland biology and breast tumorigenesis. J. Mammary Gland Biol. Neoplasia. 8:449-462. doi: 10.1023/B:JOMG.0000017431.45314.07.
Ivanov, A. I., C. A. Parkos, and A. Nusrat. 2010. Cytoskeletal regulation of epithelial barrier function during inflammation. Am. J. Pathol. 177:512-524. doi: 10.2353/ajpath.2010.100168.

Jiang, K., S. Guo, T. Zhang, Y. Yang, G. Zhao, A. Shaukat, H. Wu, and G. Deng. 2018. Downregulation of TLR4 by miR-181a Provides Negative Feedback Regulation to Lipopolysaccharide-Induced Inflammation. Front. Pharmacol. 9:142. doi: 10.3389/fphar.2018.00142.

Jin, L., Y. Qu, L. J. Gomez, S. Chung, B. Han, B. Gao, Y. Yue, Y. Gong, X. Liu, F. Amersi, C. Dang, A. E. Giuliano, and X. Cui. 2018. Characterization of primary human mammary epithelial cells isolated and propagated by conditional reprogrammed cell culture. Oncotarget. 9:11503-11514. doi: 10.18632/oncotarget.23817.

Johansson, M. E., M. Phillipson, J. Petersson, A. Velcich, L. Holm, and G. C. Hansson. 2008. The inner of the two Muc2 mucin-dependent mucus layers in colon is devoid of bacteria. Proc. Natl. Acad. Sci. U S A. 105:15064-15069. doi: 10.1073/pnas.0803124105.

Johnson, A. R., Y. Qin, A. J. Cozzo, A. J. Freemerman, M. J. Huang, L. Zhao, B. P. Sampey, J. J. Milner, M. A. Beck, B. Damania, N. Rashid, J. A. Galanko, D. P. Lee, M. L. Edin, D. C. Zeldin, P. T. Fueger, B. Dietz, A. Stahl, Y. Wu, K. L. Mohlke, and L. Makowski. 2016. Metabolic reprogramming through fatty acid transport protein 1 (FATP1) regulates macrophage inflammatory potential and adipose inflammation. Mol. Metab. 5:506-526. doi: 10.1016/j.molmet.2016.04.005.

Jonca, N., E. A. Leclerc, C. Caubet, M. Simon, M. Guerrin, and G. Serre. 2011. Corneodesmosomes and corneodesmosin: from the stratum corneum cohesion to the pathophysiology of genodermatoses. Eur. J. Dermatol. 21 Suppl 2:35-42. doi: 10.1684/ejd.2011.1264.

Josefsen, T. D., and T. Landsverk. 1996. T cell subsets and Langerhans cells in the forestomach mucosa of adult sheep and sheep foetuses. Vet. Immunol. Immunopathol. 51:101-111. doi: 10.1016/0165-2427(95)05511-8.

Julian, M. W., H. R. Strange, M. N. Ballinger, R. S. Hotchkiss, T. L. Papenfuss, and E. D. Crouser. 2015. Tolerance and Cross-Tolerance following Toll-Like Receptor (TLR)-4 and -9 Activation Are Mediated by IRAK-M and Modulated by IL-7 in Murine Splenocytes. PLoS One. 10:e0132921. doi: 10.1371/journal.pone.0132921.

Jung, H. C., L. Eckmann, S. K. Yang, A. Panja, J. Fierer, E. Morzycka-Wroblewska, and M. F. Kagnoff. 1995. A distinct array of proinflammatory cytokines is expressed in human colon epithelial cells in response to bacterial invasion. J. Clin. Invest. 95:55-65. doi: 10.1172/JCI117676.

Jura, J., P. Wegrzyn, M. Korostynski, K. Guzik, M. Oczko-Wojciechowska, M. Jarzab, M. Kowalska, M. Piechota, R. Przewlocki, and A. Koj. 2008. Identification of interleukin-1 and interleukin-6-responsive genes in human monocyte-derived macrophages using microarrays. Biochim. Biophys. Acta. 1779:383-389. doi: 10.1016/j.bbagrm.2008.04.006.

Kagnoff, M. F. 2014. The intestinal epithelium is an integral component of a communications network. J. Clin. Invest. 124:2841-2843. doi: 10.1172/JCI75225.

Karin, M., T. Lawrence, and V. Nizet. 2006. Innate immunity gone awry: linking microbial infections to chronic inflammation and cancer. Cell. 124:823-835. doi: 10.1016/j.cell.2006.02.016.

Kaser, T., J. A. Pasternak, G. Hamonic, M. Reider, K. Lai, M. Delgado-Ortega, V. Gerdts and F. Meurens. 2016. Flow cytometry as an improved method for titration of Chlamydiaceae and other intracellular bacteria. Cytometry. 89A:451-460. doi: 10.1002/cyto.a.22822.

Kastrukoff, L. F., A. S. Lau, F. Takei, M. J. Smyth, C. M. Jones, S. R. Clarke, and F. R. Carbone. 2010. Redundancy in the immune system restricts the spread of HSV-1 in the

central nervous system (CNS) of C57BL/6 mice. Virology. 400:248-258. doi: 10.1016/j.virol.2010.02.013.
Kauffman, A. L., A. V. Gyurdieva, J. R. Mabus, C. Ferguson, Z. Yan, and P. J. Hornby. 2013. Alternative functional in vitro models of human intestinal epithelia. Front. Pharmacol. 4:79. doi: 10.3389/fphar.2013.00079.
Kayama, H., and K. Takeda. 2016. Functions of innate immune cells and commensal bacteria in gut homeostasis. J. Biochem. 159:141-149. doi: 10.1093/jb/mvv119.
Kelly, B., and L. A. O'Neill. 2015. Metabolic reprogramming in macrophages and dendritic cells in innate immunity. Cell Res. 25:771-784. doi: 10.1038/cr.2015.68.
Kelly, J. M., B. W. McBride, and L. P. Milligan. 1993. In vitro ouabain-sensitive respiration and protein synthesis in ruminal epithelial papillae of Hereford steers fed either alfalfa or bromegrass hay once daily. J. Anim. Sci. 71:2799-2808. doi: 10.2527/1993.71102799x.
Kent-Dennis, C., A. Pasternak, J. C. Plaizier, and G. B. Penner. 2019. Potential for a localized immune response by the ruminal epithelium in nonpregnant heifers following a short-term subacute ruminal acidosis challenge. J. Dairy Sci. 102:7556-7569. doi: 10.3168/jds.2019-16294.
Kent-Dennis, C., J.R. Aschenbach, P.J. Griebel, and G.B. Penner. 2020. Effects of lipopolysaccharide exposure on the inflammatory response in cultured primary ruminal epithelial cells. J. Dairy Sci. (In Press).
Keogh, K., S. M. Waters, P. Cormican, A. K. Kelly, E. O'Shea, and D. A. Kenny. 2017. Effect of dietary restriction and subsequent re-alimentation on the transcriptional profile of bovine ruminal epithelium. PLoS One. 12:e0177852. doi: 10.1371/journal.pone.0177852.
Kern, M., D. Gunzel, J. R. Aschenbach, K. Tedin, A. Bondzio, and U. Lodemann. 2017. Altered Cytokine Expression and Barrier Properties after In Vitro Infection of Porcine Epithelial Cells with Enterotoxigenic Escherichia coli and Probiotic Enterococcus faecium. Mediators Inflamm. 2017:2748192. doi: 10.1155/2017/2748192.
Kern, R. J., A. K. Lindholm-Perry, H. C. Freetly, W. M. Snelling, J. W. Kern, J. W. Keele, J. R. Miles, A. P. Foote, W. T. Oliver, L. A. Kuehn, and P. A. Ludden. 2016. Transcriptome differences in the rumen of beef steers with variation in feed intake and gain. Gene. 586:12-26. doi: 10.1016/j.gene.2016.03.034.
Kesimer, M., C. Ehre, K. A. Burns, C. W. Davis, J. K. Sheehan, and R. J. Pickles. 2013. Molecular organization of the mucins and glycocalyx underlying mucus transport over mucosal surfaces of the airways. Mucosal Immunol. 6:379-392. doi: 10.1038/mi.2012.81.
Khafipour, E., D. O. Krause, and J. C. Plaizier. 2009a. Alfalfa pellet-induced subacute ruminal acidosis in dairy cows increases bacterial endotoxin in the rumen without causing inflammation. J. Dairy Sci. 92:1712-1724. doi: 10.3168/jds.2008-1656.
Khafipour, E., D. O. Krause, and J. C. Plaizier. 2009b. A grain-based subacute ruminal acidosis challenge causes translocation of lipopolysaccharide and triggers inflammation. J. Dairy Sci. 92:1060-1070. doi: 10.3168/jds.2008-1389.
Khorasani, G. R., G. De Boer, and J. J. Kennelly. 1996. Response of early lactation cows to ruminally undegradable protein in the diet. J. Dairy Sci. 79:446-453. doi: 10.3168/jds.S0022-0302(96)76384-1.
Khoury, J., J. C. Ibla, A. S. Neish, and S. P. Colgan. 2007. Antiinflammatory adaptation to hypoxia through adenosine-mediated cullin-1 deneddylation. J. Clin. Invest. 117:703-711. doi: 10.1172/JCI30049.

Kiela, P. R., and F. K. Ghishan. 2009. Ion transport in the intestine. Curr. Opin. Gastroenterol. 25:87-91. doi: 10.1097/MOG.0b013e3283260900.
Kiepe, D., S. Ciarmatori, A. Hoeflich, E. Wolf, and B. Tonshoff. 2005. Insulin-like growth factor (IGF)-I stimulates cell proliferation and induces IGF binding protein (IGFBP)-3 and IGFBP-5 gene expression in cultured growth plate chondrocytes via distinct signaling pathways. Endocrinology. 146:3096-3104. doi: 10.1210/en.2005-0324.
Kim, H. M., B. S. Park, J. I. Kim, S. E. Kim, J. Lee, S. C. Oh, P. Enkhbayar, N. Matsushima, H. Lee, O. J. Yoo, and J. O. Lee. 2007. Crystal structure of the TLR4-MD-2 complex with bound endotoxin antagonist Eritoran. Cell. 130:906-917. doi: 10.1016/j.cell.2007.08.002.
Kim, S. C., and P. H. Hwang. 2018. Up-regulation of IGF Binding Protein-3 Inhibits Colonic Inflammatory Response. J. Korean Med. Sci. 33:e110. doi: 10.3346/jkms.2018.33.e110.
Kirat, D., H. Inoue, H. Iwano, K. Hirayama, H. Yokota, H. Taniyama, and S. Kato. 2005. Expression and distribution of monocarboxylate transporter 1 (MCT1) in the gastrointestinal tract of calves. Res. Vet. Sci. 79:45-50. doi: 10.1016/j.rvsc.2004.11.007.
Kirat, D., Y. Matsuda, N. Yamashiki, H. Hayashi, and S. Kato. 2007. Expression, cellular localization, and functional role of monocarboxylate transporter 4 (MCT4) in the gastrointestinal tract of ruminants. Gene. 391:140-149. doi: 10.1016/j.gene.2006.12.020.
Kisselbach, L., M. Merges, A. Bossie, and A. Boyd. 2009. CD90 Expression on human primary cells and elimination of contaminating fibroblasts from cell cultures. Cytotechnology. 59:31-44. doi: 10.1007/s10616-009-9190-3.
Kleen, J. L., G. A. Hooijer, J. Rehage, and J. P. Noordhuizen. 2003. Subacute ruminal acidosis (SARA): a review. J. Vet. Med. A. Physiol. Pathol. Clin. Med. 50:406-414.
Klotz, J. L., R. L. t. Baldwin, R. C. Gillis, and R. N. Heitmann. 2001. Refinements in primary rumen epithelial cell incubation techniques. J. Dairy Sci. 84:183-193. doi: 10.3168/jds.S0022-0302(01)74468-2.
Kobielak, A., H. A. Pasolli, and E. Fuchs. 2004. Mammalian formin-1 participates in adherens junctions and polymerization of linear actin cables. Nat. Cell Biol. 6:21-30. doi: 10.1038/ncb1075.
Kominsky, D. J., E. L. Campbell, and S. P. Colgan. 2010. Metabolic shifts in immunity and inflammation. J. Immunol. 184:4062-4068. doi: 10.4049/jimmunol.0903002.
Kowalik, M. A., A. Columbano, and A. Perra. 2017. Emerging Role of the Pentose Phosphate Pathway in Hepatocellular Carcinoma. Front. Oncol. 7:87. doi: 10.3389/fonc.2017.00087.
Kristensen, N. B., A. Danfaer, and N. Agergaard. 1998. Absorption and metabolism of short-chain fatty acids in ruminants. Arch. Tierernahr. 51:165-175. doi: 10.1080/17450399809381916.
Kristensen, N. B., and D. L. Harmon. 2004. Splanchnic metabolism of volatile fatty acids absorbed from the washed reticulorumen of steers. J. Anim. Sci. 82:2033-2042. doi: 10.2527/2004.8272033x.
Kristensen, N. B., G. B. Huntington, and D. L. Harmon. 2005. Chapter 17 Splanchnic carbohydrate and energy metabolism in growing ruminants11Approved as publication No. 02-07-97 by the Kentucky Agricultural Experiment Station. In: D. G. Burrin and H. J. Mersmann, editors, Biology of Growing Animals No. 3. Elsevier. p. 405-432.
Kvidera, S. K., E. A. Horst, M. Abuajamieh, E. J. Mayorga, M. V. Fernandez, and L. H. Baumgard. 2017. Glucose requirements of an activated immune system in lactating Holstein cows. J. Dairy Sci. 100:2360-2374. doi: 10.3168/jds.2016-12001.

Lamouille, S., J. Xu, and R. Derynck. 2014. Molecular mechanisms of epithelial-mesenchymal transition. Nat. Rev. Mol. Cell Biol. 15:178-196. doi: 10.1038/nrm3758.
Lang, C. H., Z. Spolarics, A. Ottlakan, and J. J. Spitzer. 1993. Effect of high-dose endotoxin on glucose production and utilization. Metabolism. 42:1351-1358. doi: 10.1016/0026-0495(93)90137-d.
Lanis, J. M., D. J. Kao, E. E. Alexeev, and S. P. Colgan. 2017. Tissue metabolism and the inflammatory bowel diseases. J. Mol. Med. (Berl). 95:905-913. doi: 10.1007/s00109-017-1544-2.
Laukoetter, M. G., P. Nava, W. Y. Lee, E. A. Severson, C. T. Capaldo, B. A. Babbin, I. R. Williams, M. Koval, E. Peatman, J. A. Campbell, T. S. Dermody, A. Nusrat, and C. A. Parkos. 2007. JAM-A regulates permeability and inflammation in the intestine in vivo. J. Exp. Med. 204:3067-3076. doi: 10.1084/jem.20071416.
Lavker, R. M., and A. G. Matoltsy. 1970. Formation of horny cells: the fate of cell organelles and differentiation products in ruminal epithelium. J. Cell Biol. 44:501-512. doi: 10.1083/jcb.44.3.501.
Lee, J., J. M. Gonzales-Navajas, and E. Raz. 2008. The "polarizing-tolerizing" mechanism of intestinal epithelium: its relevance to colonic homeostasis. Semin. Immunopathol. 30:3-9. doi: 10.1007/s00281-007-0099-7.
Lennie, T. A., D. O. McCarthy, and R. E. Keesey. 1995. Body energy status and the metabolic response to acute inflammation. Am. J. Physiol. 269:R1024-1031. doi: 10.1152/ajpregu.1995.269.5.R1024.
Lewis, J. S., J. A. Lee, J. C. Underwood, A. L. Harris, and C. E. Lewis. 1999. Macrophage responses to hypoxia: relevance to disease mechanisms. J. Leukoc. Biol. 66:889-900. doi: 10.1002/jlb.66.6.889.
Li, H., J. P. Limenitakis, T. Fuhrer, M. B. Geuking, M. A. Lawson, M. Wyss, S. Brugiroux, I. Keller, J. A. Macpherson, S. Rupp, B. Stolp, J. V. Stein, B. Stecher, U. Sauer, K. D. McCoy, and A. J. Macpherson. 2015. The outer mucus layer hosts a distinct intestinal microbial niche. Nat. Commun. 6:8292. doi: 10.1038/ncomms9292.
Li, H., D. N. Sheppard, and M. J. Hug. 2004. Transepithelial electrical measurements with the Ussing chamber. J. Cyst. Fibros. 3 Suppl 2:123-126. doi: 10.1016/j.jcf.2004.05.026.
Li, M., B. van Esch, G. T. M. Wagenaar, J. Garssen, G. Folkerts, and P. A. J. Henricks. 2018. Pro- and anti-inflammatory effects of short chain fatty acids on immune and endothelial cells. Eur. J. Pharmacol. 831:52-59. doi: 10.1016/j.ejphar.2018.05.003.
Li, S., E. Khafipour, D. O. Krause, A. Kroeker, J. C. Rodriguez-Lecompte, G. N. Gozho, and J. C. Plaizier. 2012. Effects of subacute ruminal acidosis challenges on fermentation and endotoxins in the rumen and hindgut of dairy cows. J. Dairy Sci. 95:294-303. doi: 10.3168/jds.2011-4447.
Li, W., S. Yang, S. O. Kim, G. Reid, J. R. Challis, and A. D. Bocking. 2014. Lipopolysaccharide-Induced Profiles of Cytokine, Chemokine, and Growth Factors Produced by Human Decidual Cells Are Altered by Lactobacillus rhamnosus GR-1 Supernatant. Reprod. Sci. 21:939-947. doi: 10.1177/1933719113519171.
Li, X., S. Jiang, and R. I. Tapping. 2010. Toll-like receptor signaling in cell proliferation and survival. Cytokine. 49:1-9. doi: 10.1016/j.cyto.2009.08.010.
Lima, R. F., J. C. Resende Júnior, S. F. Costa, J. L. P. Daniel, T. S. Teófilo, and M. G. Cardoso. 2015. MORPHOLOGICAL RESPONSE OF THE RUMINAL AND OMASAL

MUCOSAE TO THE VARIATION IN DIET ENERGY. Ciência e Agrotecnologia. 39:574-582.
Lin, M. Y., M. R. de Zoete, J. P. van Putten, and K. Strijbis. 2015. Redirection of Epithelial Immune Responses by Short-Chain Fatty Acids through Inhibition of Histone Deacetylases. Front. Immunol. 6:554. doi: 10.3389/fimmu.2015.00554.
Liu, H., L. Kai, H. Du, X. Wang, and Y. Wang. 2019. LPS Inhibits Fatty Acid Absorption in Enterocytes through TNF-alpha Secreted by Macrophages. Cells. 8doi: 10.3390/cells8121626.
Liu, J. H., T. T. Xu, Y. J. Liu, W. Y. Zhu, and S. Y. Mao. 2013. A high-grain diet causes massive disruption of ruminal epithelial tight junctions in goats. Am. J. Physiol. Regul. Integr. Comp. Physiol. 305:R232-241. doi: 10.1152/ajpregu.00068.2013.
Liu, Y., A. Beyer, and R. Aebersold. 2016. On the Dependency of Cellular Protein Levels on mRNA Abundance. Cell. 165:535-550. doi: 10.1016/j.cell.2016.03.014.
Lochmiller, R. L., and C. Deerenberg. 2000. Trade-offs in evolutionary immunology: just what is the cost of immunity? Oikos. 88:87-98. doi: 10.1034/j.1600-0706.2000.880110.x.
Lodemann, U., and H. Martens. 2006. Effects of diet and osmotic pressure on Na+ transport and tissue conductance of sheep isolated rumen epithelium. Exp. Physiol. 91:539-550. doi: 10.1113/expphysiol.2005.032078.
Loerch, S. C. 1990. Effects of feeding growing cattle high-concentrate diets at a restricted intake on feedlot performance. J. Anim. Sci. 68:3086-3095.
Loss, H., J. R. Aschenbach, F. Ebner, K. Tedin, and U. Lodemann. 2019. Inflammatory Responses of Porcine MoDC and Intestinal Epithelial Cells in a Direct-Contact Co-culture System Following a Bacterial Challenge. Inflammation. doi: 10.1007/s10753-019-01137-4.
Loss, H., J. R. Aschenbach, K. Tedin, F. Ebner, and U. Lodemann. 2018. The Inflammatory Response to Enterotoxigenic E. coli and Probiotic E. faecium in a Coculture Model of Porcine Intestinal Epithelial and Dendritic Cells. Mediators Inflamm. 2018:9368295. doi: 10.1155/2018/9368295.
Lotter, K., K. Hocherl, M. Bucher, and F. Kees. 2006. In vivo efficacy of telithromycin on cytokine and nitric oxide formation in lipopolysaccharide-induced acute systemic inflammation in mice. J. Antimicrob. Chemother. 58:615-621. doi: 10.1093/jac/dkl270.
Lotz, M., T. Konig, S. Menard, D. Gutle, C. Bogdan, and M. W. Hornef. 2007. Cytokine-mediated control of lipopolysaccharide-induced activation of small intestinal epithelial cells. Immunology. 122:306-315. doi: 10.1111/j.1365-2567.2007.02639.x.
Mackall, C. L., T. J. Fry, and R. E. Gress. 2011. Harnessing the biology of IL-7 for therapeutic application. Nat. Rev. Immunol. 11:330-342. doi: 10.1038/nri2970.
Madara, J. L. 1987. Intestinal absorptive cell tight junctions are linked to cytoskeleton. Am. J. Physiol. 253:C171-175. doi: 10.1152/ajpcell.1987.253.1.C171.
Malmuthuge, N., M. Li, P. Fries, P. J. Griebel, and L. L. Guan. 2012. Regional and age dependent changes in gene expression of Toll-like receptors and key antimicrobial defence molecules throughout the gastrointestinal tract of dairy calves. Vet. Immunol. Immunopathol. 146:18-26. doi: 10.1016/j.vetimm.2012.01.010.
Man, W. H., W. A. de Steenhuijsen Piters, and D. Bogaert. 2017. The microbiota of the respiratory tract: gatekeeper to respiratory health. Nat. Rev. Microbiol. 15:259-270. doi: 10.1038/nrmicro.2017.14.

Marchiando, A. M., W. V. Graham, and J. R. Turner. 2010. Epithelial barriers in homeostasis and disease. Annu. Rev. Pathol. 5:119-144. doi: 10.1146/annurev.pathol.4.110807.092135.

Martel, C. A., L. K. Mamedova, J. E. Minton, M. L. Jones, J. A. Carroll, and B. J. Bradford. 2014. Continuous low-dose infusion of tumor necrosis factor alpha in adipose tissue elevates adipose tissue interleukin 10 abundance and fails to alter metabolism in lactating dairy cows. J. Dairy Sci. 97:4897-4906. doi: 10.3168/jds.2013-7777.

Martin, P. M., E. Gopal, S. Ananth, L. Zhuang, S. Itagaki, B. M. Prasad, S. B. Smith, P. D. Prasad, and V. Ganapathy. 2006. Identity of SMCT1 (SLC5A8) as a neuron-specific Na+-coupled transporter for active uptake of L-lactate and ketone bodies in the brain. J. Neurochem. 98:279-288. doi: 10.1111/j.1471-4159.2006.03878.x.

Masoud, G. N., and W. Li. 2015. HIF-1alpha pathway: role, regulation and intervention for cancer therapy. Acta Pharm. Sin. B. 5:378-389. doi: 10.1016/j.apsb.2015.05.007.

Matejuk, A. 2018. Skin Immunity. Arch. Immunol. Ther. Exp. (Warsz). 66:45-54. doi: 10.1007/s00005-017-0477-3.

McCloy, R. A., S. Rogers, C. E. Caldon, T. Lorca, A. Castro, and A. Burgess. 2014. Partial inhibition of Cdk1 in G 2 phase overrides the SAC and decouples mitotic events. Cell Cycle. 13:1400-1412. doi: 10.4161/cc.28401.

McClure, R., and P. Massari. 2014. TLR-Dependent Human Mucosal Epithelial Cell Responses to Microbial Pathogens. Front. Immunol. 5:386. doi: 10.3389/fimmu.2014.00386.

McGhee, J. R., and K. Fujihashi. 2012. Inside the mucosal immune system. PLoS Biol. 10:e1001397. doi: 10.1371/journal.pbio.1001397.

McGuinness, O. P. 2005. Defective glucose homeostasis during infection. Annu. Rev. Nutr. 25:9-35. doi: 10.1146/annurev.nutr.24.012003.132159.

McNabney, S. M., and T. M. Henagan. 2017. Short Chain Fatty Acids in the Colon and Peripheral Tissues: A Focus on Butyrate, Colon Cancer, Obesity and Insulin Resistance. Nutrients. 9doi: 10.3390/nu9121348.

McNeil, C. J., S. O. Hoskin, D. M. Bremner, G. Holtrop, and G. E. Lobley. 2016. Whole-body and splanchnic amino acid metabolism in sheep during an acute endotoxin challenge. Br. J. Nutr. 116:211-222. doi: 10.1017/S0007114516001860.

Medzhitov, R. 2008. Origin and physiological roles of inflammation. Nature. 454:428-435. doi: 10.1038/nature07201.

Meissner, S., F. Hagen, C. Deiner, D. Gunzel, G. Greco, Z. Shen, and J. R. Aschenbach. 2017. Key role of short-chain fatty acids in epithelial barrier failure during ruminal acidosis. J. Dairy Sci. 100:6662-6675. doi: 10.3168/jds.2016-12262.

Memon, R. A., K. R. Feingold, A. H. Moser, W. Doerrler, S. Adi, C. A. Dinarello, and C. Grunfeld. 1992. Differential effects of interleukin-1 and tumor necrosis factor on ketogenesis. Am. J. Physiol. 263:E301-309.

Miglior, F., A. Fleming, F. Malchiodi, L. F. Brito, P. Martin, and C. F. Baes. 2017. A 100-Year Review: Identification and genetic selection of economically important traits in dairy cattle. J. Dairy Sci. 100:10251-10271. doi: 10.3168/jds.2017-12968.

Minuti, A., A. Palladino, M. J. Khan, S. Alqarni, A. Agrawal, F. Piccioli-Capelli, F. Hidalgo, F. C. Cardoso, E. Trevisi, and J. J. Loor. 2015. Abundance of ruminal bacteria, epithelial gene expression, and systemic biomarkers of metabolism and inflammation are altered during the peripartal period in dairy cows. J Dairy Sci. 98:8940-8951. doi: 10.3168/jds.2015-9722.

Mortha, A., A. Chudnovskiy, D. Hashimoto, M. Bogunovic, S. P. Spencer, Y. Belkaid, and M. Merad. 2014. Microbiota-dependent crosstalk between macrophages and ILC3 promotes intestinal homeostasis. Science. 343:1249288. doi: 10.1126/science.1249288.

Muller, F., J. R. Aschenbach, and G. Gabel. 2000. Role of Na+/H+ exchange and HCO3- transport in pHi recovery from intracellular acid load in cultured epithelial cells of sheep rumen. J. Comp. Physiol. B. 170:337-343. doi: 10.1007/s003600000107.

Muller, F., K. Huber, H. Pfannkuche, J. R. Aschenbach, G. Breves, and G. Gabel. 2002. Transport of ketone bodies and lactate in the sheep ruminal epithelium by monocarboxylate transporter 1. Am. J. Physiol. Gastrointest. Liver Physiol. 283:G1139-1146. doi: 10.1152/ajpgi.00268.2001.

Mulligan, F. J., and M. L. Doherty. 2008. Production diseases of the transition cow. Vet. J. 176:3-9. doi: 10.1016/j.tvjl.2007.12.018.

Muscher, A. S., B. Schroder, G. Breves, and K. Huber. 2010. Dietary nitrogen reduction enhances urea transport across goat rumen epithelium. J. Anim. Sci. 88:3390-3398. doi: 10.2527/jas.2010-2949.

Nagaraja, T. G., E. E. Bartley, L. R. Fina, H. D. Anthony, and R. M. Bechtle. 1978. Evidence of endotoxins in the rumen bacteria of cattle fed hay or grain. J. Anim. Sci. 47:226-234. doi: 10.2527/jas1978.471226x.

Nagaraja, T. G., and M. M. Chengappa. 1998. Liver abscesses in feedlot cattle: a review. J. Anim. Sci. 76:287-298. doi: 10.2527/1998.761287x.

Nagaraja, T. G., and E. C. Titgemeyer. 2007. Ruminal acidosis in beef cattle: the current microbiological and nutritional outlook. J. Dairy Sci. 90 Suppl 1:E17-38. doi: 10.3168/jds.2006-478.

Najar, M., M. Krayem, N. Meuleman, D. Bron, and L. Lagneaux. 2017. Mesenchymal Stromal Cells and Toll-Like Receptor Priming: A Critical Review. Immune Netw. 17:89-102. doi: 10.4110/in.2017.17.2.89.

Neal, M. D., C. P. Sodhi, H. Jia, M. Dyer, C. E. Egan, I. Yazji, M. Good, A. Afrazi, R. Marino, D. Slagle, C. Ma, M. F. Branca, T. Prindle, Jr., Z. Grant, J. Ozolek, and D. J. Hackam. 2012. Toll-like receptor 4 is expressed on intestinal stem cells and regulates their proliferation and apoptosis via the p53 up-regulated modulator of apoptosis. J. Biol. Chem. 287:37296-37308. doi: 10.1074/jbc.M112.375881.

Neogrady, S., P. Galfi, and F. Kutas. 1989a. Effects of butyrate and insulin and their interaction on the DNA synthesis of rumen epithelial cells in culture. Experientia. 45:94-96.

Neogrady, S., P. Galfi, F. Kutas, and T. Sakata. 1989b. The effects of butyrate and glucagon on the proliferation of ruminal epithelial cells in culture. Vet. Res. Commun. 13:27-29. doi: 10.1007/bf00366849.

Nestle, F. O., P. Di Meglio, J. Z. Qin, and B. J. Nickoloff. 2009. Skin immune sentinels in health and disease. Nat. Rev. Immunol. 9:679-691. doi: 10.1038/nri2622.

Nierhaus, A., J. Linssen, M. S. Winkler, D. P. Frings, and S. Kluge. 2017. The Effects of Ex Vivo Administration of Granulocyte-Macrophage Colony-Stimulating Factor and Endotoxin on Cytokine Release of Whole Blood Are Determined by Priming Conditions. Biomed. Res. Int. 2017:9834512. doi: 10.1155/2017/9834512.

Nish, S., and R. Medzhitov. 2011. Host defense pathways: role of redundancy and compensation in infectious disease phenotypes. Immunity. 34:629-636. doi: 10.1016/j.immuni.2011.05.009.

Nocek, J. E. 1997. Bovine acidosis: implications on laminitis. J. Dairy Sci. 80:1005-1028. doi: 10.3168/jds.S0022-0302(97)76026-0.
Nomura, F., S. Akashi, Y. Sakao, S. Sato, T. Kawai, M. Matsumoto, K. Nakanishi, M. Kimoto, K. Miyake, K. Takeda, and S. Akira. 2000. Cutting edge: endotoxin tolerance in mouse peritoneal macrophages correlates with down-regulation of surface toll-like receptor 4 expression. J. Immunol. 164:3476-3479.
O'Connor, J. C., R. H. McCusker, K. Strle, R. W. Johnson, R. Dantzer, and K. W. Kelley. 2008. Regulation of IGF-I function by proinflammatory cytokines: at the interface of immunology and endocrinology. Cell Immunol. 252:91-110. doi: 10.1016/j.cellimm.2007.09.010.
Oetzel, G. R. 2017. Diagnosis and Management of Subacute Ruminal Acidosis in Dairy Herds. Vet. Clin. North Am. Food Anim. Pract. 33:463-480. doi: 10.1016/j.cvfa.2017.06.004.
Ohtsuka, Y., J. Lee, D. S. Stamm, and I. R. Sanderson. 2001. MIP-2 secreted by epithelial cells increases neutrophil and lymphocyte recruitment in the mouse intestine. Gut. 49:526-533. doi: 10.1136/gut.49.4.526.
Okumura, R., and K. Takeda. 2017. Roles of intestinal epithelial cells in the maintenance of gut homeostasis. Exp. Mol. Med. 49:e338. doi: 10.1038/emm.2017.20.
Ovsiy, I., V. Riabov, I. Manousaridis, J. Michel, K. Moganti, S. Yin, T. Liu, C. Sticht, E. Kremmer, M. C. Harmsen, S. Goerdt, A. Gratchev, and J. Kzhyshkowska. 2017. IL-4 driven transcription factor FoxQ1 is expressed by monocytes in atopic dermatitis and stimulates monocyte migration. Sci. Rep. 7:16847. doi: 10.1038/s41598-017-17307-z.
Owens, F. N., D. S. Secrist, W. J. Hill, and D. R. Gill. 1998. Acidosis in cattle: a review. J. Anim. Sci. 76:275-286.
Ozaki, K., and W. J. Leonard. 2002. Cytokine and cytokine receptor pleiotropy and redundancy. J. Biol. Chem. 277:29355-29358. doi: 10.1074/jbc.R200003200.
Pailla, K., M. Y. El-Mir, L. Cynober, and F. Blonde-Cynober. 2001. Cytokine-mediated inhibition of ketogenesis is unrelated to nitric oxide or protein synthesis. Clin. Nutr. 20:313-317. doi: 10.1054/clnu.2001.0421.
Pailla, K., S. K. Lim, J. P. De Bandt, C. Aussel, J. Giboudeau, S. Troupel, L. Cynober, and F. Blonde-Cynober. 1998. TNF-alpha and IL-6 synergistically inhibit ketogenesis from fatty acids and alpha-ketoisocaproate in isolated rat hepatocytes. JPEN J. Parenter. Enteral. Nutr. 22:286-290. doi: 10.1177/014860719802200528 6.
Pan, L. F., L. Yu, L. M. Wang, J. T. He, J. L. Sun, X. B. Wang, Z. H. Bai, H. Wang, T. L. Yan, and H. H. Pei. 2017. The Toll-like receptor 4 antagonist TAK-242 protects against chronic pancreatitis in rats. Mol. Med. Rep. 16:3863-3868. doi: 10.3892/mmr.2017.7105.
Parada, V. D., M. K. De la Fuente, G. Landskron, M. J. Gonzalez, R. Quera, G. Dijkstra, H. J. M. Harmsen, K. N. Faber, and M. A. Hermoso. 2019. Short Chain Fatty Acids (SCFAs)-Mediated Gut Epithelial and Immune Regulation and Its Relevance for Inflammatory Bowel Diseases. Front. Immunol. 10:277. doi: 10.3389/fimmu.2019.00277.
Park, B. S., and J. O. Lee. 2013. Recognition of lipopolysaccharide pattern by TLR4 complexes. Exp. Mol. Med. 45:e66. doi: 10.1038/emm.2013.97.
Park, S. J., C. P. Smith, R. R. Wilbur, C. P. Cain, S. R. Kallu, S. Valasapalli, A. Sahoo, M. R. Guda, A. J. Tsung, and K. K. Velpula. 2018. An overview of MCT1 and MCT4 in GBM: small molecule transporters with large implications. Am. J. Cancer Res. 8:1967-1976.

Paruchuri, S., and A. Sjolander. 2003. Leukotriene D4 mediates survival and proliferation via separate but parallel pathways in the human intestinal epithelial cell line Int 407. J. Biol. Chem. 278:45577-45585. doi: 10.1074/jbc.M302881200.
Pasare, C., and R. Medzhitov. 2005. Toll-like receptors: linking innate and adaptive immunity. Adv. Exp. Med. Biol. 560:11-18. doi: 10.1007/0-387-24180-9_2.
Pasternak, J. A., D. J. MacPhee, and J. C. S. Harding. 2020. Fetal cytokine response to porcine reproductive and respiratory syndrome virus-2 infection. Cytokine. 126:154883. doi: 10.1016/j.cyto.2019.154883.
Pastore, S., F. Mascia, S. Gulinelli, S. Forchap, C. Dattilo, E. Adinolfi, G. Girolomoni, F. Di Virgilio, and D. Ferrari. 2007. Stimulation of purinergic receptors modulates chemokine expression in human keratinocytes. J. Invest. Dermatol. 127:660-667. doi: 10.1038/sj.jid.5700591.
Pastuszak, M., K. Groszewski, M. Pastuszak, P. Dyrla, S. Wojtun, and J. Gil. 2015. Cytokeratins in gastroenterology. Systematic review. Prz. Gastroenterol. 10:61-70. doi: 10.5114/pg.2015.51182.
Paton, L. J., K. A. Beauchemin, D. M. Veira, and M. A. G. von Keyserlingk. 2006. Use of sodium bicarbonate, offered free choice or blended into the ration, to reduce the risk of ruminal acidosis in cattle. Can. J. Anim. Sci. 86:429-437. doi: 10.4141/A06-014.
Paupe, V., and J. Prudent. 2018. New insights into the role of mitochondrial calcium homeostasis in cell migration. Biochem. Biophys. Res. Commun. 500:75-86. doi: 10.1016/j.bbrc.2017.05.039.
Pederzolli, R. A., A. G. Van Kessel, J. Campbell, S. Hendrick, K. M. Wood, and G. B. Penner. 2018. Effect of ruminal acidosis and short-term low feed intake on indicators of gastrointestinal barrier function in Holstein steers. J. Anim. Sci. 96:108-125. doi: 10.1093/jas/skx049.
Penner, G. B., K. A. Beauchemin, and T. Mutsvangwa. 2006. An evaluation of the accuracy and precision of a stand-alone submersible continuous ruminal pH measurement system. J. Dairy Sci. 89:2132-2140. doi: 10.3168/jds.S0022-0302(06)72284-6.
Penner, G. B., K. A. Beauchemin, and T. Mutsvangwa. 2007. Severity of ruminal acidosis in primiparous holstein cows during the periparturient period. J. Dairy Sci. 90:365-375. doi: 10.3168/jds.S0022-0302(07)72638-3.
Penner, G. B., M. Oba, G. Gabel, and J. R. Aschenbach. 2010. A single mild episode of subacute ruminal acidosis does not affect ruminal barrier function in the short term. J. Dairy Sci. 93:4838-4845. doi: 10.3168/jds.2010-3406.
Penner, G. B., M. A. Steele, J. R. Aschenbach, and B. W. McBride. 2011. Ruminant Nutrition Symposium: Molecular adaptation of ruminal epithelia to highly fermentable diets. J. Anim. Sci. 89:1108-1119. doi: 10.2527/jas.2010-3378.
Penner, G. B., M. Taniguchi, L. L. Guan, K. A. Beauchemin, and M. Oba. 2009. Effect of dietary forage to concentrate ratio on volatile fatty acid absorption and the expression of genes related to volatile fatty acid absorption and metabolism in ruminal tissue. J Dairy Sci. 92:2767-2781. doi: 10.3168/jds.2008-1716.
Pennington, R. J., and T. M. Sutherland. 1956. The metabolism of short-chain fatty acids in the sheep. IV. The pathway of propionate metabolism in rumen epithelial tissue. Biochem. J. 63:618-628. doi: 10.1042/bj0630618.
Perks, C. M., C. McCaig, and J. M. Holly. 2000. Differential insulin-like growth factor (IGF)-independent interactions of IGF binding protein-3 and IGF binding protein-5 on

apoptosis in human breast cancer cells. Involvement of the mitochondria. J. Cell Biochem. 80:248-258. doi: 10.1002/1097-4644(20010201)80:2<248::aid-jcb140>3.0.co;2-4.
Peters, A. 2006. The energy request of inflammation. Endocrinology. 147:4550-4552. doi: 10.1210/en.2006-0815.
Peterson, L. W., and D. Artis. 2014. Intestinal epithelial cells: regulators of barrier function and immune homeostasis. Nat. Rev. Immunol. 14:141-153. doi: 10.1038/nri3608.
Petzl, W., J. Gunther, T. Pfister, C. Sauter-Louis, L. Goetze, S. von Aulock, A. Hafner-Marx, H. J. Schuberth, H. M. Seyfert, and H. Zerbe. 2012. Lipopolysaccharide pretreatment of the udder protects against experimental Escherichia coli mastitis. Innate Immun. 18:467-477. doi: 10.1177/1753425911422407.
Peuhkuri, K., H. Vapaatalo, and R. Korpela. 2010. Even low-grade inflammation impacts on small intestinal function. World J. Gastroenterol. 16:1057-1062. doi: 10.3748/wjg.v16.i9.1057.
Phillip, L. E., J. G. Buchanan-Smith, and W. L. Grovum. 1981. Food intake and ruminal osmolality in sheep: differentiation of the effect of osmolality from that of the products of maize silage fermentation. J. Agric. Sci. 96:439-445. doi: 10.1017/S002185960006620X.
Plaizier, J. C., M. Danesh Mesgaran, H. Derakhshani, H. Golder, E. Khafipour, J. L. Kleen, I. Lean, J. Loor, G. Penner, and Q. Zebeli. 2018. Review: Enhancing gastrointestinal health in dairy cows. Animal. 12:s399-s418. doi: 10.1017/S1751731118001921.
Plaizier, J. C., E. Khafipour, S. Li, G. N. Gozho, and D. O. Krause. 2012. Subacute ruminal acidosis (SARA), endotoxins and health consequences. Anim. Feed Sci. and Technol. 172:9-21. doi: 10.1016/j.anifeedsci.2011.12.004.
Plaizier, J. C., D. O. Krause, G. N. Gozho, and B. W. McBride. 2008. Subacute ruminal acidosis in dairy cows: the physiological causes, incidence and consequences. Vet. J. 176:21-31. doi: 10.1016/j.tvjl.2007.12.016.
Pott, J., and M. Hornef. 2012. Innate immune signalling at the intestinal epithelium in homeostasis and disease. EMBO Rep. 13:684-698. doi: 10.1038/embor.2012.96.
Puchalska, P., and P. A. Crawford. 2017. Multi-dimensional Roles of Ketone Bodies in Fuel Metabolism, Signaling, and Therapeutics. Cell Metab. 25:262-284. doi: 10.1016/j.cmet.2016.12.022.
Ragionieri, L., A. Cacchioli, F. Ravanetti, M. Botti, A. Ivanovska, R. Panu, F. Righi, A. Quarantelli, and F. Gazza. 2016. Effect of the supplementation with a blend containing short and medium chain fatty acid monoglycerides in milk replacer on rumen papillae development in weaning calves. Ann. Anat. 207:97-108. doi: 10.1016/j.aanat.2016.04.035.
Rakoff-Nahoum, S., J. Paglino, F. Eslami-Varzaneh, S. Edberg, and R. Medzhitov. 2004. Recognition of commensal microflora by toll-like receptors is required for intestinal homeostasis. Cell. 118:229-241. doi: 10.1016/j.cell.2004.07.002.
Ricciotti, E., and G. A. FitzGerald. 2011. Prostaglandins and inflammation. Arterioscler. Thromb. Vasc. Biol. 31:986-1000. doi: 10.1161/ATVBAHA.110.207449.
Richardson, R. A., and H. I. Davidson. 2003. Nutritional demands in acute and chronic illness. Proc. Nutr. Soc. 62:777-781. doi: 10.1079/PNS2003302.
Rimoldi, M., M. Chieppa, V. Salucci, F. Avogadri, A. Sonzogni, G. M. Sampietro, A. Nespoli, G. Viale, P. Allavena, and M. Rescigno. 2005. Intestinal immune homeostasis is

regulated by the crosstalk between epithelial cells and dendritic cells. Nat. Immunol. 6:507-514. doi: 10.1038/ni1192.
Rinaldo-Matthis, A., and J. Z. Haeggstrom. 2010. Structures and mechanisms of enzymes in the leukotriene cascade. Biochimie. 92:676-681. doi: 10.1016/j.biochi.2010.01.010.
Rodriguez-Prados, J. C., P. G. Traves, J. Cuenca, D. Rico, J. Aragones, P. Martin-Sanz, M. Cascante, and L. Bosca. 2010. Substrate fate in activated macrophages: a comparison between innate, classic, and alternative activation. J. Immunol. 185:605-614. doi: 10.4049/jimmunol.0901698.
Roediger, W. E., and S. Nance. 1986. Metabolic induction of experimental ulcerative colitis by inhibition of fatty acid oxidation. Br. J. Exp. Pathol. 67:773-782.
Roh J. S. and D. H. Sohn. 2018. Damage-associated molecular patterns in inflammatory disease. Immune Netw. 18:e27. doi.org/10.4110/in.2018.18.e27.
Russell, J. B., and D. B. Wilson. 1996. Why are ruminal cellulolytic bacteria unable to digest cellulose at low pH? J Dairy Sci. 79:1503-1509. doi: 10.3168/jds.S0022-0302(96)76510-4.
Russell, M. W., and P. L. Ogra. 2010. Mucosal decisions: tolerance and responsiveness at mucosal surfaces. Immunol. Invest. 39:297-302. doi: 10.3109/08820131003729927.
Sakata, T. 2019. Pitfalls in short-chain fatty acid research: A methodological review. Anim. Sci. J. 90:3-13. doi: 10.1111/asj.13118.
Schett, G., and M. F. Neurath. 2018. Resolution of chronic inflammatory disease: universal and tissue-specific concepts. Nat. Commun. 9:3261. doi: 10.1038/s41467-018-05800-6.
Schilling, J. D., S. M. Martin, C. S. Hung, R. G. Lorenz, and S. J. Hultgren. 2003. Toll-like receptor 4 on stromal and hematopoietic cells mediates innate resistance to uropathogenic Escherichia coli. Proc. Natl. Acad. Sci. U S A. 100:4203-4208. doi: 10.1073/pnas.0736473100.
Schindler, R., P. Ghezzi, and C. A. Dinarello. 1990. IL-1 induces IL-1. IV. IFN-gamma suppresses IL-1 but not lipopolysaccharide-induced transcription of IL-1. J. Immunol. 144:2216-2222.
Schmitz, H., C. Barmeyer, M. Fromm, N. Runkel, H. D. Foss, C. J. Bentzel, E. O. Riecken, and J. D. Schulzke. 1999. Altered tight junction structure contributes to the impaired epithelial barrier function in ulcerative colitis. Gastroenterology. 116:301-309. doi: 10.1016/s0016-5085(99)70126-5.
Schroder, K., and T. C. Bosch. 2016. The Origin of Mucosal Immunity: Lessons from the Holobiont Hydra. mBio. 7doi: 10.1128/mBio.01184-16.
Schurmann, B. L., M. E. Walpole, P. Gorka, J. C. Ching, M. E. Loewen, and G. B. Penner. 2014. Short-term adaptation of the ruminal epithelium involves abrupt changes in sodium and short-chain fatty acid transport. Am. J. Physiol. Regul. Integr. Comp. Physiol. 307:R802-816. doi: 10.1152/ajpregu.00035.2014.
Schwaiger, T., K. A. Beauchemin, and G. B. Penner. 2013a. The duration of time that beef cattle are fed a high-grain diet affects the recovery from a bout of ruminal acidosis: dry matter intake and ruminal fermentation. J. Anim. Sci. 91:5729-5742. doi: 10.2527/jas.2013-6471.
Schwaiger, T., K. A. Beauchemin, and G. B. Penner. 2013b. Duration of time that beef cattle are fed a high-grain diet affects the recovery from a bout of ruminal acidosis: short-chain fatty acid and lactate absorption, saliva production, and blood metabolites. J. Anim. Sci. 91:5743-5753. doi: 10.2527/jas.2013-6472.

Schweigel, M., M. Freyer, S. Leclercq, B. Etschmann, U. Lodemann, A. Bottcher, and H. Martens. 2005. Luminal hyperosmolarity decreases Na transport and impairs barrier function of sheep rumen epithelium. J. Comp. Physiol. B. 175:575-591. doi: 10.1007/s00360-005-0021-3.

Scott, A., and I. C. Gardner. 1973. Papillar form in the forestomach of the sheep. J. Anat. 116:255-267.

Scoville, E. A., M. M. Allaman, C. T. Brown, A. K. Motley, S. N. Horst, C. S. Williams, T. Koyama, Z. Zhao, D. W. Adams, D. B. Beaulieu, D. A. Schwartz, K. T. Wilson, and L. A. Coburn. 2018. Alterations in Lipid, Amino Acid, and Energy Metabolism Distinguish Crohn's Disease from Ulcerative Colitis and Control Subjects by Serum Metabolomic Profiling. Metabolomics. 14:17. doi: 10.1007/s11306-017-1311-y.

Seeley, J. J., and S. Ghosh. 2017. Molecular mechanisms of innate memory and tolerance to LPS. J. Leukoc. Biol. 101:107-119. doi: 10.1189/jlb.3MR0316-118RR.

Segain, J. P., D. Raingeard de la Bletiere, A. Bourreille, V. Leray, N. Gervois, C. Rosales, L. Ferrier, C. Bonnet, H. M. Blottiere, and J. P. Galmiche. 2000. Butyrate inhibits inflammatory responses through NFkappaB inhibition: implications for Crohn's disease. Gut. 47:397-403. doi: 10.1136/gut.47.3.397.

Sehested, J., L. Diernaes, P. D. Moller, and E. Skadhauge. 1996. Transport of sodium across the isolated bovine rumen epithelium: interaction with short-chain fatty acids, chloride and bicarbonate. Exp. Physiol. 81:79-94. doi: 10.1113/expphysiol.1996.sp003920.

Sehested, J., L. Diernaes, P. D. Moller, and E. Skadhauge. 1999a. Ruminal transport and metabolism of short-chain fatty acids (SCFA) in vitro: effect of SCFA chain length and pH. Comp. Biochem. Physiol. A. Mol. Integr. Physiol. 123:359-368.

Sehested, J., L. Diernaes, P. D. Moller, and E. Skadhauge. 1999b. Transport of butyrate across the isolated bovine rumen epithelium--interaction with sodium, chloride and bicarbonate. Comp. Biochem. Physiol. A. Mol. Integr. Physiol. 123:399-408. doi: 10.1016/s1095-6433(99)00082-3.

Sekirov, I., N. M. Tam, M. Jogova, M. L. Robertson, Y. Li, C. Lupp, and B. B. Finlay. 2008. Antibiotic-induced perturbations of the intestinal microbiota alter host susceptibility to enteric infection. Infect. Immun. 76:4726-4736. doi: 10.1128/IAI.00319-08.

Serhan, C. N., N. Chiang, and T. E. Van Dyke. 2008. Resolving inflammation: dual anti-inflammatory and pro-resolution lipid mediators. Nat. Rev. Immunol. 8:349-361. doi: 10.1038/nri2294.

Serhan, C. N., and J. Savill. 2005. Resolution of inflammation: the beginning programs the end. Nat. Immunol. 6:1191-1197. doi: 10.1038/ni1276.

Shen, H., Z. Lu, Z. Chen, Y. Wu, and Z. Shen. 2016. Rapid Fermentable Substance Modulates Interactions between Ruminal Commensals and Toll-Like Receptors in Promotion of Immune Tolerance of Goat Rumen. Front. Microbiol. 7:1812. doi: 10.3389/fmicb.2016.01812.

Shen, H., Z. Lu, Z. Xu, and Z. Shen. 2017. Diet-induced reconstruction of mucosal microbiota associated with alterations of epithelium lectin expression and regulation in the maintenance of rumen homeostasis. Sci. Rep. 7:3941. doi: 10.1038/s41598-017-03478-2.

Shklovskaya, E., B. J. O'Sullivan, L. G. Ng, B. Roediger, R. Thomas, W. Weninger, and B. Fazekas de St Groth. 2011. Langerhans cells are precommitted to immune tolerance induction. Proc. Natl. Acad. Sci. U S A. 108:18049-18054. doi: 10.1073/pnas.1110076108.

Simpson, H. L., N. C. Jackson, F. Shojaee-Moradie, R. H. Jones, D. L. Russell-Jones, P. H. Sonksen, D. B. Dunger, and A. M. Umpleby. 2004. Insulin-like growth factor I has a direct effect on glucose and protein metabolism, but no effect on lipid metabolism in type 1 diabetes. J. Clin. Endocrinol. Metab. 89:425-432. doi: 10.1210/jc.2003-031274.

Sivaprakasam, S., Y. D. Bhutia, S. Yang, and V. Ganapathy. 2017. Short-Chain Fatty Acid Transporters: Role in Colonic Homeostasis. Compr. Physiol. 8:299-314. doi: 10.1002/cphy.c170014.

Skou, J. C. 1998. Nobel Lecture. The identification of the sodium pump. Biosci. Rep. 18:155-169. doi: 10.1023/a:1020196612909.

Snyder, E., and B. Credille. 2017. Diagnosis and Treatment of Clinical Rumen Acidosis. Vet. Clin. North Am. Food Anim. Pract. 33:451-461. doi: 10.1016/j.cvfa.2017.06.003.

Song, P. I., T. A. Abraham, Y. Park, A. S. Zivony, B. Harten, H. F. Edelhauser, S. L. Ward, C. A. Armstrong, and J. C. Ansel. 2001. The expression of functional LPS receptor proteins CD14 and toll-like receptor 4 in human corneal cells. Invest. Ophthalmol. Vis. Sci. 42:2867-2877.

Sonoda, S., C. Spee, E. Barron, S. J. Ryan, R. Kannan, and D. R. Hinton. 2009. A protocol for the culture and differentiation of highly polarized human retinal pigment epithelial cells. Nat. Protoc. 4:662-673. doi: 10.1038/nprot.2009.33.

Staal-van den Brekel, A. J., M. A. Dentener, A. M. Schols, W. A. Buurman, and E. F. Wouters. 1995. Increased resting energy expenditure and weight loss are related to a systemic inflammatory response in lung cancer patients. J. Clin. Oncol. 13:2600-2605. doi: 10.1200/jco.1995.13.10.2600.

Stadnyk, A. W. 2002. Intestinal epithelial cells as a source of inflammatory cytokines and chemokines. Can. J. Gastroenterol. 16:241-246. doi: 10.1155/2002/941087.

Steele, M. A., O. AlZahal, S. L. Greenwood, J. C. Matthews, and B. W. McBride. 2013. Technical note: Use of laser capture microdissection for the localization of tissue-specific global gene expression in rumen papillae. J. Dairy Sci. 96:7748-7752. doi: 10.3168/jds.2013-6920.

Steele, M. A., O. AlZahal, S. E. Hook, J. Croom, and B. W. McBride. 2009. Ruminal acidosis and the rapid onset of ruminal parakeratosis in a mature dairy cow: a case report. Acta Vet. Scand. 51:39. doi: 10.1186/1751-0147-51-39.

Steele, M. A., J. Croom, M. Kahler, O. AlZahal, S. E. Hook, K. Plaizier, and B. W. McBride. 2011. Bovine rumen epithelium undergoes rapid structural adaptations during grain-induced subacute ruminal acidosis. Am. J. Physiol. Regul. Integr. Comp. Physiol. 300:R1515-1523. doi: 10.1152/ajpregu.00120.2010.

Steele, M. A., L. Dionissopoulos, O. AlZahal, J. Doelman, and B. W. McBride. 2012. Rumen epithelial adaptation to ruminal acidosis in lactating cattle involves the coordinated expression of insulin-like growth factor-binding proteins and a cholesterolgenic enzyme. J. Dairy Sci. 95:318-327. doi: 10.3168/jds.2011-4465.

Steele, M. A., G. B. Penner, F. Chaucheyras-Durand, and L. L. Guan. 2016. Development and physiology of the rumen and the lower gut: Targets for improving gut health. J. Dairy Sci. 99:4955-4966. doi: 10.3168/jds.2015-10351.

Steven, D. H., and A. B. Marshall. 1972. Branching mononuclear cells in the forestomach epithelium of the sheep. Q. J. Exp. Physiol. Cogn. Med. Sci. 57:267-270. doi: 10.1113/expphysiol.1972.sp002161.

Stevens, C. E., and B. K. Stettler. 1966. Factors affecting the transport of volatile fatty acids across rumen epithelium. Am. J. Physiol. 210:365-372. doi: 10.1152/ajplegacy.1966.210.2.365.
Stone, W. C. 2004. Nutritional Approaches to Minimize Subacute Ruminal Acidosis and Laminitis in Dairy Cattle. J. Dairy Sci. 87:E13-E26. doi: 10.3168/jds.S0022-0302(04)70057-0.
Straub, R. H. 2017. The brain and immune system prompt energy shortage in chronic inflammation and ageing. Nat. Rev. Rheumatol. 13:743-751. doi: 10.1038/nrrheum.2017.172.
Stumpff, F. 2018. A look at the smelly side of physiology: transport of short chain fatty acids. Pflugers Arch. 470:571-598. doi: 10.1007/s00424-017-2105-9.
Stumpff, F., M. I. Georgi, L. Mundhenk, I. Rabbani, M. Fromm, H. Martens, and D. Gunzel. 2011. Sheep rumen and omasum primary cultures and source epithelia: barrier function aligns with expression of tight junction proteins. J. Exp. Biol. 214:2871-2882. doi: 10.1242/jeb.055582.
Stumpff, F., H. Martens, S. Bilk, J. R. Aschenbach, and G. Gabel. 2009. Cultured ruminal epithelial cells express a large-conductance channel permeable to chloride, bicarbonate, and acetate. Pflugers Arch. 457:1003-1022. doi: 10.1007/s00424-008-0566-6.
Sugimoto, M. A., L. P. Sousa, V. Pinho, M. Perretti, and M. M. Teixeira. 2016. Resolution of Inflammation: What Controls Its Onset? Front. Immunol. 7:160. doi: 10.3389/fimmu.2016.00160.
Sun, M., C. He, Y. Cong, and Z. Liu. 2015. Regulatory immune cells in regulation of intestinal inflammatory response to microbiota. Mucosal Immunol. 8:969-978. doi: 10.1038/mi.2015.49.
Tadepalli, S., S. K. Narayanan, G. C. Stewart, M. M. Chengappa, and T. G. Nagaraja. 2009. Fusobacterium necrophorum: a ruminal bacterium that invades liver to cause abscesses in cattle. Anaerobe. 15:36-43. doi: 10.1016/j.anaerobe.2008.05.005.
Takeuchi, O., and S. Akira. 2010. Pattern recognition receptors and inflammation. Cell. 140:805-820. doi: 10.1016/j.cell.2010.01.022.
Takeuchi, O., K. Hoshino, T. Kawai, H. Sanjo, H. Takada, T. Ogawa, K. Takeda, and S. Akira. 1999. Differential roles of TLR2 and TLR4 in recognition of gram-negative and gram-positive bacterial cell wall components. Immunity. 11:443-451. doi: 10.1016/s1074-7613(00)80119-3.
Tamate, H., T. Kikuchi, and T. Sakata. 1974. Ultrastructural Changes in the Ruminal Epithelium after Fasting and Subsequent Refeeding in the Sheep. Tohoku J. Agric. Res. 25
Taniguchi, M., G. B. Penner, K. A. Beauchemin, M. Oba, and L. L. Guan. 2010. Comparative analysis of gene expression profiles in ruminal tissue from Holstein dairy cows fed high or low concentrate diets. Comp. Biochem. Physiol. Part D Genomics Proteomics. 5:274-279. doi: 10.1016/j.cbd.2010.07.004.
Thibault, R., F. Blachier, B. Darcy-Vrillon, P. de Coppet, A. Bourreille, and J. P. Segain. 2010. Butyrate utilization by the colonic mucosa in inflammatory bowel diseases: a transport deficiency. Inflamm. Bowel Dis. 16:684-695. doi: 10.1002/ibd.21108.
Thibault, R., P. De Coppet, K. Daly, A. Bourreille, M. Cuff, C. Bonnet, J. F. Mosnier, J. P. Galmiche, S. Shirazi-Beechey, and J. P. Segain. 2007. Down-regulation of the monocarboxylate transporter 1 is involved in butyrate deficiency during intestinal inflammation. Gastroenterology. 133:1916-1927. doi: 10.1053/j.gastro.2007.08.041.

Thomson, A., K. Smart, M. S. Somerville, S. N. Lauder, G. Appanna, J. Horwood, L. Sunder Raj, B. Srivastava, D. Durai, M. J. Scurr, A. V. Keita, A. M. Gallimore, and A. Godkin. 2019. The Ussing chamber system for measuring intestinal permeability in health and disease. BMC Gastroenterol. 19:98. doi: 10.1186/s12876-019-1002-4.

Trevisi, E., M. Amadori, F. Riva, G. Bertoni, and P. Bani. 2014. Evaluation of innate immune responses in bovine forestomachs. Res. Vet. Sci. 96:69-78. doi: 10.1016/j.rvsc.2013.11.011.

Tsukamoto, H., K. Fukudome, S. Takao, N. Tsuneyoshi, and M. Kimoto. 2010. Lipopolysaccharide-binding protein-mediated Toll-like receptor 4 dimerization enables rapid signal transduction against lipopolysaccharide stimulation on membrane-associated CD14-expressing cells. Int. Immunol. 22:271-280. doi: 10.1093/intimm/dxq005.

Tsukita, S., M. Furuse, and M. Itoh. 2001. Multifunctional strands in tight junctions. Nat. Rev. Mol. Cell Biol. 2:285-293. doi: 10.1038/35067088.

Tudela, C. V., C. Boudry, F. Stumpff, J. R. Aschenbach, W. Vahjen, J. Zentek, and R. Pieper. 2015. Down-regulation of monocarboxylate transporter 1 (MCT1) gene expression in the colon of piglets is linked to bacterial protein fermentation and pro-inflammatory cytokine-mediated signalling. Br. J. Nutr. 113:610-617. doi: 10.1017/s0007114514004231.

Untergasser, A., H. Nijveen, X. Rao, T. Bisseling, R. Geurts, and J. A. Leunissen. 2007. Primer3Plus, an enhanced web interface to Primer3. Nucleic Acids Res. 35:W71-74. doi: 10.1093/nar/gkm306.

Ussing, H. H., and K. Zerahn. 1951. Active transport of sodium as the source of electric current in the short-circuited isolated frog skin. Acta Physiol. Scand. 23:110-127. doi: 10.1111/j.1748-1716.1951.tb00800.x.

Vallee, S., S. Laforest, F. Fouchier, M. P. Montero, C. Penel, and S. Champion. 2004. Cytokine-induced upregulation of NF-kappaB, IL-8, and ICAM-1 is dependent on colonic cell polarity: implication for PKCdelta. Exp. Cell Res. 297:165-185. doi: 10.1016/j.yexcr.2004.03.007.

van Raam, B. J., W. Sluiter, E. de Wit, D. Roos, A. J. Verhoeven, and T. W. Kuijpers. 2008. Mitochondrial membrane potential in human neutrophils is maintained by complex III activity in the absence of supercomplex organisation. PloS one. 3:e2013-e2013. doi: 10.1371/journal.pone.0002013.

Vancamelbeke, M., T. Laeremans, W. Vanhove, K. Arnauts, A. S. Ramalho, R. Farre, I. Cleynen, M. Ferrante, and S. Vermeire. 2019. Butyrate Does Not Protect Against Inflammation-induced Loss of Epithelial Barrier Function and Cytokine Production in Primary Cell Monolayers From Patients With Ulcerative Colitis. J. Crohns Colitis. 13:1351-1361. doi: 10.1093/ecco-jcc/jjz064.

VandeHaar, M. J., and N. St-Pierre. 2006. Major advances in nutrition: relevance to the sustainability of the dairy industry. J. Dairy Sci. 89:1280-1291. doi: 10.3168/jds.S0022-0302(06)72196-8.

Vaure, C., and Y. Liu. 2014. A comparative review of toll-like receptor 4 expression and functionality in different animal species. Front. Immunol. 5:316. doi: 10.3389/fimmu.2014.00316.

Veldhoen, M., and B. Stockinger. 2006. TGFbeta1, a "Jack of all trades": the link with pro-inflammatory IL-17-producing T cells. Trends Immunol. 27:358-361. doi: 10.1016/j.it.2006.06.001.

Venereau, E., C. Ceriotti, and M. E. Bianchi. 2015. DAMPs from cell death to new life. Front. Immunol. 6:422. doi: 10.3389/fimmu.2015.00422

Vijay-Kumar, M., F. A. Carvalho, J. D. Aitken, N. H. Fifadara, and A. T. Gewirtz. 2010. TLR5 or NLRC4 is necessary and sufficient for promotion of humoral immunity by flagellin. Eur. J. Immunol. 40:3528-3534. doi: 10.1002/eji.201040421.

Waldron, M. R., F. N. Schrick, J. D. Quigley, J. L. Klotz, A. M. Saxton, and R. N. Heitmann. 2002. Volatile fatty acid metabolism by epithelial cells isolated from different areas of the ewe rumen. J. Anim. Sci. 80:270-278.

Wang, H., and J. Ye. 2015. Regulation of energy balance by inflammation: common theme in physiology and pathology. Rev. Endocr. Metab. Disord. 16:47-54. doi: 10.1007/s11154-014-9306-8.

Ward, G. A. 2008. Effect of pre-weaning diet on lamb's rumen development. American-Eurasian J. of Agric. & Environ. Sci. 3:561-567.

Watanabe, M., Y. Ueno, T. Yajima, Y. Iwao, M. Tsuchiya, H. Ishikawa, S. Aiso, T. Hibi, and H. Ishii. 1995. Interleukin 7 is produced by human intestinal epithelial cells and regulates the proliferation of intestinal mucosal lymphocytes. J. Clin. Invest. 95:2945-2953. doi: 10.1172/JCI118002.

Werner, S., and B. Munz. 2000. Suppression of keratin 15 expression by transforming growth factor beta in vitro and by cutaneous injury in vivo. Exp. Cell Res. 254:80-90. doi: 10.1006/excr.1999.4726.

Westerhout, J., H. Wortelboer, and K. Verhoeckx. 2015. Ussing Chamber. In: K. Verhoeckx, P. Cotter, I. Lopez-Exposito, C. Kleiveland, T. Lea, A. Mackie, T. Requena, D. Swiatecka and H. Wichers, editors, The Impact of Food Bioactives on Health: in vitro and ex vivo models, Cham (CH). p. 263-273.

Wickersham, M., S. Wachtel, T. Wong Fok Lung, G. Soong, R. Jacquet, A. Richardson, D. Parker, and A. Prince. 2017. Metabolic Stress Drives Keratinocyte Defenses against Staphylococcus aureus Infection. Cell Rep. 18:2742-2751. doi: 10.1016/j.celrep.2017.02.055.

Wierenga, K. T., T. A. McAllister, D. J. Gibb, A. V. Chaves, E. K. Okine, K. A. Beauchemin, and M. Oba. 2010. Evaluation of triticale dried distillers grains with solubles as a substitute for barley grain and barley silage in feedlot finishing diets. J. Anim. Sci. 88:3018-3029. doi: 10.2527/jas.2009-2703.

Wiese, B. I., P. Gorka, T. Mutsvangwa, E. Okine, and G. B. Penner. 2013. Short communication: Interrelationship between butyrate and glucose supply on butyrate and glucose oxidation by ruminal epithelial preparations. J. Dairy Sci. 96:5914-5918. doi: 10.3168/jds.2013-6677.

Wiese, B. I., S. Hendrick, J. G. Campbell, J. J. McKinnon, K. A. Beauchemin, T. A. McAllister, and G. B. Penner. 2017. Defining risk for low reticuloruminal pH during the diet transition period in a commercial feedlot in western Canada. J. Anim. Sci. 95:420-435. doi: 10.2527/jas.2016.0969.

Williamson, D. H., J. Mellanby, and H. A. Krebs. 1962. Enzymic determination of D(-)-beta-hydroxybutyric acid and acetoacetic acid in blood. Biochem. J. 82:90-96. doi: 10.1042/bj0820090.

Wilson, D. J., T. Mutsvangwa, and G. B. Penner. 2012. Supplemental butyrate does not enhance the absorptive or barrier functions of the isolated ovine ruminal epithelia. J. Anim. Sci. 90:3153-3161. doi: 10.2527/jas.2011-4315.

Wittkopf, N., M. F. Neurath, and C. Becker. 2014. Immune-epithelial crosstalk at the intestinal surface. J. Gastroenterol. 49:375-387. doi: 10.1007/s00535-013-0929-4.
Wolowczuk, I., C. Verwaerde, O. Viltart, A. Delanoye, M. Delacre, B. Pot, and C. Grangette. 2008. Feeding our immune system: impact on metabolism. Clin. Dev. Immunol. 2008:639803. doi: 10.1155/2008/639803.
Wong, J. M., R. de Souza, C. W. Kendall, A. Emam, and D. J. Jenkins. 2006. Colonic health: fermentation and short chain fatty acids. J. Clin. Gastroenterol. 40:235-243. doi: 10.1097/00004836-200603000-00015.
Xiao, T., S. Wu, C. Yan, C. Zhao, H. Jin, N. Yan, J. Xu, Y. Wu, C. Li, Q. Shao, and S. Xia. 2018. Butyrate upregulates the TLR4 expression and the phosphorylation of MAPKs and NK-kappaB in colon cancer cell in vitro. Oncol. Lett. 16:4439-4447. doi: 10.3892/ol.2018.9201.
Yagi, S., A. Takaki, T. Hori, and K. Sugimachi. 2002. Enteric lipopolysaccharide raises plasma IL-6 levels in the hepatoportal vein during non-inflammatory stress in the rat. Fukuoka Igaku Zasshi. 93:38-51.
Yamanaka, K., R. Clark, B. Rich, R. Dowgiert, K. Hirahara, D. Hurwitz, M. Shibata, N. Mirchandani, D. A. Jones, D. S. Goddard, S. Eapen, H. Mizutani, and T. S. Kupper. 2006. Skin-derived interleukin-7 contributes to the proliferation of lymphocytes in cutaneous T-cell lymphoma. Blood. 107:2440-2445. doi: 10.1182/blood-2005-03-1139.
Yan, X., X. Xiong, and Y. G. Chen. 2018. Feedback regulation of TGF-beta signaling. Acta Biochim. Biophys. Sin. (Shanghai). 50:37-50. doi: 10.1093/abbs/gmx129.
Yang, R. B., M. R. Mark, A. L. Gurney, and P. J. Godowski. 1999. Signaling events induced by lipopolysaccharide-activated toll-like receptor 2. J. Immunol. 163:639-643.
Yohe, T. T., H. L. M. Tucker, C. L. M. Parsons, A. J. Geiger, R. M. Akers, and K. M. Daniels. 2016. Short communication: Initial evidence supporting existence of potential rumen epidermal stem and progenitor cells. J. Dairy Sci. 99:7654-7660. doi: 10.3168/jds.2016-10880.
Yu, F., L. A. Bruce, A. G. Calder, E. Milne, R. L. Coop, F. Jackson, G. W. Horgan, and J. C. MacRae. 2000. Subclinical infection with the nematode Trichostrongylus colubriformis increases gastrointestinal tract leucine metabolism and reduces availability of leucine for other tissues. J. Anim. Sci. 78:380-390. doi: 10.2527/2000.782380x.
Zagari, F., M. Jordan, M. Stettler, H. Broly, and F. M. Wurm. 2013. Lactate metabolism shift in CHO cell culture: the role of mitochondrial oxidative activity. N. Biotechnol. 30:238-245. doi: 10.1016/j.nbt.2012.05.021.
Zaslona, Z., E. M. Palsson-McDermott, D. Menon, M. Haneklaus, E. Flis, H. Prendeville, S. E. Corcoran, M. Peters-Golden, and L. A. J. O'Neill. 2017. The Induction of Pro-IL-1beta by Lipopolysaccharide Requires Endogenous Prostaglandin E2 Production. J. Immunol. 198:3558-3564. doi: 10.4049/jimmunol.1602072.
Zebeli, Q., D. Mansmann, S. Sivaraman, S. M. Dunn, and B. N. Ametaj. 2013. Oral challenge with increasing doses of LPS modulated the patterns of plasma metabolites and minerals in periparturient dairy cows. Innate Immun. 19:298-314. doi: 10.1177/1753425912461287.
Zebeli, Q., and B. U. Metzler-Zebeli. 2012. Interplay between rumen digestive disorders and diet-induced inflammation in dairy cattle. Res. Vet. Sci. 93:1099-1108. doi: 10.1016/j.rvsc.2012.02.004.

Zeisberg, M., and E. G. Neilson. 2009. Biomarkers for epithelial-mesenchymal transitions. J Clin Invest. 119:1429-1437. doi: 10.1172/JCI36183.
Zhan, K., X. Gong, Y. Chen, M. Jiang, T. Yang, and G. Zhao. 2019. Short-Chain Fatty Acids Regulate the Immune Responses via G Protein-Coupled Receptor 41 in Bovine Rumen Epithelial Cells. Front. Immunol. 10:2042. doi: 10.3389/fimmu.2019.02042.
Zhang, J. M., and J. An. 2007. Cytokines, inflammation, and pain. Int. Anesthesiol. Clin. 45:27-37. doi: 10.1097/AIA.0b013e318034194e.
Zhang, R., W. Zhu, and S. Mao. 2016. High-concentrate feeding upregulates the expression of inflammation-related genes in the ruminal epithelium of dairy cattle. J. Anim. Sci. Biotechnol. 7:42. doi: 10.1186/s40104-016-0100-1.
Zhang, S., R. I. Albornoz, J. R. Aschenbach, D. R. Barreda, and G. B. Penner. 2013. Short-term feed restriction impairs the absorptive function of the reticulo-rumen and total tract barrier function in beef cattle. J. Anim. Sci. 91:1685-1695. doi: 10.2527/jas.2012-5669.
Zhang, S., G. Bories, C. Lantz, R. Emmons, A. Becker, E. Liu, M. M. Abecassis, L. Yvan-Charvet, and E. B. Thorp. 2019. Immunometabolism of Phagocytes and Relationships to Cardiac Repair. Front. Cardiovasc. Med. 6:42. doi: 10.3389/fcvm.2019.00042.
Zhang, W., J. Y. Du, Q. Yu, and J. O. Jin. 2015. Interleukin-7 produced by intestinal epithelial cells in response to Citrobacter rodentium infection plays a major role in innate immunity against this pathogen. Infect. Immun. 83:3213-3223. doi: 10.1128/IAI.00320-15.
Zhang, Z., Z. Zi, E. E. Lee, J. Zhao, D. C. Contreras, A. P. South, E. D. Abel, B. F. Chong, T. Vandergriff, G. A. Hosler, P. E. Scherer, M. Mettlen, J. C. Rathmell, R. J. DeBerardinis, and R. C. Wang. 2018. Differential glucose requirement in skin homeostasis and injury identifies a therapeutic target for psoriasis. Nat. Med. 24:617-627. doi: 10.1038/s41591-018-0003-0.
Zhao, K., Y. H. Chen, G. B. Penner, M. Oba, and L. L. Guan. 2017. Transcriptome analysis of ruminal epithelia revealed potential regulatory mechanisms involved in host adaptation to gradual high fermentable dietary transition in beef cattle. BMC Genomics. 18:976. doi: 10.1186/s12864-017-4317-y.
Zheng, Y., Y. Song, Q. Han, W. Liu, J. Xu, Z. Yu, R. Zhang, and N. Li. 2018. Intestinal epithelial cell-specific IGF1 promotes the expansion of intestinal stem cells during epithelial regeneration and functions on the intestinal immune homeostasis. Am. J. Physiol. Endocrinol. Metab. 315:E638-E649. doi: 10.1152/ajpendo.00022.2018.
Zinn, R. A., F. N. Owens, and R. A. Ware. 2002. Flaking corn: processing mechanics, quality standards, and impacts on energy availability and performance of feedlot cattle. J. Anim. Sci. 80:1145-1156. doi: 10.2527/2002.8051145x.
Zouboulis, C. C., J. Adjaye, H. Akamatsu, G. Moe-Behrens, and C. Niemann. 2008. Human skin stem cells and the ageing process. Exp. Gerontol. 43:986-997. doi: 10.1016/j.exger.2008.09.001.